

NEW SYNTHETIC RECEPTORS FOR MOLECULAR RECOGNITION OF ANIONS AND THEIR PRACTICAL APPLICATIONS

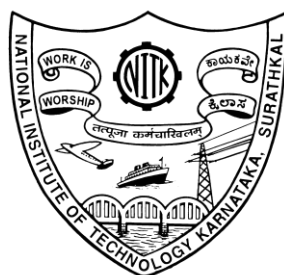
Thesis

Submitted in partial fulfilment of the requirements for the degree of

DOCTOR OF PHILOSOPHY

By

MADHUPRASAD



DEPARTMENT OF CHEMISTRY

NATIONAL INSTITUTE OF TECHNOLOGY KARNATAKA,

SURATHKAL, MANGALORE – 575 025

March, 2014

DECLARATION

I hereby *declare* that the Research Thesis entitled “New Synthetic Receptors for Molecular Recognition of Anions and Their Practical Applications” which is being submitted to the National Institute of Technology Karnataka, Surathkal in partial fulfilment of the requirements for the award of the Degree of Doctor of Philosophy in Chemistry is a *bonafide report of the research work carried out by me*. The material contained in this Research Thesis has not been submitted to any University or Institution for the award of any degree.

Madhuprasad

Reg. No. 100544CY10F02

Department of Chemistry

Place: NITK - Surathkal

Date:

CERTIFICATE

This is to certify that the Research Thesis entitled “New Synthetic Receptors for Molecular Recognition of Anions and Their Practical Applications” submitted by Mr. Madhuprasad (Register Number: 100544CY10F02) as the record of the research work carried out by him is accepted as the Research Thesis submission in partial fulfilment of the requirements for the award of degree of Doctor of Philosophy.

Dr. Darshak R. Trivedi
Research Guide
Date:

Chairman – DRPC
Date:

DEDICATED TO MY

PARENTS

&

FAMILY

ACKNOWLEDGMENT

Completing Ph.D. degree is probably the most challenging activity of my life. It has been a great privilege to spend time in the Department of Chemistry, National Institute of Technology Karnataka. In this regard, I would like to acknowledge people who helped me throughout this journey.

My first gratitude must go to my advisor, Dr. Darshak R. Trivedi, who patiently provided me the vision and necessary guidance as well as support to reach the vision. This work would not have been possible without his supervision and encouragement throughout the research program. Along with the subject he taught me how to tackle the difficulties of life and ultimately to reach the goals successfully. I am sure it will support me to move forward in my career and life as well.

I thank NITK, Surathkal, for providing financial assistance and all the necessary facilities to make this research peaceful.

I am thankful to Prof. B. R. Bhat, Head, Department of Chemistry and Chairman-DRPC, members of RPAC, Prof. A.C. Hegde, Ex-Head, Department of Chemistry Dr. Jagadeesh Babu, Department of Chemical Engineering for their support, guidance and helpful suggestions. Their guidance has aided me well and I owe them my earnest appreciation.

I thank Prof. A. N. Shetty, Prof. A. V. Adhikari, Prof. D. K. Bhat, Dr. A. M. Isloor, Dr. D. Udaya Kumar and Dr. Sib Sankar Mal for their encouragement, timely help and support.

I am obliged to Dr. D. Amilan Jose, Assistant Professor, National Institute of Technology Kurukshetra for the valuable scientific advices, Prof. Parthasarathi Dastidar, Professor and Head, and Uttam Kumar Das, Department of Organic Chemistry, Indian Association for the Cultivation of Science for SCXRD analysis, CSMCRI Bhavnagar, Optoelectronics laboratory; Dept. of Physics; NITK, CFTRI, Mysore, Manipal Institute of Technology, Manipal and Sri Ramachandra Medical Centre, Chennai for providing analytical support. I extend my gratitude to Department of Science and Technology, Govt. of India for providing SCXRD facility to Department of Chemistry, NITK Surathkal, under FIST program.

I am indebted to my research colleagues, Dr. Subrahmanya Ishwar Bhat, Mrs. Madhavi Oruganti and groupmembers as well as other researchers in the department who supported me during my research programme.

Special thanks to my closest comrades Balakrishna S. G, INM–Leibniz Institute for New Materials, Germany and Surendra B, Team leader, Biocon, Bangalore who were sources of laughter, joy and support. In addition, I thank each and every person who helped me directly or indirectly in my career.

I extend my appreciation to non-teaching staff members of Chemistry Department Mrs. Kasthuri, Mr. Prashant, Mrs. Sharmila, Mr. Ashok, Mr. Pradeep, Mr. Harish and Mrs. Deepa for their timely help in the department.

Last but not the least, I would like to pay the respects and dedicate this work to my Mother, Durgavathi; Father, Shambhayya; Brother, Pradeep and Sisters, Nimmi Mohan and Roopa. Their love and unconditional support provided my inspiration and was and will be my driving force. I owe them everything and wish I could show them just how much I love and appreciate them. I hope that this work makes them proud. A special thanks to my sister in law, Nayana who helped me to improve language. My wife, Rashmi, whose love and encouragement allowed me to finish this journey. So I will just give her ‘heartfelt’ thanks.

MADHUPRASAD

ABSTRACT

Among the wide range of anions, the detection of fluoride ion has gained greater attention because of its privileged usage in clinical applications which made it beneficial to human health. However, the excess of fluoride consumption is health concern as it can be a cause of many lethal diseases including bone cancer. Apart from this fluoride ion detection, the detection of dicarboxylates is also a field of prominence as they play vital role in the numerous metabolic processes such as glyoxalate cycle, generation of high energy phosphate bonds etc.

Considering the significance of the field, six new series of receptors based on various backbones such as 1-naphthohydrazide, benzohydrazide, aminophenol and triphenylphosphonium salts have been designed and synthesised for the colorimetric detection of fluoride ion and dicarboxylate ions and utilized for versatile applications of environmental concern. All the receptors have been characterised using different techniques such as ^1H NMR, FT-IR, elemental analysis and ESI-MS. The selected receptors have been considered for three-dimensional structural elucidation using Single Crystal X-Ray diffraction (SCXRD) studies.

The quantitative analysis of anions with the receptors has been carried out using UV-vis titration. The binding constant for the receptor-anion complex has been calculated using Benesi–Hildebrand equation. The binding mechanism has been proposed based on UV-vis titration and the same has been confirmed by ^1H NMR titration.

Based on the experimental results, it has been concluded that the simple organic molecules could act as very good colorimetric receptors for biologically important anions such as fluoride and dicarboxylate ions. Along with colorimetric detection, these receptors could show vivid analytically as well as environmentally significant applications such as quantitative analysis of fluoride ion present in sea water/mouthwash, determination of percentage composition in binary solvent mixture and extraction of fluoride ions from sea water.

Keywords: Anion Receptors; Colorimetric detection; Solvatochromism; Aqueous media; Extraction; Deprotonation; Charge transfer; Acidic proton.

CONTENTS

DECLARATION

CERTIFICATE

ACKNOWLEDGEMENT

ABSTRACT

CONTENTS

i

NOMENCLATURE

vii

CHAPTER 1

INTRODUCTION AND LITERATURE REVIEW

1.1	SUPRAMOLECULAR CHEMISTRY	1
1.2	ANIONS	2
1.2.1	Biological and environmental importance of anions	2
1.2.2	Fluoride ion	2
1.2.3	Dicarboxylate ions	3
1.3	ANION RECEPTOR CHEMISTRY	4
1.3.1	Host-guest chemistry	4
1.3.2	Challenges in anion receptor chemistry	5
1.3.3	History of synthetic anion receptor chemistry	6
1.3.4	Classification of colorimetric receptors	7
1.3.5	Substitution methodology	8
1.3.6	Reaction based methodology	8
1.3.7	Binding methodology	9
1.4	BRIEF LITERATURE REVIEW	12
1.4.1	Literature on F ⁻ ion detection	13
1.4.2	Literatures on carboxylate ion detection	23
1.5	SCOPE OF THE WORK	27
1.6	OBJECTIVES OF THE CURRENT WORK	29

CHAPTER 2

DESIGN AND SYNTHESIS OF 1-NAPHTHOHYDRAZIDE BASED RECEPTORS AND THEIR APPLICATION AS FLUORIDE ION RECEPTORS

2.1	INTRODUCTION	31
2.2	EXPERIMENTAL	33
2.2.1	Materials and methods	33
2.2.2	Synthesis of intermediate S 2.5	34
2.2.3	Synthesis of receptors S1R1, S1R2 and S1R3	34
2.3	RESULTS AND DISCUSSION	39
2.3.1	Colorimetric detection of anions	39
2.3.2	UV-vis spectral studies of receptors	41
2.3.3	¹ H NMR titration and binding mechanism	46
2.3.4	Practical application	50
2.4	CONCLUSIONS	51

CHAPTER 3

DESIGN AND SYNTHESIS OF BENZOHYDRAZIDE BASED RECEPTORS FOR THE DETECTION OF INORGANIC FLUORIDE ION IN AQUEOUS MEDIA

3.1	INTRODUCTION	53
3.2	EXPERIMENTAL	54
3.2.1	Materials and methods	54
3.2.2	Synthesis of intermediates S 3.3 and S 3.6	55
3.2.3	Synthesis of receptors S2R1, S2R2 and S2R3	56
3.2.4	Synthesis of receptor S2R4	56
3.3	RESULTS AND DISCUSSION	63
3.3.1	Colorimetric detection of anions	63
3.3.2	UV-vis spectral studies of receptors	65
3.3.3	Practical applications	68
3.3.4	Binding mechanism	71
3.3.5	¹ H NMR titration studies	72

3.4	CONCLUSIONS	73
-----	-------------	----

CHAPTER 4

DESIGN AND SYNTHESIS OF AMINOPHENOL BASED FLUORIDE ION RECEPTOR, SOLVATOCHROMIC STUDY AND ITS MOLECULAR SWITCH APPLICATION

4.1	INTRODUCTION	75
4.2	EXPERIMENTAL	76
4.2.1	Materials and methods	76
4.2.2	Synthesis of receptors S3R1, S3R2 and S3R3	77
4.2.3	Stoichiometric ratio determination using Job's plot method	82
4.3	RESULTS AND DISCUSSION	82
4.3.1	Colorimetric detection of anions	82
4.3.2	UV-vis spectral studies of receptors	84
4.3.3	Binding mechanism of anion	85
4.3.4	¹ H NMR titration studies	86
4.3.5	Solvatochromic studies	87
4.3.6	Application of solvatochromism	88
4.3.7	Detailed study in ACN solvent	90
4.3.8	Colorimetric detection and binding mechanism of cation	92
4.3.9	Logic gate application of receptor S3R1	93
4.4	CONCLUSIONS	95

CHAPTER 5

DESIGN AND SYNTHESIS OF AMINOPHENOL BASED RECEPTORS FOR COLORIMETRIC DISCRIMINATION OF ISOMERIC DICARBOXYLATES AND THEIR APPLICATION IN DETECTING FLUORIDE IONS

5.1	INTRODUCTION	97
5.2	EXPERIMENTAL	99
5.2.1	Materials and methods	99
5.2.2	Synthesis of receptors S4R1, S4R2, S4R3 and S4R4 (Scheme 5.1)	99

5.2.3	Synthesis of tetrabutylammonium salts	104
5.2.4	Stoichiometric ratio determination using Job's plot method	104
5.3	RESULTS AND DISCUSSION	104
5.3.1	Discrimination of isomeric dicarboxyltes	104
5.3.2	Detection of F ⁻ ions	112
5.4	CONCLUSIONS	117

CHAPTER 6

DESIGN AND SYNTHESIS OF BENZOHYDRAZIDE BASED RECEPTORS FOR DISCRIMINATION OF MALEATE OVER FUMARATE AND RATIO METRIC FLUORIDE ION DETECTION

6.1	INTRODUCTION	119
6.2	EXPERIMENTAL	121
6.2.1	Materials and methods	121
6.2.2	Synthesis of intermediates S 6.3 and S 6.7	121
6.2.3	Synthesis of receptors S5R1 and S5R2 (Scheme 6.3)	122
6.2.4	Synthesis of receptors S5R3 (Scheme 6.4)	123
6.2.5	General procedure for the synthesis of tetrabutylammonium salts	127
6.3	RESULTS AND DISCUSSION	127
6.3.1	Discrimination of isomeric dicarboxyltes	127
6.3.2	Detection of F ⁻ ions	134
6.4	CONCLUSIONS	141

CHAPTER 7

DESIGN AND SYNTHESIS OF RECEPTORS WITH ACTIVE METHYLENE GROUP AS BINDING SITE FOR EXTRACTION OF FLUORIDE IONS FROM SEA WATER

7.1	INTRODUCTION	143
7.2	EXPERIMENTAL	144
7.2.1	Materials and methods	144
7.2.2	Synthesis of S 7.2 and S 7.3 (Scheme 7.1)	145

7.2.3	Synthesis of S6R3 (Scheme 7.2)	145
7.2.4	Synthesis of S6R4 (Scheme 7.3)	146
7.2.5	Synthesis of S 7.4 and S 7.5 (Scheme 7.4)	146
7.2.6	Synthesis of S6R1 and S6R2 (Scheme 7.5)	147
7.2.7	Extraction efficiency measurement of receptor S6R2	153
7.3	RESULTS AND DISCUSSION	153
7.3.1	Fluoride ion detection	153
7.3.2	Extraction of inorganic fluoride ion from aqueous media	161
7.4	CONCLUSIONS	163
 CHAPTER 8		
SUMMARY AND CONCLUSIONS		
8.1	SUMMARY	165
8.2	CONCLUSIONS	166
 REFERENCES		
PUBLICATIONS		
CURRICULAM VITAE		

NOMENCLATURE

ABBREVIATIONS

EDC.HCl	1-ethyl-3-(3-dimethylaminopropyl)carbodiimide hydrochloride
HOBt	1-Hydroxybenzotriazole
AcO ⁻	Acetate ion
ACN	Acetonitrile
Br ⁻	Bromide ion
Cl ⁻	Chloride ion
<i>J</i>	Coupling constant
DCM	Dichloromethane
H ₂ PO ₄ ⁻	Dihydrogenphosphate ion
DMSO	Dimethyl sulfoxide
DMSO- <i>d</i> ₆	Dimethyl sulfoxide-deuterated
DMF	Dimethylformamide
ESI	Electrospray ionization
EtOH	Ethanol
equiv.	Equivalence
Fig.	Figure
F ⁻	Fluoride ion
FT-IR	Fourier transform infrared
FID	Free induction decay
HPLC	High-performance liquid chromatography
NH ₂ NH ₂	Hydrazine hydrate
HCl	Hydrochloric acid
HSO ₄ ⁻	Hydrogensulphate ion
ICT	Intramolecular charge transfer
I ⁻	Iodide ion
MS	Mass spectra
m.p.	Melting point

MeOH	Methanol
NO ₃ ⁻	Nitrate ion
ORTEP	Oak ridge thermal ellipsoidal plot
POCl ₃	Phosphorousoxychloride
¹ H NMR	Proton nuclear magnetic resonance
RT	Room temperature
SCXRD	Single crystal X-ray diffraction
NaF	Sodium fluoride
Na ₂ SO ₄	Sodium sulphate
TBA	Tetrabutylammonium
THF	Tetrahydrofuran
TMS	Tetramethylsilane
TLC	Thin layer chromatography
SOCl ₂	Thionyl chloride
UV-vis	Ultraviolet-visible
WHO	World health organization

SYMBOLS AND UNITS

α	Alpha
β	Beta
cm	Centimetre
$^{\circ}$	Degree
$^{\circ}\text{C}$	Degree Celsius
δ	Delta
γ	Gamma
g	Gram
>	Greater than
h	Hour
Hz	Hertz
$^{-1}$	Inverse
λ	Lamda
<	Less than
L	Litre
MHz	Mega hertz
mL	millilitre
mmol	millimole
min	Minute
M	Molar
μ	Mu
nm	Nanometre
ppm	Parts per million
θ	Theta

CHAPTER 1

INTRODUCTION AND LITERATURE REVIEW

In this chapter, a brief introduction about supramolecular chemistry, anions and anion binding chemistry has been discussed. In addition challenges in anion detection, history of anion receptors, a brief literature review, scope and objectives of the current work have been described.

1.1 SUPRAMOLECULAR CHEMISTRY

Supramolecular chemistry has been defined by Jean-Marie Lehn as ‘*the chemistry of molecular assemblies and of the intermolecular bond*’, who shared the Nobel Prize for this work in the year 1987. Broadly, the supramolecular chemistry can be expressed as ‘chemistry beyond the molecule’. Perhaps it can also be defined as ‘the chemistry of the non-covalent bond’ and ‘non-molecular chemistry’. The supramolecular chemistry was defined in terms of the non-covalent interaction between a ‘host’ and a ‘guest’ molecule (Steed et al. 2009). The traditional chemistry focuses on the covalent bond; whereas supramolecular chemistry concentrates on the weaker and reversible non-covalent interactions between molecules. Thus the supramolecular division focuses on the chemical systems made up of a discrete number of assembled molecular subunits or components. The simple illustration to compare molecular chemistry with supramolecular chemistry is given in Fig 1.1.

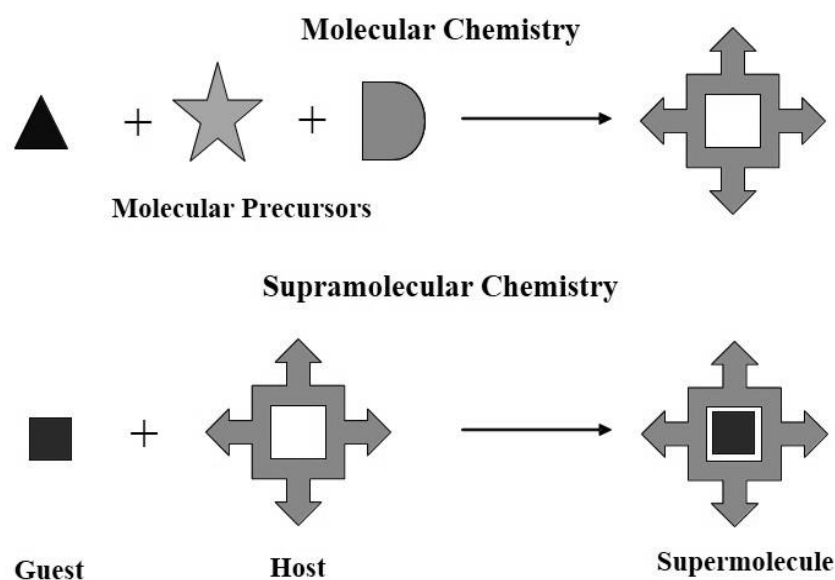


Fig. 1.1 Comparison between molecular and supramolecular chemistry

1.2 ANIONS

An atom or a molecule which possesses more number of electrons than protons is called anion. The resulting charge over the atom or molecule is negative. The atoms that form anions most easily are Group 17 (or VII) atoms, or the halogens such as fluorine, chlorine, bromine, iodine etc. These halogens can readily gain one extra electron to carry a -1 charge (negative charge) and thus form respective anions (halides). Oxygen and sulphur can carry -2 charges; nitrogen and phosphorous can carry -3 charges to form respective anions. The molecules such as cyanide (CN^-), thiocyanate (SCN^-), carboxylate (COO^-) and phosphate (PO_4^{3-}) etc. are anions as these molecules carry negative charges.

1.2.1 Biological and environmental importance of anions

Anions are responsible for many biological processes and to regulate several environmental processes. Generally, anions are directly involved in various biological parameters such as retaining the cell volume, osmotic pressure, production of electrical signals, activation of pathways to transfer genetic information etc. (Alberts et al. 1994) Thus, anions directly influence on many genetic disorders such as Pendred's syndrome (Scott et al. 1999; Yoshida et al. 2002), Bartter's syndrome (Simon et al. 1997) Dent's disease (Devuyst et al. 1999), cystic fibrosis (Anderson et al. 1991) and osteopetrosis (Kornak et al. 2001). Anions are indispensable component in the interaction between RNA/DNA and proteins as well as in many of the enzymatic complexes and they are the energy source for the enzymatic transformation. Further, anions act as environmental pollutants which includes contamination of drinking water with fluoride, carcinogenesis (process by which normal cells are transformed into cancer cells) by metabolites of acetate (Glidewell 1990), eutrophication (uncontrolled growth of algae due to the excess of nutrients in water bodies) caused by phosphate/nitrates containing fertilizers (Moss 1996). Though the disadvantages associate with anions some of them are still essential for the normal health.

1.2.2 Fluoride ion

Among the wide range of anions, fluoride has attained significance in the scientific community because of its dual functionality. This biologically important

anion has a vital role in preventing dental decay (Kirk 1991; Featherstone 1999) and in the treatment of osteoporosis (Riggs 1984; Kleerekoper 1998). Therefore, small quantity of fluoride ions is essential as well as beneficial to human health. In contradictory, excess of fluoride consumption can cause dental fluorosis (Weatherall 1969; Wiseman 1970; Kaminsky 1990; Browne et al. 2005) or mottled enamel and skeletal fluorosis (Shivarajashankara et al. 2001; Schwarzenbach et al. 2006), a bone disease which is a major problem in India. It has been assessed that excess of fluoride can inhibits over 100 different enzyme systems. Acute fluoride exposure may cause collagen breakdown, depression in the thyroid activity, bone cancer, immune system disturbance and anaemia (Carton 2006; Bassin et al. 2006; Schwarzenbach et al. 2006; Connet 2007; Yu et al. 2008; Kim et al. 2011). Recently, fluoride has also been suspected for many lethal diseases including damaging the hippocampal area of brain. Despite of knowing these facts, continued introduction of fluoride to the environment by excessive usage of fertilizers and industrial wastes is of great concerned.

1.2.3 Dicarboxylate ions

Generally, dicarboxylates are the anions which contain two carboxylic acid functional groups in a molecule. The dicarboxylic acids gain significance due to their wide spread applications in pharmaceutical industries and food industries. Apart from these, the dicarboxylates are used in many materials such as fragrances, polyamides/nylons, adhesives, lubricants, polyurethane foams, leather tanning and polyesters. Furthermore, the dicarboxylates are biologically very important as they play crucial roles in numerous metabolic processes such as glyoxalate cycle, generation of high energy phosphate bonds and in dicarboxylate cycle for autotrophic carbon dioxide (CO₂) fixation (Berg et al. 2012). The dicarboxylate isomers such as maleate and fumarate plays significant role in many biological processes. For example; fumarate is generated in the Krebs cycle and maleate is used to inhibit the Krebs cycle (Gougoux et al. 1976; EiamOng et al. 1995). The *cis*-aconitate is produced during the citric acid cycle whereas *trans*-aconitate is a good inhibitor of both aconitase and fumarase (Kata et al. 2004).

1.3 ANION RECEPTOR CHEMISTRY

In general, anion receptors are the molecules which can recognize or sense the anions (i.e. negatively charged species). Though instrumental methods such as anion monitor probes are available for the detection of anion, it consumes more time and requires skilled efforts to operate. On the other hand, colorimetric method of detection is widely accepted due to the low cost, instantaneous detection, easy/safe to handle, equally selective and sensitive as instrumental methods. Therefore, designing novel synthetic receptors for the colorimetric detection of anions acquired considerable attention and as a result, from couple of decades the colorimetric anion receptor chemistry has been studied extensively (Garcia-Garrido et al. 2007; Steed 2009; Kubik 2009; Caltagirone and Gale 2009; Gale and Gunlaugsson 2010; Lau et al. 2011; Gale 2011; Dydio et al. 2011; Moragues et al. 2011; Ngo et al. 2012; Yin et al. 2013; Gale et al. 2014). However, most of the comprehensive studies follow host-guest and non-covalent binding approach to design the various receptors.

1.3.1 Host-guest chemistry

It is important to define the binding in the process of non-covalent binding. Generally binding is the process where a molecular 'guest' binds to another molecule 'host' to form a supermolecule or a 'host-guest' complex (Fig. 1.2). Commonly the host is a large molecule or an enzyme or a synthetic cyclic molecule which possesses a central hole or cavity. The guest may be monatomic cation, or simple monatomic inorganic anion or sometimes small synthetic anions. More precisely the host is defined as the molecular entity possessing 'convergent' binding sites such as Lewis basic donor atoms or hydrogen bond donors. The guest possesses 'divergent' binding sites such as Lewis acid metal cations or hydrogen bond acceptor halide anions.

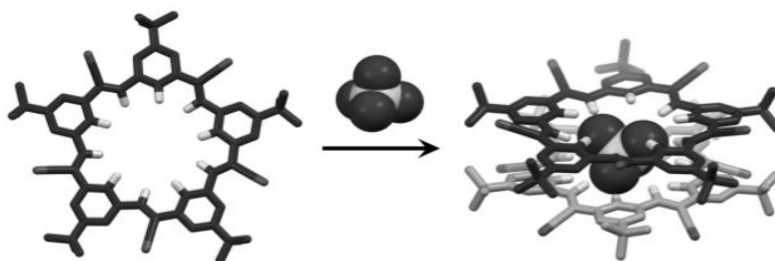


Fig. 1.2 Schematic representation of host-guest chemistry (Amar Flood Research Group)

According to Donald Cram the host-guest relationship can be defined as,

“Complexes are composed of two or more molecules or ions held together in unique structural relationships by electrostatic forces other than those of full covalent bonds, molecular complexes are usually held together by hydrogen bonding, by ion pairing, by π -acid to π -base interactions, by metal-to-ligand binding, by van der Waals attractive forces, by solvent reorganising, and by partially made and broken covalent bonds (transition states). High structural organisation is usually produced only through multiple binding sites. A highly structured molecular complex is composed of at least one host and one guest component. A host–guest relationship involves a complementary stereo electronic arrangement of binding sites in host and guest. The host component is defined as an organic molecule or ions whose binding sites converge in the complex and the guest component as any molecule or ion whose binding sites diverge in the complex.”

1.3.2 Challenges in anion receptor chemistry

The anion binding chemistry with non-covalent host guest approach is an old concept. However, the designing an anion receptor is still challenging when compared to the same for cation. This difficulty is because of the following reasons;

- ❖ Anions are relatively larger in size than the equivalent isoelectric cations. For example; one of the smallest anions, F^- (1.33Å) is comparable in ionic radius with K^+ (1.38Å). Therefore, they have lower charge to radius ratio and thus, binding interactions are less effective than corresponding isoelectric cations
- ❖ Anions are pH sensitive and easily get protonated at low pH to lose their negative charge. Thus, receptors must work within the pH range of the target anion
- ❖ Anions are usually coordinatively saturated. Therefore, binding of anions should take place only through weak forces such as hydrogen bonding or van der Waals interactions
- ❖ Anionic species have wide range of geometries (Fig. 1.3) and therefore generally a higher degree of design and complementarity is required to make receptors that are selective for a particular anionic guest than for most simple cations

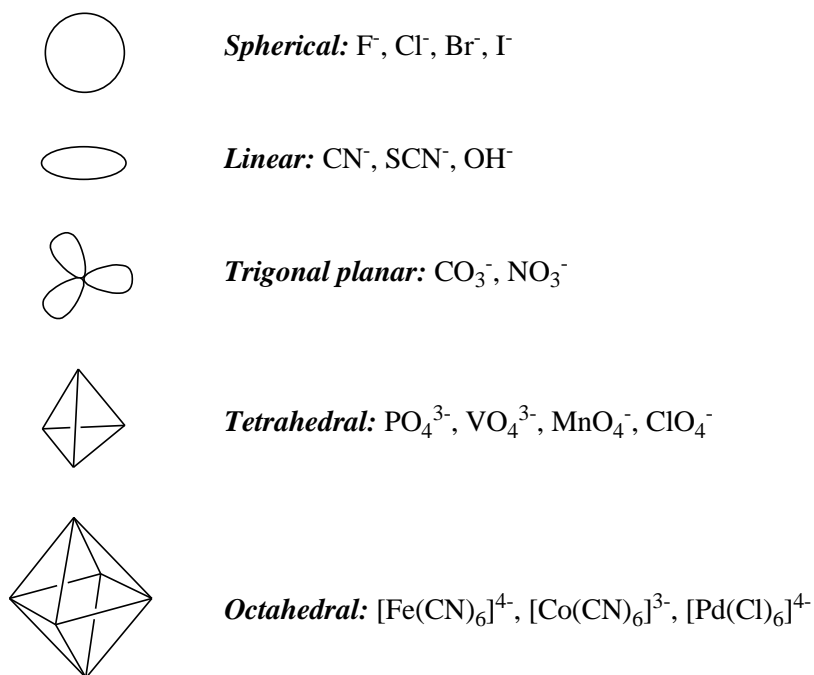


Fig. 1.3 Different shapes of anions

- ❖ In comparison to cations of similar size, anions have high free energies of solvation. Therefore, anions readily get solvated in polar protic solvents and for the detection of these anions the receptor must compete more effectively with the surrounding medium

Thus, anion complexation with the receptor is relatively different from cation receptors, where detection involves the metal coordination.

1.3.3 History of synthetic anion receptor chemistry

The first synthetic anion receptor was reported by Park and Simmons in late 60s (Park and Simmons 1968). This work has been communicated the halide binding properties of macrobicyclic receptor containing two ammonium centres bridged by three alkyl linkers.

Following Park and Simmons work Lehn and Graf (1975) synthesized ammonium based macrobicyclic and macrotricyclic receptors. These cryptand-like receptors with four amine centres were able to bind halide anions particularly chloride ions within the cavity (Graf and Lehn 1976). Iodide was too large to fit into the cavity and therefore relatively less strongly bound to the receptor. The crystal structure of

chloride bound receptor was reported by Metz, Rosalky and Weiss in the year 1976 which confirmed chloride ion bound to the center of this cryptand-like receptor. In the year 1978, Lehn and co-workers synthesized hexa-protonated cryptands which was found to be highly selective towards linear anions such as azide (N_3^-).

Later in early 80s, Schimidtchen produced a series of receptors based on quaternary ammonium groups (Schimidtchen 1980; Schimidtchen 1981; Schimidtchen and Muller 1984), which do not depend on the hydrogen bonding interactions to bind anions. The receptor was arranged in tetrahedral manner and hence anion bound very easily with in the cage-like arrangement with electrostatic interactions. The selectivity of these receptors was able to 'tune' by altering length of alkyl chain between the ammonium centres. In the year 1986, Pascal et al. synthesized first anion receptor with amide $-\text{NH}$ linkage (Pascal et al. 1986). This receptor was found to have affinity towards fluoride ions in $\text{DMSO}-d_6$ solution and this was confirmed by ^1H NMR and ^{19}F NMR studies.

Reinhoudt and co-workers synthesized a series of amide and sulphonamide based acyclic tripodal receptors in 1993 (Reinhoudt et al. 1993). These receptors selectively bound to the dihydrogen phosphate ions over other halide anions and hydrogen sulphate. Subsequently, the anion receptor chemistry extensively studied during the past couple of decades.

1.3.4 Classification of colorimetric receptors

After the first synthetic anion receptor, developed by Park and Simmons (Park and Simmons 1968), the coordination of anions was not comprehensively explored for many years. However, from the past couple of decades the field of anion detection and anion coordination was extensively studied owing to potential applications of anions in the various fields such as biology, environmental science and chemical science (Bowman-James and Garcia-Espana 1997; Sessler et al. 2006). Initial research on the anion receptor chemistry was focused on the design and synthesis of the organic molecules which could detect the anions in organic environment (Suksai and Tuntulani 2003). Recently, anion receptor chemistry is concentrating on developing the new receptors for the detection of anions in aqueous media (Kubik 2010), for the removal of anions from aqueous media using extraction method (Das et al. 2011), to

detect anionic pollutants in low concentrations (Kim and Gabbai 2009) and *in vivo* detection of biologically important anions (Ojida et al. 2008). However, all these detection process follows three main methodologies based on the detection mechanism of receptors which are discussed in following sections.

1.3.5 Substitution methodology

The substitution methodology consists of a receptor which contains a binding site and a signalling unit which are non-covalently bound together to form a complex molecule. When an anion is introduced to the solution of this complex molecule, it substitutes the signalling unit and free signalling unit in the solution incorporates colour change in system (Fig. 1.4). However, in this methodology the presence of signalling unit in same system may interfere with actual detection process of anions as signalling unit can compete with the anions for non-covalent interactions.

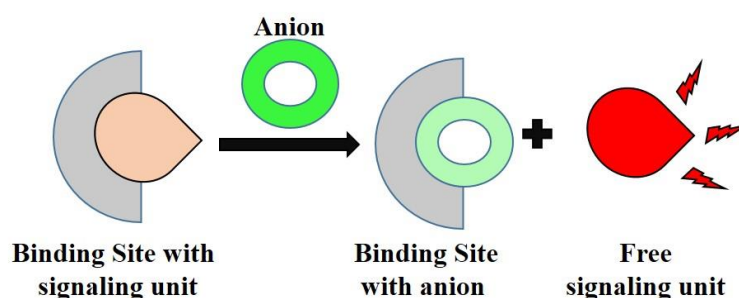


Fig. 1.4 Schematic representation of anion detection through substitution methodology

1.3.6 Reaction based methodology

In this methodology anion induced chemical reactions are used for the detection process of anions. This detection process does not contain any non-covalent interactions such as hydrogen bonding or coordination bonding. Therefore, strictly the term receptor cannot be used. Instead it can be called chemodosimeters. In this case the detection process of anions is irreversible as the resulting molecule is different from the starting molecule. Therefore, the photophysical properties of the final molecule should change which allows detection of anions. For example; silyl deprotection using fluoride ions. Fig 1.5 represents schematic representation of this methodology. Though, reaction based methodology is more selective towards anions,

it perhaps consumes more time. Therefore the detection process may not be instantaneous.

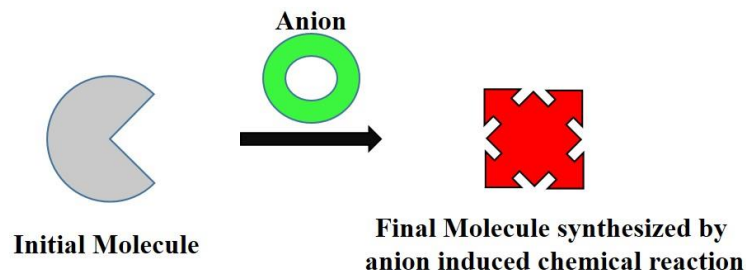


Fig. 1.5 Schematic representation of anion detection through reaction based methodology

1.3.7 Binding methodology

The receptors used in this methodology generally comprise of two parts namely a binding site and a signalling unit. These two parts attached together with covalent linker. Fig. 1.6 illustrates the detection process of anions via binding methodology. The incoming anion binds non-covalently (generally through hydrogen bonding) to binding site of the receptor. This binding of anion, modifies the photophysical properties of receptor which will be transformed to optical/visible changes by signalling units. Signalling unit generally consists of a chromophore which is responsible for the visible colour change in molecule upon binding of anion. The detection process involves non-covalent interaction and therefore this process is reversible.

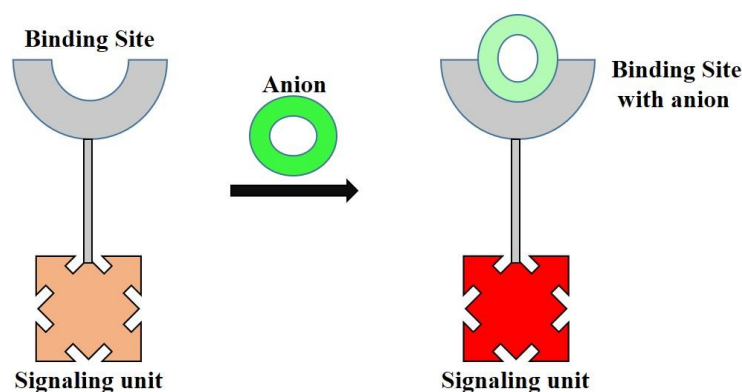


Fig. 1.6 Schematic representation of anion detection through binding methodology

Generally, in binding methodology of detection process the most common non-covalent interaction is hydrogen bonding as it is more directional compared to other non-covalent interactions. This directionality allows designing the receptors with unequivocal hydrogen bond arrangements so that it can discriminate anions of different geometries (Beer and Gale 2001). Based on this ideology, receptors with various hydrogen bond donors such as urea/thiourea (Li et al, 2010), amide (Dydio, 2011), pyrrole (Zielinski and Jurczak 2005; Bates et al. 2008), aminopyrrole (Gale, 2005), indole (Pfeffer et al. 2007; Caltagirone et al. 2008) and other chemical backbones (Duke et al, 2010) were reported (Fig. 1.7).

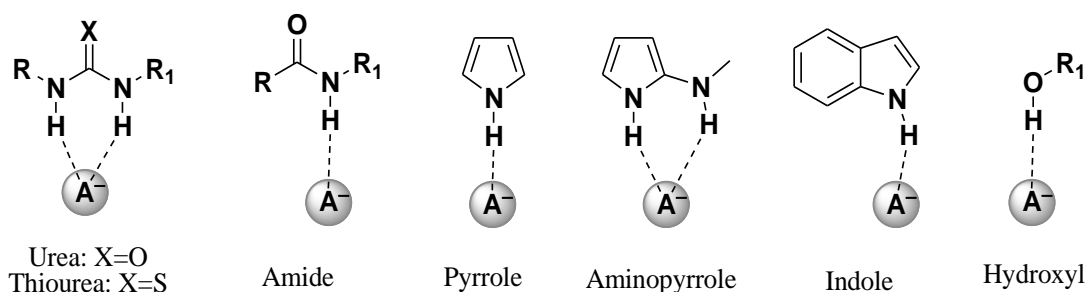


Fig. 1.7 Different hydrogen bond donors reported for the detection of anions

The detection ability of receptors with urea, thiourea, amide and pyrrole/imidazole/indole functional groups where $-NH$ acts as the binding site depends on the acidity of $-NH$ proton (Amendola et al 2006). However, this acidity can be tuned by inserting different electron withdrawing groups to molecular backbone. As acidity of $-NH$ increases, the hydrogen bond donor tendency of $-NH$ also increases and at extreme acidity the receptor experiences deprotonation. This deprotonation establishes various types of signalling mechanisms such as internal/intramolecular charge transfer-ICT (Duke et al, 2011), photoinduced electron transfer-PET (Gunnlaugsson et al, 2001) etc. This leads to the formation of charge transfer complexes. As a result significant colours change of the solution with a large bathochromic shift will be achieved and hence the naked eye detection of anion becomes feasible. Thus, the stability of charge transfer complexes directly depends on the acidic nature of $-NH$ proton (Park et al, 2011).

Applying the above said approaches, a number of colorimetric receptors for anion were designed and synthesised (Gale 2000; Gale 2001; Llinares et al. 2003;

Davis and Joos 2003; Martinez-Manez and Sanceno 2003; Moragues et al. 2011; Dydio et al. 2011). Majority of these reported receptors could be operational in non-competitive organic solvents for the detection of tetrabutylammonium fluoride (TBAF) and in absolute non-aqueous conditions. This is perhaps due to the higher acidity of water than that of protons which involved in binding process and hence the F^- ion readily gets solvated even with the trace amount of water. Though the receptors working in non-aqueous conditions for the detection of organic F^- ion source is important, the detection of inorganic fluoride such as sodium fluoride in aqueous conditions is of equal significance owing to its real-life applications.

Few receptors capable of detecting fluoride ion in aqueous solutions (organic/water mixture) have been reported. In addition, some researchers have reported unique receptors for the detection of inorganic fluorides which was used to develop test papers (Lin et al. 2006). Though these test papers requires several minutes for the detection process, the visual detection associated with it could be useful for the real life applications such as detection of inorganic fluoride in ground water. Recently, Das et al. (2011) designed and synthesized a receptor to show practical applicability by detecting inorganic fluoride ions in organic media and extracting them from ground water to organic solvent. Nevertheless, the design and synthesis of receptors with real-life applications, such as detection of inorganic fluoride in aqueous media is yet a daunting task.

Moving away from inorganic anion detection process, few research groups have developed selective receptors for the colorimetric detection of organic molecules. As a result of their efforts very few receptors for colorimetric discriminative detection of organic amines were reported (Rakow et al. 2005; Tang et al. 2010). As an addition, the researchers synthesised organic receptors using naphthalenediimide (NDI) which can discriminate the positional isomers of organic molecules by charge transfer (CT) mechanism (Trivedi et al. 2008, Trivedi et al. 2009). Among the widespread organic molecules the detection of dicarboxylates ions attains substantial prominence, due to the vital applications in the various metabolic and biological processes (Voet and Voet, 1995; Krueger et al., 2009; El-Sherif, 2010; Song et al. 2011; Xu and Liu, 2012). Considering this, few receptors have been

reported for the selective detection of dicarboxylates (Karl et al., 1995; Gunnlaugsson et al., 2002; Raker and Glass, 2002; Liu et al., 2005; Jadhav and Schmidtchen, 2006; Ghosh et al., 2010). However, amongst the dicarboxylates, the discrimination of geometrical isomeric dicarboxylates such as *cis/trans* isomers (Scheme 1.1; maleate and fumarate ions) gains significance because of their different biological behaviours. For example, fumarate is produced during Krebs cycle on the other hand maleate is used as Krebs cycle inhibitor (Gougoux et al., 1976; EiamOng et al., 1995).



Scheme 1.1 Example of *cis/trans* dicarboxylates

Owing to the similar chemical and physical properties, it is difficult to discriminate isomeric dicarboxylates with the conventional analytical methods. Nevertheless, this challenging task of discriminating geometrical isomeric dicarboxylates can be achieved with colorimetric/fluorometric detection approach, where the receptors selectively differentiate the isomers. Based on this strategy, few research groups recently reported receptors which can discriminate maleate ion and fumarate ion either colorimetrically or fluorometrically (Sancenon et al. 2003; Yen et al. 2006; Costero et al. 2006; Lin et al. 2007; Tseng et al. 2007; Lin et al. 2009). However, these receptors are complicated molecules which require skilled processes and tedious synthetic procedures for synthesis. Therefore, the development of new receptors for the discrimination of isomers such as maleate and fumarate are further need to be explored.

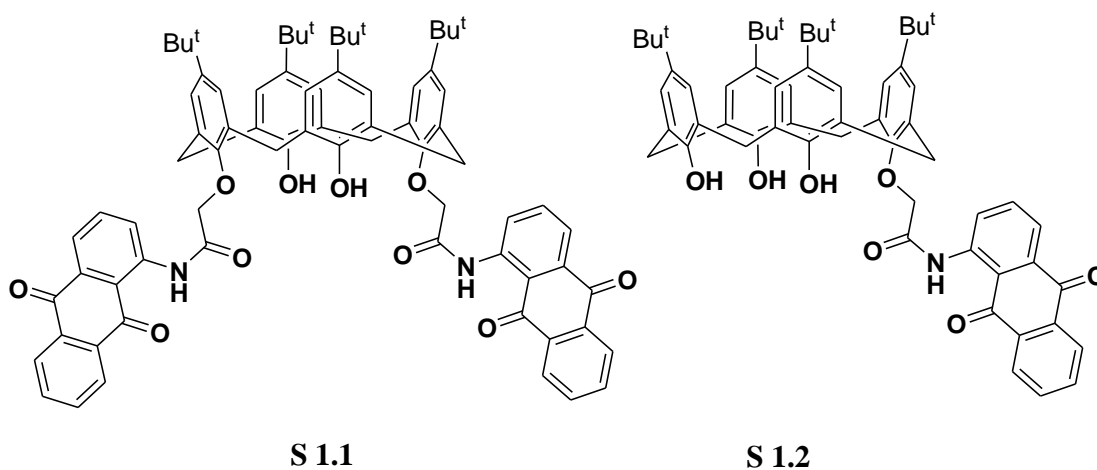
1.4 BRIEF LITERATURE REVIEW

The anion receptors with numerous binding sites based on amide, thioamide, sulfonamide, urea, thiourea, indole, pyrrole subunits are reporting in the literature from several years. However, the selective binding of anion is still a challenging task and needs to be explored further. To overcome the challenges and to understand the anion receptor chemistry in depth, a detailed literature review was carried out. Since

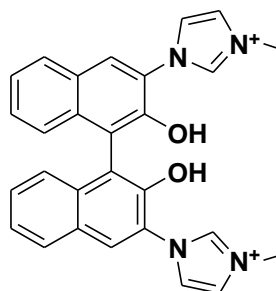
the current research is focussed on colorimetric and selective detection of anions, a brief literature survey relevant to present study has been discussed.

1.4.1 Literature on F⁻ ion detection

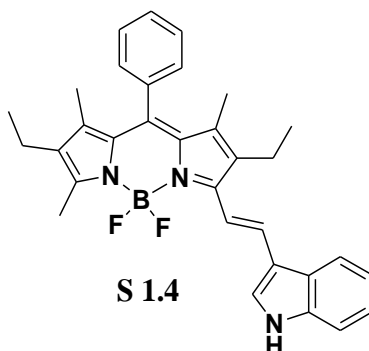
New fluorescent receptors **S 1.1** and **S 1.2** with amidoanthraquinone groups coupled to lower rim of *p-tert*-butylcalix[4]arene have been synthesized by Jung et al. (2009). The significant changes in the absorption and fluorescence bands confirm that these receptors are selective toward F⁻ over other anions such as Cl⁻, Br⁻, I⁻, AcO⁻, H₂PO₄⁻, HSO₄⁻ and OH⁻. The excited state intramolecular proton transfer (ESIPT) process of this receptor, inhibited by the F⁻ ion induces hydrogen bonding followed by deprotonation of -NH of the amidoanthraquinone and this is responsible for the detection process. The absorption and fluorescence variations upon adding F⁻ ion have been observed by naked-eyes as well as by optical responses. However, other anions were not induced any changes in optical responses.



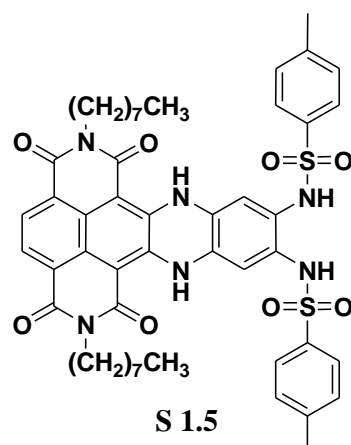
Lu et al. (2009) investigated the activity of imidazolium-functionalized binaphthol (BINOL) receptor **S 1.3**, towards the F⁻ ion. The molecule showed good colorimetric as well as fluorescent responses in presence of F⁻ ion. A brilliant yellow colour was established from colourless solution of receptor upon the addition of fluoride ions. The mechanism for the colour change involves initial deprotonation of hydroxyl groups which is followed by ESIPT in receptor-anion complex.

**S 1.3**

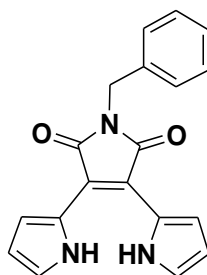
A Boron-dipyrromethene (BODIPY)–indole conjugated receptor **S 1.4** has been developed by Shiraishi and co-workers (2009). This receptor behaves as a colorimetric and fluorometric probe for selective detection of F^- . The F^- ion interacts with indole –NH of the receptor via a hydrogen bonding to form 1:1 receptor: F^- ion complex which resulted in a colour change from blue to green as well as quenching of orange fluorescence. The quenching of fluorescence perhaps due to the establishment of charge transferred excited state between receptor and F^- ion complex.

**S 1.4**

The synthesis and characterization of a highly fluorescent core-substituted naphthalene diimide receptor **S 1.5** containing a bis-sulfonamide group has been described by Bhosle and associates (2009). This receptor shows a unique selectivity and reactivity for the F^- ion over other anions in $CHCl_3$ by a two-stage deprotonation process which results in a colorimetric response. In DMSO solution, the receptor displays high selectivity for F^- ions ($K_a \sim 10^6 M^{-1}$) over other anions. The uses of this receptor in various sensing applications as well as in anion transport and purification have been discussed.



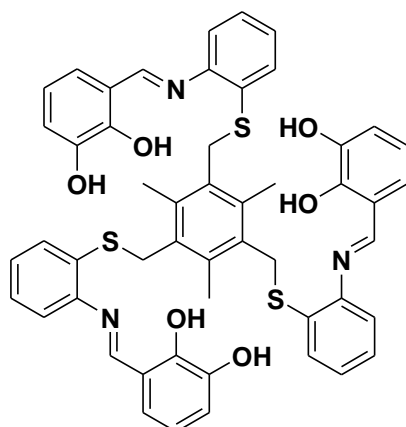
A class of disubstituted maleimide dye based receptor **S 1.6** with two symmetrical -NH binding sites has been synthesised by Lin et al. (2009). This receptor has been investigated for the colour change and fluorescence quenching effect on adding fluoride, cyanide, and dihydrogen phosphate anions. The intense red emission displayed apparent solvatochromic shift which indicates a strong charge transfer character of the receptor. It has been found that the interactions between receptor and anions were variable depending on the amine substituents at C (3, 4) of the maleimides. The -NH protons get deprotonated on addition of more basic anions such as fluoride or cyanide in the receptor with two pyrrolyl binding sites. The formation of a chelate with H_2PO_4^- through hydrogen bonds has been observed for the receptors with two indolyl binding sites. The theoretical estimation using B3LYP/6-31G supported the formation of 1:1 complexes between receptor and anion.



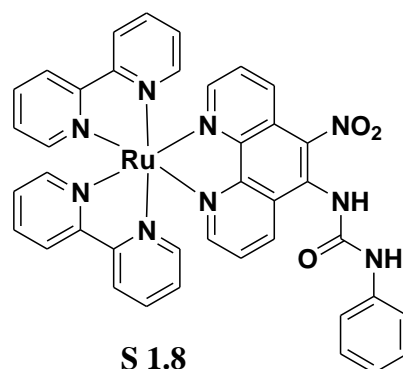
S 1.6

A neutral tripodal Schiff base receptor **S 1.7** with catechol as end groups was synthesized and characterized by Bhardwaj and co-workers (2009). The receptor serves as a visually detectable optical receptor for F^- ions in DMSO and is sensitive enough to recognize the F^- ions up to a concentration of 1×10^{-5} M with naked eye.

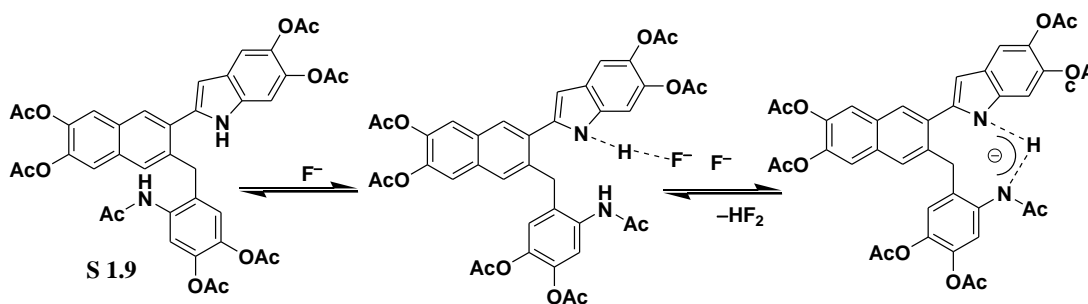
The colorimetric response is based on deprotonation of the highly acidic catechol moieties in the receptor on adding highly basic F^- ions in a polar solvent like DMSO. This receptor has been designed to provide anion recognition through hydrogen bonding interactions employing $-OH$ groups of catechol. However, the results showed the deprotonation rather than the hydrogen bonding which was the key factor to trigger colorimetric change. This deprotonation is facilitated by the high acidity of catechol groups and high basicity F^- ions in polar solvent like DMSO. The researchers compared the sensing ability of tripodal receptor with monopodal receptor and proved that the tripodal receptor provides much enhanced response towards the F^- ion.

**S 1.7**

A new receptor **S 1.8** based on ruthenium(II)-polypyridyl complex having a urea functionality as a binding site for anions has been synthesized by Ghosh et al. (2009). The binding affinity of this receptor towards various oxy anions and halides has been studied. The complex was found to be selective colorimetric receptor only for F^- among halides and for $AcO^-/H_2PO_4^-$ among oxy anions. The relative binding affinity of different anions towards this receptor was tested with the help of quantum chemical calculations. Surprisingly, this complex is also acts as a colorimetric receptor for neutral molecules like DMSO and DMF with the weaker binding compared to anions. The relative acidity of two $-NH$ atoms of urea functional group was compared with that of one from the related complex by using pKa calculations. These calculations revealed that the $-NH$ proton closer to the phenanthroline moiety is more acidic than that of the $-NH$ hydrogen closer to the phenyl group in the complex.

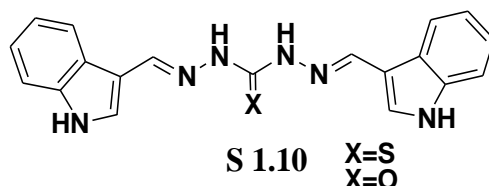


The indole based receptor **S 1.9** was designed and synthesized by Panzella et al. (2009). The molecule was found to be a fluorometric receptor for F^- ion in organic media. This F^- ion sensing receptor was obtained by a variant of the classic acid promoted trimerization of indoles. The mild one-pot conversion of 5,6-dihydroxyindole to receptor S 1.9 provides an expedient and practical access route to the 2-(2-amidobenzyl)-3-(indol-3-yl)quinoline system. This fluorescent F^- ion sensing receptor was operated in the turn-on mode. The mechanism involves initial hydrogen bond formation between indole $-NH$ and F^- ions, which is followed by deprotonation.

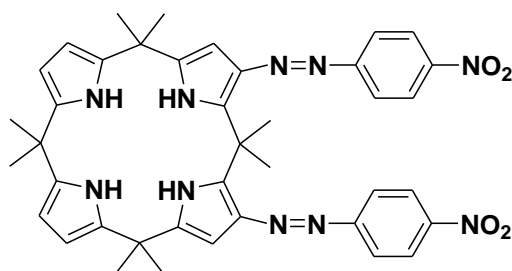


Bose and Ghosh (2010) synthesized receptor **S 1.10** consisting indole unit conjugated with thiourea/urea functional group. These receptors exhibited selective binding properties towards the F^- ion which results in colorimetric change in the organic media. Furthermore, the thiourea and urea derivatives show intense colour change in presence of F^- along with an absorption maxima at 936 nm and 904 nm (near IR region) respectively. The receptor has three types of acidic protons, *viz.* thiourea/urea $-NH$, imine $-CH$ and indole $-NH$ that can bind anion and based on the basicity and equiv. of the anion, multiple acidic protons could be deprotonated.

Owing to this multiple deprotonation, the receptor shows absorption spectra with NIR signature. Thus, the receptor could be useful to avoid the interference from endogenous chromophores and thus, would be more beneficial in biological systems.

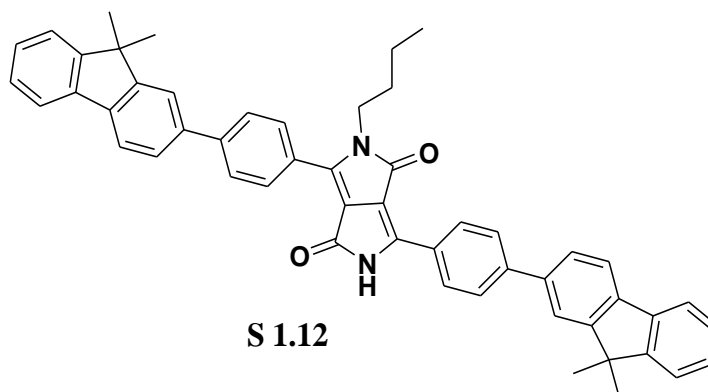


A receptor **S 1.11** based on octamethyl calix[4]pyrrole substituted with azo derivative has been prepared and studied as potential anion receptors for, F^- , AcO^- and $H_2PO_4^-$ ions by Garg and co-workers (2010). This receptor not only allows the colorimetric detection but also helps to discriminate the geometrically different anions. The selectivity trends in the binding affinities of the receptor was studied by the researches for anions in DMSO and found to be $F^- > AcO^- > H_2PO_4^- > HSO_4^- > Cl^-$. This binding order was rationalized based on guest basicity.

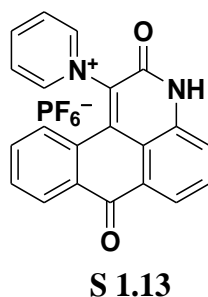


S 1.11

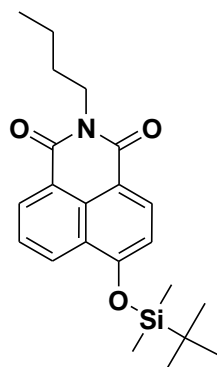
New diketopyrrolopyrrole (DPP) based receptor **S 1.12** was designed and synthesized by Qu and associates (2010). It was found to be a very good colorimetric and ratiometric red fluorescent sensors for F^- ions with high sensitivity and selectivity. The recognition mechanism follows the intermolecular proton transfer between a hydrogen atom on the lactam N positions of the diketopyrrolopyrrole moiety and the fluoride anion. The receptor displays orange-to-red absorption colour change and yellow-to-red emission colour change upon adding F^- ions in DCM due to deprotonation. Upon adding fluoride, the ICT transition enhances from the amide anion to the electron-withdrawing moiety, which is facilitated by the deprotonation of the amide moiety.



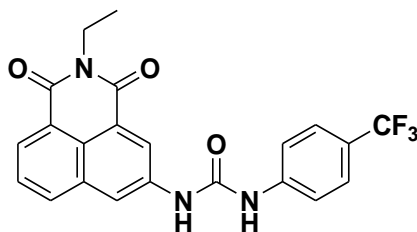
Receptor **S 1.13** bearing pyridinium unit conjugated to anthrapyridone moiety has been developed by Luxami et al. (2010). It opens double channel in absorbance at 490nm (orange) between 5 μ M and 75 μ M of F⁻ ions and at 630 nm (green) between 75 μ M and 600 μ M of F⁻ ions. The fluoride ions induced fluorescence enhancement (>25 times) in this receptor at 510 nm enables selective estimation of 0.5 μ M–5 μ M fluoride ions which is much less than the desirable concentration range for the maximum contaminant level of fluoride ions in drinking water. More importantly the presence of hydroxide ion which is a common interfering anion in hydrogen bonding based F⁻ ion receptors; do not interfere in the estimation of fluoride ions.



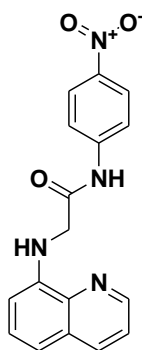
Ren et al. (2011) synthesised 4-substituted 1,8-naphthalimide derivatives (**S 1.14**) which on addition of F⁻ in CH₃CN solution showed transition from colourless to yellow along with the prominent change in UV-vis spectra. The molecule found to be a very good selective sensor for fluoride ion detection. The selectivity is due to the cleavage of Si-O bond in the molecule by fluoride which leads to bathochromic shift in absorption maxima by 112 nm. The detection limit was calculated to be 0.59 mM.

**S 1.14**

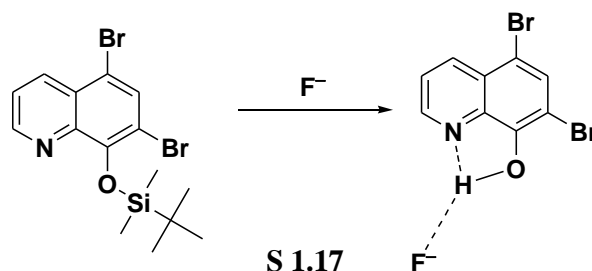
Duke et al. (2011) reported 3-urea-1,8-naphthalinimide derivatives (**S 1.15**) as highly fluoride selective colorimetric sensors. The receptors based on 1,8-naphthalimide with substitution at 3-position of naphthalimide ring has been used to incorporate the anion recognition moiety. The molecule shows significant change in both absorption and emission spectra which red shifted upon interacting with fluoride ion in DMSO.

**S 1.15**

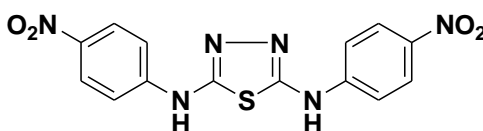
Park et al. (2011) synthesised a quinoline derivative (**S 1.16**) which is coupled to 4-nitroaniline with an amide linkage. The receptor utilizes amide N–H and amine N–H, to bind anions through hydrogen bonds. In addition, the receptor acts as an efficient naked eye detector for fluoride and pyrophosphate.

**S 1.16**

Bao et al. (2011) reported 8-hydroxy quinoline derivatives (**S 1.17**) which showed ratiometric fluorescent chemosensing property towards fluoride ions. The fluorescent property of the molecule is due to the combination of desilylation and excited state proton transfer from the desilylation product to fluoride ion. The sensor showed rapid response and excellent selectivity towards fluoride ion.

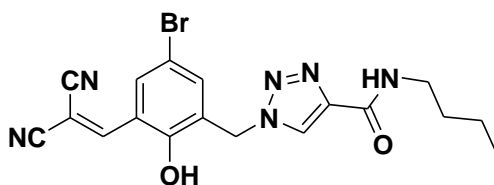


A neutral acyclic receptor **S 1.18** containing –NH binding sites with a thiadiazole spacer has been developed by Basu and Das (2012). This receptor has been extensively studied for halide ions binding both in solution state as well as in solid state. The receptor forms 1:1 hydrogen bonded complex with fluoride ion. On the other hand, in case of chloride and bromide, the receptor binds to two halide anions along with formation of a halide bridged 1D polymeric chain network. The receptor behaves as an efficient colorimetric sensor for fluoride ions by displaying optical changes on adding excess of fluoride ions. Furthermore, the incremental addition of fluoride ions leads to the formation of hydrogen bonded complex formation and subsequently the stepwise deprotonation of –NH groups. This stepwise mechanism could be visually monitored by a stepwise colour change, initially from yellow to pink at lower concentration and from pink to blue at higher concentration of anions.

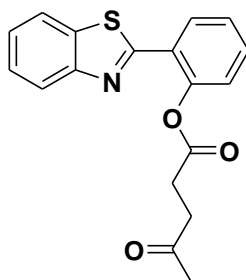


Xu et al (2012) synthesised a triazole containing receptor **S 1.19** which is combined with different types of hydrogen bond donors such as OH, NH and CH groups. The receptor shows colorimetric and fluorescent responses only in presence of

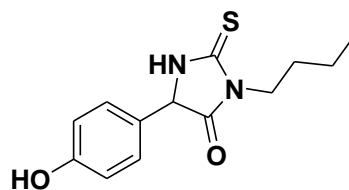
fluoride. On the other hand the receptor shows evident ^1H NMR response to both fluoride and sulphate by the free rotation of the sub methyl group.

**S 1.19**

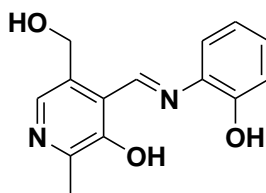
The levulinate ester of 2-(benzothiazol-2-yl)phenol, **S 1.20**, has been developed by Chen and co-workers (2012). This was found to be a ratiometric fluorescent probe for identifying and quantitating sulphite anions. The mechanism of detection is based on the sulphite triggered cleavage of the levulinate functionality to give 2-(benzothiazol-2-yl)phenol, which upon excitation at 310 nm, decays to its ground state via ESIPT.

**S 1.20**

Yong et al (2013) synthesised a chemosensor **S 1.21**, based on 2-thiohydantoin which showed high selectivity for the fluoride ions over other anions. The receptor follows two step binding process, initially with hydroxyl functionality of the receptor followed by the involvement of -NH unit at higher concentration. This results in two step colour change, initially from colourless to yellow upon adding fluoride ions (0-3 equiv.) and in second step the colour changed from yellow to purple (3 to 6 equiv.). The receptor was further used to develop a test paper to detect the fluoride ions in solid state wherein it showed the detection limit as low as 1.9 ppm.

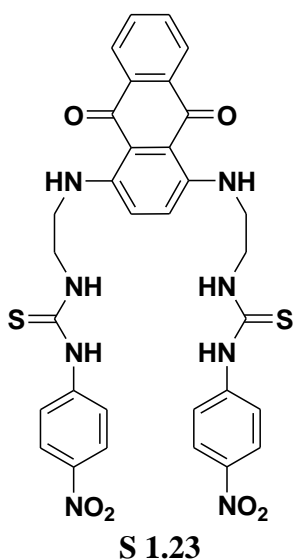
**S 1.21**

Sharma et al. (2013) synthesized a receptor **S 1.22**, by combining vitamin B₆ cofactor pyridoxal with 2-aminophenol. The receptor displays a colour change from yellow to red in the presence of fluoride and acetate owing to the formation of a polymeric complex in 1:1 stoichiometry through multiple hydrogen bonding. This polymeric complex formation locks C=N bond of the receptor to prevent its rapid isomerisation which results in the 'turn-on' of fluorescence only in presence of fluoride ions. The detection limit of this receptor was found to be 7.39×10^{-8} M.

**S 1.22**

1.4.2 Literatures on carboxylate ion detection

Tseng et al. in 2007, designed organic receptor (**S 1.23**) for the discriminative detection of isomeric dicarboxylates such as maleate ions over fumarate ions. Upon addition of maleate ions to receptor in DMSO, the receptor showed a significant colour change from dark-blue to dark-red, which can be distinguishable by naked eye. This prominent colour changes perhaps due to the deprotonation of the thiourea moiety of the 4-nitronaphthyl chromophore. However, upon addition of fumarate ion to the same receptor, colour of the receptor solution changed from dark-blue to bright yellow. Thus, these receptors are very good optical chemosensors for selective recognition of maleate ion over fumarate ion.



The colour change observed is owing to the formation of a stable complex between maleate ion and the receptor. The receptor is designed in such a way that during complexation the maleate ion with its *cis* conformation exactly fits in the molecule (Fig. 1.8). On the other hand, fumarate ion has *trans* conformation and hence it weakly binds to the receptor which results in the weak colour change.

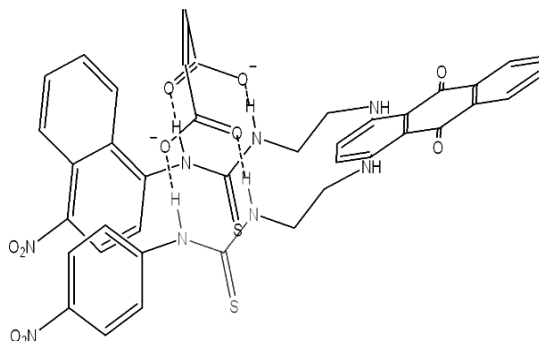
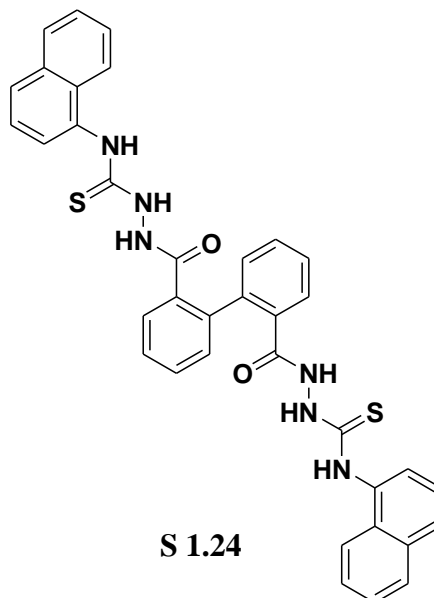


Fig. 1.8 Possible binding model of receptor with maleate ion

A Thiourea based molecular clip has been synthesised by Lin et al. (2007), which could fluorometrically discriminate isomeric dicarboxylates. The receptor (**S 1.24**) comprises two thiourea-based binding groups and two naphthalene units as fluorophores, which acts as a fluorescent chemosensor to distinguish *o*-phthalate from two other isomers of it. Upon the addition of *o*-phthalate, the emission intensity at 420 nm decreases drastically through Photoinduced Electron Transfer (PET) and when the system excited at 380 nm, a new emission band at 460 nm gradually develops upon

the addition of the *o*-phthalate ion. However, no such observation was observed with the addition of other two isomers.



It has been depicted that the clipping behaviour is responsible for the fluorometric change of receptor. Upon addition of *o*-phthalate ion the receptor attains twisted conformation and the naphthyl rings positions close enough to exhibit new emission (Fig. 1.9).

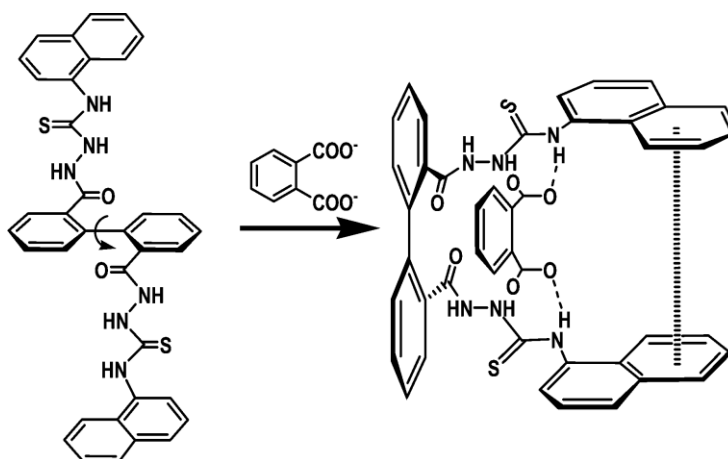
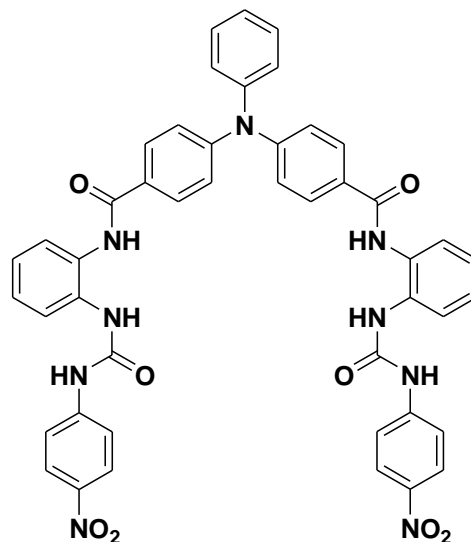


Fig. 1.9 Proposed binding of *o*-phthalate to the receptor

A new triphenylamine-based receptor (**S 1.25**) for the recognition of aliphatic dicarboxylates with varying chain lengths was synthesised by Ghosh et al (2010). The receptor has been designed in such a way that it can utilize the amide–urea conjugate

system for binding dicarboxylates. The receptor was found to bind the dicarboxylates under a semi rigid, propeller shaped, fluorescent triphenylamine spacer.



S 1.25

The binding strength of receptor was increased along with the chain length of dicarboxylates. The binding of these dicarboxylates were achieved via hydrogen bonding and shown in the Fig. 1.10.

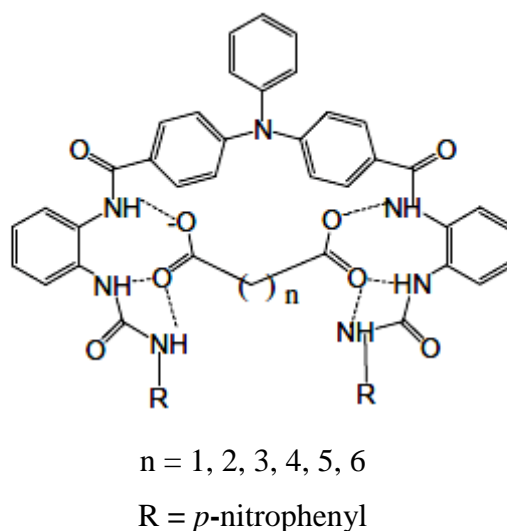
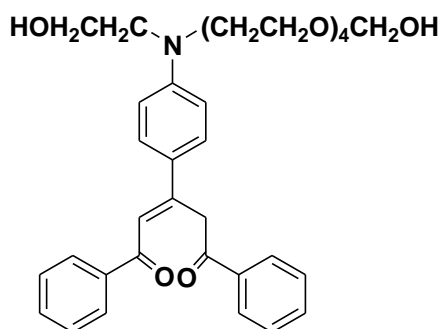


Fig. 1.10 Proposed hydrogen bonding structure of receptor with dicarboxylates

Sancenon et al. (2003) designed and synthesised a receptor based on 1,3,5-triarylpent-2-en-1,5-diones (**S 1.26**) which colorimetrically detects the dicarboxylates. The receptor also discriminates isomeric dicarboxylates ions such as maleate ion and

fumarate ion. The receptors are capable of selective discrimination between *cis/trans* dicarboxylates and *ortho/meta/para* dicarboxylates in water/organic solvent mixtures at nearly neutral pH values.



S 1.26

The recognition process, involves cyclization of 1,3,5-triaryl-2-en-1,5-diones (Fig. 1.11) upon adding the carboxylates with *cis* conformation and has proved to be very sensitive towards these ions. The literature gains the great attention of scientific community due to its shape-induced cyclization which leads to the colorimetric recognition of certain organic isomers.

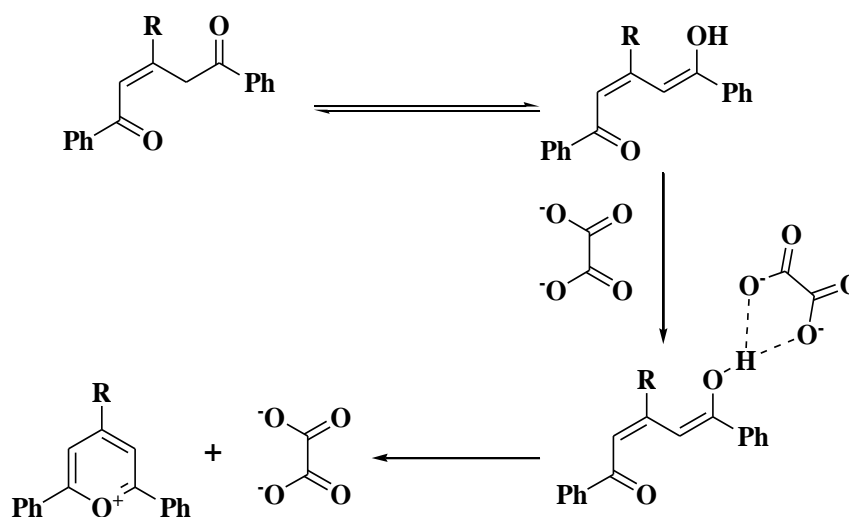


Fig. 1.11 Mechanism for the detection of carboxylate ions

1.5 SCOPE OF THE WORK

The detection of F^- ions has gained prime significance among environmental science, biomedical research and in chemical logics in recent years owing to its dual functionality. Consumption of fluoride in controlled quantities is beneficial to human

health as it prevents dental decay and it is used in clinical applications such as in the treatment of osteoporosis. However, excessive intake of fluoride can cause dental and skeletal fluorosis which is a concerning problem in India and various developing countries around the world. From the literature survey it can be concluded that the design and synthesis of receptors for fluoride ion is well established area in the field of supramolecular chemistry. However, these investigations have some shortcomings which includes,

- ❖ Majority of the receptors involve complicated molecules which require complicated organic synthesis. Therefore, these receptors are not much cost effective and environmental friendly
- ❖ Majority of them are based on the fluorometric detection, which requires the help of complicated instruments for the detection process
- ❖ Detection of fluoride at ppm level still needs to be explored
- ❖ Though the receptor which works only with noncompeting organic media is important, for the real-life application the receptors should work in aqueous media. Thus, along with the organic media, the receptors which are capable of detecting inorganic fluoride ion source in aqueous media gain more significance

The organic anions plays vital role in the numerous metabolic processes such as glyoxalate cycle, generation of high energy phosphate bonds and in dicarboxylate cycle for autotrophic carbon dioxide (CO₂) fixation. Therefore the detection of organic anions for instance dicarboxylate ions gain more prominence along with the inorganic anions. Along with the dicarboxylates, the detection/discrimination of isomeric dicarboxylates (such as *cis/trans* isomers) is a field of interest because these isomers behave differently in biological systems. Owing to the similar physical properties, the discrimination of these isomeric anions is difficult task using conventional analytical methods. Though the discrimination of these geometrical isomeric dicarboxylates was achieved with colorimetric/fluorometric detection approach, the receptors used are complicated organic molecules which require skilled processes and difficult synthetic procedures for synthesis. Therefore, the development

of new 'easy to synthesis' receptors for the discrimination of geometrical isomers such as maleate and fumarate are still a challenging task which need to be focussed.

1.6 OBJECTIVES OF THE CURRENT WORK

Looking at the scope in the field of anion receptor chemistry, the current research concentrated on following objectives,

- ❖ To synthesize simple organic receptors for the colorimetric detection of fluoride ions and for the discriminative detection of dicarboxylate isomers namely, maleate ion and fumarate
- ❖ To synthesize simple organic receptors for the detection of fluoride ions in the aqueous media
- ❖ To evaluate the real life applications of receptors such as detection of fluoride ions in commercial mouth wash and sea water, extraction of fluoride from aqueous fluoride ion solution and from sea water and solvatochromism
- ❖ To quantify the amount of fluoride present in the commercial mouth wash and sea water using receptors
- ❖ To characterize the receptors by ^1H NMR, FT-IR, elemental analysis and ESI-MS
- ❖ Single Crystal X-Ray diffraction (SCXRD) studies of selected receptors for three-dimensional structural elucidation
- ❖ To investigate the shift in absorption maxima (λ_{max}) before and after complexation of anions with receptors, using UV-vis spectroscopy
- ❖ To determine receptor to anion complexation ratio either with Job's Plot method or with Benesi-Hildebrand method
- ❖ To calculate the binding constant for the receptor-anion complex using Benesi-Hildebrand equation
- ❖ To study the quantitative analysis of anion complexation with receptor molecule using UV-vis titration
- ❖ To study the effect of anion binding with the receptor using ^1H NMR titration

Conclusively, the current research work concentrated on design and syntheses of new, simple organic molecules for the molecular recognition of anions. Further, the practical applications of these molecules were studied. Therefore, in the present work six series of receptors were designed and synthesised for the molecular recognition of anions. The **Chapter 2** deals synthesis of 1-naphthohydrazide based receptors for the colorimetric detection of fluoride ions in organic media. Further, the detection of inorganic fluoride ions in organo-aqueous media owing to deprotonation of base labile hydroxyl functionality was deployed. **Chapter 3** describes syntheses and characterization of new benzohydrazide based colorimetric receptors for the expeditious detection of inorganic fluoride ions such as NaF. The colorimetric anion sensing properties, detection mechanism were explored and the real-life applications of these receptors have been demonstrated by detecting fluoride ions in commercial mouthwash as well as in sea water. In **Chapter 4**, syntheses of new aminophenol based colorimetric receptors for fluoride ion detection have been discussed. The colorimetric anion sensing properties, detection mechanism, solvatochromic effect and logic gate application of these receptors have been studied in detail. **Chapter 5** comprises syntheses of new aminophenol Schiff's base derivatives for discriminative detection of maleate ions over fumarate. In addition, the receptors were studied for colorimetric detection of other biologically important anions such as fluoride. **Chapter 6** encompasses syntheses of new benzohydrazide based receptors. The detailed studies about discrimination of maleate ions over fumarate ions using these receptors have been discussed. The colorimetric detection of fluoride ions and concentration dependency of the receptors were incorporated. **Chapter 7** encloses design and syntheses of receptors based on triphenylphosphonium salts with active methylene group which acts as binding site. The selectivity of the receptors towards fluoride ions has been discussed in detail. The real-life applicability of these receptors has been examined by extracting fluoride ions from aqueous solutions and sea water. Towards the end, **Chapter 8** summarizes the conclusion and outcome of the present research work.

CHAPTER 2

***DESIGN AND SYNTHESIS OF 1-NAPHTHOHYDRAZIDE
BASED RECEPTORS AND THEIR APPLICATION AS
FLUORIDE ION RECEPTORS***

*This chapter comprises the synthesis of 1-naphthohydrazide based receptors for the colorimetric detection of fluoride ions. The receptor **SIR1** found to be useful for the detection of fluoride ions in absolute organic media and on the other hand receptor **SIR2** was able to detect the inorganic fluoride ions in organo-aqueous media.*

2.1 INTRODUCTION

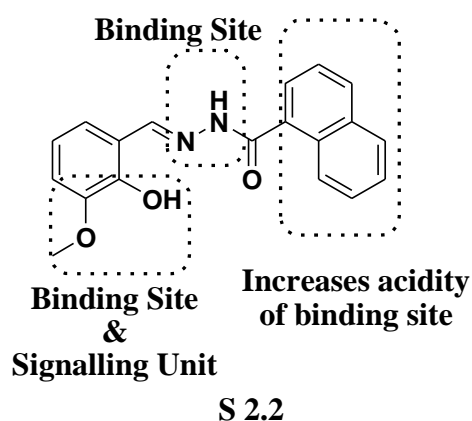
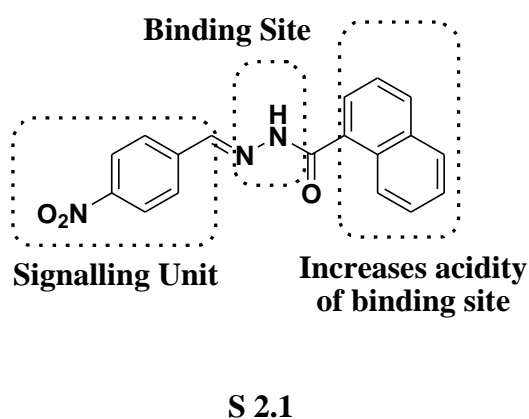
Conventional fluoride ion detection using electrode is costly, time consuming and requires complicated instrumentation with confusing handling procedures (Frant and Ross 1966). On the other hand, colorimetric receptors appear to be attractive because of their simplicity, high sensitivity, high selectivity and real-time ‘naked eye’ detection. This colorimetric detection of fluoride could be achieved by designing a host molecule where the binding of anion can change the colour of host molecule. Based on this strategy, a number of receptors have been reported for the selective binding of fluoride (Gale et al. 2008; Li et al 2010; Dydio et al. 2011; Santos-Figueroa et al. 2013). The well-known functional groups such as urea/thiourea, amides, pyrrole and imidazolium are proved themselves as effective binding sites for the fluoride ion through the formation of a hydrogen bond with N–H unit of these functional groups (Piatek and Jurczak 2002; Kang et al. 2003; Nie et al. 2004; Xu and Tarr 2004; Zhang et al. 2004; Liu and Tian, 2005; Shang, et al. 2007; Danil de Namor et al. 2007; Yang et al. 2008; Aydogan et al. 2008; Cametti and Rissanen 2009; Bose and Ghosh 2010; Li et al. 2013). Silyl group deprotection based colorimetric receptors for fluoride ions were also studied in various literatures (Rao et al. 2010; Buckland et al. 2011; Bao et al. 2011; Lu et al. 2011). The affinity of a boron atom toward fluoride ions were well utilized for the detection of fluoride ions (Dusemund et al. 1995; Cooper et al. 1998; Chiu and Gabbai 2006; Lee et al. 2007; Galbraith et al 2008; Hudnall et al. 2008; Kim and Gabbai 2009; Guliyev et al. 2012). Unfortunately, majority of them are capable of detecting fluoride ions only in absolute non-aqueous conditions and to detect the organic fluoride sources such as tetrabutylammonium fluoride (TBAF). Therefore these receptors cannot be used for the real-life applications. Alternatively, if the receptor could detect inorganic fluorides such as

sodium fluoride in aqueous media which is a real source of environmental pollutant, then it could be useful for the real-life application.

The detection ability, selectivity and sensitivity of a receptor depend on the acidity of protons where the F^- ions bind (Amendola et al. 2006). If the acidity of these protons is lesser than that of water then the F^- ions get solvated. Hence, contamination of receptor even with trace amount of water could result in the failure of colorimetric detection process. However, this drawback can be resolved to some extent by designing a receptor where the F^- ion binding protons are more acidic than water or by incorporating a base labile group such as hydroxyl (-OH) functionality, which can readily deprotonated with the basic ions such as F^- ion (Li et al. 2009; Bharadwaj et al. 2009).

Few receptors which are capable of detecting fluoride ions in organo-aqueous solvent mixture were reported recently. Unfortunately, majority of them are limited to organic fluoride source such as TBAF (Zhang et al. 2009; Mahapatra et al. 2010; Sokkalingam and Lee 2011) or to make test papers, which is not instantaneous towards detection process (Lin et al. 2006a; Lin et al 2006b). On the other hand, there are few reports which showed admirable results such as detection of inorganic fluoride ions in aqueous media (Gunnlaugsson et al. 2005) and removal of inorganic fluoride ions by extracting them to organic media (Das et al. 2011). Nevertheless, the synthesis of receptors for the practical or real-life applications still persist as the detection of fluoride ions in 'water-only' conditions are hard to achieve.

Keeping this in mind, efforts have been made to design new receptors based on 1-naphthohydrazide Schiff's base.



The receptors **S1R1** (S 2.1) and **S1R2** (S 2.2) comprises of –NH which acts as binding site for F⁻ ions. The presence of carbonyl group adjacent to –NH group increases the acidity of corresponding proton and thus, increases the sensitivity of the receptor. The presence of imine linkage in the receptors provides extended conjugation and hence increases the colorimetric sensitivity towards fluoride ion. The receptor **S1R2** encompasses base labile hydroxyl (-OH) functional group and therefore it enable the detection of F⁻ ion in the form of NaF in organo-aqueous mixture (ACN:H₂O 9:1 ratio). The receptor **S1R3** was designed and synthesised to depict the role of aromatic substitution (which acts as signalling unit) to 1-naphthohydrazide backbone.

2.2 EXPERIMENTAL

2.2.1 Materials and methods

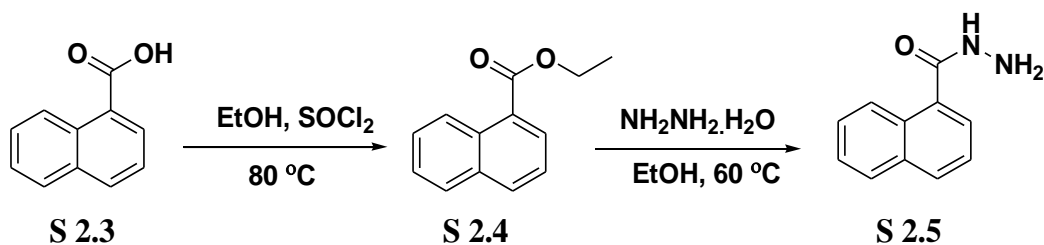
All chemicals were purchased from Sigma-Aldrich, Alfa Aesar or from Spectrochem and used without further purification. All solvents were procured from SD Fine, India with High-performance liquid chromatography (HPLC) grade and used without further distillation.

The proton nuclear magnetic resonance (¹H NMR) spectra were recorded on a Bruker, Avance II (500 MHz) instrument using tetramethylsilane (TMS) as internal reference and deuterated Dimethyl sulphoxide (DMSO-*d*₆) as solvent. The raw free induction decay (FID) data was processed with MestReNova 7.0.0-8331 software. Resonance multiplicities are described as s (singlet), br s (broad singlet), d (doublet), t (triplet), q (quartet) and m (multiplet). The chemical shifts (δ) are reported in parts per million (ppm) and coupling constant (*J*) values are given in Hz. Melting points were determined with Stuart- SMP3 melting-point apparatus in open capillaries and are uncorrected. Infrared (IR) spectra were recorded on a Thermo Nicolet Avatar-330 FT-IR spectrometer; signal designations: s (strong), m (medium), w (weak), br.m (broad medium) and br.w (broad weak). Mass spectra were recorded on Waters Micromass Q-ToF micro spectrometer with Electrospray Ionization (ESI) source. The single-crystal X-ray diffraction (SCXRD) was performed on Bruker AXS APEX II system. UV-vis spectroscopy was carried out with Ocean Optics SD2000-Fibre Optics Spectrometer and Analytikjena Specord S600 Spectrometer in standard 3.5 mL quartz

cells (2 optical windows) with 10 mm path length. Elemental analyses were done using Flash EA1112 CHNS analyser (Thermo Electron Corporation). All reactions were monitored by thin layer chromatography (TLC) on pre-coated silica gel 60 F₂₅₄ plates which were procured from Merck.

2.2.2 Synthesis of intermediate S 2.5

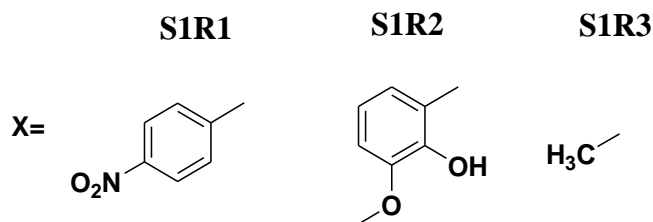
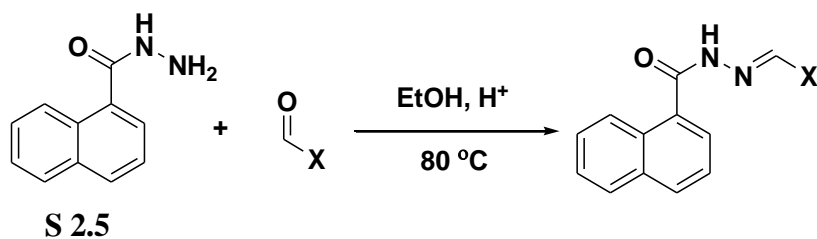
A solution of 1-naphthoic acid **S 2.3** (5.8 mmol) in ethanol taken in round bottom (RB) flask and thionylchloride (6.4 mmol) was added. The reaction was catalysed by a drop of dimethylformamide (DMF). The reaction mixture was refluxed for 4 h. Completion of the reaction was confirmed by thin layer chromatography. Excess of ethanol from the reaction mixture was removed by evaporation, diluted with dichloromethane and washed with water. Organic layer was separated, dried over anhydrous Na₂SO₄ and the solvent was evaporated to yield corresponding ester (**S 2.4**). Thus obtained ester **S 2.4** (5.75 mmol) was treated with hydrazine hydrate (28.75 mmol) in ethanol and heated to 60°C for 2.5 h. The reaction mixture was cooled below 5 °C. The solid formed was filtered and dried to yield pale yellow coloured solid intermediate **S 2.5** (Scheme 2.1).



Scheme 2.1 Synthesis of intermediate S 2.5

2.2.3 Synthesis of receptors S1R1, S1R2 and S1R3

A mixture of aldehyde (2.69 mmol) and 1-naphthohydrazide **S 2.5** (2.69 mmol) reacted in RB flask using ethanol as solvent under reflux condition for 5h. The reaction was catalysed by a drop of acetic acid. After cooling, the formed solid was filtered and washed with ethanol to obtain the target compounds (**S1R1**, **S1R2** and **S1R3**, Scheme 2.2).



Scheme 2.2 Synthesis of the receptors **S1R1**, **S1R2** and **S1R3**

The single crystal of the receptors **S1R2** suitable for X-ray diffraction analysis was obtained by slow evaporation of methanol-chloroform (1:1) solution at room temperature. The ORTEP diagram (50% probability) of the receptor **S1R2** is given in Fig. 2.1. The receptor **S1R2** was crystallised in orthorhombic lattice. The detailed crystallographic data of receptor **S1R2** is given in the Table 2.1.

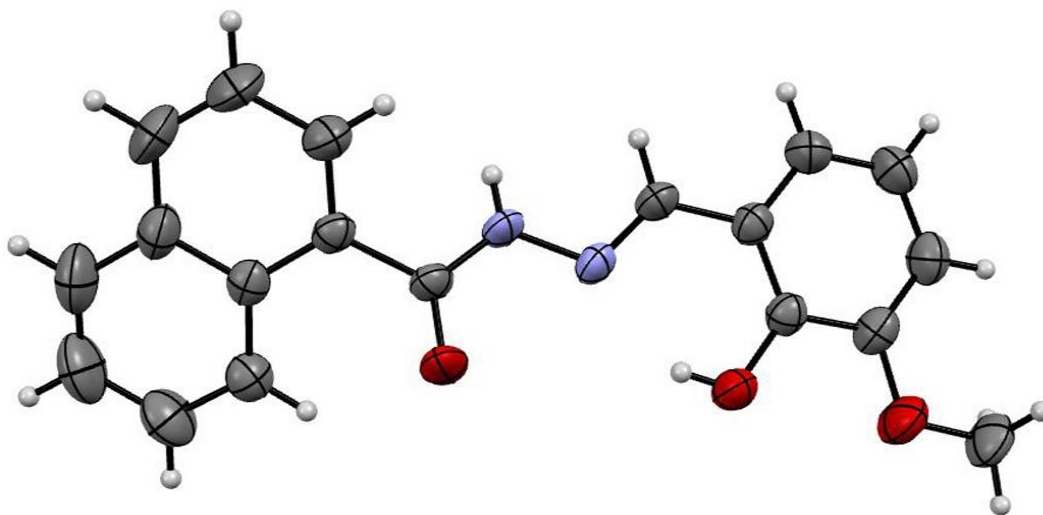


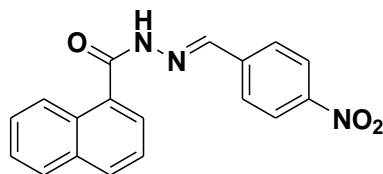
Fig. 2.1 ORTEP diagram (50% probability) of receptor **S1R2**

Table 2.1 Crystallographic data of receptor **S1R2**

Receptor	S1R2
CCDC No.	938645
Chemical formula	C ₁₉ H ₁₆ N ₂ O ₃
Formula weight	320.34
Crystal System	Orthorhombic
Space group	P b c a
a (Å)	13.8637(14)
b (Å)	8.5605(9)
c (Å)	27.679(3)
α (°)	90.00
β (°)	90.00
γ (°)	90.00
V (Å) ³	3284.9(6)
Z	8
Crystal size	0.49 × 0.45 × 0.39
F (000)	1344
R-factor (%)	4.3

All compounds and receptors were characterized by spectral analysis. The characterization data has been compiled and given below.

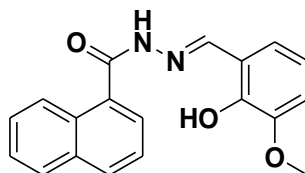
(E)-N'-(4-nitrobenzylidene)-1-naphthohydrazide (S1R1).



Yield: 92%; m.p.: 313 – 314 °C. Elemental analysis Calculated for C₁₈H₁₃N₃O₃ (%): C 67.71, H 4.10, N 13.16, Experimental: C 67.53, H 4.23, N 13.24. ¹H NMR (DMSO-*d*₆): δ 12.34 (s, 1H, NH), δ 8.45 (s, 1H, -CH), δ 8.34 (d, 2H, ArH, *J* = 8.5 Hz), δ 8.24 (d, 1H, ArH, *J* = 7.5 Hz), δ 8.14 (d, 1H, ArH, *J* = 8.0 Hz), δ 8.04 (d, 2H, ArH, *J* = 8.0 Hz), δ 7.80 (d, 1H, ArH, *J* = 7.0 Hz), δ 7.63 (d, 3H, ArH, *J* = 6.0

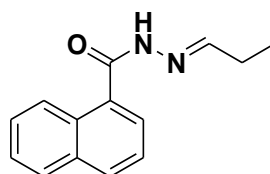
Hz). FT-IR in cm^{-1} : 3163.5 (br.w), 3005.7 (br.m), 2842.0 (br.w), 1640.7 (s), 1556.6 (m), 1509.9 (s), 1334.6 (s), 1293.0 (s), 1254.1 (m), 1201.1 (m), 1143.8 (w), 1075.1 (w), 1027.5 (w), 779.9 (m); MS (ESI) m/z Calculated: 318.3062 $[\text{M-H}]^-$, Experimental: 318.0919 $[\text{M-H}]^-$.

(E)-N'-(2-hydroxy-3-methoxybenzylidene)-1-naphthohydrazide (S1R2)



Yield: 90%; m.p.: 169 – 170 °C. Elemental analysis Calculated for $\text{C}_{19}\text{H}_{16}\text{N}_2\text{O}_3$ (%): C 71.24, H 5.03, N 8.74, Experimental: C 71.28, H 5.09, N 8.76. ^1H NMR ($\text{DMSO}-d_6$): δ 12.22 (s, 1H, -NH), δ 10.89 (s, 1H, -OH), δ 8.56 (s, 1H, -CH), δ 8.26 (d, 1H, ArH, $J = 9.0$ Hz), δ 8.13 (d, 1H, ArH, $J = 8.5$ Hz), δ 8.04-8.03 (m, 1H, ArH), δ 7.81 (d, 1H, ArH, $J = 8.5$ Hz), 7.64-7.60 (m, 3H, ArH), 7.19 (d, 1H, ArH, $J = 8.5$ Hz), δ 7.07 (d, 1, ArH, $J = 8.0$ Hz), δ 6.87 (t, 1H, ArH, $J = 8.25$ Hz), δ 3.83 (s, 3H, - CH_3). FT-IR in cm^{-1} : 3170.3 (w), 3041.1 (w), 2856.2 (w), 1640.0 (s), 1564.5 (m), 1468.5 (m), 1245.8 (s), 722.8 (w), 659.5 (w).

(E)-N'-propylidene-1-naphthohydrazide (S1R3)



Yield: 88%; m.p.: 191 – 192 °C. Elemental analysis Calculated for $\text{C}_{14}\text{H}_{14}\text{N}_2\text{O}$ (%): C 74.31, H 6.24, N 12.32, Experimental: C 74.23, H 6.21, N 12.41. ^1H NMR ($\text{DMSO}-d_6$): δ 11.58 (s, 1H, NH), δ 8.16-8.12 (m, 1H, ArH), δ 8.07 (d, 1H, -CH, $J = 8.5$ Hz), δ 8.01-8.7.98 (m, 1H, ArH), δ 7.67-7.64 (m, 2H, ArH), δ 7.60-7.57 (m, 3H, ArH), δ 2.33-2.28 (m, 2H, - CH_2), δ 1.08 (t, 3H, - CH_3 , $J = 7.5$ Hz). FT-IR in cm^{-1} : 3181.1 (br.m), 3034.6 (m), 2068.0 (m), 1870.3 (br.w), 1633.6 (s), 1549.1 (s), 1352.8 (m), 1295.6 (m), 1252.7 (m), 1147.4 (w), 777.6 (s). MS (ESI) m/z Calculated: 249.2635 $[\text{M}+\text{Na}]^+$, Experimental: 249.1578 $[\text{M}+\text{Na}]^+$.

The representative spectra of receptors have been given below.

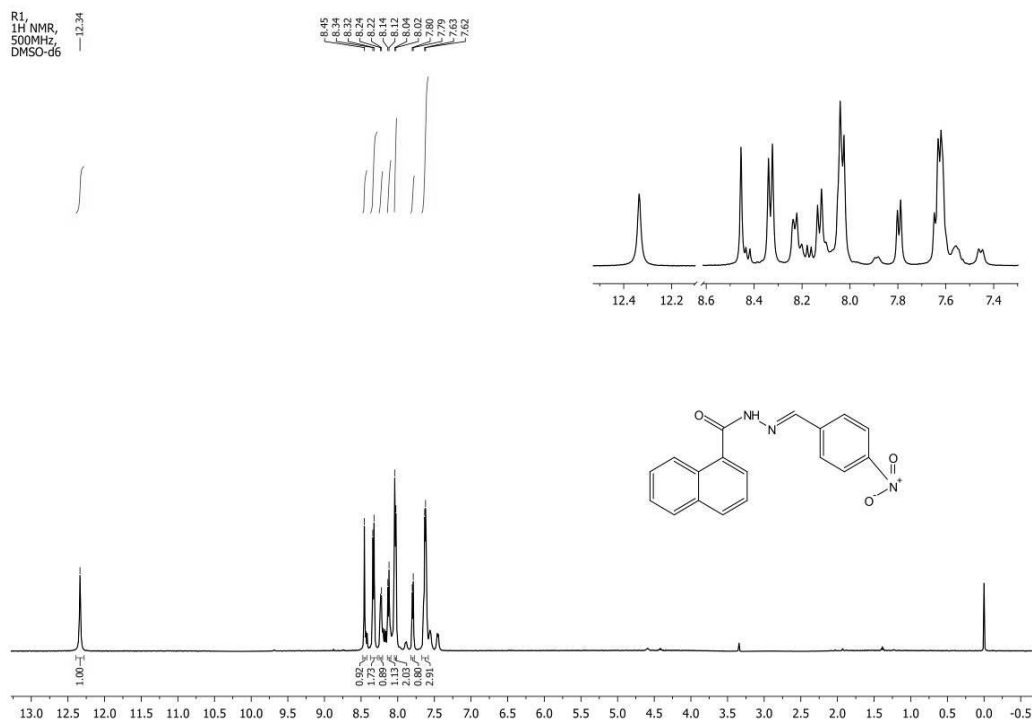


Fig. 2.2 ^1H NMR spectrum of S1R1

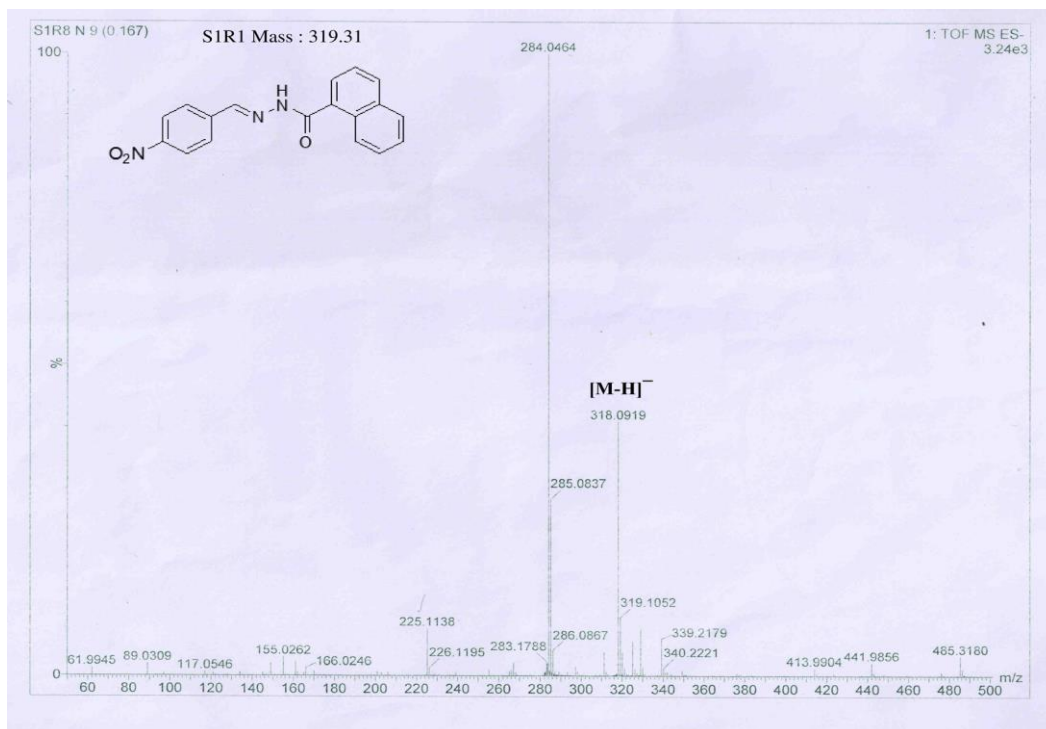


Fig. 2.3 ESI-MS of S1R1

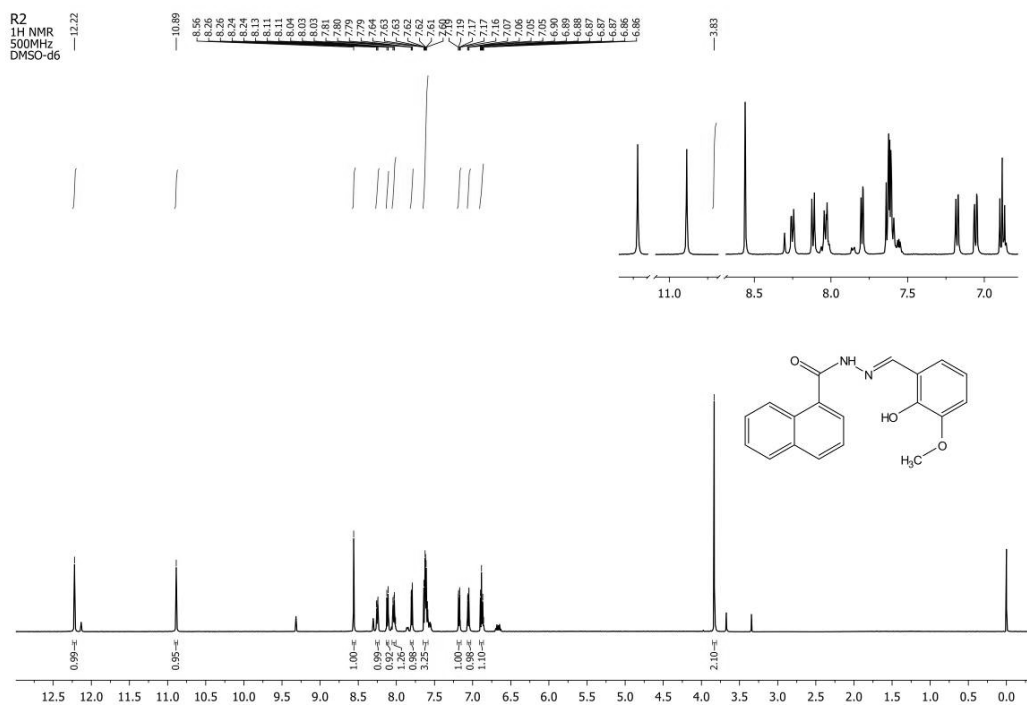


Fig. 2.4 ^1H NMR spectrum of **S1R2**

2.3 RESULTS AND DISCUSSION

2.3.1 Colorimetric detection of anions

The receptors **S1R1** and **S1R2** were initially investigated for selective colorimetric detection of F^- ion over other anions in DMSO solvent. The receptors (2.5×10^{-5} M) were treated with 1 equiv. of various anions such as fluoride, chloride, bromide, iodide, acetate, hydrogensulphate and dihydrogenphosphate in the form of tetrabutylammonium (TBA) salts. A colour change from colourless to red and colourless to bright yellow was observed instantaneously upon adding F^- ions and AcO^- ions to the receptors **S1R1** (Fig. 2.5) and **S1R2** (Fig. 2.6) respectively. The colour intensity was more in case of F^- ion for both the receptors which indicates strong binding of F^- ion to the receptors whereas, a much weaker interaction between receptors and AcO^- ion was resulted in decreased intensity in colorimetric detection.

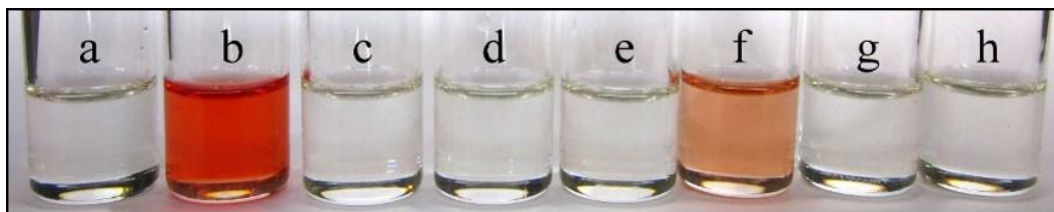


Fig. 2.5 Change in colour of **S1R1** (2.5×10^{-5} M) in DMSO solution on adding 1 equiv. of TBA anions; (a) Free Receptor **S1R1**, (b) F^- , (c) Cl^- , (d) Br^- , (e) I^- , (f) AcO^- , (g) HSO_4^- and (h) $H_2PO_4^-$ ions

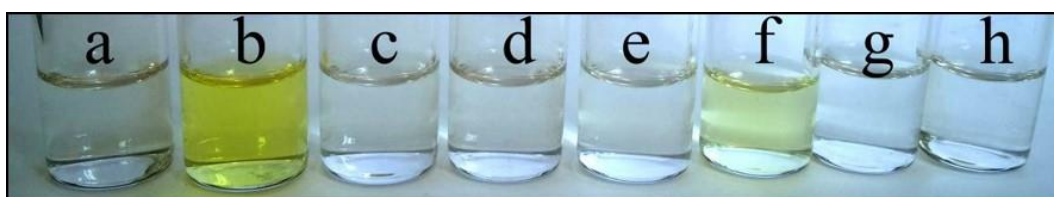


Fig. 2.6 Change in colour of **S1R2** (2.5×10^{-5} M) in DMSO solution on adding of 1 equiv. of TBA anions; (a) Free Receptor **S1R2**, (b) F^- , (c) Cl^- , (d) Br^- , (e) I^- , (f) AcO^- , (g) HSO_4^- and (h) $H_2PO_4^-$ ions

The colorimetric detecting ability of receptors **S1R1** and **S1R2** were studied in ACN solvent. Unfortunately, the receptor **S1R1** was partially soluble in ACN and therefore, it was not able to study for colorimetric detection. The receptor **S1R2** displayed similar colour change from colourless to bright yellow on addition of F^- ions and AcO^- ions (Fig. 2.7). However, the colour intensity for AcO^- ion was less when compared to F^- ion because of the weaker interaction of AcO^- ion with receptor **S1R2**.

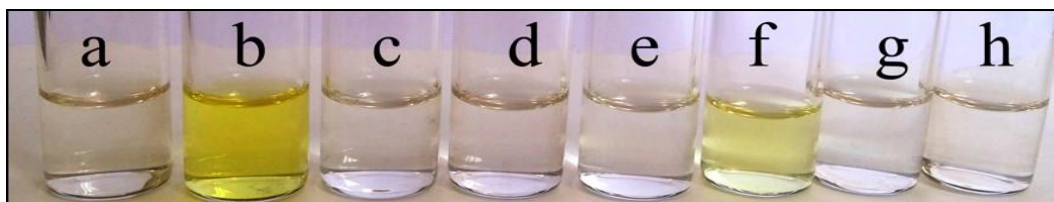


Fig. 2.7 Change in colour of **S1R2** (2.5×10^{-5} M) in ACN solution on adding 1 equiv. of TBA anions; (a) Free Receptor **S1R2**, (b) F^- , (c) Cl^- , (d) Br^- , (e) I^- , (f) AcO^- , (g) HSO_4^- and (h) $H_2PO_4^-$ ions

The receptor **S1R3** was evaluated for colorimetric detection of F^- ions over other anions in DMSO. The colour of receptor was not changed even after adding 20 equiv. of any anions (Fig. 2.8) as it does not has signalling unit.

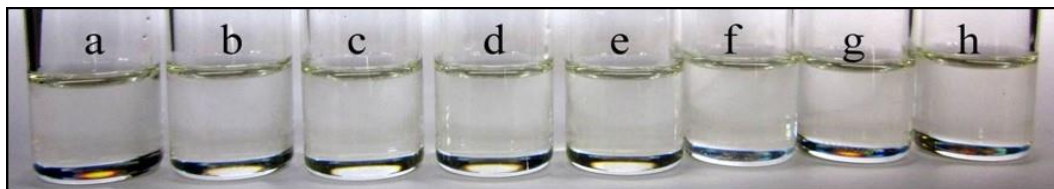


Fig. 2.8 Change in colour of **S1R3** (5×10^{-5} M) in DMSO solution with addition of 20 equiv. of TBA anions; (a) Free Receptor **S1R3**, (b) F^- , (c) Cl^- , (d) Br^- , (e) I^- , (f) AcO^- , (g) HSO_4^- and (h) $H_2PO_4^-$ ions

In order to examine the selectivity towards F^- ion over other anions, receptor **S1R1** was treated with 1 equiv. of F^- ion in presence of Cl^- , Br^- , I^- , HSO_4^- and $H_2PO_4^-$ ions (1 equiv.). As shown in Fig. 2.9, presence of other ions virtually made no difference on the colorimetric detection of F^- ion. Thus, receptor **S1R1** could selectively detect the fluoride ion even in presence of other competing anions.

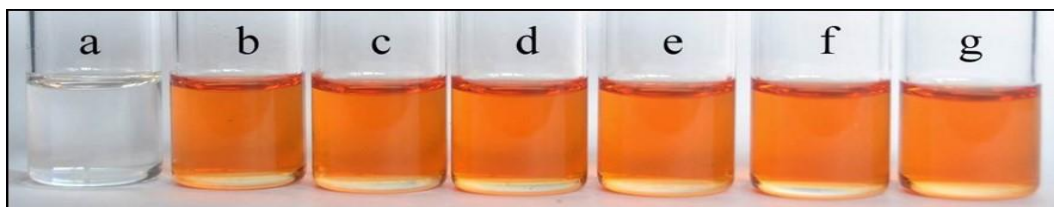


Fig. 2.9 Competitive study of receptor **S1R1** solution (2.5×10^{-5} M) in DMSO after adding 1 equiv. of F^- and 1 equiv. of other anions; (a) Free Receptor **S1R1**, (b) F^- , (c) $Cl^- + F^-$, (d) $Br^- + F^-$, (e) $I^- + F^-$, (f) $HSO_4^- + F^-$ and (g) $H_2PO_4^- + F^-$

2.3.2 UV-vis spectral studies of receptors

The selectivity of receptor **S1R1** was further evaluated with UV-vis spectroscopy. The significant shift in the absorption band was observed upon addition of F^- ions and AcO^- ions. The intensity of this newly generated absorption band after addition of AcO^- ions was much less than that of F^- ions (Fig. 2.10). However, all other anions did not show any change in UV-vis absorption band. This indicates either these anions are not interacted with receptor **S1R1** or the interaction was much weaker to create any changes in colorimetric detection and in UV-vis absorption.

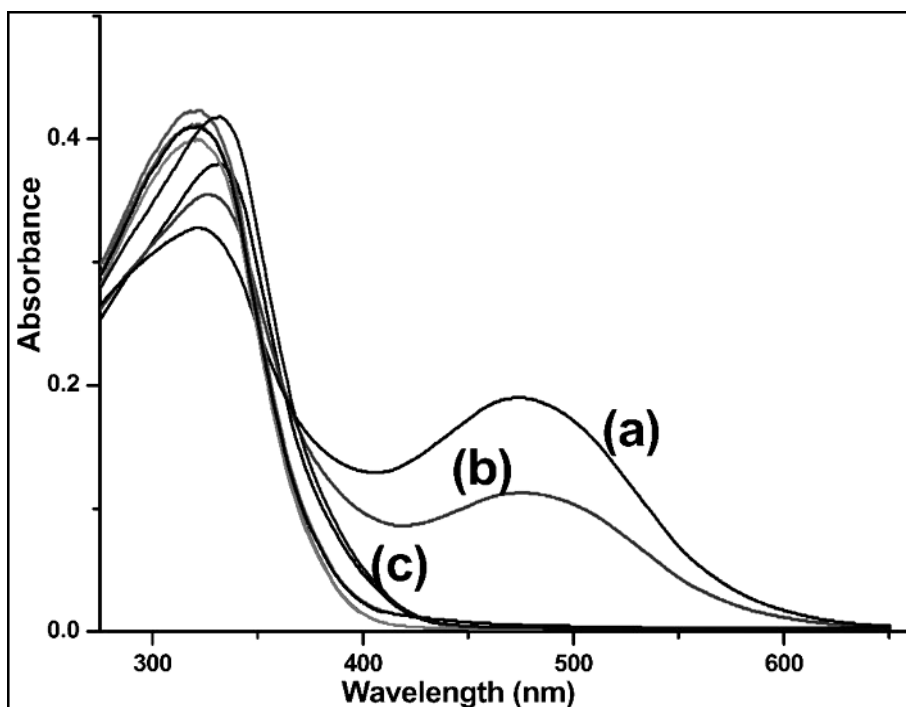


Fig. 2.10 UV-vis spectral changes of **S1R1** (2.5×10^{-5} M) in DMSO after adding 10 equiv. of (a) F^- , (b) AcO^- and (c) Cl^- , Br^- , I^- , HSO_4^- and $H_2PO_4^-$ as TBA salts

The UV-vis confirmation for selectivity was extended to the receptor **S1R2** in DMSO as well as in ACN solvents (Fig. 2.11, A and B, respectively). In both the solvents the receptor **S1R2** showed substantial shift in the absorption band only upon adding F^- ions and AcO^- ions. However, the intensity of absorption band was much lesser upon adding AcO^- ions, which clearly indicates the interaction between receptor **S1R2** and AcO^- ion is much weaker.

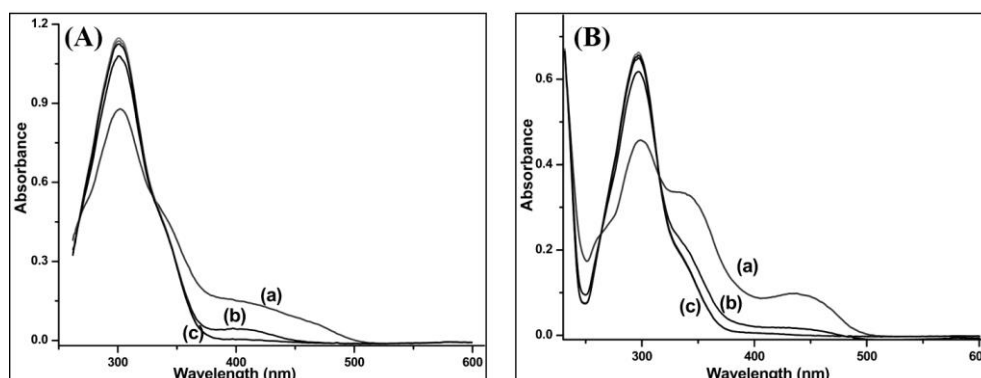


Fig. 2.11 UV-vis changes of **S1R2** in (A) DMSO and (B) ACN (2.5×10^{-5} M) after adding 10 equiv. of anions. (a) F^- , (b) AcO^- (c) Cl^- , Br^- , I^- , HSO_4^- and $H_2PO_4^-$

The absorbance in UV-vis spectroscopy was not changed with the addition of any anions (Fig. 2.12) to the receptor **S1R3**. Therefore, it is clear that, the presence of aromatic unit attached to naphthohydrazone unit is indispensable for the F^- ion detection process.

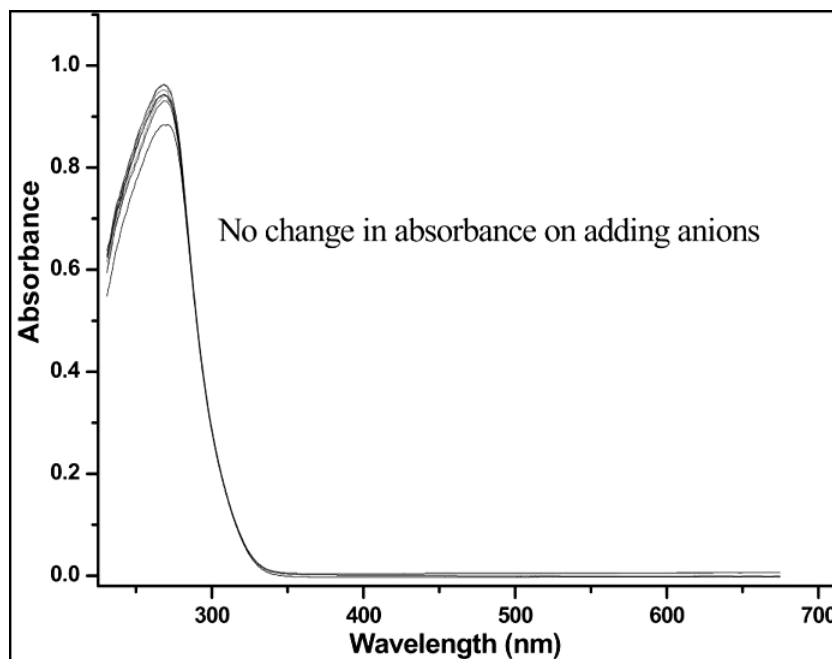


Fig. 2.12 UV-vis changes of **S1R3** in DMSO (2.5×10^{-5} M) after the addition of 20 equiv. of anions

To understand the nature of the receptor–anion interactions, a UV-vis titration was performed by increasing addition of TBAF to **S1R1** (2.5×10^{-5} M) in DMSO. The constant increase in the concentration of TBAF resulted in steady decrease in intensity of absorbance band at 328 nm. Meanwhile, a new absorption band at 476 nm with the formation of a clear isosbestic point at 362 nm (Fig. 2.13) was appeared. This bathochromic shift of 148 nm was attributed to the intramolecular charge transfer transition in the receptor **S1R1** on F^- ion binding.

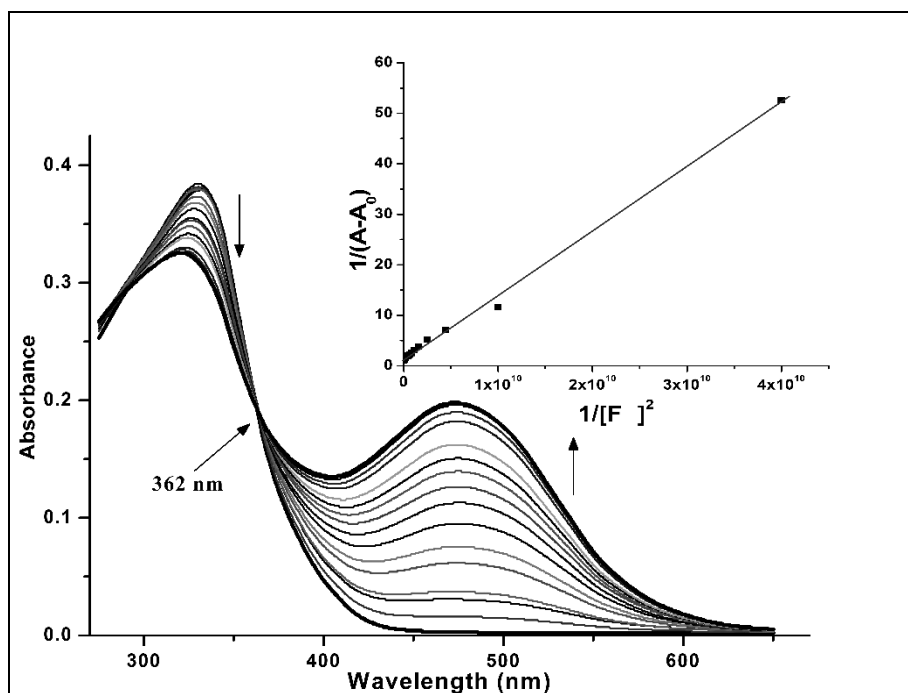


Fig. 2.13 UV-vis titration of **S1R1** (2.5×10^{-5} M) with TBAF (0–15 equiv.) in DMSO; Inset: Benesi - Hildebrand plot of receptor **S1R1** binding with F^- ion associated with absorbance change at 476 nm in DMSO

The UV-vis titration of receptor **S1R2** was carried out in both DMSO as well as ACN solutions. The DMSO solution showed constant decrease in the absorption band at 301 nm with gradual increasing addition of F^- ions. Simultaneously, a new band centred at 413 nm was appeared and intensity of this absorption band was increased continuously with increasing concentration of F^- ions (Fig. 2.14, A).

On gradual addition of F^- ions to receptor **S1R2** in ACN, a new absorption peak at 440 nm corresponding to intramolecular charge transfer was established. Concurrently, the absorption maxima corresponding to $-OH$ functional group at 296 nm gradually shifted to a new absorption maxima at 344 nm creating an isosbestic point at 315 nm (Fig. 2.14, B). This 48 nm bathochromic shift in the absorption maxima was due to the stabilization of *keto* tautomer of hydroxyl functional group. However, this *enol* to *keto* tautomeric shift was not observed in case of DMSO solution as the *keto* tautomer itself is more stable in polar solvents like DMSO (Beyramabadi et al. 2011; Laurella et al. 2012). The DMSO solvent forms hydrogen

bond with the $-C=O$ of *keto* tautomer and therefore, *keto* tautomer becomes stable in receptor **S1R2**. As a result, *keto* tautomer predominates over *enol* tautomer in DMSO solvent and the $-C=O$ functional group of *keto* tautomer has no binding site to participate in the detection process.

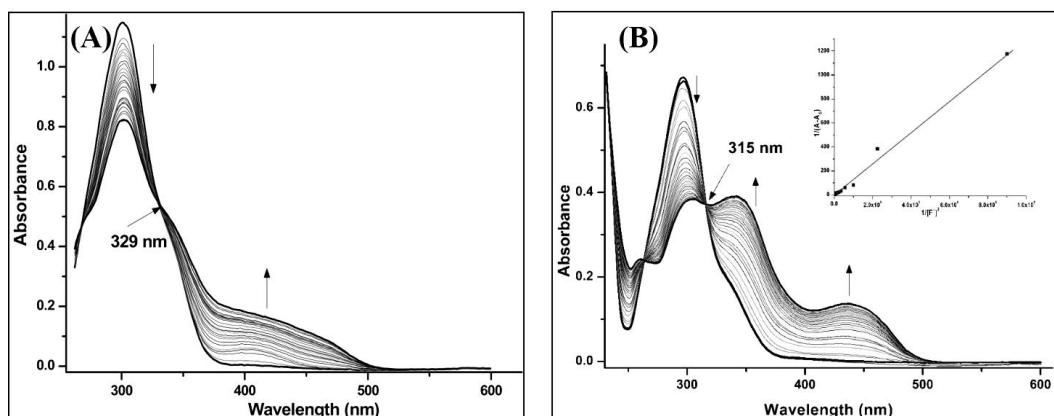


Fig. 2.14 UV-vis titration of **S1R2** (2.5×10^{-5} M) with TBAF (0–15 equiv.) in (A) DMSO and (B) ACN; Inset: Benesi - Hildebrand plot of receptor **S1R2** binding with F^- ion associated with absorbance change at 440 nm in ACN

The stoichiometry of the anion complexation for both receptors **S1R1** and **S1R2** was determined by Benesi-Hildebrand method (Benesi and Hildebrand 1949) using UV-vis spectrometric titration data at 476 nm and 440 nm respectively (Fig. 2.13, Inset and Fig. 2.14, B Inset). The linearity in graph confirms formation of a stable 1:2 stoichiometric complex for both receptors with F^- ions. The binding constant was calculated using Benesi-Hildebrand equation (Eq. 2.1).

$$\frac{1}{(A - A_0)} = \frac{1}{(A_{max} - A_0)} + \frac{1}{K[F^-]^n(A_{max} - A_0)} \dots \dots \dots \text{(Eq. 2.1)}$$

Where, A_0 , A , A_{max} are the absorption considered in the absence of F^- , at an intermediate, and at a concentration of saturation. K is binding constant, $[F^-]$ is concentration of F^- ion and n is the stoichiometric ratio.

The values of $A - A_0$, $A_{max} - A_0$ and $[F^-]$ were obtained by the titration plot which was plotted using UV-vis spectrometric titration data at 476 nm (Fig. 2.15).

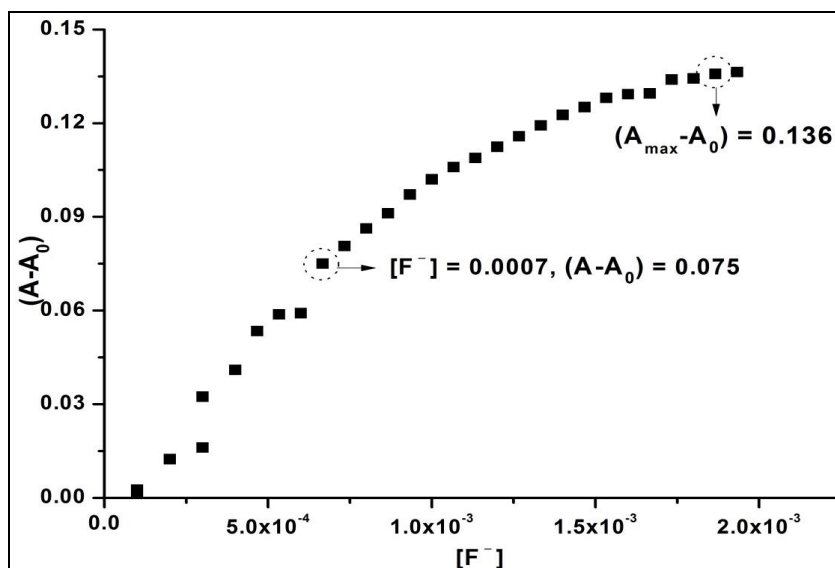


Fig. 2.15 Titration plot at 476 nm in DMSO, $(A-A_0)$ vs. $[F^-]$

The values of $(A-A_0)$, $(A_{max} - A_0)$, $[F^-]$ and n were substituted in Eq. 2.1 as shown below.

$$\frac{1}{0.075} = \frac{1}{0.136} + \frac{1}{K(0.0007)^2 \times (0.136)}$$

$$\text{Therefore, } K = 2.5 \times 10^6$$

The same calculations were repeated two more UV-vis titration data and average of all three ' K ' values with a standard deviations were calculated to obtain the binding constant. Thus, the binding constants for receptors **S1R1** and **S1R2** were found to be $2.36 \pm 0.33 \times 10^6 \text{ M}^{-2}$ and $0.973 \pm 0.09 \times 10^6 \text{ M}^{-2}$ respectively.

2.3.3 ^1H NMR titration and binding mechanism

^1H NMR titration experiments of **S1R1** and **S1R2** with F^- ion (as TBA salt) were carried out in $\text{DMSO-}d_6$ to understand the mechanism of receptor-anion interactions. The proton H_a at δ 12.34 corresponding to $-\text{NH}$ of receptor **S1R1** was initially disappeared on adding TBAF (1 equiv.) as a result of fast proton exchange. The signals at δ 8.15 (H_c) and δ 8.05 (H_d) corresponding to nitro phenyl group were merged together till 2 equiv. of F^- ions due to the fast proton exchange through the receptor **S1R1**. At 5 equiv. of F^- ions the $-\text{NH}$ of receptor deprotonates and a conjugated quinonoid form of receptor **S1R1** was stabilized. As a result, splitting of

the signals corresponding to nitro phenyl group reappeared (Fig. 2.16). As the concentration of F^- ion increased from 1 equiv. to 5 equiv., signal at δ 8.45 corresponding to imine proton (H_b) was slowly shifted to upfield owing to the formation of exocyclic double bond during detection process. The deprotonation lead to increase in electron density over receptor **S1R1** which resulted in upfield shift of aromatic protons.

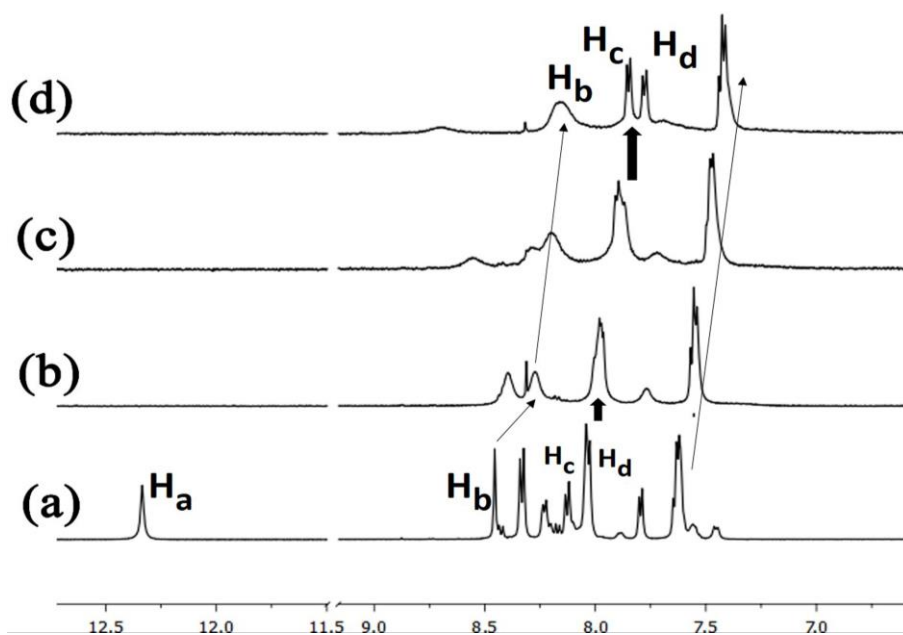


Fig. 2.16 Partial 1H NMR spectra of receptor **S1R1** in $DMSO-d_6$ after adding (a) 0, (b) 1, (c) 2 and (d) 5 equiv. of F^- ions

The most important result observed in 1H NMR titration was appearance of a new peak at δ 16.1 (Fig. 2.17) at higher concentration (5 equiv.) of F^- ion. This corresponds to hydrogen difluoride (Boiocchi et al. 2004) which clearly shows the deprotonation of $-NH$ proton in receptor **S1R1**.

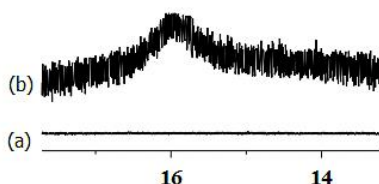
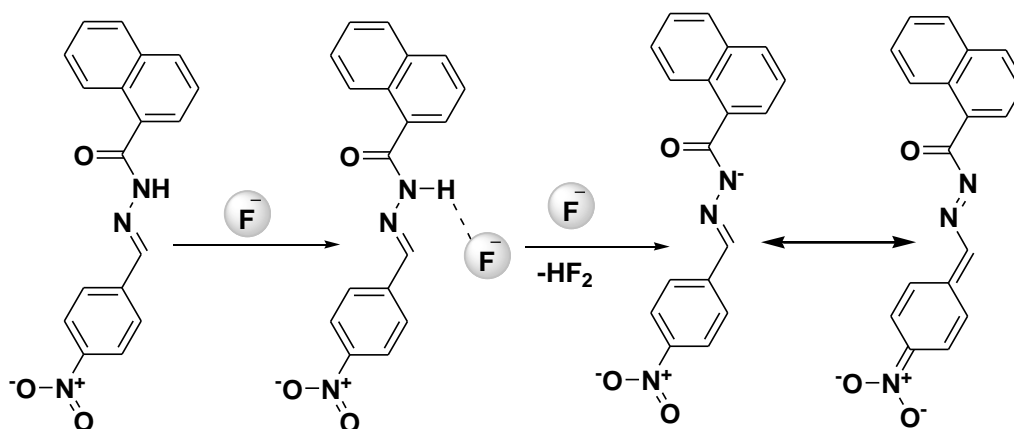


Fig. 2.17 (a) No peak at 16.1 at 0 equiv. F^- ions and (b) peak corresponding to HF_2 on adding 5 equiv. of F^- ions

The binding mechanism of receptor **S1R1** to F^- ions was proposed by evaluating the results obtained from UV-vis titration and 1H NMR titration (Scheme 2.3). The F^- ion detection using receptor **S1R1** is two-step process. At first, F^- ion binds through hydrogen bonding to the $-NH$ proton of the receptor **S1R1** which results in 1:1 adduct and **S1R1**••• F^- complex formation (Ghosh et al. 2009). Further, the second F^- ion induces deprotonation of $-NH$ proton in the receptor **S1R1** and as a result, the electron density increases over the deprotonated receptor **S1R1**. Thus, the charge separation in the receptor is introduced which results in ICT transition between the electron deficient $-NO_2$ group at *p*- position and electron rich $-N^-$ which lead to intense colorimetric change (Cho et al. 2005).



Scheme 2.3 Proposed mechanism for binding of F^- ions with receptor **S1R1**

As stated previously, the *keto* tautomer of receptor **S1R2** will be predominated over the *enol* tautomer in polar solvents such as DMSO. This tautomerism is confirmed by 1H NMR spectrum where the proton at δ 12.25 (H_a) corresponds to $-CONH$ and proton at δ 10.9 (H_b) corresponds to $-NH$ of $-CONH$. In 1H NMR titration of receptor **S1R2**, both the protons corresponding to $-NH$ at δ 12.25 and at δ 10.9, were disappeared upon adding 1 equiv. of F^- ions (Fig. 2.18), which is owing to the formation of hydrogen bond between F^- ion and $-NH$ proton of $-CONH$ followed by fast proton exchange. Surprisingly, no other major changes were observed in 1H NMR signals corresponding to the aromatic protons while adding F^- ions up to 2 equiv. However, at higher concentration of F^- ions (5 equiv.) the proton H_a deprotonates and this result in the charge transfer transition in receptor **S1R2**. Consequently, the

aromatic signals corresponding to naphthyl protons (H_d) were merged together. This deprotonation leads to increased electronic density over the phenyl group and signals corresponding to these protons (H_e) experiences slightly upfield shift. The imine proton H_c in receptor **S1R2** has not participated in the detection process. This was confirmed by ^1H NMR titration spectra where the signals at δ 8.6 was not shifted either upfield or downfield even after adding 5 equiv. of F^- ions.

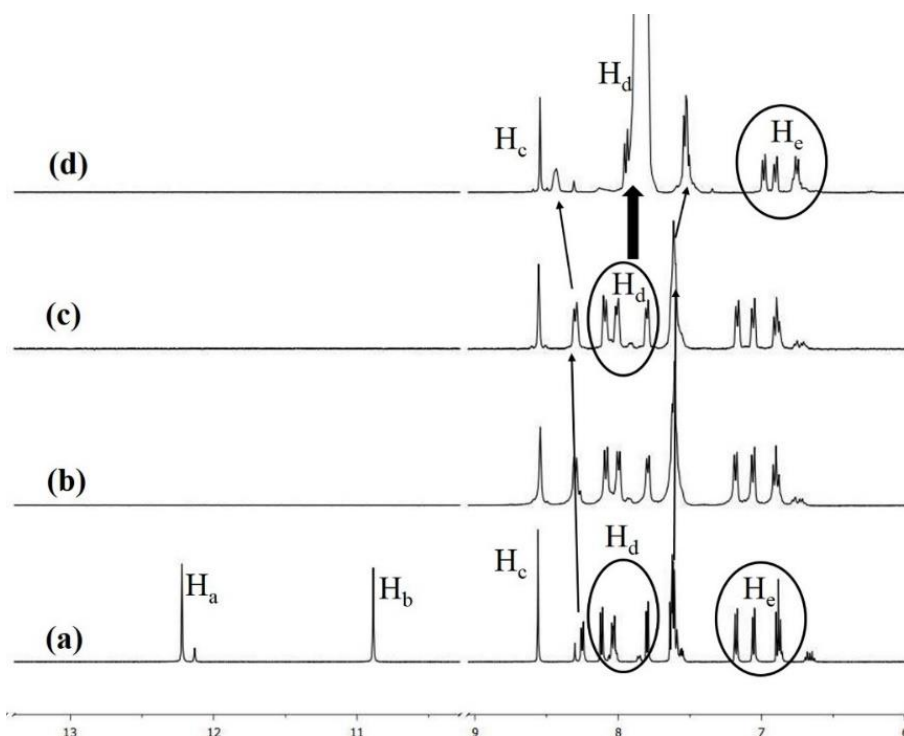
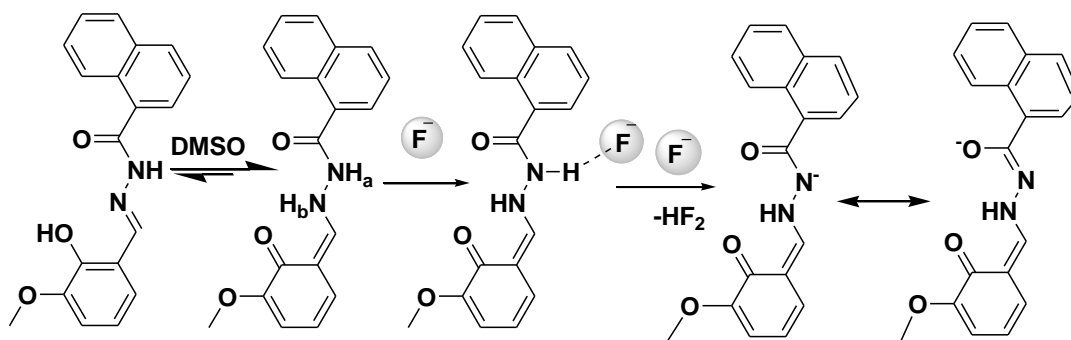


Fig. 2.18 Partial ^1H NMR spectra of receptor **S1R2** in $\text{DMSO}-d_6$ after adding (a) 0, (b) 1, (c) 2 and (d) 5 equiv. of F^- ions

Thus, the results of UV-vis titration and ^1H NMR titration were compiled to determine the binding mechanism of receptor **S1R2** with F^- ions (Scheme 2.4). Keto tautomer being more stable in DMSO, the $-\text{NH}$ proton of receptor **S1R2** initially forms hydrogen bond with F^- ion to stabilize a $\text{S1R2}\cdots\text{F}^-$ adduct. Further the addition of F^- ion persuades deprotonation of the $-\text{NH}$ proton in receptor **S1R2** and thus establishes charge on the receptor. This leads to charge transfer transition within the receptor **S1R2** and thus the receptor show a significant colour change.



Scheme 2.4 Proposed mechanism for binding of fluoride ions with receptor **S1R2**

2.3.4 Practical application

To evaluate real-life applicability of any receptor, it is necessary to detect the inorganic fluoride ions such as sodium fluoride particularly in aqueous media. Therefore, to ensure the real-life significance, the receptors **S1R1** and **S1R2** were subjected for the colorimetric detection of sodium fluoride in 9:1 (1×10^{-3} M solution) organo-aqueous (ACN:H₂O) mixture. Though the receptor **S1R1** showed remarkable colour change in organic solvents for the detection of TBAF, it failed to detect inorganic fluoride ions in aqueous media. However, the receptor **S1R2** showed a significant colour change from colourless to pale yellow on adding 3 equiv. of sodium fluoride in aqueous media (Fig. 2.19).

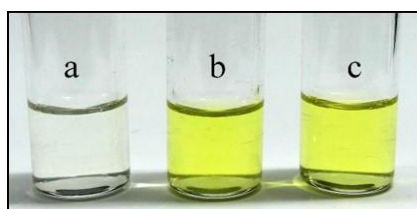
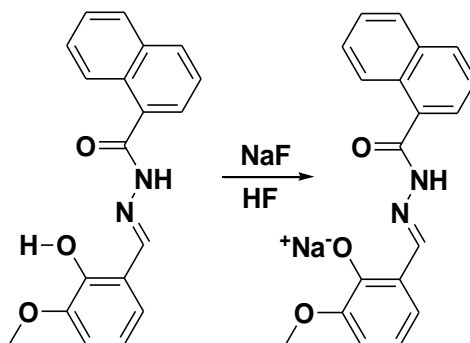


Fig. 2.19 Colour change of the receptor **S1R2** after adding the F⁻ ions in 9:1 ACN:H₂O solvent mixture (a) **S1R2**, (b) **S1R2** + 3 equiv. NaF and (c) **S1R2** + 3 equiv. TBAF

The receptor **S1R2** showed same colour change even with the addition of 3 equiv. TBAF as F⁻ ion source in aqueous media. Unfortunately, UV-vis studies were unable to perform as the receptor concentration exceeded absorption limit.

The receptor **S1R1** was failed to detect inorganic fluoride ions as the binding site (-NH) readily gets solvated in presence of water even the in trace amounts. On

the other hand, receptor **S1R2** has a phenolic $-OH$ which is highly base labile and immediately binds with basic inorganic fluoride ions to form respective salt. As a result, upon adding sodium fluoride to the receptor **S1R2**, phenolic $-OH$ readily gets deprotonated to form corresponding sodium salt (Scheme 2.5) and this deprotonation leads to the colour change of receptor **S1R2** from colourless to pale yellow.



Scheme 2.5 Proposed mechanism for detection of inorganic fluoride ions in aqueous media

2.4 CONCLUSIONS

To summarize, the receptors **S1R1** and **S1R2** were designed and synthesised based on 1-naphthohydrazide Schiff's base for the selective colorimetric detection of F^- ions over other anions. The detection process involves initial 1:1 receptor- F^- ion adduct formation followed by deprotonation of receptor at higher concentration of F^- ions. This resulted in charge transfer transition through the receptors and thus remarkable colour change from colourless to red in case of receptor **S1R1** and colourless to bright yellow for receptor **S1R2** was observed. The binding of F^- ion to receptor **S1R1** is much stronger than that of **S1R2** which resulted in higher binding constant in case of receptor **S1R1**. Though the receptor **S1R1** displayed prominent colour change in organic media, it failed to show the same result for the detection of inorganic fluoride ions in aqueous media as the binding site easily gets solvated with trace amount of water. Alternatively, the receptor **S1R2** was able to detect inorganic fluoride in aqueous media. This observation was owing to the presence of base labile $-OH$ functionality in receptor **S1R2** which will get deprotonated in presence basic F^- ions, even in aqueous media.

CHAPTER 3

***DESIGN AND SYNTHESIS OF BENZOHYDRAZIDE
BASED RECEPTORS FOR THE DETECTION OF
INORGANIC FLUORIDE ION IN AQUEOUS MEDIA***

The chapter consists of design, syntheses and characterization of new benzohydrazide based colorimetric receptors for the expeditious detection of inorganic fluoride ions such as NaF. The colorimetric anion sensing properties, detection mechanism were explored and the real-life applications of these receptors have been demonstrated by detecting fluoride ions in commercial mouthwash as well as in sea water.

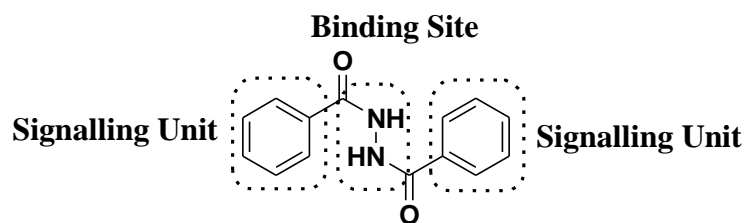
3.1 INTRODUCTION

Colorimetric receptors with high selectivity, sensitivity, being easy and safe to handle have received significant attention and thus, a number of colorimetric receptors have been reported that are capable of detecting fluoride ions (Piatek and Jurczak 2002; Jose et al. 2004; Rose-Lis et al. 2007; Veale et al. 2007; Gong et al. 2008; Gale et al. 2008; Li et al. 2010; Kumar et al. 2010; Bose and Ghosh, 2010; Park et al. 2011; Dydio et al. 2011.). However, majority of these receptors could be operated only in noncompetitive organic solvents for the detection of tetrabutylammonium fluoride (TBAF) and in absolute nonaqueous conditions. This drawback is due to the higher acidity of water than that of protons which is involved in binding process and hence the F^- ion readily gets solvated even with the trace amount of water. Conversely, design and synthesis of receptor molecules capable of detecting inorganic fluoride such as sodium fluoride in aqueous conditions for real-life applications is a daunting task and yet to be explored by chemists.

The detection ability of receptors with urea, thiourea, amide and pyrrole/imidazole/indole functional groups where $-NH$ acts as the binding site, depends on the acidity of $-NH$ proton (Amendola et al. 2006). However, this acidity can be tuned by inserting different electron withdrawing groups to molecular backbone. As acidity of $-NH$ increases, the hydrogen bond donor tendency of $-NH$ also increases, which at extreme acidity leads to deprotonation of the receptor. This deprotonation establishes the charge transfer complexes which results in significant colour change of the solution with a large bathochromic shift and hence the naked eye detection of anion becomes feasible. Thus the stability of charge transfer complexes directly depends on the acidic nature of $-NH$ proton (Park et al. 2011).

The receptors in this series are based on phenylcarbonylbenzohydrazide (**S 3.1**).

Notably two carbonyl ($-C=O$) groups adjacent to $-NH$ and a nitro group ($-NO_2$) at p -position of the phenyl ring was incorporated in case of **S2R1** and **S2R2** to increase the acidity of $-NH$ proton. Hence these receptors would compete with water to bind with inorganic fluoride for naked eye detection.



S 3.1

The receptors **S2R1-S2R3** were designed to demonstrate the effect of nitro substitution at p - position of phenyl ring on intramolecular charge transfer (ICT). Receptor **S2R4** was synthesized to study the role of $-NH$ in fluoride ion binding process.

3.2 EXPERIMENTAL

3.2.1 Materials and methods

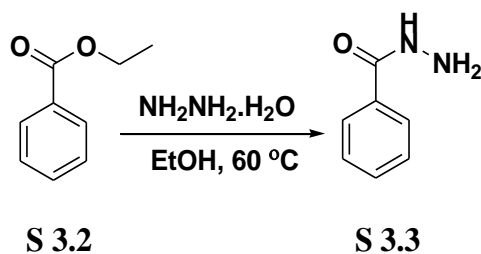
All chemicals were purchased from Sigma-Aldrich, Alfa Aesar or from Spectrochem and used without further purification. All solvents were procured from SD Fine, India with HPLC grade and used without further distillation.

The 1H NMR spectra were recorded on a Bruker, Avance II (500 MHz) instrument using TMS as internal reference and $DMSO-d_6$ as solvent. The raw FID data was processed with MestReNova 7.0.0-8331 software. Resonance multiplicities are described as s (singlet), br s (broad singlet), d (doublet), t (triplet), q (quartet) and m (multiplet). The chemical shifts (δ) are reported in ppm and coupling constant (J) values are given in Hz. Melting points were determined with Stuart- SMP3 melting-point apparatus in open capillaries and are uncorrected. IR spectra were recorded on a Thermo Nicolet Avatar-330 FT-IR spectrometer; signal designations: s (strong), m (medium), w (weak), br.m (broad medium) and br.w (broad weak). Mass spectra were recorded on Waters Micromass Q-ToF micro spectrometer with ESI source. The SCXRD was performed on Bruker AXS APEX II system. UV-vis spectroscopy was carried out with Ocean Optics SD2000-Fibre Optics Spectrometer and Analytikjena

Specord S600 Spectrometer in standard 3.5 mL quartz cells (2 optical windows) with 10 mm path length. Elemental analyses were done using Flash EA1112 CHNS analyser (Thermo Electron Corporation). All reactions were monitored by TLC on pre-coated silica gel 60 F₂₅₄ plates which were procured from Merck.

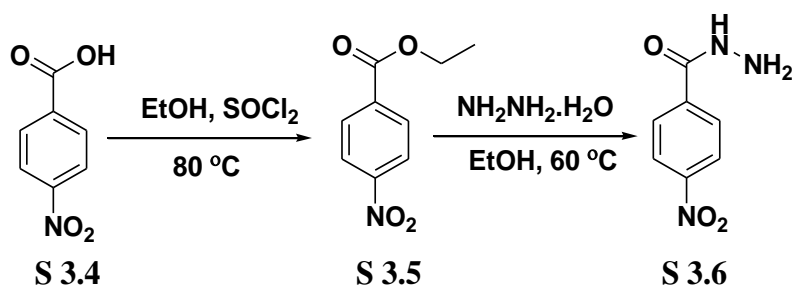
3.2.2 Synthesis of intermediates S 3.3 and S 3.6

The ethyl benzoate **S 3.2** (6.65 mmol) was treated with hydrazine hydrate (33.29 mmol) in presence of ethanol and heated to 60°C for 2.5 h. The reaction mixture was cooled below 5°C. The solid formed was filtered and dried to give colourless solid intermediate **S 3.3** (Scheme 3.1)



Scheme 3.1 Synthesis of intermediate **S 3.3**

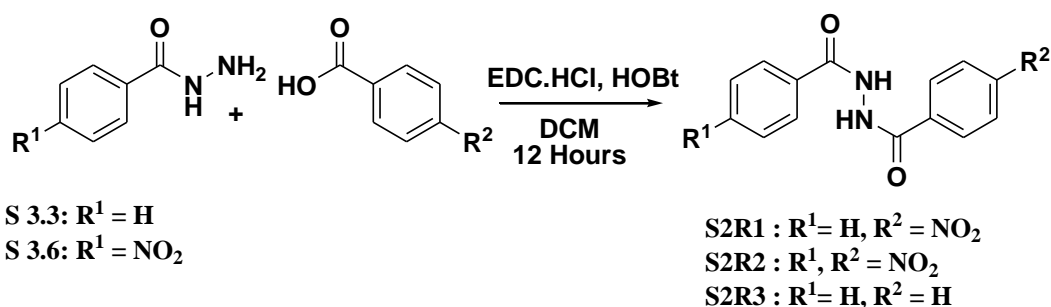
To a solution of 4-nitrobenzoic acid **S 3.4** (2.99 mmol) in ethanol, thionylchloride (3.3 mmol) was added. The reaction was catalysed by a drop of dimethylformamide (DMF). The reaction mixture was then refluxed for 4 h. Completion of the reaction was confirmed by thin layer chromatography. Excess of ethanol was removed by evaporation from the reaction mixture, diluted with dichloromethane and washed with water. Organic layer was separated, dried over anhydrous Na₂SO₄ and evaporated to yield corresponding ester (**S 3.5**). Thus obtained ester **S 3.5** (2.6 mmol) was treated with hydrazine hydrate (12.8 mmol) in presence of ethanol and heated to 60 °C for 2.5 h. The reaction mixture was cooled below 5 °C. The solid formed was filtered and dried to give pale yellow coloured solid intermediate **S 3.6** (Scheme 3.2).



Scheme 3.2 Synthesis of intermediate S 3.6

3.2.3 Synthesis of receptors S2R1, S2R2 and S2R3

To a solution of 1-ethyl-3-(3-dimethylaminopropyl)carbodiimide hydrochloride (EDC.HCl) (2.94 mmol) in 3 mL of dichloromethane, 1-Hydroxybenzotriazole (HOBt) (0.147 mmol), benzoic acid derivative (1.47 mmol) and triethylamine (2.94 mmol) were added and stirred for 30 min. The starting material S 3.3/S 3.6 (1.47 mmol) was then added to the reaction mixture and stirred at room temperature for overnight. The reaction mixture was diluted with 2 mL of dichloromethane, washed with 2N HCl (3 mL×2) followed by 10% sodium bicarbonate solution (3 mL×2). The organic layer was separated, dried over anhydrous Na₂SO₄ and concentrated under reduced pressure to yield the product (Scheme 3.3).

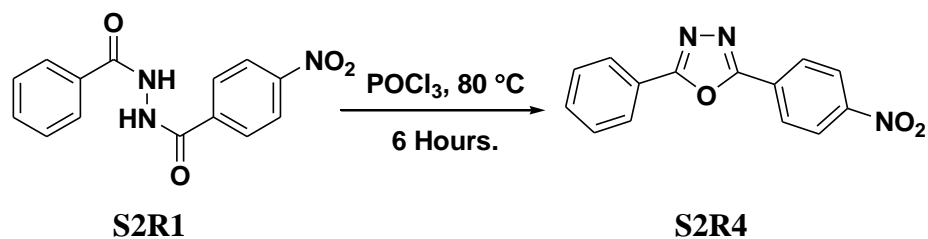


Scheme 3.3 Synthesis of S2R1, S2R2 and S2R3

3.2.4 Synthesis of receptor S2R4

A mixture of compound S2R1 (0.35 mmol) and 2 mL of phosphorousoxychloride was heated at 80 °C for 6 h. The reaction mixture was cooled to room temperature and poured into 20 mL ice cold water. The resulting precipitate was filtered, washed with water and dried to yield the compound S2R4

(Scheme 3.4).



Scheme 3.4 Synthesis of **S2R4**

The single crystal of the receptors **S2R2** suitable for X-ray diffraction analysis was obtained by slow evaporation of dimethylformamide (DMF) solution at room temperature. The ORTEP diagram with 50% probability is given in Fig. 3.1.

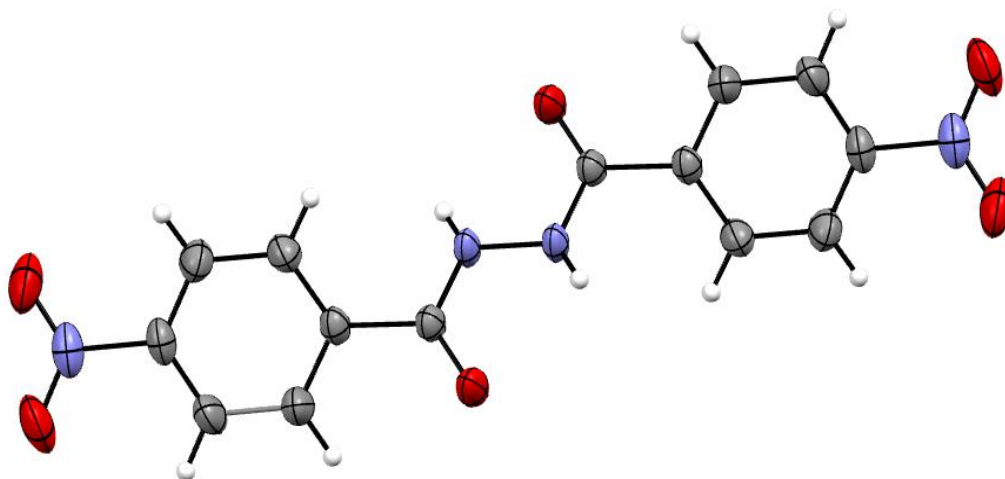


Fig. 3.1 ORTEP diagram of receptor **S2R2** with 50% probability

The receptors **S2R2** was crystallised in monoclinic lattice. Detailed crystallographic data is given in the Table 3.1.

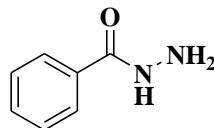
Table 3.1 Crystallographic data of receptor **S2R2**

Receptor	S2R2
Chemical formula	$C_{14}H_{10}N_4O_6$
Formula weight	330.25
Crystal System	Monoclinic
Space group	P2(1)/c

a (Å)	4.7966(2)
b (Å)	9.9017(5)
c (Å)	14.9138(6)
α (°)	90.00
β (°)	98.839(3)
γ (°)	90.00
V (Å)³	699.911
Z	2
Crystal size	0.45 × 0.33 × 0.24
F (000)	340
R-factor (%)	3.92

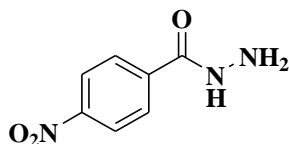
All compounds and receptors were characterized by spectral analysis. The characterization data has been compiled and given below.

Benzohydrazide (S 3.3)

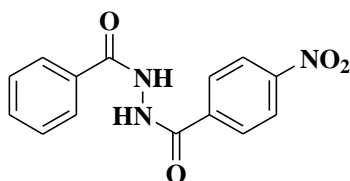


Yield: 92%; m.p.: 114-115°C. Elemental analysis Calculated for C₇H₈N₂O (%) : C 71.75, H 5.92, N 20.58. Experimental: C 71.65, H 5.98, N 20.38. FT-IR in cm⁻¹: 3292.9 (m), 3190.4 (s), 3010.4 (s), 1607.9 (s), 1559.5 (s), 1335.5 (s), 671.9 (s).

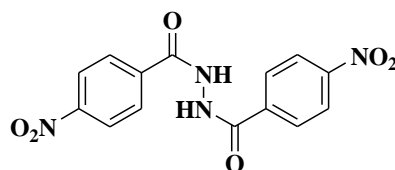
4-nitrobenzohydrazide (S 3.6)



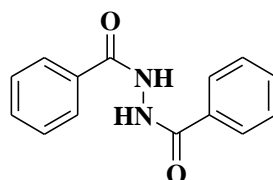
Yield: 89%; m.p.: 216-217°C. Elemental analysis Calculated for C₇H₇N₃O₃ (%) : C 46.41, H 3.89, N 23.20. Experimental: C 46.25, H 3.62, N 23.38. FT-IR in cm⁻¹: 3316.8 (m), 3037.6 (w), 1608.6 (m), 1511.6 (s), 1313.8 (m), 926.2 (m), 857.1 (m), 589.7 (m).

4-nitro-*N'*-(phenylcarbonyl)benzohydrazide (S2R1)

Yield: 89%; m.p.: 234-235 °C. Elemental analysis Calculated for $C_{14}H_{11}N_3O_4$ (%): C 58.95, H 3.89, N 14.73. Experimental: C 58.65, H 3.95, N 14.78. 1H NMR (DMSO- d_6): δ 10.88 (s, 1H, NH), δ 10.65 (s, 1H, NH), δ 8.40 (d, 2H, ArH, $J = 8.5$ Hz), δ 8.17 (d, 2H, ArH, $J = 9$ Hz), δ 7.94 (d, 2H, ArH, $J = 7.5$ Hz), δ 7.62 (t, 1H, ArH, $J = 7.25$ Hz), δ 7.54 (t, 2H, ArH, $J = 7.5$ Hz). FT-IR in cm^{-1} : 3341.5 (br.m), 3201.7 (br.m), 3060.5 (m), 1679.8 (w), 1641.2 (s), 1598.7 (m), 1516.9 (s), 1337.5 (s), 1270.0 (s), 690.2 (m). MS (ESI) m/z Calculated: 284.2469 $[M-H]^-$ Experimental: 284.0241 $[M-H]^-$

4-nitro-*N'*-[(4-nitrophenyl)carbonyl]benzohydrazide (S2R2)

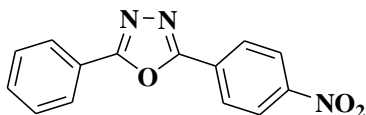
Yield: 86%; m.p.: 234-235 °C. Elemental analysis Calculated for $C_{14}H_{10}N_4O_6$ (%): C 50.92, H 3.05, N 16.96. Experimental: C 51.03, H 2.98, N 16.89. 1H NMR (DMSO- d_6): δ 11.00 (s, 2H, NH), δ 8.41 (d, 4H, ArH, $J = 8.5$ Hz), δ 8.18 (d, 4H, ArH, $J = 9.0$ Hz). FT-IR in cm^{-1} : 3381.2 (br.m), 3211.8 (s), 3108.8 (m), 1578.9 (s), 1519.0 (s), 1455.7 (s), 1345.9 (s), 860.9 (m), 704.3 (m). MS (ESI) m/z Calculated: 331.2603 $[M+H]^+$ Experimental: 331.2208 $[M+H]^+$

***N'*-(phenylcarbonyl)benzohydrazide (S2R3)**

Yield: 89%; m.p.: 139-140 °C. Elemental analysis Calculated for $C_{14}H_{12}N_2O_2$ (%): C 69.99, H 5.03, N 11.66. Experimental: C 69.74, H 5.10, N 11.68. 1H NMR (DMSO- d_6): δ 11.56 (s, 2H, NH), δ 7.80-7.75 (m, 5H, ArH), δ 7.58 (t, 2H, ArH, $J =$

7.75 Hz), δ 7.49 (t, 3H, ArH, $J = 7.75$ Hz). FT-IR in cm^{-1} : 3382.7 (br.m), 3265.5 (s), 3058.6 (m), 1696.6 (s), 1651.7 (s), 1246.8 (s), 688.9 (m). MS (ESI) m/z Calculated: 241.2652 $[\text{M}+\text{H}]^+$ Experimental: 241.1732 $[\text{M}+\text{H}]^+$

2-(4-nitrophenyl)-5-phenyl-1,3,4-oxadiazole (S2R4)



Yield: 92%; m.p. 212-213 °C. Elemental analysis Calculated for $\text{C}_{14}\text{H}_9\text{N}_3\text{O}_3$ (%): C 62.92, H 3.39, N 15.72. Experimental: C 63.01, H 3.36, N 15.68. ^1H NMR ($\text{DMSO}-d_6$): δ 8.48 (d, 2H, ArH, $J = 9$ Hz), δ 8.42 (d, 2H, ArH, $J = 9$ Hz), δ 8.20 (d, 2H, ArH, $J = 7.75$ Hz), δ 7.65-7.70 (m, 3H, ArH). FT-IR in cm^{-1} : 3382.7 (br.m), 3265.5 (s), 3058.6 (m), 1696.6 (s), 1651.7 (s), 1246.8 (s), 688.9 (m).

The representative spectra of receptors have been given below.

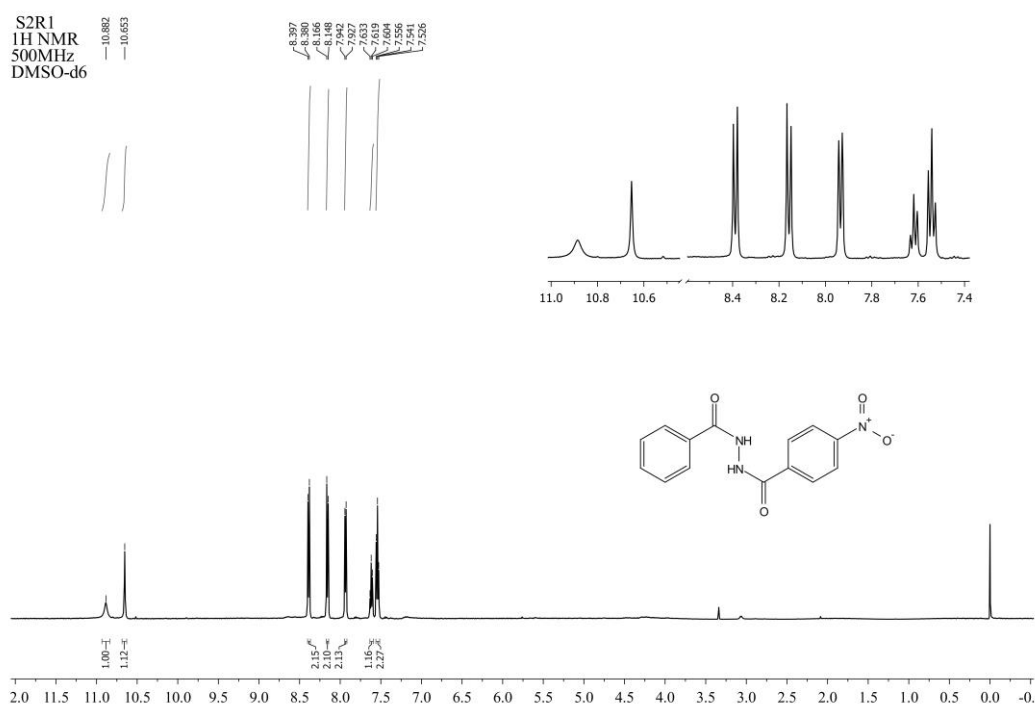
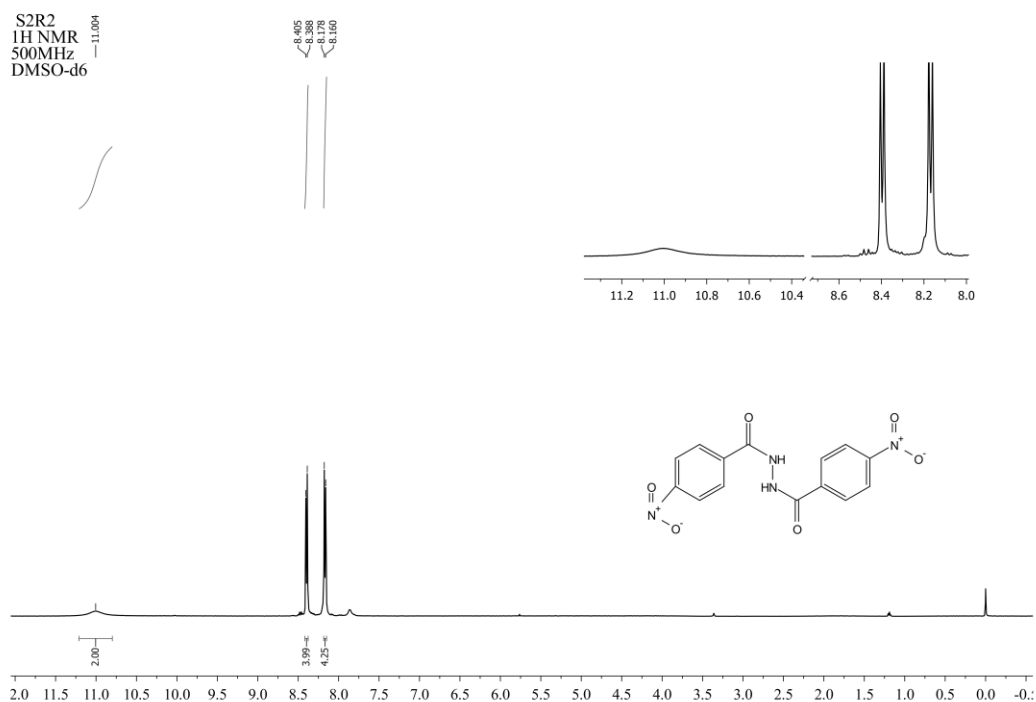
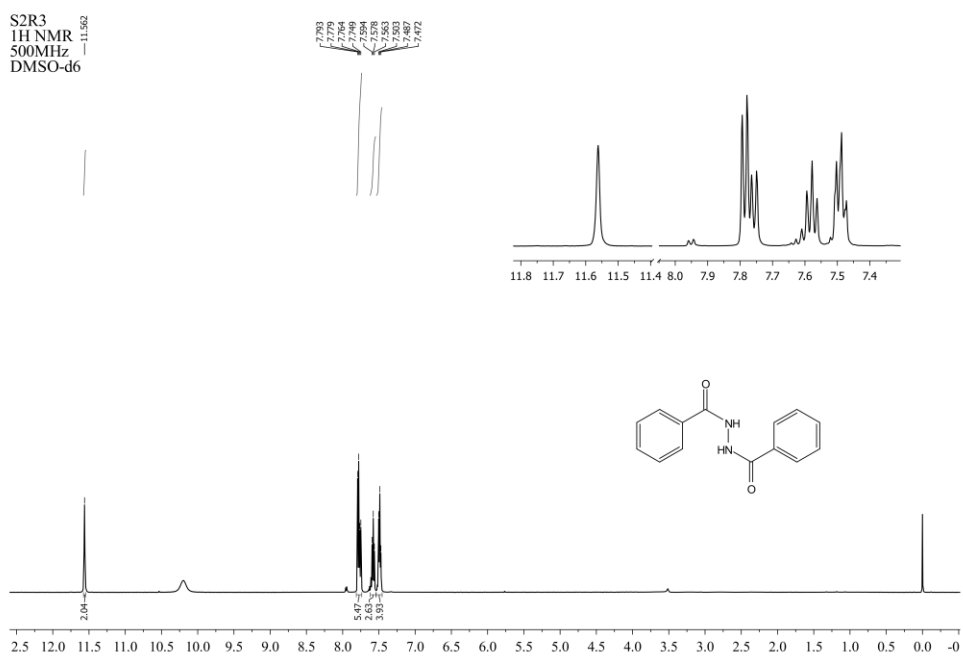


Fig. 3.2 ^1H NMR spectrum of S2R1

Fig. 3.3 ^1H NMR spectrum of S2R2Fig. 3.4 ^1H NMR spectrum of S2R3

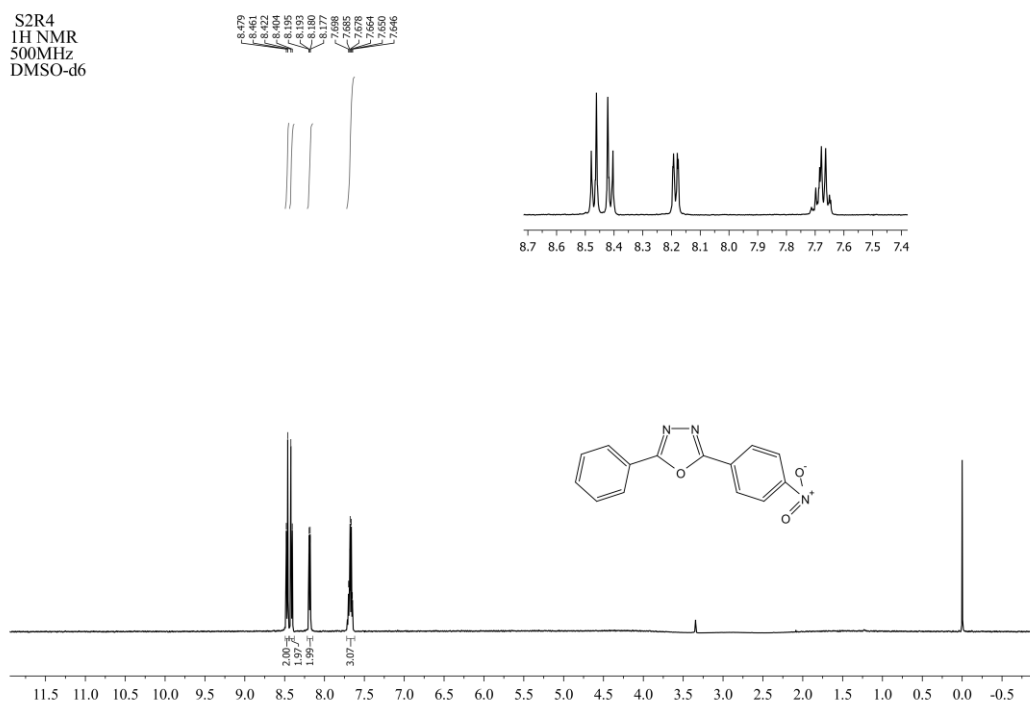


Fig. 3.5 FT-IR spectrum of S2R4

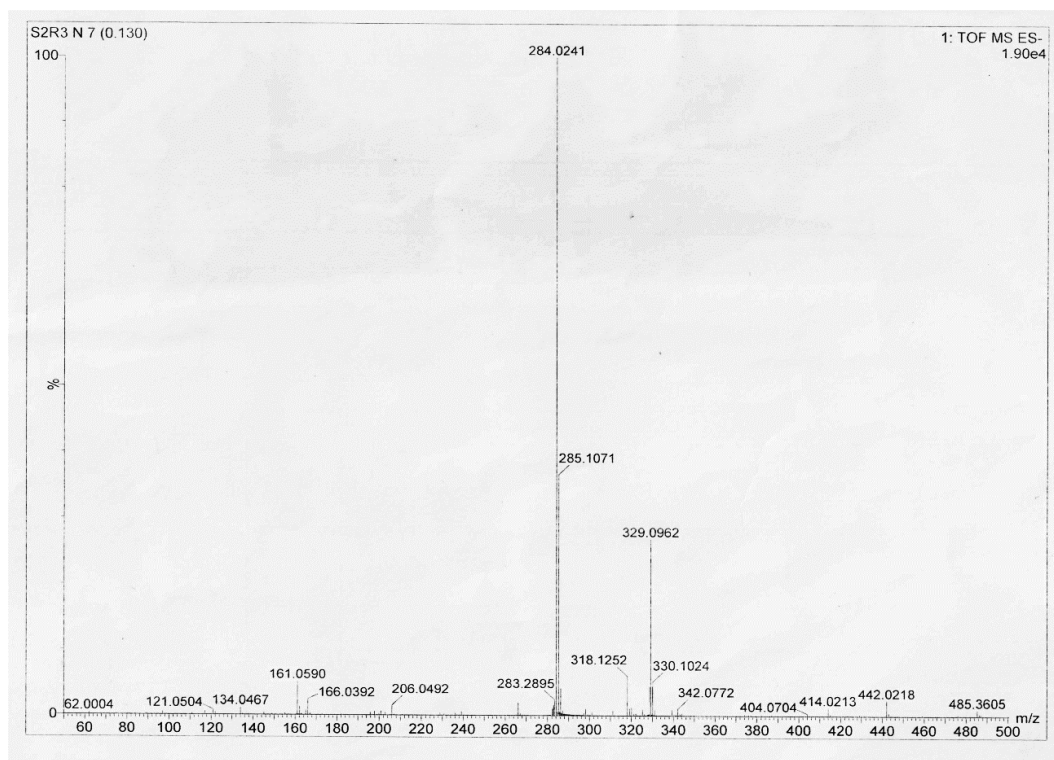


Fig. 3.6 ESI-MS spectrum of S2R1

3.3 RESULTS AND DISCUSSION

3.3.1 Colorimetric detection of anions

Initially the receptors **S2R1** and **S2R2** were investigated for colorimetric detection application by adding different anions in DMSO solvent. Both the receptor solutions (2.5×10^{-5} M) were treated with different anions (1 equiv.) such as fluoride, chloride, bromide, iodide, nitrate, hydrogensulphate, dihydrogenphosphate and acetate in the form of tetrabutylammonium (TBA) salts. These receptors showed remarkable colour change from colourless to red instantaneously with F^- ion whereas that associated with AcO^- ion was less intense. This confirms selective binding of F^- ion to the receptors. However, no colour change was observed on addition of other anions. Fig. 3.7 and Fig 3.8 show the change in the colour of receptors **S2R1** and **S2R2** respectively, on addition of 1 equiv. of different anion solutions as TBA salts.

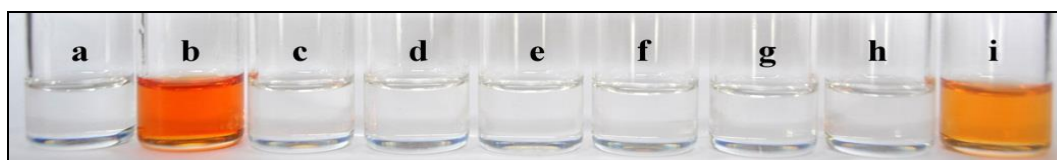


Fig 3.7 Change in colour of **S2R1** (2.5×10^{-5} M) in DMSO after adding 1 equiv. of TBA anions; (a) Free **S2R1**, (b) F^- , (c) Cl^- , (d) Br^- (e) I^- , (f) NO_3^- , (g) HSO_4^- , (h) $H_2PO_4^-$ and (i) AcO^-

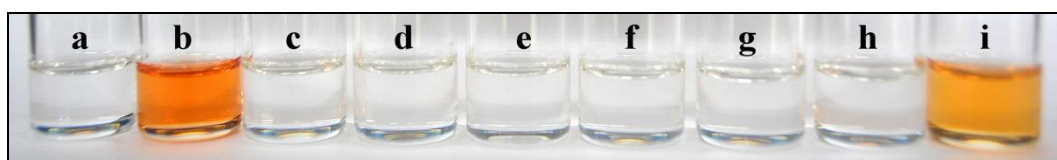


Fig 3.8 Change in colour of **S2R2** (2.5×10^{-5} M) in dry DMSO after adding 1 equiv. of TBA anions; (a) Free **S2R2**, (b) F^- , (c) Cl^- , (d) Br^- (e) I^- , (f) NO_3^- , (g) HSO_4^- , (h) $H_2PO_4^-$ and (i) AcO^-

The colorimetric study was carried out for receptors **S2R3** and **S2R4** as well. On adding 1 equiv. of TBA anions to the receptors **S2R3** and **S2R4**, change in the colour was not observed. Therefore, 10 equiv. of TBA anions were used. Receptor **S2R3** showed a slight colour change from colourless to pale yellow (Fig. 3.9) only for F^- ions. However, in case of **S2R4** no colour change was observed which confirms the role of $-NH$ in binding process of F^- ion (Fig. 3.10).

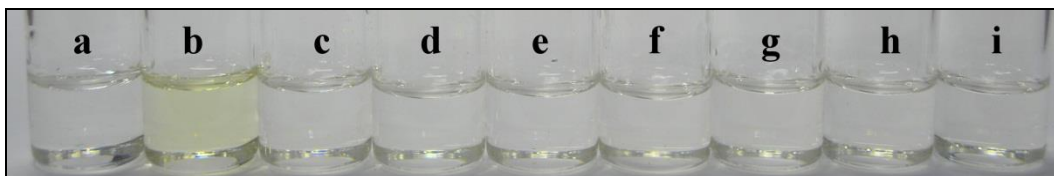


Fig 3.9 Change in colour of **S2R3** (2.5×10^{-5} M) in DMSO after adding 10 equiv. of TBA anions; (a) Free **S2R3**, (b) F^- , (c) Cl^- , (d) Br^- (e) I^- , (f) NO_3^- , (g) HSO_4^- , (h) $H_2PO_4^-$ and (i) AcO^-

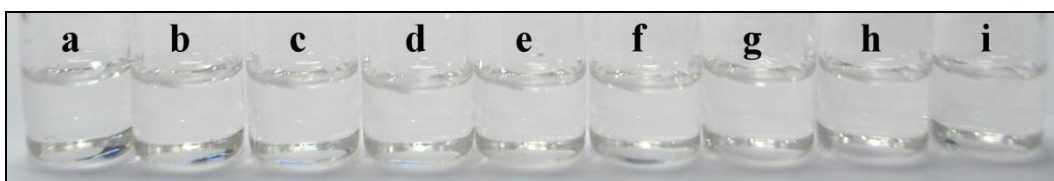


Fig 3.10 Change in colour of **S2R4** (2.5×10^{-5} M) in DMSO solution with the addition of 10 equiv. of TBA anions; (a) Free **S2R4**, (b) F^- , (c) Cl^- , (d) Br^- (e) I^- , (f) NO_3^- , (g) HSO_4^- , (h) $H_2PO_4^-$ and (i) AcO^-

In order to examine the selectivity, a competitive study of receptors **S2R1** and **S2R2** were carried out by treating 1 equiv. of TBAF in presence of other anions. The presence of other anions virtually makes no difference on the colorimetric detection of F^- ions (Fig. 3.11 for **S2R1** and Fig. 3.12 for **S2R2**).



Fig. 3.11 **S2R1** solution (2.5×10^{-5} M) in DMSO after adding 1 equiv. of TBAF and 1 equiv. of other anions; (a) Free **S2R1**, (b) F^- , (c) $Cl^- + F^-$, (d) $Br^- + F^-$ (e) $I^- + F^-$, (f) $NO_3^- + F^-$, (g) $HSO_4^- + F^-$ and (h) $H_2PO_4^- + F^-$

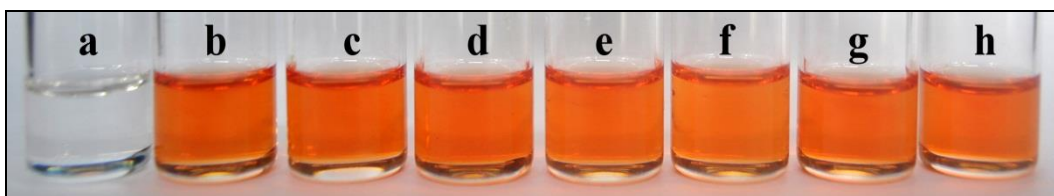


Fig. 3.12 **S2R2** solution (2.5×10^{-5} M) in DMSO after adding 1 equiv. of TBAF and 1 equiv. of other anions; (a) Free **S2R2**, (b) F^- , (c) $Cl^- + F^-$, (d) $Br^- + F^-$, (e) $I^- + F^-$, (f) $NO_3^- + F^-$, (g) $HSO_4^- + F^-$ and (h) $H_2PO_4^- + F^-$

3.3.2 UV-vis spectral studies of receptors

As a justification for selectivity, changes in UV-vis absorption of receptors **S2R1** and **S2R2** were recorded in dry DMSO (2.5×10^{-5} M), after adding 10 equiv. of different anions. As shown in Fig 3.13 only F^- ion and AcO^- ion induced instantaneous bathochromic shift in the absorption maxima and all other anions did not cause any change in the absorption.

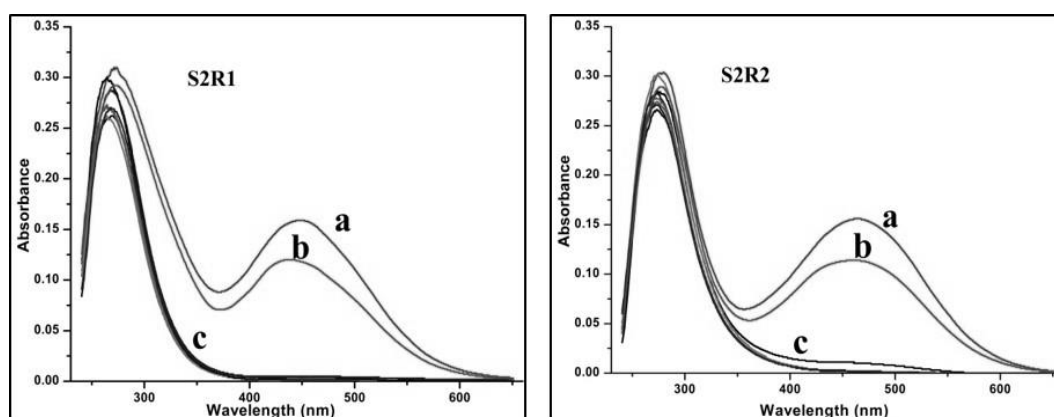


Fig. 3.13 UV-vis spectral changes of **S2R1** and **S2R2** (2.5×10^{-5} M) in DMSO after addition of 10 equiv. of (a) F^- , (b) AcO^- and (c) other anions as TBA salts

The sensing ability of receptor **S2R1** in dry DMSO solution (2.5×10^{-5} M) was investigated using UV-vis spectrophotometric titration experiments by gradually adding a standard solution of TBAF. Fig. 3.14 shows the UV-vis spectral changes of **S2R1** on titrating with F^- ions. With the constant increase in the concentration of F^- ion, the peak at 268 nm was slightly increased due to change in $\pi \rightarrow \pi^*$ transition. A new band at 446 nm formed and developed with a bathochromic shift of 178 nm, which was ascribed to the formation of intramolecular charge transfer (ICT) complex. The receptor reached the saturation (Fig. 3.14, inset) at 3 equiv. of TBAF.

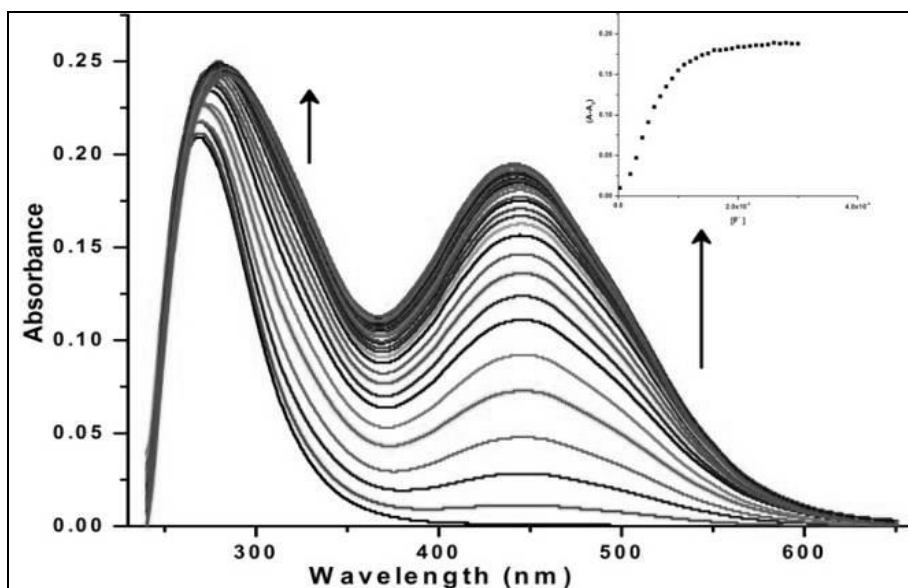


Fig. 3.14 UV-vis titration of **S2R1** (2.5×10^{-5} M) with the increasing addition of TBAF (0–10 equiv.) in DMSO; Inset: Titration plot at 446 nm ($A - A_0$) vs. $[F^-]$

The similar trend was observed in case of the receptor **S2R2** (Fig. 3.15).

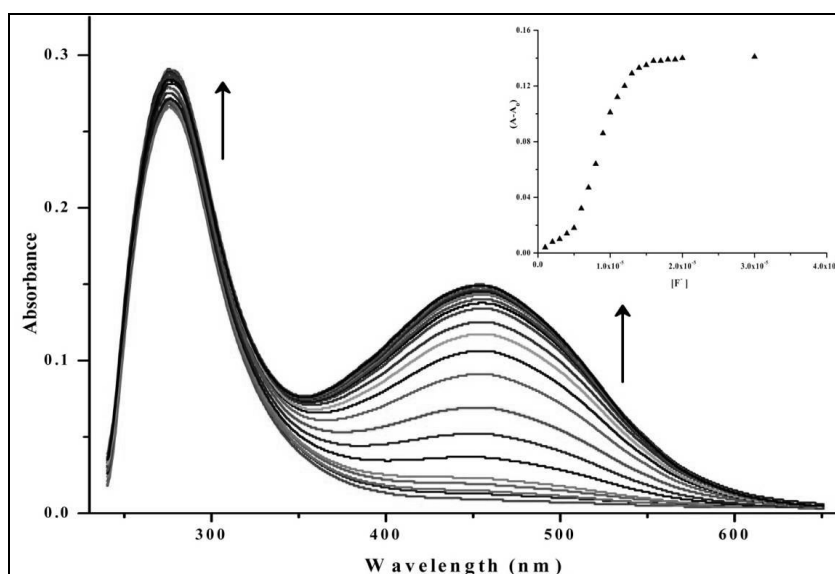


Fig. 3.15 UV-vis spectra of **S2R2** (2.5×10^{-5} M) with the increasing addition of TBAF (0–10 equiv.) in DMSO; Inset: Titration plot at 452 nm ($A - A_0$) vs. $[F^-]$

Upon constant incremental addition of F^- ion to the receptor **S2R2** solution in DMSO, a slight increase in the absorption peak at 275 nm was observed. This slight increase was attributed to the change in $\pi \rightarrow \pi^*$ transition. Simultaneously, a new peak

at 452 nm with a bathochromic shift of 177 nm was appeared and developed. This new peak was associated to the intramolecular charge transfer between receptor and F^- ion.

To explore the applicability of receptor **S2R1**, UV-vis titration was carried out in aqueous DMSO (9:1 v/v) using sodium fluoride (NaF) solution in water as fluoride source (Fig. 3.16).

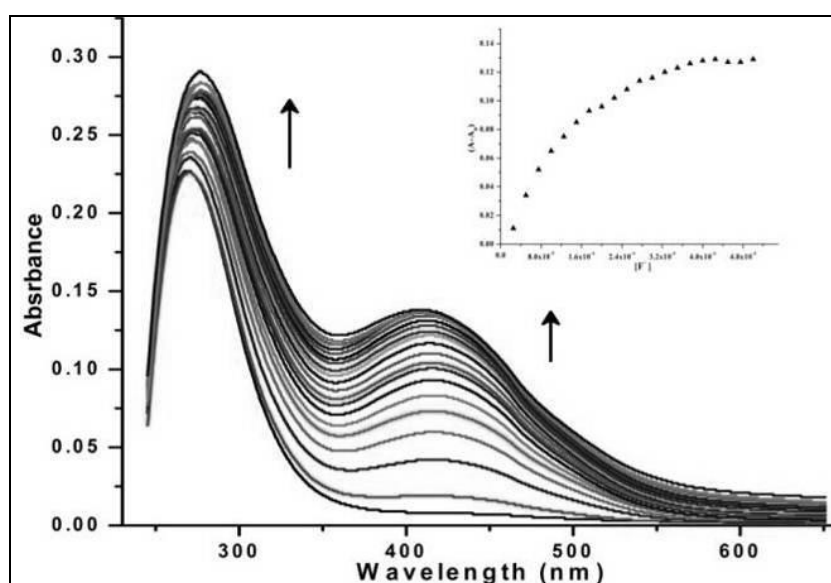


Fig. 3.16 UV-vis spectra of **S2R1** (2.5×10^{-5} M) with the increasing addition of NaF (0–20 equiv.) in DMSO:H₂O (9:1 v/v); Inset: Titration plot at 417 nm ($A-A_0$) vs. $[F^-]$

Upon increasing addition of NaF to receptor **S2R1**, the intensity of peak at 268 nm slightly increased and a new peak at 417 nm with the $\Delta\lambda_{\max}$ of 149 was observed. This new absorption peak was ascribed to the formation of new charge transfer complex. The saturation point reached after the addition of 15 equiv. of NaF solution in water. The receptor **S2R2** showed a new peak at 431 nm with a bathochromic shift of 147 nm (Fig 3.17). These results revealed that the titration spectra did not show much difference on addition of inorganic fluoride to aqueous receptor solution (DMSO:H₂O, 9:1; v/v) when compared to TBAF with dry DMSO solution of **S2R1**. The 10% aqueous solution of receptor **S2R1** was further titrated with TBAF which showed similar spectral changes. This indicates that the same ICT mechanism was followed in case of organic and aqueous media for the detection of F^- ion.

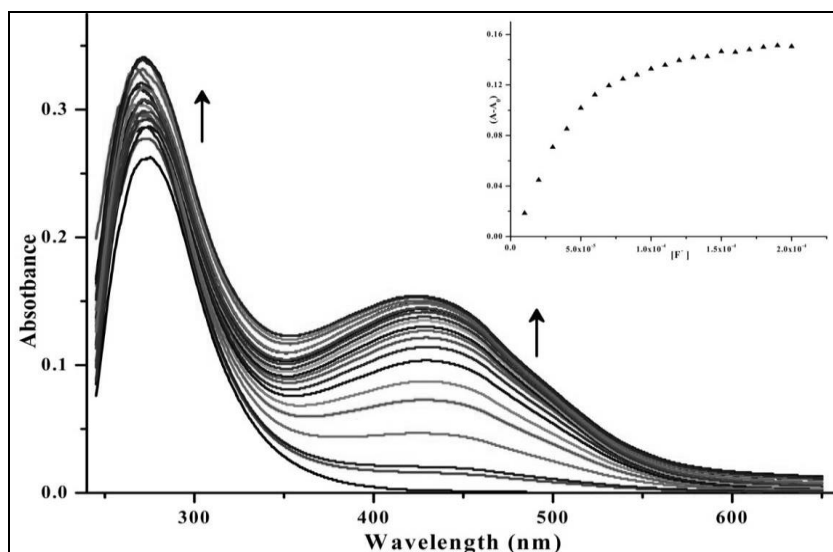


Fig. 3.17 UV-vis spectra of **S2R2** (2.5×10^{-5} M) with increasing addition of NaF (0–20 equiv.) in DMSO:H₂O (9:1 v/v); Inset: Titration plot at 431 nm ($A-A_0$) vs. $[F^-]$

Presence of two carbonyl groups adjacent to $-NH$ and nitro substitution at *p*-position of phenyl ring made the $-NH$ protons highly acidic (Clayden et al. 2001) and hence the receptor **S2R1** and **S2R2** readily get deprotonated in presence of basic F^- ion. Thus, these receptors can detect both organic as well as inorganic fluorides. However, the slight less bathochromic shift in case of aqueous DMSO when compared to dry DMSO was observed perhaps due to the solvation of F^- ions in water which decreased its binding with receptors (Kumar et al. 2008).

3.3.3 Practical applications

The practical application of receptor was evaluated by adding inorganic fluoride ions to 10% aqueous solution of receptor. The receptors **S2R1** and **S2R2** showed a colour change from colourless to yellow (Fig. 3.18). Experimental studies showed that the receptors **S2R1** and **S2R2** could colorimetrically detect the presence of inorganic fluoride even at 0.5 ppm level which is much lower than the WHO permissible F^- ions (maximum of 1 ppm) in drinking water (Fawell et al. 2001, WHO Technical Report, 1994). Furthermore, the receptor **S2R1** was tested for the detection of F^- ions in sea water, collected from Arabian Sea (Latitude $13^\circ 0' 33.99''$, Longitude $74^\circ 47' 17.23''$) and commercial mouthwash. When a drop of sea water/mouthwash was added to the DMSO solution of receptor **S2R1**, a permanent change in colour from

colourless to yellow was observed (Fig. 3.18).



Fig 3.18 Receptor **S2R1** showing colour change upon addition of NaF, seawater and commercial mouthwash

Thus, the F^- ion in sample water can be detected with naked eye by adding a drop of water sample containing F^- ion to the receptor solution. The amount of F^- ions in sea water/mouthwash was determined using a calibration curve which was established by plotting absorbance vs. concentration of F^- ions (Fig. 3.19). The curve showed 1.54 ppm of F^- ions in sea water (215.5 ppm in mouthwash), which is comparable with standard values (WHO Technical Report, 1994).

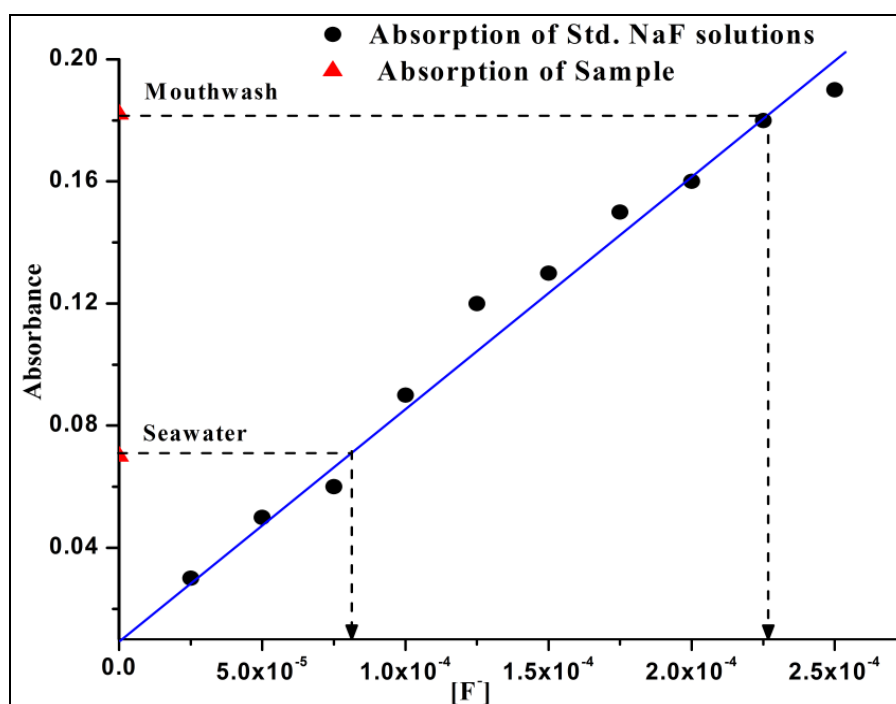


Fig. 3.19 Calibration curve to determine the amount of F^- ions in seawater/mouthwash sample

The $\Delta\lambda_{\max}$ for organic and aqueous solutions of receptors **S2R1-S2R4** upon

addition of TBAF and NaF are summarized in Table 3.2. In case of **S2R1** and **S2R2**, extended conjugation was observed upon binding of F⁻ ion due to the presence of –NO₂ group at *p*- position to phenyl ring and as a result ICT was achieved with a maximum bathochromic shift of 178 nm and 177 nm (149 nm and 147 nm in case of 10% aqueous solution) respectively. However, in case of **S2R2**, the presence of additional –NO₂ group at *p*- position of second phenyl rings did not make much difference in the sensitivity. As the receptor **S2R3** being deficient of –NO₂ group, ICT was not feasible and hence only the broad band centred at 313 nm with a bathochromic shift of 39 nm was observed due to hydrogen bonding on addition of F⁻ ion. The receptor **S2R4** did not showed any shift in absorbance on addition of F⁻ ion. This further confirms the –NH protons are responsible for binding process of F⁻ ion.

Table 3.2 Change in absorption ($\Delta\lambda_{\max}$) of receptors **S2R1-S2R4** (2.5×10^{-5} M) in the presence of F⁻ ion (10 equiv.)

Receptor (R) ^a	λ_{\max}	λ_{\max}	$\Delta\lambda_{\max}$	$\Delta\lambda_{\max}$
	(R+TBAF) ^b	(R+NaF) ^c	(Organic)	(Aqueous)
S2R1	446 nm	417 nm	178 nm	149 nm
S2R2	452 nm	431 nm	177 nm	147 nm
S2R3	313 nm	274 nm	39 nm	0 nm
S2R4	311 nm	311 nm	0 nm	0 nm

^a Absorption spectra were taken for receptors at a concentration of 2.5×10^{-5} M in DMSO. ^b TBAF solution (10 equiv. in dry DMSO) was added to receptor solution (dry DMSO). ^c NaF solution (10 equiv. in H₂O) was added to receptor solution (DMSO:H₂O, 9:1; v/v)

The stoichiometry of the F⁻ ion complexation with receptor **S2R1** in DMSO:H₂O (9:1 v/v) was determined by Benesi-Hildebrand method (Benesi and Hildebrand, 1948) using NaF. This clearly confirmed the formation of a stable 1:2 stoichiometric complex between receptor **S2R1** and F⁻ ions (Fig.3.20).

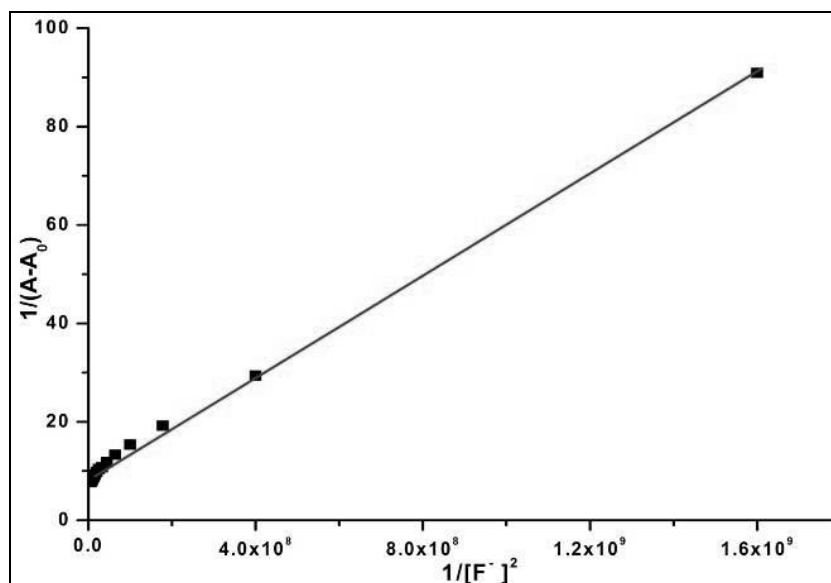


Fig. 3.20 Benesi - Hildebrand plot of receptor **S2R1** binding with F⁻ ion (NaF) associated with absorbance change at 417 nm in DMSO:H₂O (9:1 v/v) solvent

The binding constant was determined using Benesi-Hildebrand equation (Eq. 3.1) for the receptor **S2R1** in organic medium and aqueous solution was found to $4.26 \pm 0.66 \times 10^8 \text{ M}^{-2}$ and $8.64 \pm 0.23 \times 10^7 \text{ M}^{-2}$ respectively. Thus, the receptor **S2R1** strongly binds to the F⁻ ions even in aqueous solutions.

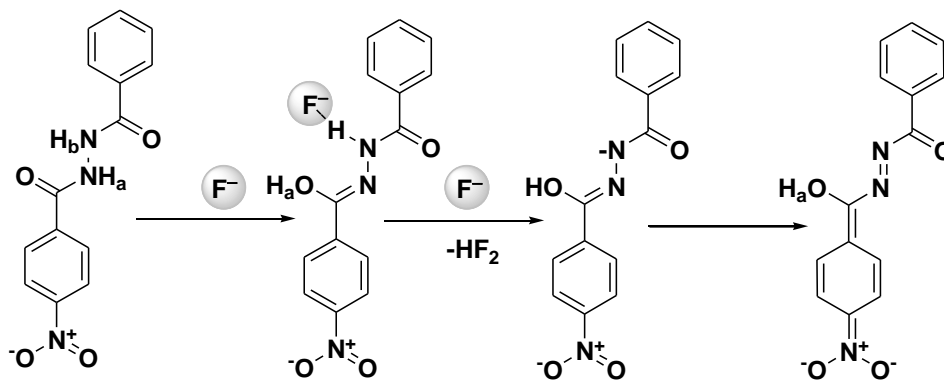
$$\frac{1}{(A - A_0)} = \frac{1}{(A_{max} - A_0)} + \frac{1}{K[F^-]^n(A_{max} - A_0)} \dots \dots \dots (\text{Eq. 3.1})$$

Where, A_0 , A , A_{max} are the absorption considered in the absence of F⁻, at an intermediate, and at a concentration of saturation. K is binding constant, $[F^-]$ is concentration of F⁻ ion and n is the stoichiometric ratio.

3.3.4 Binding mechanism

From the stoichiometric studies it is clear that F⁻ ion detection using receptor **S2R1** is a two-step process. At first, a F⁻ ion binds to receptor through hydrogen bonding and thus a 1:1 adduct is generated to form a **S2R1**···F⁻ complex (Ghosh et al. 2009). The second F⁻ ion causes deprotonation of -NH proton in receptor **S2R1** which resulted in increased electron density over the complex system. This induced a charge separation in the molecule (Scheme 3.5) and hence intramolecular charge transfer (ICT) interaction was increased between electron deficient nitro group and

electron rich $-N^-$ which resulted in the optical colour change (Cho et al. 2005). However, the formation of ICT complex was not observed in case of receptor **S2R3** as it has no electron withdrawing group attached. This resulted in low sensitivity of receptor **S2R3** while detecting the F^- ion.



Scheme 3.5 Predicted mechanism for the fluoride ion binding to receptor **S2R1**

The $-NH$ proton H_a tautomerizes to imidic acid from amide form under basic condition. However, at lower concentration (0-2 equiv.) of TBAF the fast exchange of this proton between two tautomers could be observed and at a higher concentration (5 equiv.) of TBAF, imidic acid tautomer was stabilized.

3.3.5 1H NMR titration studies

As an evidence for the binding mechanism, a 1H NMR titration was carried out in $DMSO-d_6$ using TBAF. The process of tautomerism was clearly observed in 1H NMR titration (Fig. 3.21). Due to the fast exchange between two tautomers, the proton H_a was unavailable for resonance. As a result, the signal at δ 10.9 was completely disappeared. At higher concentration (5 equiv.) the reappearance of signal at δ 10.4 confirmed the formation of stable imidic acid tautomer. Upto 2 equiv. of F^- ion the resonance signal corresponding to H_b (δ 10.65), showed a broadening and splitting patterns in the aromatic region retained. On the other hand, at higher concentration of F^- ion (5 equiv.) the peak corresponding to H_b as well as the splitting pattern in the aromatic region completely disappeared. This indicates the formation of $NH \cdots F^-$ hydrogen bonding followed by deprotonation (Cho et al. 2005) of receptor **S2R1**. Due to the formation of ICT, electron density of the phenyl rings increased and this resulted in upfield shifts in the signals (Boiocchi et al. 2004) of all aromatic

protons. Furthermore, splitting in the signals of aromatic protons had completely disappeared (Fig. 3.21). This observation was due to the fast proton exchange within the molecule.

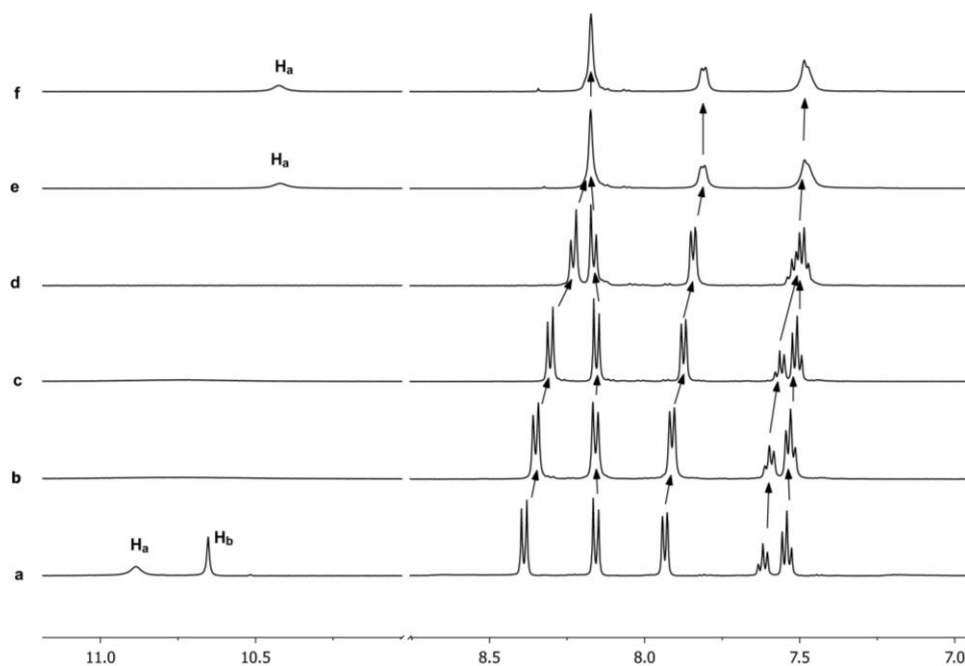


Fig. 3.21 Partial ^1H NMR spectra of receptor **S2R1** in $\text{DMSO-}d_6$ after adding (a) 0, (b) 0.5, (c) 1, (d) 2, (e) 5 and (f) 10 equiv. of TBAF

3.4 CONCLUSIONS

To summarize, the receptors **S2R1**, **S2R2** based on benzohydrazide derivatives were designed and synthesized for the instantaneous and selective detection of inorganic fluoride (NaF) in aqueous media. The receptors possess high sensitivity towards F^- ion with a detection limit of 0.5 ppm in aqueous media which is much less than WHO permissible level (1 ppm) in drinking water. The mechanism followed for the detection process is ICT and formation of stable imidic acid tautomer which was evidenced by ^1H NMR titrations. Hence on interaction with F^- ion the receptors **S2R1** and **S2R2** showed brilliant colour change from colourless to yellow with a large bathochromic shift of 149 nm and 147 nm respectively. These derivatives proved themselves as potent colorimetric fluoride ion receptors by detecting the presence of fluoride in sea water and commercial mouthwash.

CHAPTER 4

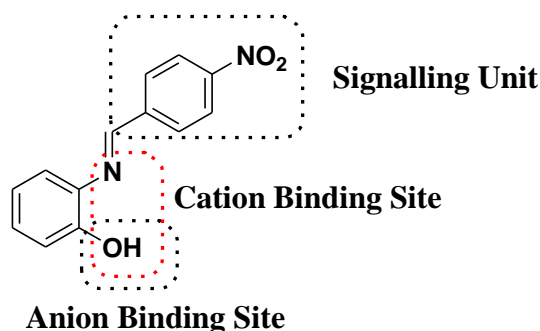
***DESIGN AND SYNTHESIS OF AMINOPHENOL BASED
FLUORIDE ION RECEPTOR, SOLVATOCHROMIC
STUDY AND ITS MOLECULAR SWITCH APPLICATION***

In this chapter, the design, syntheses and characterization of aminophenol based new colorimetric receptors for fluoride ion detection have been discussed in detail. The colorimetric anion sensing properties, detection mechanism solvatochromic effect and logic gate application of these receptors have been studied.

4.1 INTRODUCTION

Being an essential component of molecular computing operations and molecular devices, the molecular logic gates for converting chemical input signal into the measurable output signals has become an exciting research area in supramolecular chemistry. Subsequently, increasing attention was attained for the logic gate applications based on anion/cation detecting receptors (Gunnlaugsson et al. 2001; de Silva and McClenaghan 2004; Rosenbaum et al. 2011; Mandal et al. 2012; Elstner et al. 2012). Various types of logic gate functions can be achieved by applying two-input systems. Even though, molecular analogues of many logic gate functions (based on two-input systems) are reported in the literature (de Silva et al. 1994; D'Souza 1996; Asakawa et al. 1997; Crediet et al. 1997; de Silva et al. 1999; Baytekin and Akkaya 2000; Banthia and Samanta 2005; Singh and Kumar 2006; Suresh et al. 2007a; Lee et al. 2007; Suresh et al. 2007b; Luxami and Kumar 2008; Suresh et al. 2008; Magri et al. 2009; Zhang et al. 2012; Mahato et al. 2012), only few of them are based on colorimetric receptors (Upadhyay et al. 2010; Liu et al. 2011; Luxami and Kumar 2012; Kaur and Kumar 2012; Luxami and Kumar 2012). Accordingly, the colorimetric receptor based molecular logic gates attained interest among supramolecular chemists. Further, molecular logic gate application gains attention as it can be used for molecular switching applications (Kim et al. 2012). The receptors which can shift between two or more stable states as a response to change in the physical or chemical parameters are called molecular switches. These molecular switches are good as well as simple examples for the molecular machines.

The receptors in this chapter have been designed in such a way that it is capable of detecting anion as well as cation, to be specific F^- ions and Cu^{2+} ions with naked eye. The receptor **S3R1** (**S 4.1**) encompasses hydroxyl ($-OH$) functional group, which detects F^- ion by deprotonation mechanism and phenolic oxygen ($-O$) along with imine nitrogen ($=N$) for the detection of Cu^{2+} via complex formation.



S 4.1

The **S3R1** served as effective receptor for the detection of F⁻ ion as well as Cu²⁺ with the logic gate function. In addition, this receptor showed remarkable solvatochromic property by displaying different colours in different solvents only in presence of F⁻ ion. This solvatochromic property of the receptor molecule has indispensable applications in many fields of chemistry including characterization of mixed solvent systems, solid surfaces and polymers, chemical sensors to detect the presence of water in polymers and to study the behaviour of solute-solvent interactions in supercritical fluids (Nigam and Rutan 2001). The receptor **S3R2** was synthesised to verify the substitution position of -OH functional group in detection process and receptor **S3R3** was synthesised to examine the role of -OH as binding site in detection process.

4.2 EXPERIMENTAL

4.2.1 Materials and methods

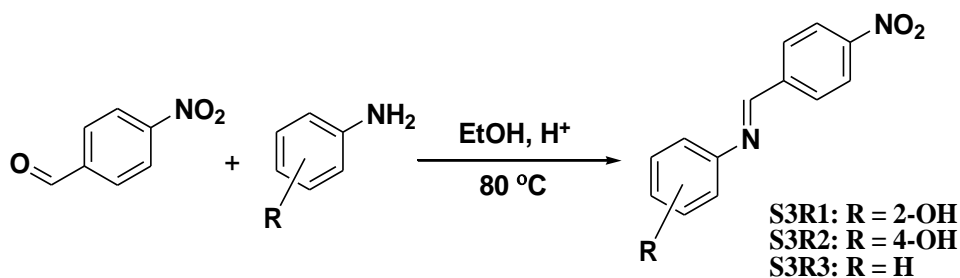
All chemicals were purchased from Sigma-Aldrich, Alfa Aesar or from Spectrochem and used without further purification. All solvents were procured from SD Fine, India with HPLC grade and used without further distillation.

The ¹H NMR spectra were recorded on a Bruker, Avance II (500 MHz) instrument using TMS as internal reference and DMSO-d₆ as solvent. The raw FID data was processed with MestReNova 7.0.0-8331 software. Resonance multiplicities are described as s (singlet), br s (broad singlet), d (doublet), t (triplet), q (quartet) and m (multiplet). The chemical shifts (δ) are reported in ppm and coupling constant (J) values are given in Hz. Melting points were determined with Stuart- SMP3 melting-point apparatus in open capillaries and are uncorrected. IR spectra were recorded on a

Thermo Nicolet Avatar-330 FT-IR spectrometer; signal designations: s (strong), m (medium), w (weak), br.m (broad medium) and br.w (broad weak). Mass spectra were recorded on Waters Micromass Q-Tof micro spectrometer with ESI source. The SCXRD was performed on Bruker AXS APEX II system. UV-vis spectroscopy was carried out with Ocean Optics SD2000-Fibre Optics Spectrometer and Analytikjena Specord S600 Spectrometer in standard 3.5 mL quartz cells (2 optical windows) with 10 mm path length. Elemental analyses were done using Flash EA1112 CHNS analyser (Thermo Electron Corporation). All reactions were monitored by TLC on pre-coated silica gel 60 F254 plates which were procured from Merck.

4.2.2 Synthesis of receptors **S3R1**, **S3R2** and **S3R3**

A mixture of 4-nitrobenzaldehyde (1.32 mmol) and substituted amines (2.69 mmol) reacted in ethanol under reflux for 5h. The reaction was catalysed by a drop of acetic acid. The reaction mixture was cooled to room temperature. The solid formed was filtered and washed with ethanol to obtain the pure compounds (Scheme 4.1).



Scheme 4.1 Synthesis of **S3R1**, **S3R2** and **S3R3**

The single crystal of the receptors **S3R1** suitable for X-ray diffraction analysis was obtained by slow evaporation of dichloromethane solution at room temperature and the single crystals of receptors **S3R2** and **S3R3** were obtained directly from reaction media (ethanol used as solvent). The ORTEP diagrams (50% probability) of the receptor **S3R1**, **S3R2** and **S3R3** are given in Fig. 4.1.

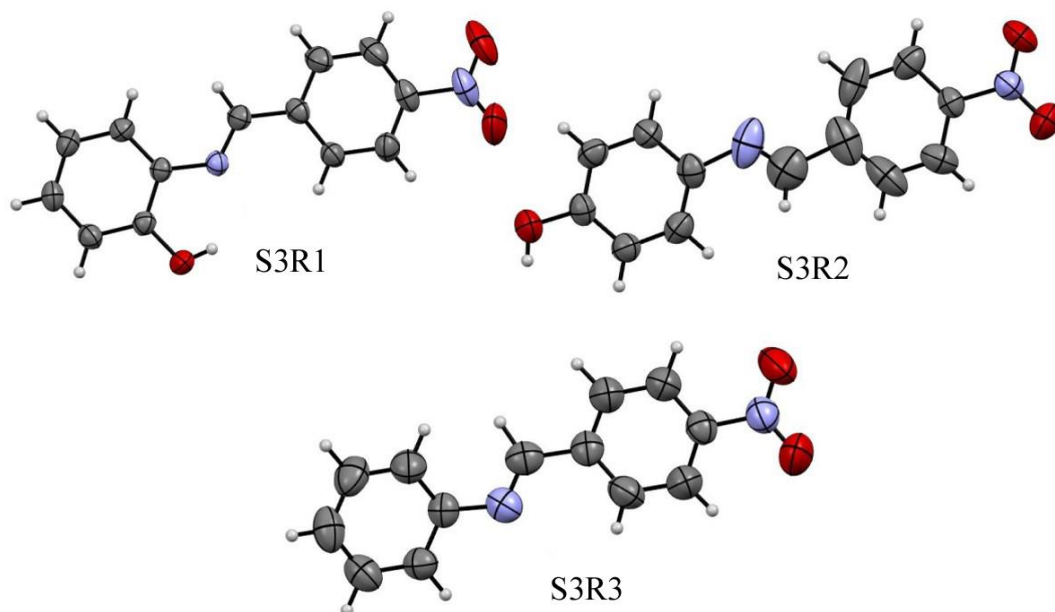


Fig. 4.1 The ORTEP diagrams (50% probability) receptors **S3R1**, **S3R2** and **S3R3**

The receptors **S3R1** and **S3R3** were crystallised in monoclinic lattice whereas **S3R2** crystallised in triclinic lattice. Detailed crystallographic data of receptor **S3R1**, **S3R2** and **S3R3** are given in the Table 4.1.

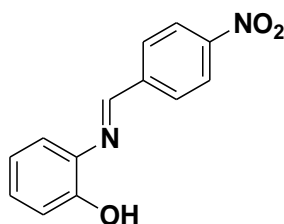
Table 4.1 Crystallographic data of receptor **S3R1**, **S3R2** and **S3R3**

Receptor	S3R1	S3R2	S3R3
CCDC No	912057	939306	939305
Chemical formula	C ₁₃ H ₁₀ N ₂ O ₃	C ₁₃ H ₁₀ N ₂ O ₃	C ₁₃ H ₁₀ N ₂ O ₂
Formula weight	242.23	242.23	226.23
Crystal System	Monoclinic	Triclinic	Monoclinic
Space group	P2(1)/c	P $\bar{1}$	P2(1)/n
a (Å)	11.9767 (8)	12.3048(9)	14.6480(2)
b (Å)	5.9302 (4)	13.3933(10)	10.8265(2)
c (Å)	16.1269 (10)	15.7190(12)	14.7278(2)
α (°)	90.00	72.812(4)	90.00

β (°)	96.635 (2)	67.370(4)	101.940 (2)
γ (°)	90.00	76.718(4)	90.00
V (Å) ³	1137.73 (13)	2264.4(3)	2285.10 (6)
Z	4	8	8
Crystal size	0.47 × 0.30 × 0.27	0.45 × 0.31 × 0.21	0.47 × 0.33 × 0.26
F (000)	504	1008	944
R-factor (%)	5.23	9.72	6.85

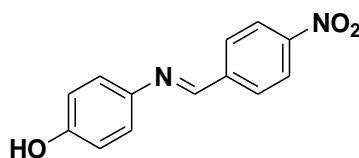
All intermediates and receptors were characterized by spectral analysis. The characterization data have been compiled and given below.

(E)-2-(4-nitrobenzylideneamino)phenol (S3R1)



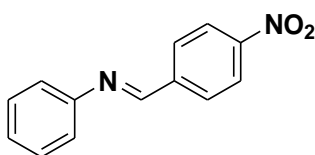
Yield: 79%; m.p.: 165 - 166°C. Elemental analysis Calculated for C₁₃H₁₀N₂O₃ (%): C 64.46, H 4.16, N 11.56. Experimental: C 64.26, H 4.30, N 11.60. ¹H NMR (DMSO-*d*₆): δ 9.27(s, 1H, -OH); δ 8.88(s, 1H, =CH); δ 8.34 (d, 2H, Ar-H, *J*=8Hz), δ 8.30 (d, 2H, Ar-H, *J*=8Hz), δ 7.30(d, 1H, Ar-H, *J*=7.5 Hz), δ 7.16 (t, 1H, Ar-H, *J*=7.25Hz), δ 6.95 (d, 1H, Ar-H, *J*=8 Hz), δ 6.86 (t, 1H, Ar-H, *J*=7 Hz). FT-IR in cm⁻¹: 3367.3 (m), 1586.2 (m), 1508.8 (m), 1331.7 (s), 1230.2 (m), 1096.4 (w), 1027.5 (w), 779.9 (m). MS (ESI) *m/z* Calculated: 243.2380 [M+H]⁺ Experimental: 243.2590 [M+H]⁺

(E)-4-(4-nitrobenzylideneamino)phenol (S3R2)



Yield: 80%; m.p.: 174 - 175°C. Elemental analysis Calculated for $C_{13}H_{10}N_2O_3$ (%): C 64.46, H 4.16, N 11.56. Experimental: C 64.32, H 4.28, N 11.48. 1H NMR (DMSO- d_6): δ 9.72(s, 1H, -OH), δ 8.77 (s, 1H, =CH), δ 8.32 (d, 2H, Ar-H, $J=8$ Hz), δ 8.12 (d, 2H, Ar-H, $J=8.5$ Hz), δ 7.32(d, 2H, Ar-H, $J=8.5$ Hz), δ 6.85 (d, 2H, Ar-H, $J=8$ Hz). FT-IR in cm^{-1} : 3434.3 (s), 1582.7 (m), 1500.6 (s), 1328.4 (s), 1252.5 (m), 1197.9 (m), 1195.7 (w).

(E)-N-(4-nitrobenzylidene)benzenamine (S3R3)



Yield: 63%; m.p.: 94 - 95°C. Elemental analysis Calculated for $C_{13}H_{10}N_2O_2$ (%): C 69.02, H 4.46, N 12.38. Experimental: C 68.98, H 4.50, N 12.39. 1H NMR (DMSO- d_6): δ 8.79 (s, 1H, =CH), δ 8.35 (d, 2H, Ar-H, $J=8.5$ Hz), δ 8.19 (d, 2H, Ar-H, $J=8.5$ Hz), δ 7.47 (t, 2H, Ar-H, $J=7.5$ Hz), δ 7.29- δ 7.35 (m, 3H, Ar-H). FT-IR in cm^{-1} : 3063.5 (w), 1588.1 (m), 1510.3 (s), 1330.6 (s).

The representative spectra of receptors have been given below.

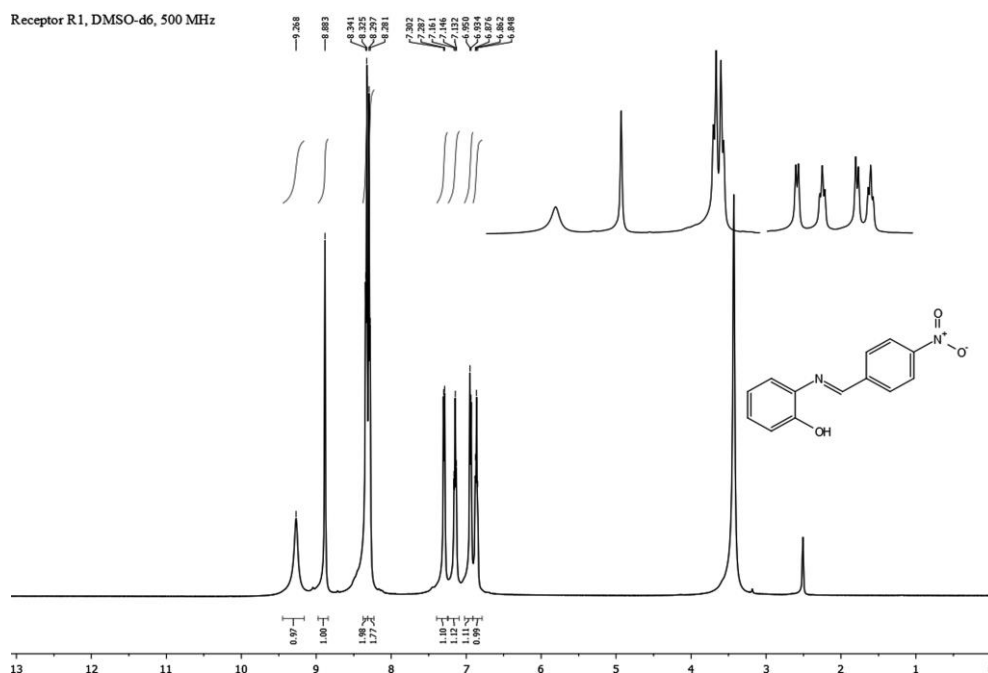
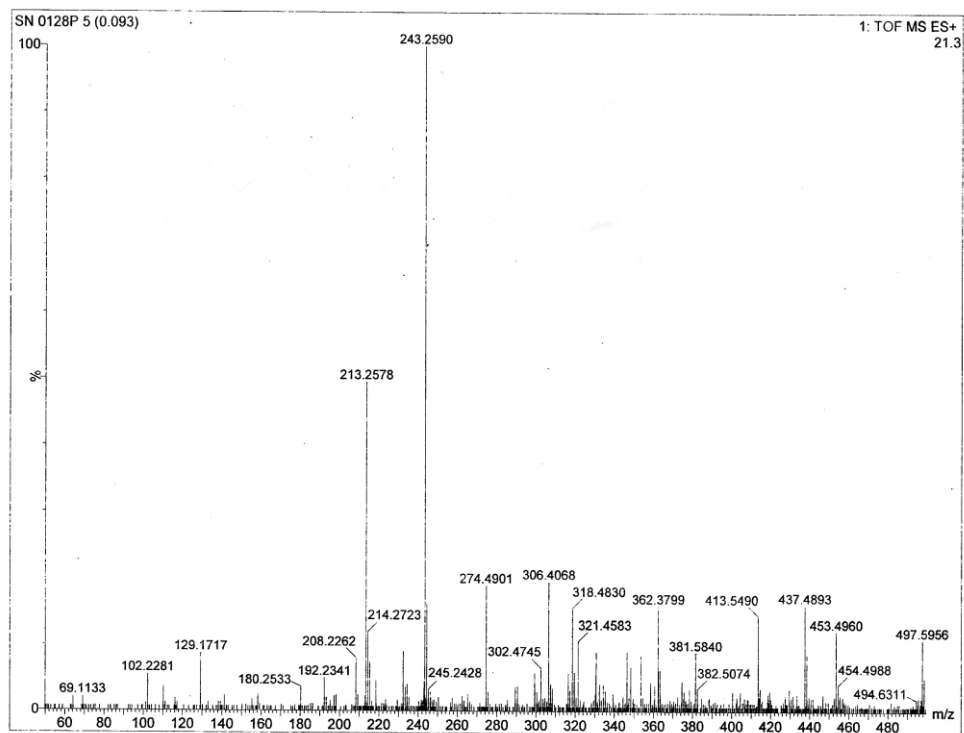
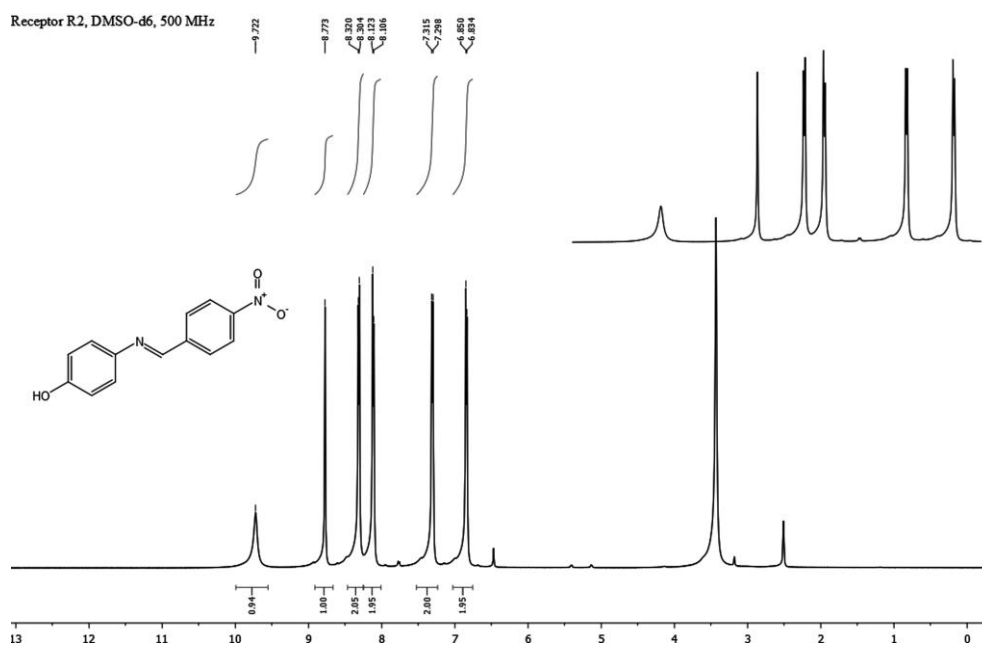


Fig. 4.2 1H NMR spectrum of **S3R1**

**Fig. 4.3** ESI-MS spectrum of S3R1**Fig. 4.4** ¹H NMR spectrum of S3R2

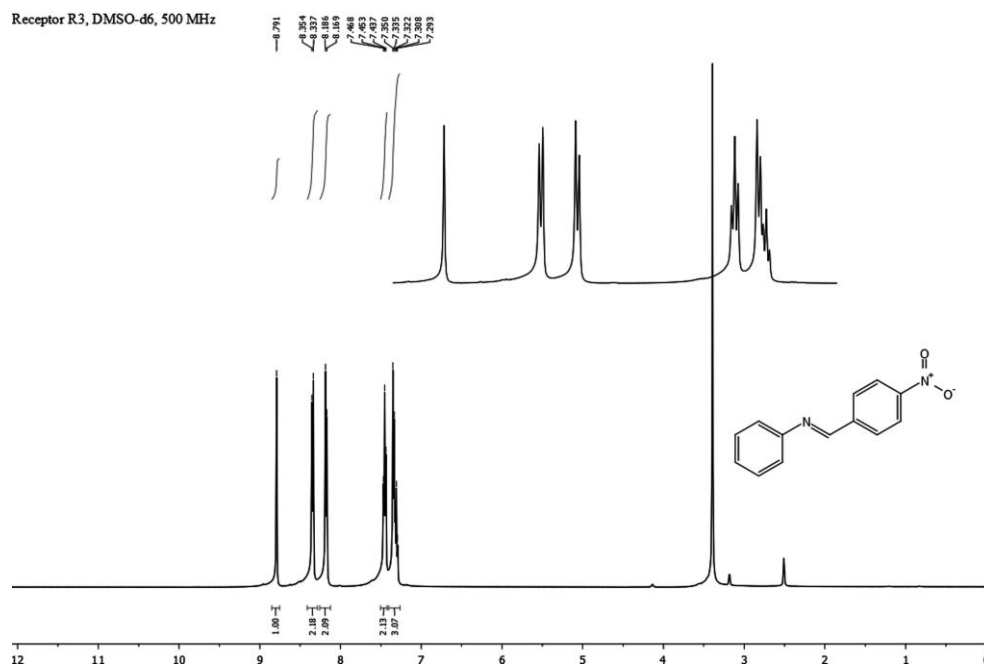


Fig. 4.5 ^1H NMR spectrum of S3R3

4.2.3 Stoichiometric ratio determination using Job's plot method

A Job plot is used to determine the binding stoichiometry. In this method, the total molar concentration of anion and receptor are kept constant. However, the molar ratio of the anion as well as the receptor is continuously varied. The UV-vis absorbance was measured for each fraction. This absorbance was plotted against the mole fractions of the two components. The maximum absorbance on the plot corresponds to the stoichiometry of the two species.

4.3 RESULTS AND DISCUSSION

4.3.1 Colorimetric detection of anions

Initially, the receptors S3R1 and S3R2 were evaluated for colorimetric detection of F^- ions over other anions (chloride, bromide, iodide, nitrate, hydrogensulphate, dihydrogenphosphate and acetate) in dry DMSO solvent. Both the receptors have hydroxyl ($-\text{OH}$) functionality as electron donor and nitro ($-\text{NO}_2$) functionality as electron acceptor. Due to this donor-acceptor (D-A) interactions these receptors are pale yellow in colour. These receptors (5×10^{-5} M) were treated with tetrabutylammonium (TBA) salt of different anions (1 equiv.) in DMSO. A significant colour change from pale yellow to blue (receptor S3R1) and greenish blue (receptor

S3R2), was observed instantaneously with the addition of F^- ion. A slight colour variation from pale yellow to greenish yellow in case of receptor **S3R1** and pale yellow to dark yellow in case of receptor **S3R2** were observed upon adding the acetate ion. On the other hand, no colour change was noticed on addition of other anions (Fig. 4.6 and Fig. 4.7).

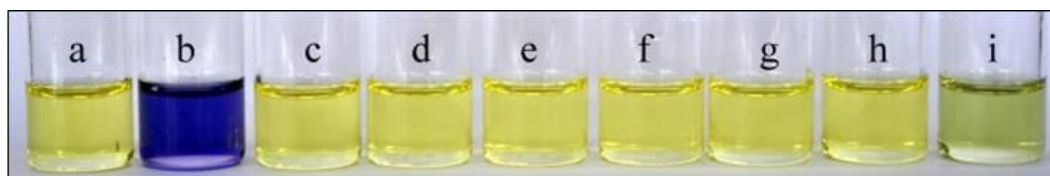


Fig. 4.6 Change in colour after adding 1 equiv. of TBA anions to receptor solution in DMSO (5×10^{-5} M); (a) Free **S3R1**, (b) F^- , (c) Cl^- , (d) Br^- (e) I^- , (f) NO_3^- , (g) HSO_4^- , (h) $H_2PO_4^-$ and (i) AcO^-

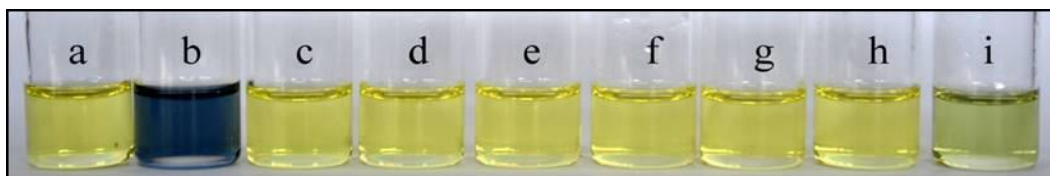


Fig. 4.7 Change in colour of **S3R2** (5×10^{-5} M) in dry DMSO with the addition of 1 equiv. of TBA anions; (a) Free **S3R2**, (b) F^- , (c) Cl^- , (d) Br^- (e) I^- , (f) NO_3^- , (g) HSO_4^- , (h) $H_2PO_4^-$ and (i) AcO^-

In order to examine the selectivity towards F^- ion over other anions, 1 equiv. of F^- ion was added to the receptor **S3R1** in presence of other anions such as Cl^- , Br^- , I^- , NO_3^- , HSO_4^- and $H_2PO_4^-$ ions. The presence of any other anions virtually makes no difference on colorimetric detection of the F^- ion (Fig. 4.8). Thus, the receptor **S3R1** could selectively detect the fluoride ion even in presence of other competing anions.

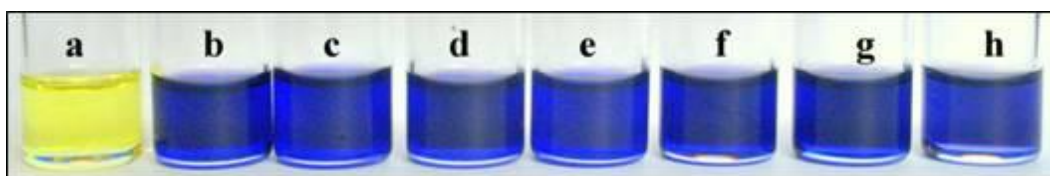


Fig.4.8 Competitive study of receptor **S3R1** (5×10^{-5} M) in DMSO by adding 1 equiv. F^- ion and 1 equiv. of other anions; (a) Free **S3R1**, (b) F^- , (c) $Cl^- + F^-$, (d) $Br^- + F^-$, (e) $I^- + F^-$, (f) $NO_3^- + F^-$, (g) $HSO_4^- + F^-$ and (h) $H_2PO_4^- + F^-$

4.3.2 UV-vis spectral studies of receptors

The colorimetric selectivity of receptors **S3R1** and **S3R2** for the detection of F^- ion was further confirmed using UV-vis spectroscopy (Fig. 4.9).

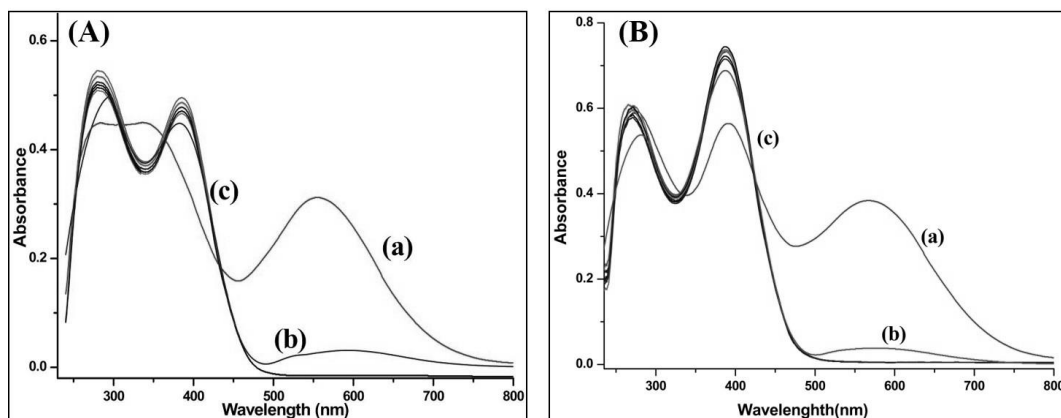


Fig.4.9 UV-vis changes of (A) **S3R1** and (B) **S3R2** in DMSO (5×10^{-5} M) after adding 20 equiv. of (a) F^- ion, (b) AcO^- ion and (c) other anions as TBA salts

As a part of quantitative analysis, the UV-vis spectrophotometric titration of receptor **S3R1** with TBAF in dry DMSO was carried out. On gradual increasing concentration of F^- ion, the intensity of peaks at 282 nm corresponding to imine ($-N=C-$) linkage and 385 nm corresponding to $-OH$ group, decreased gradually. This was followed by appearance of new bathochromic bands at 339 nm and 555 nm (Fig. 4.10, A).

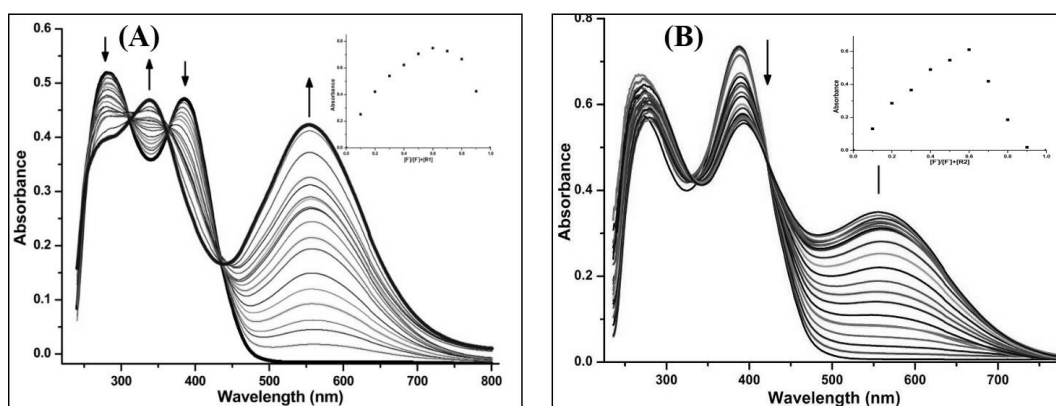
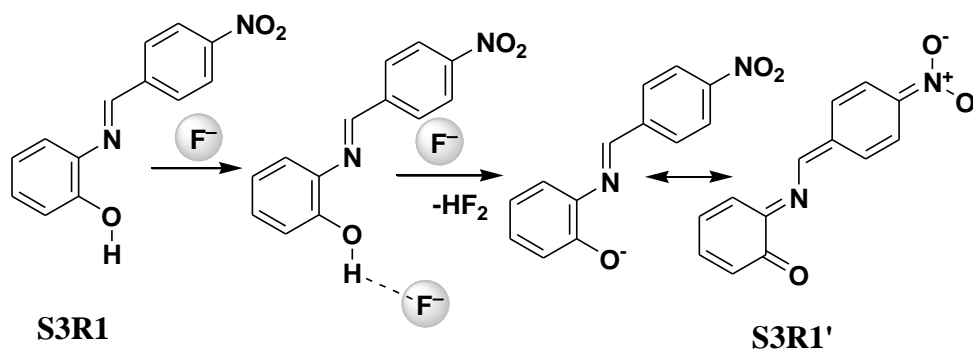


Fig. 4.10 UV-vis spectra of (A) **S3R1** and (B) **S3R2** (5×10^{-5} M) with increasing concentration of TBAF (0–25 equiv.) in dry DMSO; Inset: Jobs plot for **S3R1** and **S3R2** with F^- ion at 555 nm and 558 nm in dry DMSO respectively

The development of new band at 339 nm was attributed to the formation of exocyclic imine when the receptor undergoes enol to keto tautomerisation (due to the deprotonation of 2-hydroxyl group) and the new band at 555 nm was ascribed to the development of Intramolecular Charge Transfer (ICT) transition. This constant decrease of two absorption bands and generation of two new absorption bands resulted in the formation of three clear isosbestic points at 309 nm, 361 nm and 433 nm which evidently suggests the generation of two species in the system during the detection process. In case of receptor **S3R2**, the titration resulted in constant decrease in the intensity of absorption band at 388 nm due to the deprotonation of hydroxyl group. Simultaneously, a new bathochromic band at 558 nm was appeared which was attributed to the generation of ICT transition (Fig. 4.10, B).

4.3.3 Binding mechanism of anion

The stoichiometry of receptor- F^- ion system was determined by Jobs plot obtained from UV-vis spectrophotometric titration data for receptor **S3R1** at 555 nm and **S3R2** at 558 nm in DMSO solution (Fig. 4.10, inset). A maximum absorbance was observed, when the mole fraction was 0.66. This confirms the formation of 1:2 (Host/Guest) stoichiometric ratios between receptors and F^- ions. Hence, it is evident that F^- ion detection using these receptors is a two-step process. The proposed mechanism for receptor **S3R1** is as shown in Scheme 4.2.



Scheme 4.2 Proposed mechanism for fluoride ion binding to receptor **S3R1**

At the first instance, F^- ion binds through hydrogen bonding to the hydroxyl proton of receptor **S3R1** resulting in 1:1 adduct to give **S3R1**•• F^- complex (Ghosh et al. 2009). In the next step the second F^- ion induces deprotonation of phenolic $-OH$ proton of receptor **S3R1** and as a result, the electron density over the deprotonated

receptor **S3R1** was increased. Thus, the charge separation in the receptor was introduced which resulted in ICT transition between the electron deficient $-\text{NO}_2$ group at *p*- position and electron rich $-\text{O}^-$ which lead to intense colorimetric change (Cho et al. 2005).

4.3.4 ^1H NMR titration studies

^1H NMR titration was carried out in dry $\text{DMSO-}d_6$ to confirm the binding mechanism (Fig. 4.11). Upon addition of 0.5 equiv. TBAF, the $-\text{OH}$ peak at δ 9.26 (H_a) disappeared completely and thus confirms the deprotonation of phenolic $-\text{OH}$ (Bharadwaj et al. 2009).

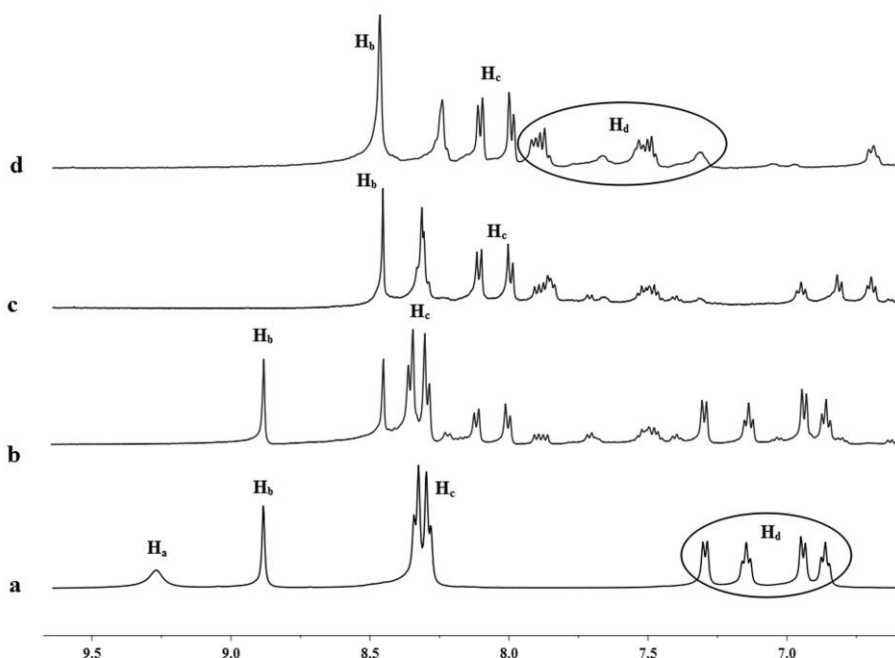


Fig. 4.11 Partial ^1H NMR titration spectra of receptor **S3R1** with F^- ion at different concentrations in $\text{DMSO-}d_6$; (a) 0, (b) 0.5, (c) 1.0 and (d) 2.0 equiv. TBAF

The signal H_b at δ 8.88 corresponding to imine $-\text{CH}-$ experienced upfield shift to δ 8.45 due to the formation of exocyclic double bond and aromatic protons of 4-nitrophenyl group at δ 8.3, δ 8.33 were shifted to δ 8.10, δ 7.98 respectively (H_c). These upfield shifts represent the increase in electron density over the 4-nitrophenyl group of receptor molecule upon F^- ion binding. In contrast the protons of 2-aminophenol group shifted from δ range 6.86-7.29 (H_d) to δ range 7.30-8.87. This downfield shift was due to the decrease in electron density over the 4-aminophenol

group of the receptor **S3R1** which resulted in the deshielding of corresponding protons on F⁻ ion binding. Therefore the hydroxyl phenyl group acts as an electron donor and the nitrophenyl group acts as an electron acceptor, thus forming an ICT transition. Furthermore, at 0.5 equiv. and 1.0 equiv., the ¹H NMR illustrates both structures **S3R1** and **S3R1'** (Scheme 4.2), wherein the receptor undergoes keto-enol tautomerism. Finally, the keto tautomer gets stabilized at 2 equiv. of F⁻ ion.

4.3.5 Solvatochromic studies

Astonishingly, when 1 equiv. of F⁻ ion was added to the receptor **S3R1** solution in dry ACN (5×10^{-5} M), a colour change from pale yellow to pink was observed. This dissimilarity in colour change (in DMSO pale yellow to blue and in ACN pale yellow to pink) was due to the solvatochromic effect of receptor **S3R1**. This study was further extended to other aprotic solvents such as 1,4-dioxane, tetrahydrofuran (THF), dichloromethane (DCM), Acetone and DMSO where the receptor **S3R1** showed different coloration (Fig. 4.12) only in presence of F⁻ ion with respect to the solvent polarity. The colour of the receptor **S3R1** was changed from pale yellow to red in 1,4-dioxane, brown in THF and DCM, purple in acetone, pink in ACN and blue in DMSO. Similar trend was observed in case of **S3R2** where the colour was changed from pale yellow to orange in 1,4-dioxane, dark yellow in THF and DCM, dark brown in acetone, light brown in ACN and blue in DMSO upon addition of 1 equiv. of F⁻ ions (Fig. 4.13). As receptor solution does not have any charge separation and charge transfer (CT) transitions, it did not show any solvatochromism in the absence of F⁻ ion. However, addition of F⁻ ion to the receptor solutions induced charge separation. Therefore, charge transfer transition was established due to which receptor attains different dipole moments in its ground and lower energy singlet excited state. These newly established dipole moments were interacted by the solvent dipole moments to change the energy levels of receptor and as solvent polarity increased these energy levels decreased. As a result the peaks corresponding to CT transitions in UV-vis spectroscopy will red shifted (positive solvatochromism; Hadjmohammadi et al. 2008; Marini et al. 2010; Homocianu et al. 2011; Saroj et al. 2011) with increasing solvent polarity. Same mechanism is responsible for the solvatochromism in receptor **S3R2**.

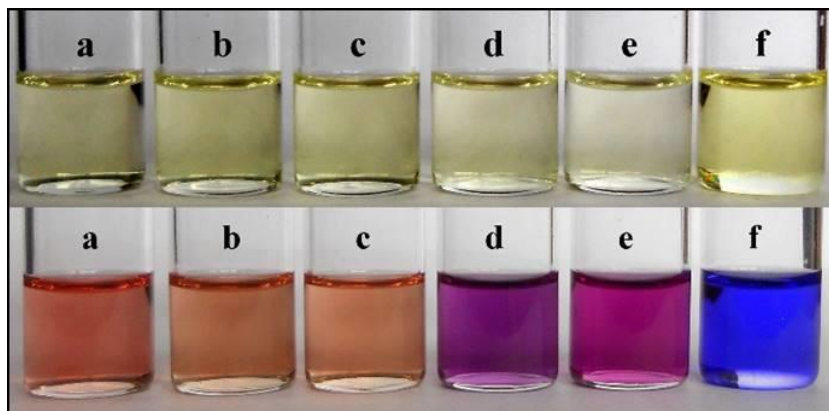


Fig. 4.12 Solvatochromism in **S3R1** upon adding 1 equiv. of F^- ions in different solvents; Top row: **S3R1** (5×10^{-5} M) in different solvents. Bottom row: **S3R1**+ F^- ions; (a) 1,4-dioxane, (b) THF, (c) DCM, (d) Acetone, (e) ACN and (f) DMSO

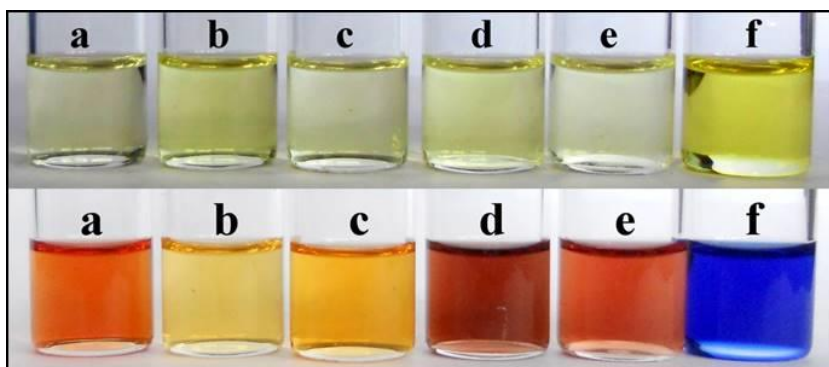


Fig. 4.13 Solvatochromism in **S3R2** upon adding 1 equiv. of F^- ions in different solvents; Top row: **S3R2** (5×10^{-5} M) in different solvents. Bottom row: **S3R2**+ F^- ions; (a) 1,4-dioxane, (b) THF, (c) DCM, (d) Acetone, (e) ACN and (f) DMSO

4.3.6 Application of solvatochromism

The percentage composition of solvent mixture is generally determined by measuring their physical properties such as viscosity, refractive index or density. On the other hand, the photophysical property such as solvatochromism is not much explored to determine composition of the solvent mixture. The receptor **S3R1** being solvatochromic in presence of F^- ions, was applied to determine the percentage composition of two different solvents. This experiment was demonstrated by inspecting colour change of receptor **S3R1** upon adding F^- ions in proportionate mixture of DCM and DMSO. The receptor **S3R1** was dissolved in a mixture of two solvents (by varying compositions between 0% and 100% of DMSO in DCM) to

prepare 5×10^{-5} M solution. Upon adding F^- ions (10 equiv.) to each solution, a colour change between brown and blue was observed (Fig. 4.14).



Fig. 4.14 Colour change of **S3R1** with varying composition of DMSO in DCM on adding F^- ions; (a) 0% i.e. 100% DCM, (b) 20%, (c) 40%, (d) 60%, (e) 80% of DMSO in DCM and (f) 100% of DMSO

This colorimetric change was confirmed with the UV-vis spectroscopy wherein the bathochromic shift in λ_{\max} was observed with the increasing percentage of DMSO in DCM (Fig. 4.15). A shift of approximately 7.5 nm in λ_{\max} was observed for each 20% increase of DMSO in the solvent mixture.

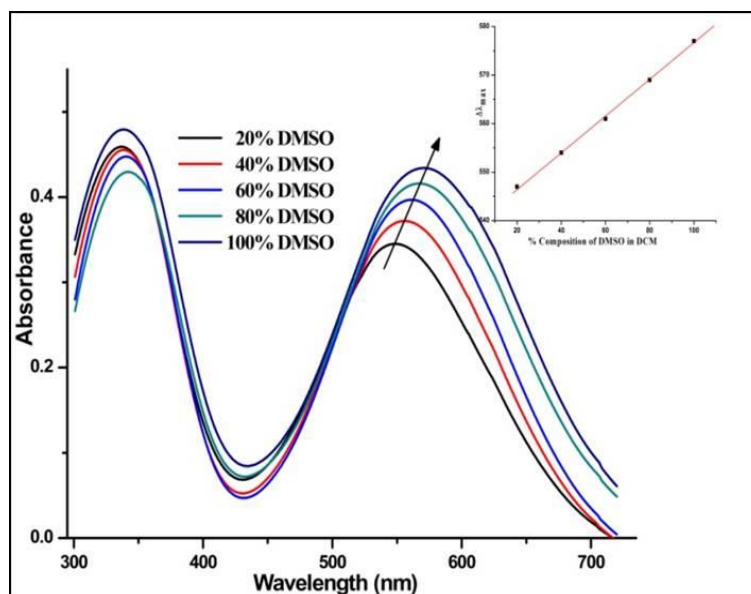


Fig. 4.15 UV-vis changes of **S3R1** (5×10^{-5} M) on adding F^- ions with varying compositions of DMSO in DCM; Inset: Calibration curve plotted with % composition of DMSO in DCM vs. Shift in λ_{\max}

A calibration curve was plotted with this bathochromic shift and the percentage composition of DMSO in DCM (Fig. 4.15, inset). A linear graph was

obtained with the increasing percentage of DMSO in DCM. The percentage composition of unknown solvent mixture (DMSO:DCM) can be easily determined using this calibration curve.

4.3.7 Detailed study in ACN solvent

The selectivity of receptor **S3R1** and **S3R2** towards F^- ion in ACN followed the same trend as in DMSO solution. When the ACN solution of receptors **S3R1** and **S3R2** (5×10^{-5} M) were treated with TBA salt of different anions (1 equiv.), only the addition of F^- ion induced instantaneous colour change from pale yellow to pink (Fig. 4.16) and pale yellow to salmon (Fig. 4.17) respectively, whereas the other anions did not persuade any colour change.

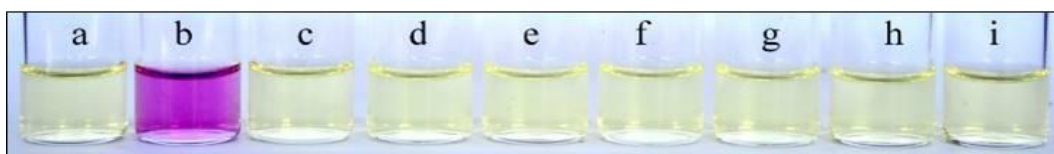


Fig. 4.16 Change in colour after adding 1 equiv. of different anions to **S3R1** in ACN (5×10^{-5} M); (a) Free **S3R1**, (b) F^- , (c) Cl^- , (d) Br^- (e) I^- , (f) NO_3^- , (g) HSO_4^- , (h) $H_2PO_4^-$ and (i) AcO^-

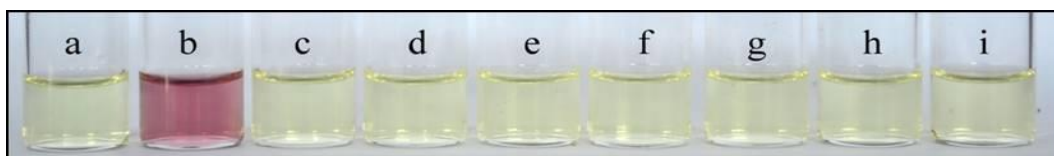


Fig. 4.17 Change in colour after adding 1 equiv. of different anions to **S3R2** solution in ACN (5×10^{-5} M); (a) Free **S3R2**, (b) F^- , (c) Cl^- , (d) Br^- (e) I^- , (f) NO_3^- , (g) HSO_4^- , (h) $H_2PO_4^-$ and (i) AcO^-

The UV-vis titration was carried out for receptor **S3R1** in dry ACN solution. On increasing concentration of F^- ion, the peak at 284 nm increased slightly due to the change in $\pi \rightarrow \pi^*$ transition. On the other hand, the peak at 375 nm was decreased constantly and a new bathochromic band centred at 511 nm was developed, thus forming two clear isosbestic points at 350 nm and 400 nm (Fig. 4.18, A). This new peak developed at 511 nm was ascribed to the formation of ICT transition.

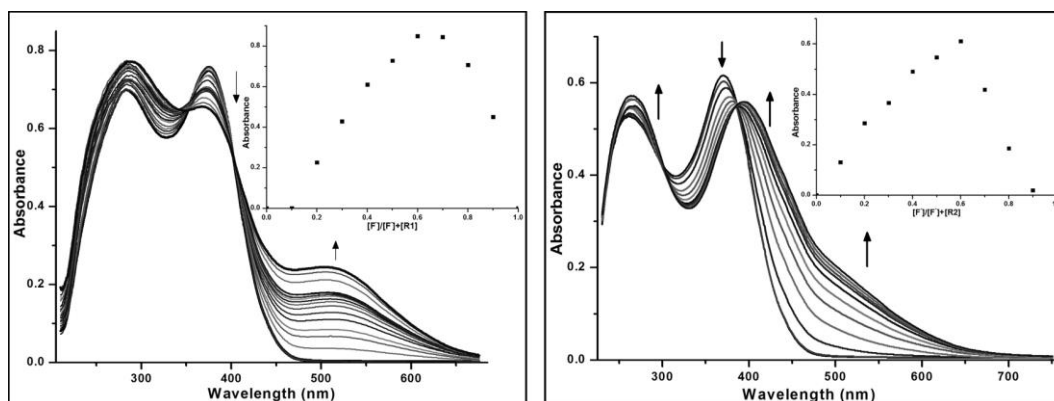


Fig. 4.18 UV-vis spectra of **S3R1** and **S3R2** (5×10^{-5} M) in ACN with increasing concentration of TBAF (0–25 equiv.); Inset: Jobs plot for **S3R1** and **S3R2** with F^- ion at 511 nm and 500 nm in dry ACN respectively

The gradual addition of F^- ion to receptor **S3R2** (5×10^{-5} M) in ACN resulted in the bathochromic shift of absorption band from 371 to 393 nm with a broadened band centred at 500 nm, along with the formation of two isosbestic points at 299 nm and 385 nm (Fig. 4.18, B). In contrast, the molecule **S3R3**, which lacks hydroxyl ($-OH$) functional group, not showed any colour change (Fig. 4.19) neither in DMSO nor in ACN (Fig. 4.20). This clearly indicates that the phenolic $-OH$ is binding site for F^- ion and hence responsible for colorimetric detection.

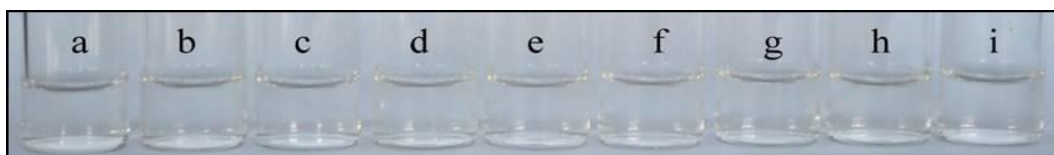


Fig. 4.19 Change in colour of **S3R3** (5×10^{-5} M) in DMSO with adding 1 equiv. of TBA anions; (a) Free **S3R3**, (b) F^- , (c) Cl^- , (d) Br^- (e) I^- , (f) NO_3^- , (g) HSO_4^- , (h) $H_2PO_4^-$ and (i) AcO^-

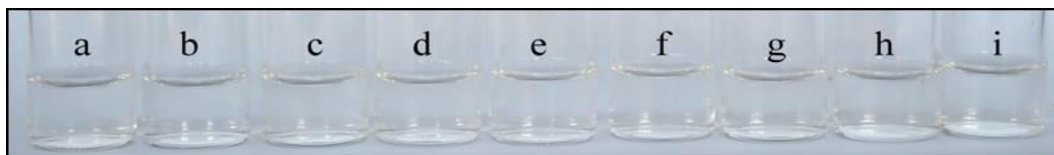


Fig. 4.20 Change in colour of **S3R3** (5×10^{-5} M) in ACN after adding of 1 equiv. of TBA anions; (a) Free **S3R3**, (b) F^- , (c) Cl^- , (d) Br^- (e) I^- , (f) NO_3^- , (g) HSO_4^- , (h) $H_2PO_4^-$ and (i) AcO^-

The shift in absorption maxima after addition of F^- ion to receptor solutions in dry ACN and dry DMSO is summarised in Table 4.2. The 170 nm shift in DMSO over 136 nm in ACN for receptor **S3R1**, confirms the stronger binding of F^- ion due to the establishment of more stable ICT transition in DMSO. The binding constant was calculated using Benesi-Hildebrand equation (Benesi and Hildebrand 1949) and found to be $7.15 \pm 0.31 \times 10^6 \text{ M}^{-2}$ for DMSO and $2.13 \pm 0.13 \times 10^6 \text{ M}^{-2}$ for ACN. This indicates the binding of F^- ion to the receptor is much stronger in case of DMSO than ACN.

Table 4.2 Change in absorption ($\Delta\lambda_{\text{max}}$) of receptors **S3R1-S3R3** ($5 \times 10^{-5} \text{ M}$) in the presence of TBAF

Receptor	$\lambda_{\text{max}}(\text{ACN})^a$	$\lambda_{\text{max}}(\text{DMSO})^b$	$\Delta\lambda_{\text{max}}(\text{ACN})$	$\Delta\lambda_{\text{max}}(\text{DMSO})$
S3R1	511 nm	555 nm	136 nm	170 nm
S3R2	500 nm	558 nm	129 nm	170 nm
S3R3	293 nm	294 nm	0 nm	0 nm

^a 10 equiv. of TBAF was added to receptor solutions in dry ACN.

^b 10 equiv. of TBAF was added to receptor solutions in dry DMSO.

4.3.8 Colorimetric detection and binding mechanism of cation

The receptor **S3R1** was evaluated for the binding ability towards cations in ACN and found to be Cu^{2+} ion active. The colorimetric detection experiment was carried out to check selectivity of Cu^{2+} ion over other cations such as Mg^{2+} , Ca^{2+} , Co^{2+} , Ni^{2+} , Zn^{2+} , Cd^{2+} , Hg^{2+} and Pb^{2+} (dissolved in water) in the form of their nitrates. The receptor **S3R1** was able to bind selectively to Cu^{2+} ions which resulted in a remarkable colour change from pale yellow to orange-red (Fig. 4.21), whereas no colour change was observed with all other cations.

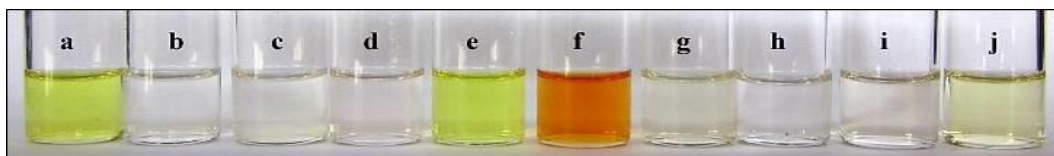
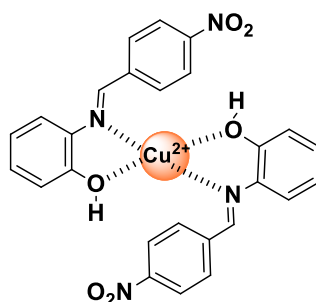


Fig. 4.21 Change in colour after addition of 3 equiv. of different cations to the receptor solution in ACN ($5 \times 10^{-5} \text{ M}$); (a) Receptor **S3R1**, (b) Mg^{2+} , (c) Ca^{2+} , (d) Co^{2+} , (e) Ni^{2+} , (f) Cu^{2+} , (g) Zn^{2+} , (h) Cd^{2+} , (i) Hg^{2+} and (j) Pb^{2+}

The stoichiometry of **S3R1**– Cu^{2+} system was determined using Job's plots where the absorbance at 427 nm was plotted against mole fraction of the Cu^{2+} . A maximum absorbance corresponding to the mole fraction of Cu^{2+} was at 0.33. This confirms the formation of 2:1 (Host/Guest) stoichiometric complex and it could be represented as shown in the Scheme 4.3.



Scheme 4.3 Proposed complexation of Cu^{2+} with receptor **S3R1**

4.3.9 Logic gate application of receptor **S3R1**

As stated previously, the receptor **S3R1** changed colour from pale yellow to pink on addition of F^- ions (2 equiv.) in dry ACN and as a result a new band centred at 511 nm with an absorbance of 0.13 was observed (Fig. 4.22, i).

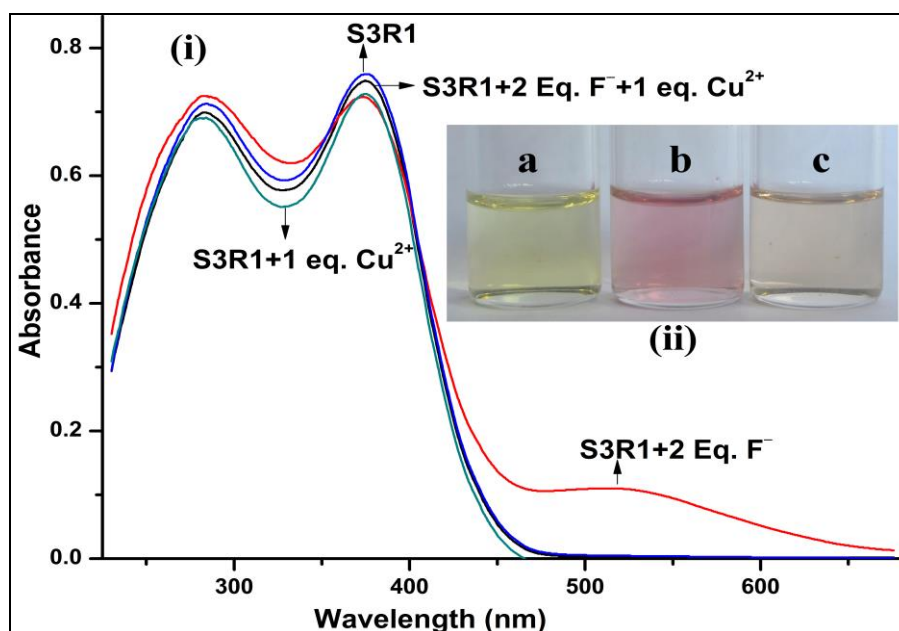


Fig. 4.22 (i) Reversal of the UV–vis spectral pattern of receptor **S3R1** + 2 equiv. of F^- upon addition of Cu^{2+} ions; (ii) Colour changes of **S3R1** in ACN; (a) Free **S3R1**, (b) **S3R1** + 2 equiv. of F^- and (c) **S3R1** + 2 equiv. of F^- + 1 equiv. Cu^{2+}

Amazingly, upon adding 1 equiv. of Cu^{2+} ions to this **S3R1**- F^- ion complex resulted in the disappearance of the pink colour and the original pale yellow colour of receptor **S3R1** was restored (Fig. 4.22, ii). This reverting of the colour was confirmed by UV-vis spectroscopy where the band at 511 nm (due to ICT) was disappeared and the band at 375 nm corresponding to receptor **S3R1** was restored (Fig. 4.18, i). This property of receptor **S3R1** was further applied for the molecular logic gate and ‘ON-OFF’ switching operation.

The system is said to be ‘switch ON’ when the receptor **S3R1** shows optical output from pale yellow to pink in presence of F^- ion and system is said to be ‘switch OFF’ when Cu^{2+} ion was added to the same solution as the pale yellow colour of the receptor **S3R1** reappears. These observations can be correlated for demonstrating a logic gate operation, where the output signals (change in colour) could be controlled by input signals (addition of F^- ion and Cu^{2+} ion). The receptor **S3R1** showed no absorbance at 511 nm which is accounted for the Boolean value of “0” and with the addition of F^- ion it showed an absorbance of 0.13 which is accounted for the Boolean value of “1”. The process of ‘switch ON’ and ‘switch OFF’ represented in the molecular logic gate through truth table as shown in the Table 4.3.

Table 4.3 Truth table for INH functions. Input A: 2 equiv. F^- ion Input B: 1 equiv. Cu^{2+} ion. Output: Absorbance at 511 nm (High absorbance: 1 low absorbance: 0)

Input A	Input B	Outputs
0	0	0
1	0	1
0	1	0
1	1	0

Output signals in the form of spectral change at 511 nm was observed upon supplying input signals in the form of F^- ion and Cu^{2+} represents INHIBIT (INH) logic gate (Gunnlaugsson et al. 2000). The outputs of the receptor **S3R1** are in agreement with complementary INH logic function (Fig. 4.23).

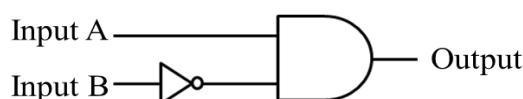
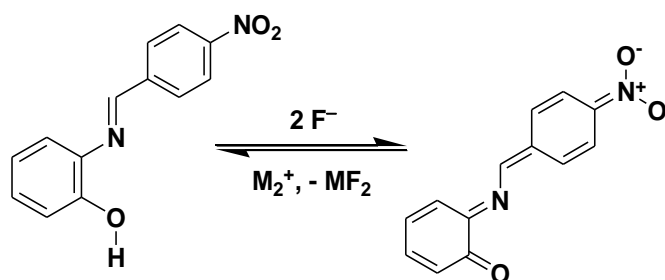


Fig. 4.23 A schematic representation of a complementary output INH circuit

The colour restoration mechanism was observed even with the addition of other metal ions such as Co^{2+} , Ni^{2+} , Zn^{2+} , Cd^{2+} and Hg^{2+} (Mg^{2+} , Ca^{2+} and Pb^{2+} salts were not soluble in organic solvent like ACN) instead of Cu^{2+} . This confirms formation of stable MF_2 salt (metal–fluoride salt). Thus, the receptor **S3R1** becomes free after the addition of 1 equiv. of M^{2+} ions to the **S3R1**+ 2 equiv. of F^- solution as demonstrated in Scheme 4.4.



Scheme 4.4 Reversal process of the receptor **S3R1** on addition of Cu^{2+} to the **S3R1**+ F^- in ACN solution

However, the addition of 10 equiv. of F^- ion to the **S3R1**- Cu^{2+} complex did not show any colour change. This confirms the stable complex formation between receptor **S3R1** and Cu^{2+} ion.

4.4 CONCLUSIONS

To conclude, a receptor **S3R1** was designed and synthesised, for the colorimetric dual ion sensing application. The receptor **S3R1** colorimetrically detected F^- ions over other anions. The binding mechanism for the selective detection involves the establishment of ICT transitions between F^- ions and the receptor. This receptor showed unique solvatochromic property only in presence of F^- ions as it establishes charge separation in the receptor. The receptor displayed different colorations in different solvents upon adding F^- ions. This colorimetric discrimination in different solvents was successfully applied to determine the percentage composition of binary solvent mixture. A strong binding was established with receptor **S3R1** and F^- ions with a binding constant of $7.15 \pm 0.31 \times 10^6 \text{ M}^{-2}$. The receptor **S3R1** colorimetrically discriminated Cu^{2+} ions over other cations by showing a colour change from pale yellow to orange-red. It acts as a molecular switch which is said to be ‘switch ON’ in presence of F^- ions and ‘switch OFF’ when Cu^{2+} ions were

added. This 'ON-OFF' switching process was demonstrated by logic gate functions. The receptor **S3R1** gave output signals corresponding to the INH circuit with input signals which can be implemented to molecular computing operations and molecular devices.

CHAPTER 5

***DESIGN AND SYNTHESIS OF AMINOPHENOL BASED
RECEPTORS FOR COLORIMETRIC DISCRIMINATION
OF ISOMERIC DICARBOXYLATES AND THEIR
APPLICATION IN DETECTING FLUORIDE IONS***

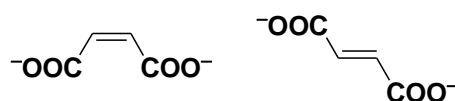
In this chapter, the design, syntheses and characterization of new aminophenol Schiff's base derivatives as colorimetric receptors for discriminative detection of maleate ions over fumarate ions have been discussed in detail. The colorimetric anion sensing properties and detection mechanism of these receptors have been incorporated. In addition, the receptors were studied for colorimetric detection of other biologically important anions such as fluoride. The binding model of receptor with fluoride ion was proposed on the basis of UV-vis spectral studies.

5.1 INTRODUCTION

Though instrumental methods are available to detect anions, colorimetric anion receptors attain significance due to its simplicity, instantaneous detection, equal selectivity and sensitivity. A colorimetric receptor for anion detection generally comprises of an organic molecule with a binding site where the anion binds to the molecule and a signalling unit which transforms the binding information through optical change. The binding site contains acidic proton/s to which anion binds non-covalently and the signalling units with an electron withdrawing chromophores changes the colour of organic molecule upon non-covalent binding. Applying this strategy, various anion receptors with different binding sites have been reported. However, majority of these receptors are restricted for the recognition of only inorganic anions.

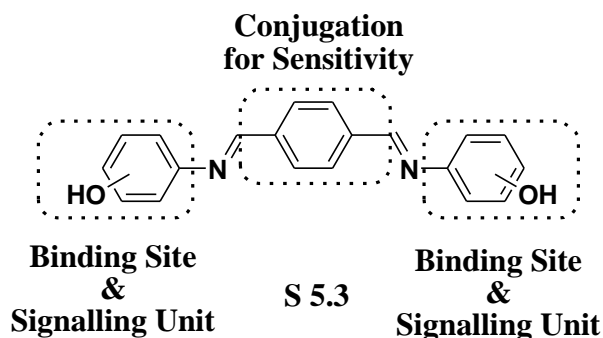
Though the majority of research community concentrated on inorganic anion detection, few researchers focused on design and synthesis of receptors for the detection of organic molecules. As an outcome of their efforts, recently reports on colorimetric discrimination of isomeric organic molecules using naphthalenediimide (NDI) based receptors by grinding methods were published (Trivedi et al. 2008; Trivedi et al. 2009). In addition, the colorimetric discriminative detection of organic amines was reported (Rakow et al. 2005; Tang et al. 2010). Consequently, designing the receptors for detection of organic anions acquires considerable attention. Notably, dicarboxylate anions attains much deliberation as they play critical role in the various metabolic and biological processes (Voet and Voet 1995; Nisbet et al. 2009; Sherif 2010; Shin et al. 2011; Xu et al. 2012). In the past decade researchers reported many receptors with diverse functional groups for the selective detection of dicarboxylates

anions (Karl et al. 1995; Gunnlaugsson et al. 2002; Raker and Glass 2002; Liu et al. 2005; Jadhav and Schmidtchen 2006; Ghosh et al. 2010). Among the dicarboxylates the differentiation of geometrical isomers (such as *cis/trans* dicarboxylates) in particular, maleate (**S 5.1**) and fumarate (**S 5.2**) gain significance. This importance is not only because of their conformational isomerism but also owing to their different biological behaviours, such as, fumarate is produced during Krebs cycle whereas maleate is used as Krebs cycle inhibitor and used in kidney related disorders (Gougoux et al., 1976; EiamOng et al., 1995).

**S 5.1****S 5.2**

Recently, few chemists demonstrated the isomeric detection of dicarboxylates using hydrogen bonding synthons. These reports are based on receptors with urea/thiourea (Costero et al. 2006; Yen and Ho 2006; Lin et al 2007; Tseng et al. 2007; Lin et al. 2009) and some other functional groups (Sancenon et al. 2003) which were able to detect the geometrical isomers either colorimetrically or fluorometrically. However, these molecules are structurally complicated and thus required skilled labour for the synthesis. Furthermore, these receptors were not demonstrated for the detection of other biologically important anions and it would be an added advantage, if a receptor could detect other important anions in particular, fluoride ions considering its vital role in clinical applications as well as disadvantages associated with it (Wiseman 1970; Dreisbuch 1980; Riggs 1984; Krik 1991; Kleerekoper 1998; Shivarajashankara et al. 2001; Ozsvath 2009).

In current chapter the receptors based on aminophenol Schiff's base (**S 5.3**) have been synthesised where the hydroxyl groups are present at *o*-, *m*-, and *p*-positions of phenyl ring. These receptors were synthesised to check the role of positions of binding sites in detection process. The aminophenol units are connected together with a phenyl ring at *1* and *4* positions. This provides extended conjugation for more sensitive recognition of anions. An additional receptor which does not contain any hydroxyl group was synthesised to justify the binding site of receptors.



5.2 EXPERIMENTAL

5.2.1 Materials and methods

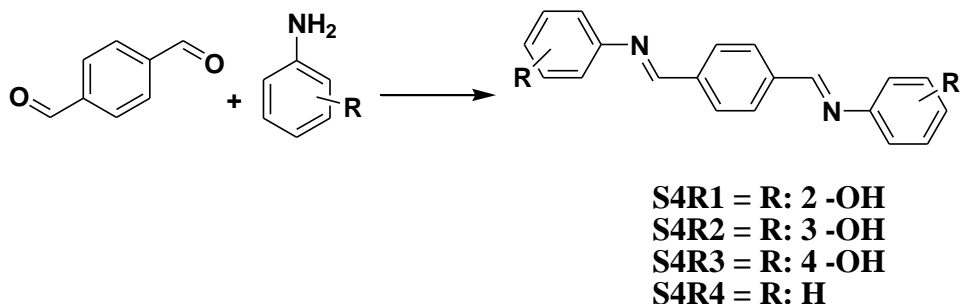
All chemicals were purchased from Sigma-Aldrich, Alfa Aesar or from Spectrochem and used without further purification. All solvents were procured from SD Fine, India with HPLC grade and used without further distillation.

The ^1H NMR spectra were recorded on a Bruker, Avance II (500 MHz) instrument using TMS as an internal reference and $\text{DMSO-}d_6$ as solvent. The raw FID data was processed with MestReNova 7.0.0-8331 software. Resonance multiplicities are described as s (singlet), br s (broad singlet), d (doublet), t (triplet), q (quartet) and m (multiplet). The chemical shifts (δ) are reported in ppm and coupling constant (J) values are given in Hz. Melting points were determined with Stuart- SMP3 melting-point apparatus in open capillaries and are uncorrected. IR spectra were recorded on a Thermo Nicolet Avatar-330 FT-IR spectrometer; signal designations: s (strong), m (medium), w (weak), br.m (broad medium) and br.w (broad weak). Mass spectra were recorded on Waters Micromass Q-Tof micro spectrometer with ESI source. The SCXRD was performed on Bruker AXS APEX II system. UV-vis spectroscopy was carried out with Ocean Optics SD2000-Fibre Optics Spectrometer and Analytikjena Specord S600 Spectrometer in standard 3.5 mL quartz cells (2 optical windows) with 10 mm path length. Elemental analyses were done using Flash EA1112 CHNS analyser (Thermo Electron Corporation). All reactions were monitored by TLC on pre-coated silica gel 60 F_{254} plates which were procured from Merck.

5.2.2 Synthesis of receptors S4R1, S4R2, S4R3 and S4R4

A mixture of terphthalaldehyde (0.373 mmol) and amine derivatives (0.746 mmol) reacted in ethanol with a catalytic amount of acetic acid under reflux condition

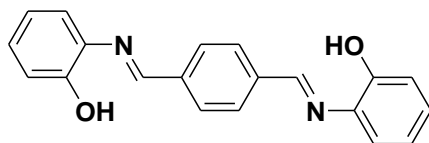
for 3 h. The reaction mixture was cooled to room temperature and the solid formed was filtered, washed with ethanol to obtain the pure solid target compounds (**S4R1**, **S4R2**, **S4R3** and **S4R4**; Scheme 5.1).



Scheme 5.1 Synthetic scheme of receptors **S4R1**, **S4R2**, **S4R3** and **S4R4**

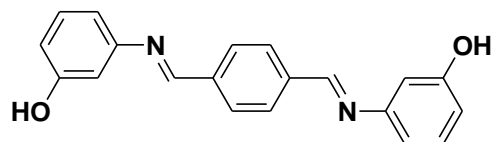
All receptors were characterized by spectral analysis. The characterization data have been compiled and given below.

2,2'-{benzene-1,4-diylbis[(*E*)methylylidenenitrilo]}diphenol (**S4R1**)



Yield: 79%; m.p.: 219 – 221 °C. Elemental analysis Calculated for $C_{20}H_{15}N_2O_2$ (%): C 76.17, H 4.79, N 8.88. Experimental: C 76.15, H 4.76, N 8.91. 1H NMR (500 MHz, $DMSO-d_6$): δ 9.10 (s, 2H, -OH); δ 8.80 (s, 2H, =CH); δ 8.16 (s, 4H, Ar-H, $J=8$ Hz), δ 7.27 (d, 2H, Ar-H, $J=6.5$ Hz), δ 7.11 (t, 2H, Ar-H, $J=7.75$ Hz), δ 6.93 (d, 2H, Ar-H, $J=8$ Hz), δ 6.86 (t, 2H, Ar-H, $J=7.5$ Hz). FT-IR in cm^{-1} : 3356.9 (m), 1585.9 (m), 1478.3 (s), 1374.2 (m), 1230.9 (s), 728.7 (s). MS (ESI) m/z: Calculated: 315.3453 $[M-H]^-$ Experimental: 315.2749 $[M-H]^-$

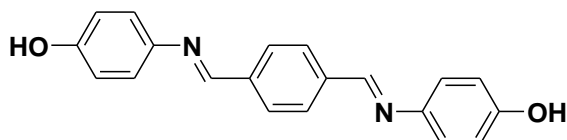
3,3'-{benzene-1,4-diylbis[(*E*)methylylidenenitrilo]}diphenol (**S4R2**)



Yield: 80%; m.p.: > 300 °C. Elemental analysis Calculated for $C_{20}H_{15}N_2O_2$ (%): C 76.17, H 4.79, N 8.88. Experimental: C 76.18, H 4.81, N 8.84. 1H NMR (500

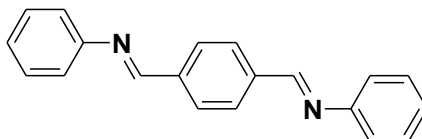
MHz, DMSO- d_6): δ 9.58 (s, 2H, -OH), δ 8.66 (s, 2H, =CH), δ 8.06 (s, 4H, Ar-H), δ 7.2-7.23 (m, 2H, Ar-H), δ 6.75 (d, 2H, Ar-H, $J=7.5$ Hz), δ 6.67-6.69 (m, 4H, Ar-H). FT-IR in cm^{-1} : 3357.8 (s), 3040.8 (w), 1586.8 (m), 1480.5 (s), 1233.8 (s), 731.4 (s). MS (ESI) m/z : Calculated: 315.3453 $[\text{M-H}]^-$ Experimental: 315.1485 $[\text{M-H}]^-$

4,4'-{benzene-1,4-diylbis(*E*)methylidenenitrilo}diphenol (S4R3)



Yield: 93%; m.p.: 271 – 273 °C. Elemental analysis Calculated for $\text{C}_{20}\text{H}_{15}\text{N}_2\text{O}_2$ (%): C 76.17, H 4.79, N 8.88. Experimental: C 76.16, H 4.79, N 8.87. ^1H NMR (500 MHz, DMSO- d_6): 9.59 (s, 2H, -OH), δ 8.69 (s, 2H, =CH), δ 8.0 (s, 4H, Ar-H), δ 7.27 (d, 4H, Ar-H, $J=8.5$ Hz), δ 6.83 (d, 4H, Ar-H, $J=9.0$ Hz). FT-IR in cm^{-1} : 3359.9 (s), 1587.4 (m), 1490.5 (m), 1234.1 (s), 822.8 (s). MS (ESI): m/z : Calculated: 315.3453 $[\text{M-H}]^-$ Experimental: 315.2896 $[\text{M-H}]^-$

N,N'-[benzene-1,4-diyl-di(*E*)methylidene]dianiline (S4R4)



Yield: 91%; m.p.: 166 – 167 °C. Elemental analysis Calculated for $\text{C}_{20}\text{H}_{16}\text{N}_2$ (%): C 84.48, H 5.67, N 9.85. Experimental: C 84.45, H 5.68, N 9.87. ^1H NMR (500 MHz, DMSO- d_6): δ 8.72 (s, 2H, =CH), δ 8.09 (s, 4H, Ar-H), δ 7.45 (t, 4H, Ar-H, $J=7.75$ Hz), δ 7.27 – 7.33 (m, 6H, Ar-H). FT-IR in cm^{-1} : 3047.8 (w), 2867.2 (w), 1572.8 (m), 1454.2 (m), 828.0 (s), 753.4 (s), 686.5 (s). MS (ESI): m/z : Calculated: 285.3618 $[\text{M-H}]^-$ Experimental: 285.1545 $[\text{M-H}]^-$

The representative spectra of receptors have been given below.

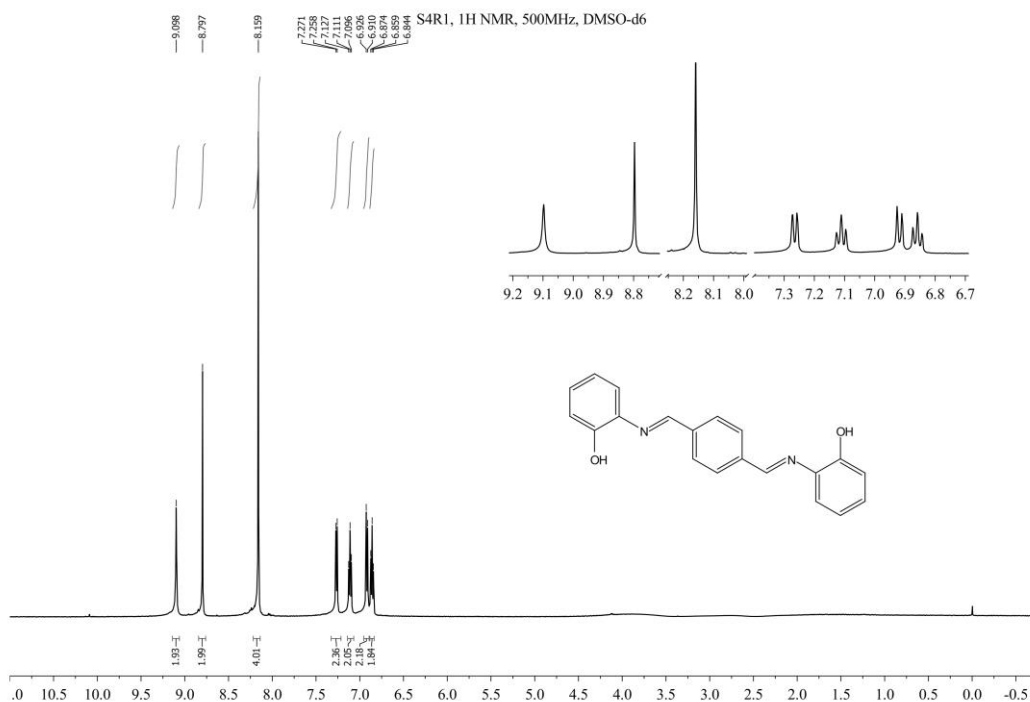
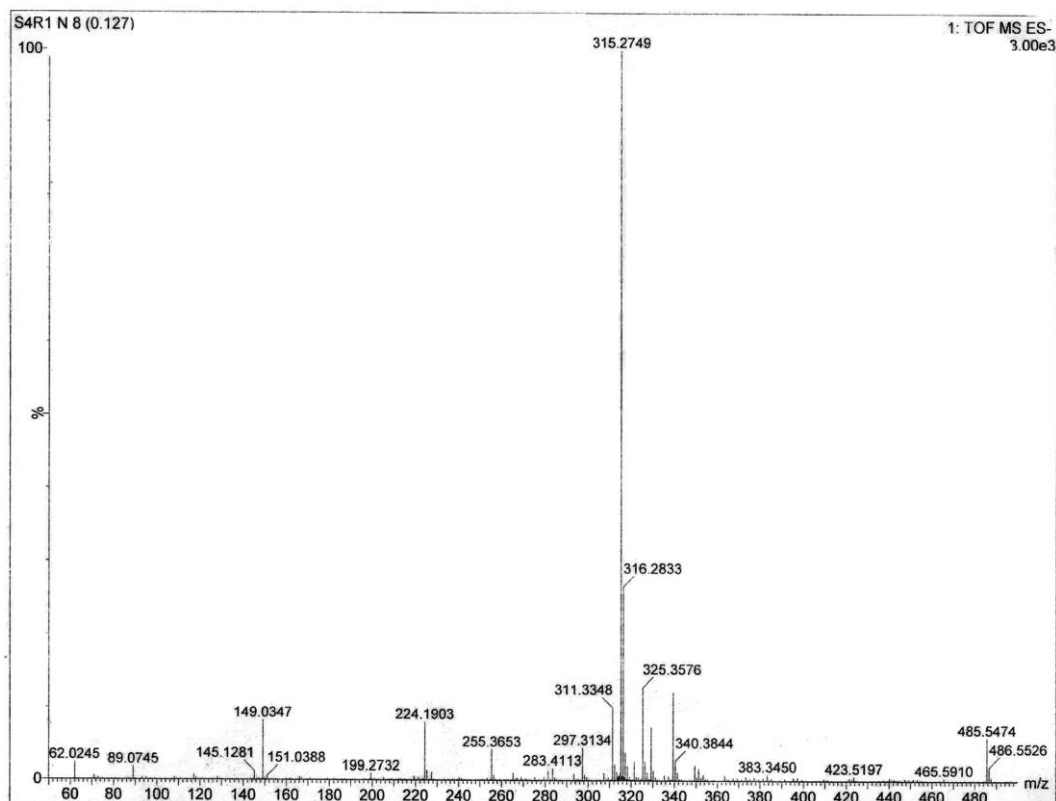
Fig. 5.1 ^1H NMR spectrum of S4R1

Fig. 5.2 ESI-MS spectrum of S4R1

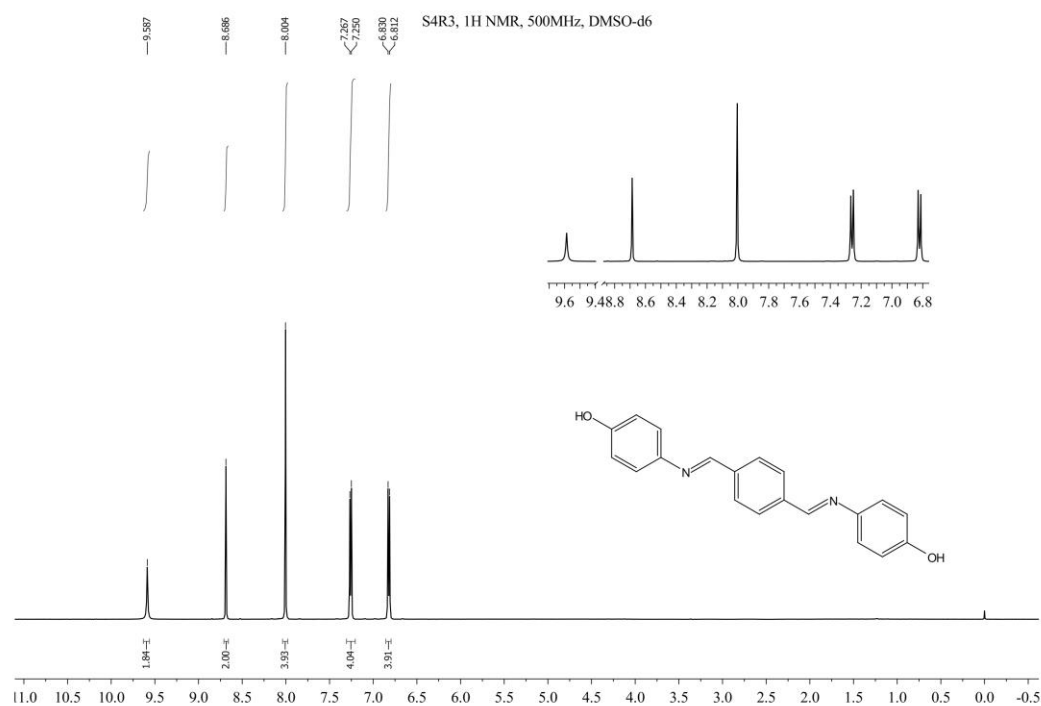
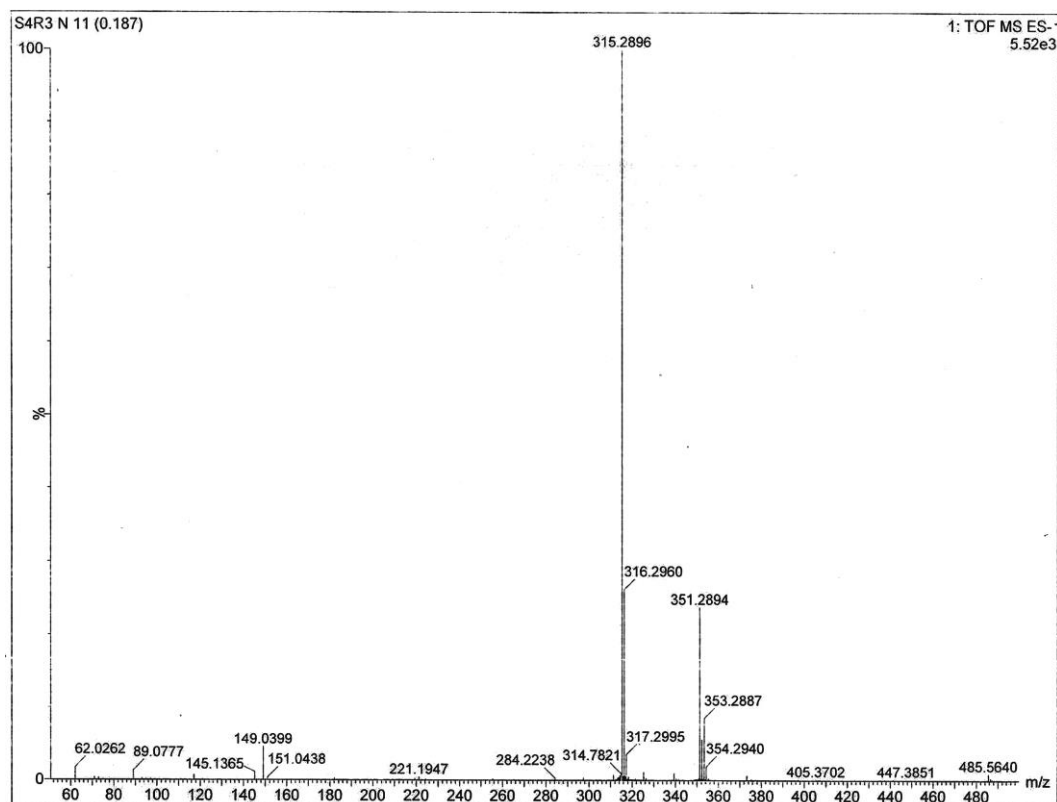
Fig. 5.3 ^1H NMR spectrum of S4R3

Fig. 5.4 ESI-MS spectrum of S4R3

5.2.3 Synthesis of tetrabutylammonium salts

To a stirred solution of a dicarboxylic acid (2.5 mmol) in dry methanol (5 mL), a 1.0 M solution of tetrabutylammonium hydroxide in methanol (2.0 equiv.) was added. The reaction mixture was stirred at room temperature for 2 h. The solvent was evaporated under reduced pressure and dried over P₂O₅ to obtain tetrabutylammonium salt of corresponding dicarboxylic acid and the salt was used immediately for further applications.

5.2.4 Stoichiometric ratio determination using Job's plot method

A Job plot is used to determine the binding stoichiometry. In this method, the total molar concentration of anion and receptor are kept constant. However, the mole fraction of both is continuously varied. The UV-vis absorbance was measured for each fraction. This absorbance was plotted against the mole fractions of the two components. The maximum absorbance on the plot corresponds to the stoichiometry of the two species.

5.3 RESULTS AND DISCUSSION

5.3.1 Discrimination of isomeric dicarboxylates

The colorimetric isomeric detection ability of the receptors **S4R1** in dry DMSO solution (5×10^{-5} M) was investigated by adding 2 equiv. of maleate and fumarate ions in the form of tetrabutylammonium (TBA) salts. A colour change of pale yellow to reddish pink was observed only with the addition of maleate ions. However, no change in colour was observed with fumarate ions (Fig. 5.5).

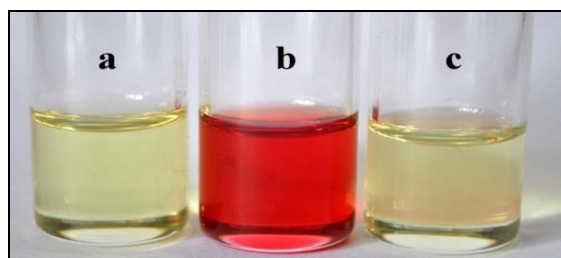


Fig. 5.5 Change in colour on adding 2 equiv. of anions in the form of TBA salt. (a) Free **S4R1** (5×10^{-5} M), (b) **S4R1**+ maleate ions and (c) **S4R1**+ fumarate ions

The colorimetric selectivity of receptor for maleate ions over fumarate ions was further confirmed with the UV-vis spectrometry (Fig. 5.6) where the receptor

with maleate ions showed a new absorption band at 508 nm and no new band was observed after the addition of fumarate ions.

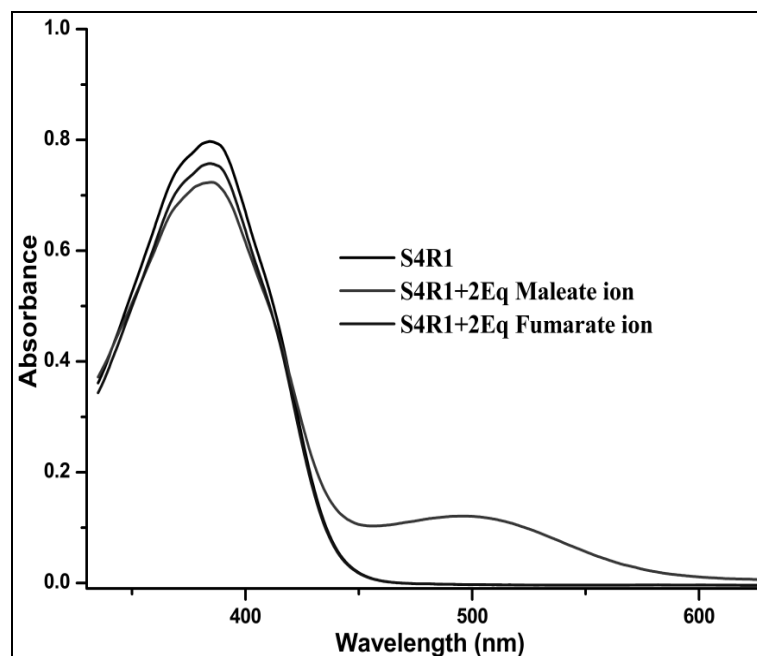


Fig. 5.6 UV–vis spectral changes of **S4R1** (5×10^{-5} M) in dry DMSO after adding 2 equiv. of maleate and fumarate in the form of TBA salts

The quantitative analysis was carried out using UV–vis titrations where the receptor **S4R1** solution (5×10^{-5} M) was treated with maleate ion solution in dry DMSO as TBA salt (Fig. 5.7). Upon incremental addition of maleate ions from 1 equiv. to 25 equiv. in DMSO, the intensity at 375 nm corresponding to phenolic –OH decreased constantly and a new band at 508 nm with a bathochromic shift of 133 nm was generated. Simultaneously, the colour of the solution turned from pale yellow to reddish pink. The formation of clear isosbestic point at 423 nm indicated the complex formation between receptor **S4R1** and maleate ion was due to hydrogen bonding electrostatic interactions (Yen and Ho 2006). The colour change and generation of new absorption band was attributed to establishment of charge transfer complex between receptor **S4R1** and maleate ion.

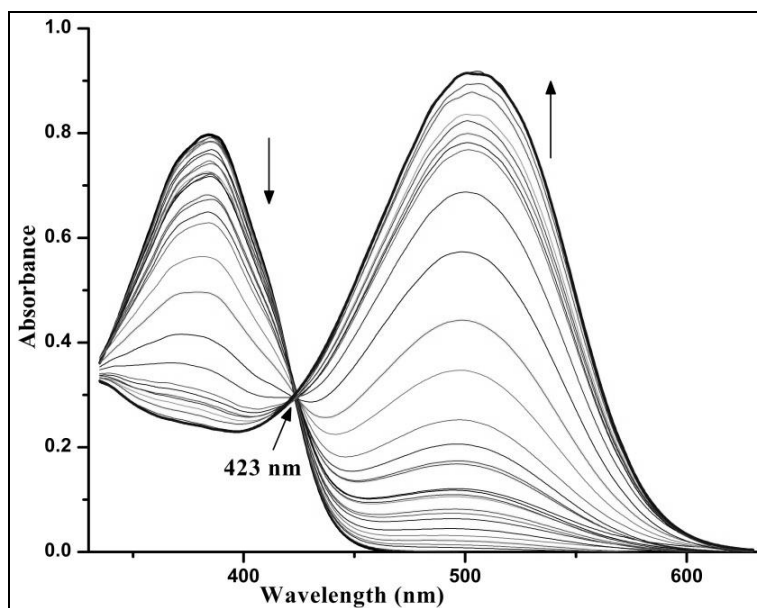


Fig. 5.7 UV-vis titration of **S4R1** (5×10^{-5} M) in DMSO with standard solution of maleate ions (0–25 equiv.)

Job's plot method was used to determine the binding stoichiometry between the receptor **S4R1** and the maleate ion (Fig. 5.8). A maximum absorbance change was observed when the mole fraction of **S4R1** versus maleate ion was 0.5, at 508 nm. This clearly confirmed the formation of 1:1 stoichiometry between **S4R1** and maleate ion.

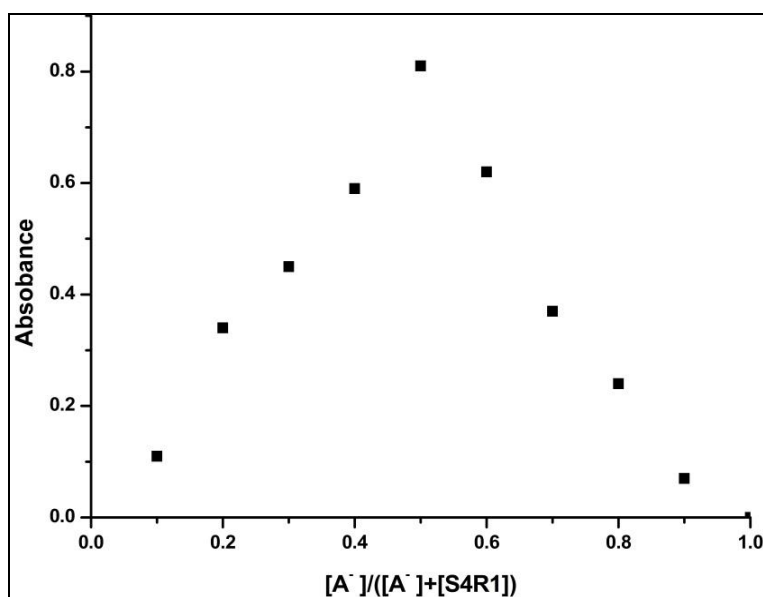


Fig. 5.8 Jobs plot at 508 nm which indicates 1:1 complexation ratio between **S4R1** and maleate ion

The binding constant was determined using Benesi – Hildebrand equation (Eq. 5.1, Benesi and Hildebrand, 1949) which was found to be $2.71 \pm 0.06 \times 10^3 \text{ M}^{-1}$.

$$\frac{1}{(A - A_0)} = \frac{1}{(A_{max} - A_0)} + \frac{1}{K[F^-]^n(A_{max} - A_0)} \dots \dots \dots (Eq.5.1)$$

Where, A_0 , A , A_{max} are the absorption considered in the absence of F^- , at an intermediate, and at a concentration of saturation. K is binding constant, $[F^-]$ is concentration of F^- ion and n is the stoichiometric ratio.

This colorimetric discrimination study was further extended to other receptors **S4R2**, **S4R3** and **S4R4**. In case of receptor **S4R2** where the $-OH$ is attached to m -position of phenyl ring showed neither colour change (Fig. 5.9, i) nor UV–vis spectral change (Fig. 5.9, ii) upon addition of maleate ions. This is because, the lone pair of oxygen at m - position is not in conjugation with the azomethine ($-C=N-$) group. Therefore, the receptor **S4R2** does not show any spectral or optical changes with the addition of maleate ions.

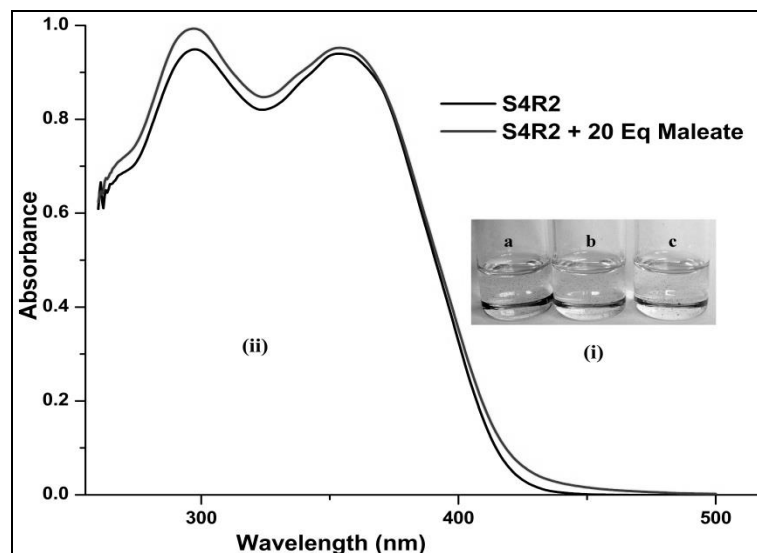


Fig. 5.9 (i) Change in colour on adding 2 equiv. of anions as TBA salt; (a) Free **S4R2** ($5 \times 10^{-5} \text{ M}$), (b) **S4R2**+ 2 equiv. maleate ions and (c) **S4R2**+ 2 equiv. fumarate ions; (ii) UV–vis spectral changes of **S4R2** ($5 \times 10^{-5} \text{ M}$) in DMSO after adding 20 equiv. of maleate ions as TBA salt

The receptor **S4R4** failed to show any optical (Fig. 5.10, i) or spectral changes (Fig. 5.10, ii) as it does not contain any hydroxyl functional group for the binding of ions.

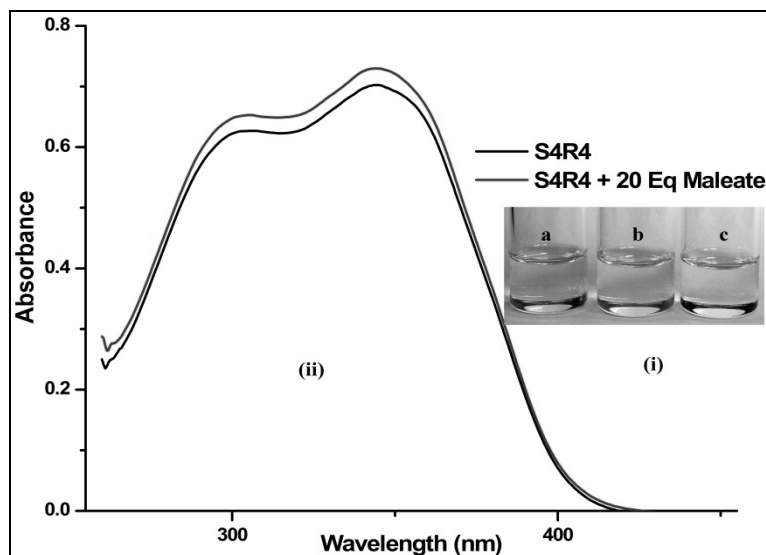


Fig. 5.10 (i) Change in colour on adding 2 equiv. of anions as TBA salt; (a) Free **S4R4** (5×10^{-5} M), (b) **S4R4**+ 2 equiv. maleate ions and (c) **S4R4**+ 2 equiv. fumarate ions; (ii) UV-vis spectral changes of **S4R4** (5×10^{-5} M) in DMSO after adding 20 equiv. of maleate ions as TBA salt

However, the dry DMSO solution of receptor **S4R3** (5×10^{-5} M) where the –OH group is at *p*- position of the phenyl ring, showed similar observations by changing its colour from pale yellow to reddish pink upon adding 2 equiv. of maleate ion whereas no change was observed (Fig. 5.11) on adding fumarate ion.

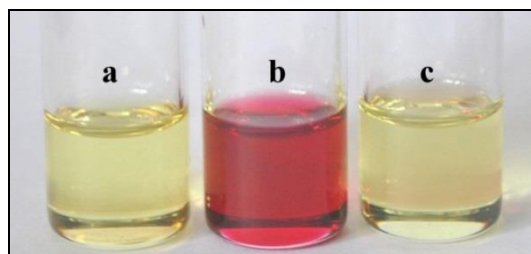


Fig. 5.11 Change in colour on adding 2 equiv. of anions as TBA salt; (a) Free **S4R3** (5×10^{-5} M), (b) **S4R3**+ 2 equiv. maleate ions and (c) **S4R3**+ 2 equiv. fumarate ions

As a part of quantitative study, the UV–vis titration was carried out by titrating **S4R3** with maleate ions in DMSO solution. The UV–vis titration curve for receptor **S4R3** showed similar changes as the receptor **S4R1** (Fig. 5.12).

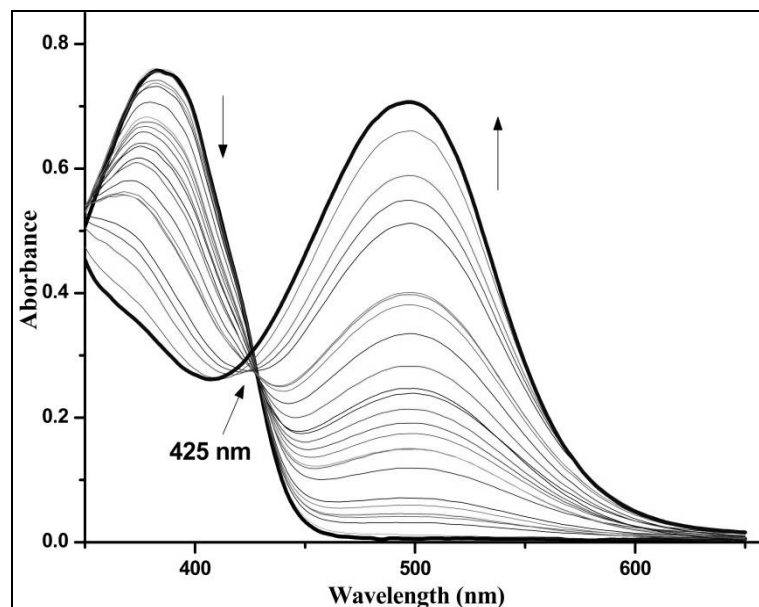


Fig. 5.12 UV-vis titration of **S4R3** (5×10^{-5} M) in DMSO with standard solution of maleate ions (0 – 25 equiv.)

Upon gradual increasing addition from 0 equiv. to 25 equiv. of maleate ion to the receptor **S4R3** solution (5×10^{-5} M) in dry DMSO, a constant decrease in the intensity of absorption at 371 nm which corresponds to –OH functional group was observed and a new absorption band at 500 nm with a bathochromic shift of 129 nm was developed. This new band was ascribed to the generation of charge transfer complex between receptor **S4R3** and maleate ion. The formation of an isobestic point at 425 nm indicated the complex formation was due to hydrogen bonding electrostatic interactions between receptor **S4R3** and maleate ion (Yen and Ho, 2006).

Stoichiometric ratio of the complex between receptor **S4R3** and maleate ion was determined using Job's plot method at 500 nm. This revealed the formation of a stable complex between receptor **S4R3** and maleate ion (Fig. 5.13) with 1:1 complexation ratio. The binding constant was calculated using Benesi – Hildebrand equation and found to be $2.42 \pm 0.05 \times 10^3 \text{ M}^{-1}$.

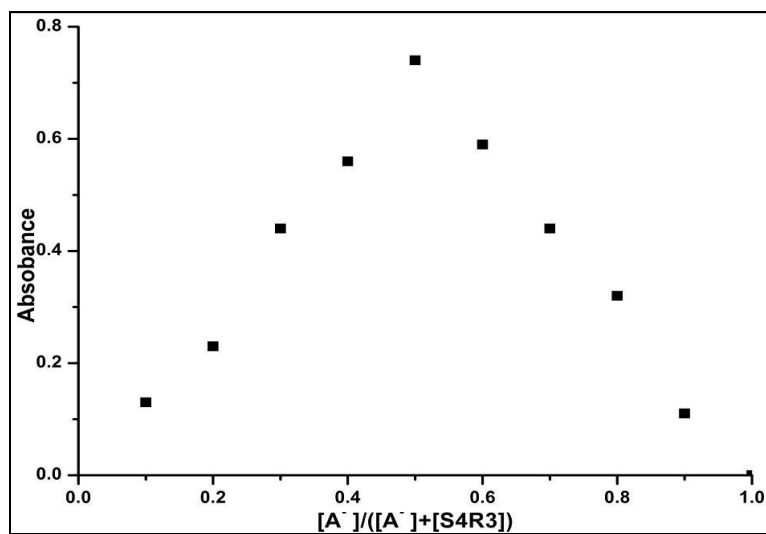


Fig. 5.13 Jobs plot at 500 nm which indicates 1:1 complexation ratio between **S4R3** and maleate ion

The binding mechanism was studied by ^1H NMR titration (Fig. 5.14) of receptor **S4R3** in dry $\text{DMSO-}d_6$ with the increasing addition of maleate ions.

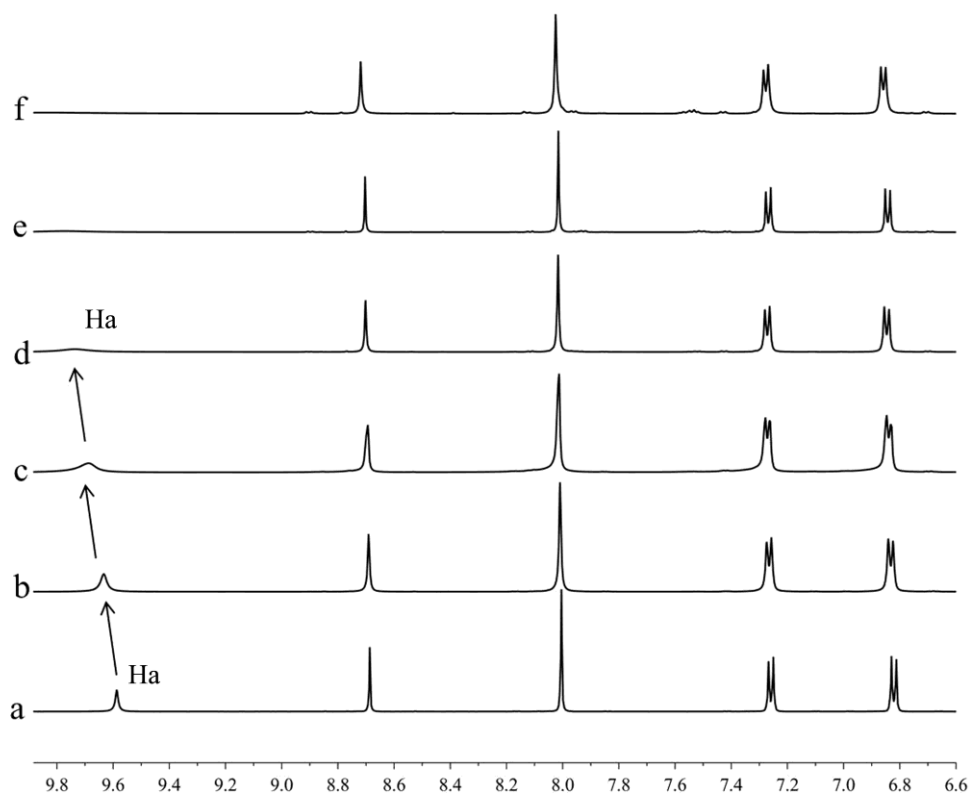
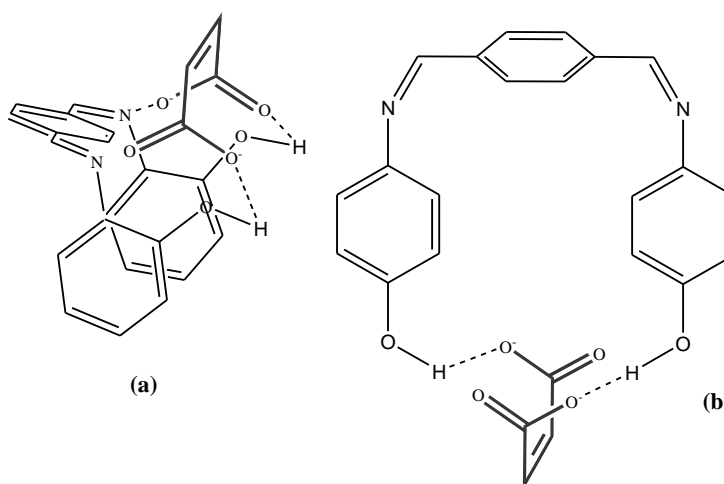


Fig. 5.14 Partial ^1H NMR spectra of **S4R3** in $\text{DMSO-}d_6$ after adding (a) 0, (b) 0.5, (c) 1, (d) 2, (e) 5 and (f) 10 equiv. of maleate ion as TBA salt

Upon adding 0.5 equiv. of maleate ion, the phenolic –OH at δ 9.58 started broadening and experienced a slight downfield shift. This indicates the decrease in electron density over the phenolic –OH due to the formation of hydrogen bonding. This trend of downfield and broadening continued till the addition of 2 equiv. of maleate ions to the receptor **S4R3**. After adding 5 equiv. of maleate ion, the peak corresponding to proton ‘Ha’ of phenolic –OH disappeared perhaps due to the fast exchange of protons between maleate ion and phenolic –OH. The other aromatic protons were not changed which further confirms the detection process is due to the formation of hydrogen bonding between the maleate ion and phenolic –OH.

However, the binding of maleate ion with receptor **S4R3** ($2.42 \pm 0.05 \times 10^3 \text{ M}^{-1}$) was less when compared to receptor **S4R1** ($2.71 \pm 0.06 \times 10^3 \text{ M}^{-1}$). This observation possibly due to the formation of more stable complex with receptor **S4R1** and maleate ions than the complex between receptor **S4R3** and maleate ions.



Scheme 5.2 Proposed binding models of (a) **S4R1** and (b) **S4R3** with maleate ion

The selectivity and colour change of the receptors can be related to the receptor orientation which perhaps changes the geometry depending upon the anion stereochemistry. Thus, the receptors with hydroxyl functional group at *ortho* and *para* positions of the phenyl group can easily bind to the maleate ion which has *cis* conformation, whereas the fumarate cannot easily fit into the receptor due to its *trans* conformation. The structure for the complex formed after binding the maleate ion could be proposed as shown in the Scheme 5.2. At the same time basicity of the

maleate ion and fumarate ion can take part significantly during the detection process as maleate ion is more basic than fumarate ion (maleic acid, pK_{a1} : 5.0, pK_{a2} : 18.8; fumaric acid, pK_{a1} : 9.0, pK_{a2} : 11.0 in DMSO; Choi et al. 2002).

All the receptors were further explored for the isomeric detection of aromatic dicarboxylates such as phthalate, isophthalate and terephthalate in the form of TBA salt. Unfortunately, these receptors did not show any colour change with the aromatic dicarboxylates. Therefore, these receptors are not useful for the discrimination of aromatic dicarboxylates.

5.3.2 Detection of F^- ions

Furthermore, the receptors **S4R1** and **S4R3** were subjected to the colorimetric detection of other biologically important anions wherein these receptors were able to colorimetrically detect the F^- ions and AcO^- ions. As shown in Fig. 5.15, upon adding 2 equiv. of anions such as fluoride, chloride, bromide, iodide, nitrate, hydrogensulfate, dihydrogenphosphate and acetate to the receptor **S4R1** (5×10^{-5} M) in dry DMSO, only F^- ion displayed colour change from pale yellow to blood red and AcO^- ions showed a colour change from pale yellow to orange.

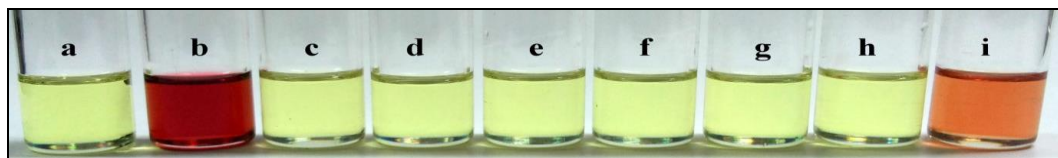


Fig. 5.15 Change in colour after adding 2 equiv. of different anions as TBA salt to receptor solution in DMSO (5×10^{-5} M); (a) Free **S4R1**, (b) F^- , (c) Cl^- , (d) Br^- (e) I^- , (f) NO_3^- , (g) HSO_4^- , (h) $H_2PO_4^-$ and (i) AcO^-

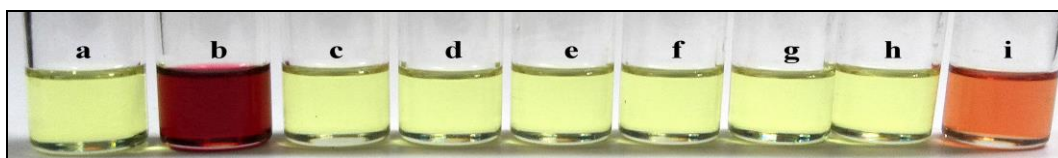


Fig. 5.16 Change in colour after adding 2 equiv. of different anions as TBA salt to the receptor **S4R3** solution in DMSO (5×10^{-5} M); (a) Free **S4R3**, (b) F^- , (c) Cl^- , (d) Br^- (e) I^- , (f) NO_3^- , (g) HSO_4^- , (h) $H_2PO_4^-$ and (i) AcO^-

This discrimination in colour upon adding F^- ions and AcO^- ions to the receptor **S4R1**, suggests that the F^- ions bind more strongly than AcO^- ions. The

colorimetric discrepancy study was extended to the receptor **S4R3** in DMSO (Fig. 5.16) wherein similar changes were observed. Upon adding 2 equiv. of different anions to the receptor **S4R3** solution in dry DMSO, colour changes from pale yellow to blood red for F^- ions and pale yellow to orange for AcO^- ions were observed. All other anions did not display any colour change.

The colorimetric discrepancy in detection of F^- ions and AcO^- ions with other anions was confirmed by UV-vis experiment. The UV-vis spectra of receptor **S4R1** showed significant shift in the absorption band upon addition of F^- ions and AcO^- ions. However, the intensity of this newly generated absorption band after addition of AcO^- ions was much less than that of F^- ions (Fig. 5.17). This clearly indicates the interaction of receptor **S4R1** with AcO^- ion is considerably weaker when compared to the interaction of receptor **S4R1** with F^- ion. All other anions did not show any changes in UV-vis absorption band, which signified either these anions are not interacted with receptor **S4R1** or the interaction was much weaker to create any change in UV-vis absorption.

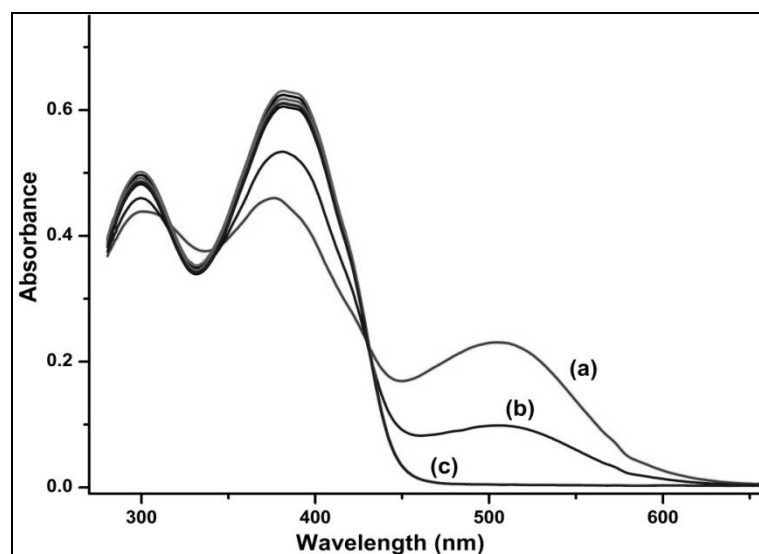


Fig. 5.17 UV-vis spectral changes of **S4R1** (5×10^{-5} M) in DMSO after adding 10 equiv. of (a) F^- , (b) AcO^- and (c) Cl^- , Br^- , I^- , HSO_4^- and $H_2PO_4^-$ as TBA salts

Similarly, the receptor **S4R3** showed significant shift in the absorption band on adding F^- ions and AcO^- ions. Owing to the weaker interaction of AcO^- ions with receptor **S4R3**, the intensity of this shifted absorption band was less when compared

to that of F^- ions. Conversely, other anions failed to generate any change to UV-vis spectra (Fig. 5.18).

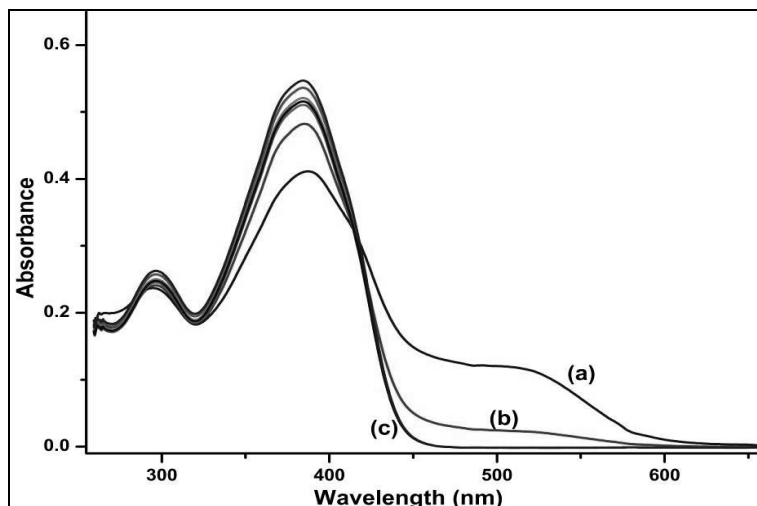


Fig. 5.18 UV-vis spectral changes of **S4R3** (5×10^{-5} M) in DMSO after adding 10 equiv. of (a) F^- , (b) AcO^- and (c) Cl^- , Br^- , I^- , HSO_4^- and $H_2PO_4^-$ as TBA salts

An UV-vis titration experiment of receptor **S4R1** with F^- ions was carried out quantitatively to understand the significance of receptor-anion interactions. The spectral changes of receptor **S4R1** as a function of F^- are shown in Fig. 5.19.

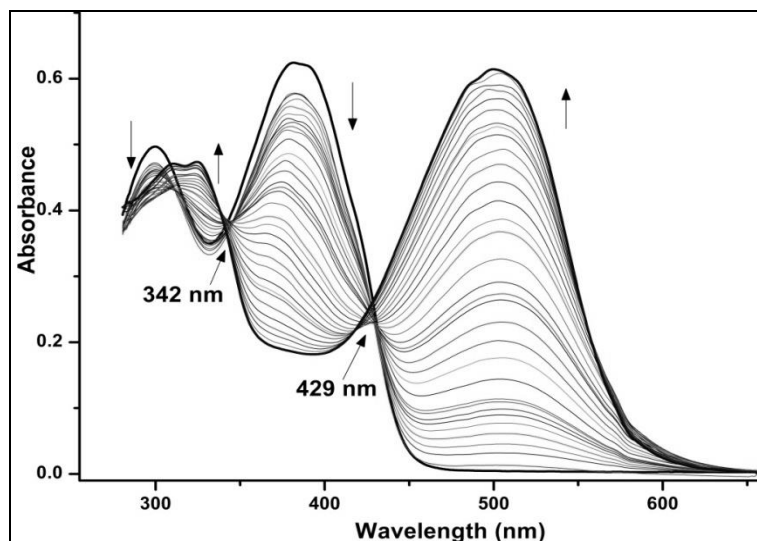


Fig. 5.19 UV-vis titration of **S4R1** (5×10^{-5} M) in DMSO with standard solution of F^- ions (0 – 15 equiv.)

Upon constant addition of F^- ion to the receptor **S4R1** solution in DMSO (5×10^{-5} M) an absorption peak at 299 nm which corresponds to azomethine ($-HC=N-$) shifted to 326 nm. As concentration of F^- ions increased from 0 equiv. to 15 equiv., the intensity of the absorption peak at 383 nm which corresponds to $-OH$ group decreased and a new absorption peak at 503 nm progressively developed with a bathochromic shift of 120 nm. This phenomenon could be attributed to the intermolecular proton transfer interaction. As the F^- ions binds to receptor **S4R1**, an intermolecular proton transfer interaction established between phenolic oxygen and F^- ions which further lead to intramolecular charge transfer (ICT). The ICT of the receptor therefore directly depends on the proton transfer abilities of phenolic oxygen in the presence and absence of fluoride ions. In the absence of F^- ions, the proton transfer interaction is not feasible and the ICT is incompetent. In presence of F^- ions, the ICT is permitted because of the proton transfer interaction between phenolic oxygen and F^- ions which results in visual colour change in the receptor **S4R1**. Continued addition of F^- ions after 15 equiv. resulted negligible change in the intensity of absorption peaks. The UV-vis titration of receptor **S4R3** with F^- ions displayed similar changes in DMSO solution (Fig. 5.20).

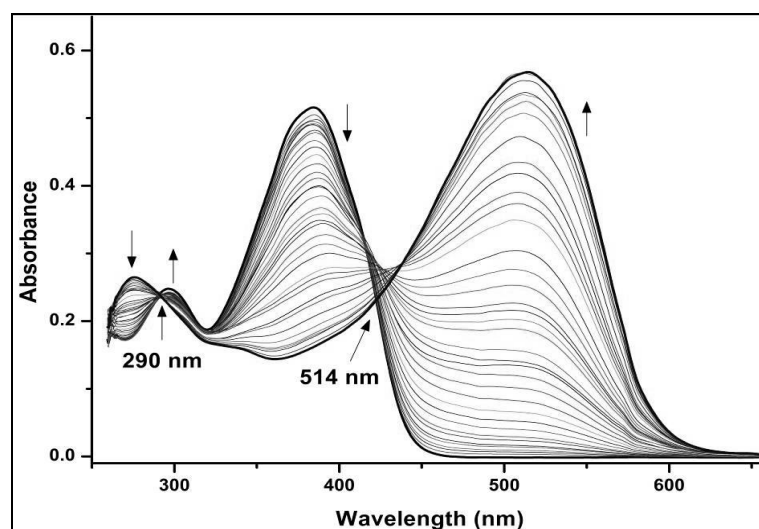


Fig. 5.20 UV-vis titration of **S4R3** (5×10^{-5} M) in DMSO with standard solution of F^- ions (0 – 15 equiv.)

The incremental addition of F^- ions to the receptor solution in DMSO (5×10^{-5} M) resulted in decreased intensity of absorption peaks at 276 nm and 384 nm corresponding to azomethine linkage and $-OH$ group respectively. Simultaneously, a new absorption peaks at 297 nm and 514 nm gradually developed with a bathochromic shift of 21 nm and 130 nm respectively. Similar to the previous discussion, the ICT was established owing to the intermolecular proton transfer between oxygen atom of receptor **S4R3** and F^- ions which employed in the colour change of receptor **S4R3**.

Job's method was used to determine the stoichiometric ratio of the receptor (both **S4R1** and **S4R3**) to F^- ions. Job's plot for receptor **S4R1** in Fig. 5.21, A showed a maximum absorption corresponding to mole ratio of F^- ion at 0.66 which indicated 1:2 complexation between receptor **S4R1** and F^- ions. Job's plot for receptor **S4R3** (Fig.5.21, B) revealed the 1:2 complexation between receptor **S4R3** and F^- ion as it showed maximum absorption corresponding to mole ratio of F^- ion at 0.67.

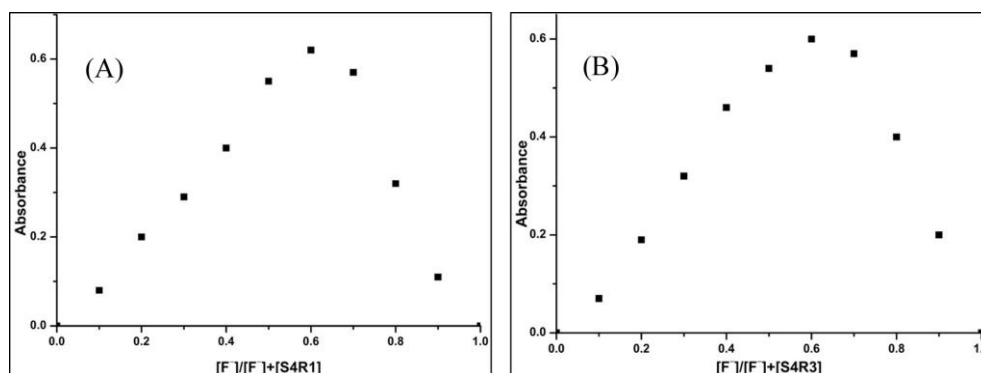
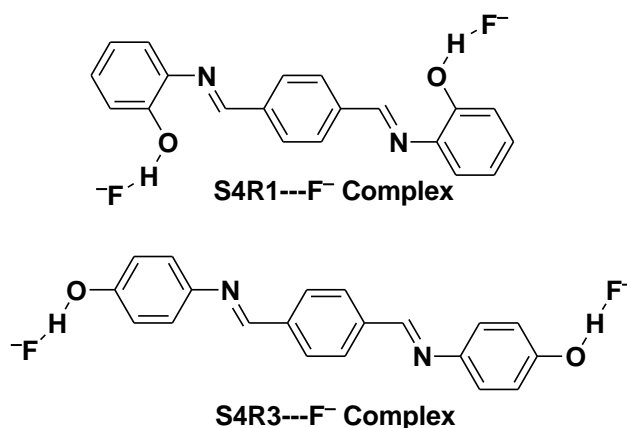


Fig. 5.21 Job's plot which indicates 1:2 complexation ratio between (A) **S4R1** and F^- ion at 503 nm and (B) **S4R3** and F^- ion at 514 nm

Based on the results obtained from UV-vis titration spectra and Job's plot, a possible binding model between receptors and F^- ion was proposed as shown in Scheme 5.3.



Scheme 5.3 Possible binding model of receptor **S4R1** and **S4R3** with F^- ion

5.4 CONCLUSIONS

In conclusion, new receptors **S4R1**- **S4R4** were designed and synthesised to demonstrate geometrical isomeric discrimination of dicarboxylate anions in particular, maleate and fumarate ions. Among these receptors, **S4R1** and **S4R3** showed a prominent colour change from pale yellow to reddish pink only with the addition of maleate ions. The colour change was resulted in a bathochromic shift of 133 nm and 129 nm in UV-vis spectra for receptor **S4R1** and **S4R3** respectively. This shift was owing to the formation of charge transfer complex between the receptors and maleate ion. The binding of maleate ion to the receptor was through hydrogen bonding which was confirmed by 1H NMR titrations. The selectivity with notable colour change of the receptors can be correlated with the change in receptor orientation upon binding with maleate ion. In addition, these receptors colorimetrically detected F^- ions by a colour change from pale yellow to blood red. This colorimetric detection was owing to the intermolecular proton transfer interaction, established between phenolic oxygen and F^- ions which further lead to intramolecular charge transfer between F^- ion and receptors. Therefore, both receptors **S4R1** and **S4R3** can be potential colorimetric receptors not only to discriminate maleate ions over fumarate ions but also to detect biologically important F^- ions over other anions.

CHAPTER 6

***DESIGN AND SYNTHESIS OF BENZOHYDRAZIDE
BASED RECEPTORS FOR DISCRIMINATION OF
MALEATE OVER FUMARATE AND RATIOMETRIC
FLUORIDE ION DETECTION***

The chapter comprises design, synthesis and characterization of new benzohydrazide based receptors. The discriminative property for geometrical isomers of these receptors was discussed in detail. The colorimetric detection of fluoride ions and concentration dependency of the receptors were explored.

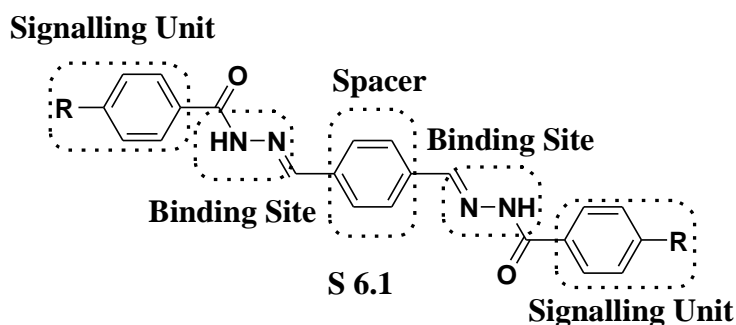
6.1 INTRODUCTION

Majority of the receptors follow binding methodology for the detection of anions. The receptors designed in this methodology comprises two parts *viz.* signalling unit and binding site which are attached together with a covalent linker. Upon binding of anions to the binding site the physical properties of the receptor changes which are transformed to optical changes by signalling unit (Gale 2000; Gale 2001; Beer and Gale 2001). In this methodology, the binding takes place via non-covalent interactions, generally hydrogen bond formation which makes this detection methodology reversible. Based on this methodology, substantial efforts have been devoted by the researchers to establish new receptors that are capable of detecting anions (Gunnlaugsson et al. 2006; Su et al. 2010; Xu et al. 2010; Kim et al. 2011; Tetilla et al. 2011; Villamil-Ramos and Yatsimirsky 2011; Park 2011). However, majority of these efforts restricted for the detection of inorganic anions, mainly fluoride (Cametti and Rissanen 2009; Duke et al. 2010; Gale 2010; Li et al. 2010; Dydio et al. 2011; Kim et al. 2011; Ren et al. 2011; Xu et al. 2012; Kundu et al. 2012; Liu et al. 2012; Zhao et al. 2012; Santos-Figueroa et al. 2012; Gao et al. 2012; Santos-Figueroa et al. 2013; Cametti and Rissanen 2013; Sharma et al. 2013a; Sharma et al. 2013b; Sharma et al. 2013c) and cyanide (Niu et al. 2008; Shiraishi et al. 2009; Chen et al. 2010; Odago et al. 2010; Park et al. 2011b; Kumari et al. 2011; Lin et al. 2012).

On the other hand, apart from the inorganic anion the detection of organic molecule gains significance because of their prevalent applications in the biological field. Among the widespread organic molecules the detection of dicarboxylates ions attains substantial prominence, due to the vital applications in the various metabolic and biological processes (Voet and Voet 1995; Nisbet et al. 2009; El-Sherif 2010; Shin et al. 2011; Xu et al. 2012). Owing to this importance, few receptors have been reported for the selective detection of dicarboxylates (Karl et al. 1995; Raker and Glass 2002; Gunnlaugsson et al. 2002; Liu et al. 2005; Jadhav and Schmidtchen 2006;

Ghosh et al. 2010). However, amongst the dicarboxylates the discrimination of geometrical isomeric dicarboxylates such as *cis/trans* isomers gains significance because of their different biological behaviours (Gougoux et al. 1976; EiamOng et al. 1995). The challenging task of discriminating geometrical isomeric dicarboxylates can be achieved with colorimetric/fluorometric detection approach, where the receptors selectively differentiate the isomers. Based on this strategy, recently few research groups reported receptors which discriminated maleate ion over fumarate ion either colorimetrically or fluorometrically (Sancenon et al. 2003; Costero et al. 2006; Yen and Ho 2006; Lin et al 2007; Tseng et al. 2007; Lin et al. 2009). Nevertheless, the development of new receptors for the discrimination of geometrical isomers such as maleate and fumarate are needs to be explored. The receptor gets added advantage if it could colorimetrically detect other biologically important anions. Among the other biologically important anions, colorimetric detection of fluoride ions gains importance owing to its health benefits (Kirk 1991) and health hazardous roles (WHO 2002).

The receptor in this chapter encompasses two benzohydrazide functionalities (S 6.1) as binding sites for the colorimetric discrimination of maleate ions over fumarate ions. These binding sites are separated by a spacer in between, to make the molecule more flexible. Two new receptors were synthesised, one with nitro group substituted at *p*- position of the terminal phenyl ring. This nitro group participates in the extended conjugation while detecting the anions and hence enhances the colorimetric sensitivity. Third receptor was synthesised to evaluate the role of carbonyl functionality in the receptor. In addition, these receptors were evaluated for the colorimetric detection of fluoride ions. Consequently, these receptors acquire added advantage over other reported receptors.



6.2 EXPERIMENTAL

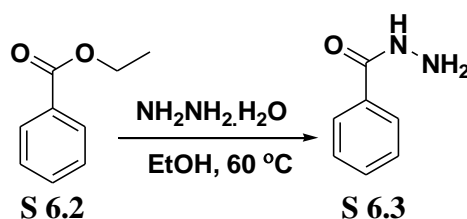
6.2.1 Materials and methods

All chemicals were purchased from Sigma-Aldrich, Alfa Aesar or from Spectrochem and used without further purification. All solvents were procured from SD Fine, India with HPLC grade and used without further distillation.

The ^1H NMR spectra were recorded on a Bruker, Avance II (500 MHz) instrument using TMS as internal reference and $\text{DMSO-}d_6$ as solvent. The raw FID data was processed with MestReNova 7.0.0-8331 software. Resonance multiplicities are described as s (singlet), br s (broad singlet), d (doublet), t (triplet), q (quartet) and m (multiplet). The chemical shifts (δ) are reported in ppm and coupling constant (J) values are given in Hz. Melting points were determined with Stuart- SMP3 melting-point apparatus in open capillaries and are uncorrected. IR spectra were recorded on a Thermo Nicolet Avatar-330 FT-IR spectrometer; signal designations: s (strong), m (medium), w (weak), br.m (broad medium) and br.w (broad weak). Mass spectra were recorded on Waters Micromass Q-ToF micro spectrometer with ESI source. The SCXRD was performed on Bruker AXS APEX II system. UV-vis spectroscopy was carried out with Ocean Optics SD2000-Fibre Optics Spectrometer and Analytikjena Specord S600 Spectrometer in standard 3.5 mL quartz cells (2 optical windows) with 10 mm path length. Elemental analyses were done using Flash EA1112 CHNS analyser (Thermo Electron Corporation). All reactions were monitored by TLC on pre-coated silica gel 60 F_{254} plates which were procured from Merck.

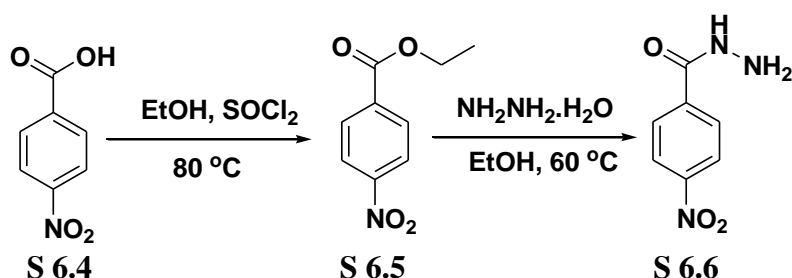
6.2.2 Synthesis of intermediates S 6.3 and S 6.7

The ethylbenzoate S 6.2 (6.65 mmol) was treated with hydrazine hydrate (33.29 mmol) in presence of ethanol and heated to 60°C for 2.5 h. The reaction mixture was cooled below 5°C . The solid formed was filtered and dried to give colourless solid intermediate S 6.3 (Scheme 6.1)



Scheme 6.1 Synthesis of intermediate S 6.3

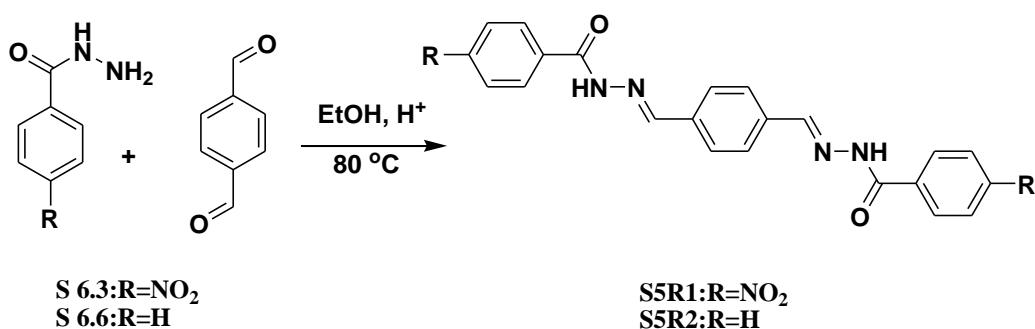
To a solution of 4-nitrobenzoic acid **S 6.4** (2.99 mmol) in ethanol, thionylchloride (3.3 mmol) was added. The reaction was catalysed by a drop of dimethylformamide (DMF). Reaction mixture was refluxed for 4 h. Completion of the reaction was confirmed by thin layer chromatography. Excess of ethanol was removed by concentration from the reaction mixture, diluted with dichloromethane and washed with water. Organic layer was separated, dried over anhydrous Na_2SO_4 and evaporated to yield corresponding ester (**S 6.5**). Thus obtained ester **S 6.5** (2.6 mmol) was treated with hydrazine hydrate (12.8 mmol) in presence of ethanol and heated to $60\text{ }^\circ\text{C}$ for 2.5 h. The reaction mixture was cooled below $5\text{ }^\circ\text{C}$. The solid formed was filtered and dried to give pale yellow coloured solid intermediate **S 6.6** (Scheme 6.2).



Scheme 6.2 Synthesis of intermediate **S 6.6**

6.2.3 Synthesis of receptors **S5R1** and **S5R2**

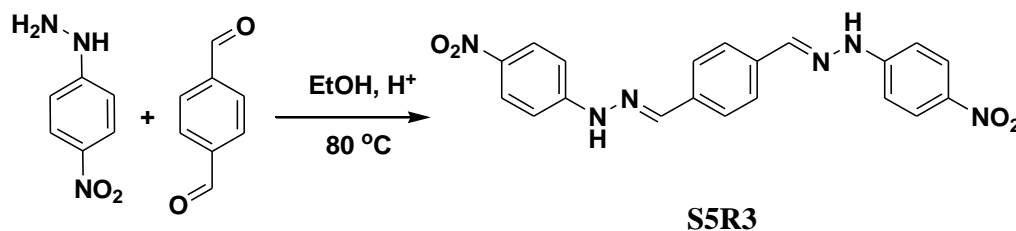
A mixture of terphthalaldehyde (0.75 mmol) and intermediate **S 6.3** or **S 6.6** (1.5 mmol) reacted in ethanol under reflux for 5 h. The reaction was catalysed by a drop of acetic acid. After cooling, the solid was filtered and washed with ethanol to obtain the solid target compounds (**S5R1** and **S5R2**); Scheme 6.3.



Scheme 6.3 Synthesis of the receptors **S5R1** and **S5R2**

6.2.4 Synthesis of receptors S5R3

A mixture of terephthalaldehyde (0.75 mmol) and 4-nitrophenylhydrazine (1.5 mmol) was reacted in ethanol under reflux condition for 5 h. The reaction was catalysed by a drop of acetic acid. After cooling, the solid was filtered and washed with ethanol to obtain the solid target compound **S5R3** (Scheme 6.4).



Scheme 6.4 Synthesis of the receptor **S5R3**

The single crystal of the receptors **S5R2** suitable for X-ray diffraction analysis was obtained by slow evaporation of DMF solution at room temperature. The ORTEP diagram (50% probability) of the receptor **S5R2** is given in Fig. 6.1.

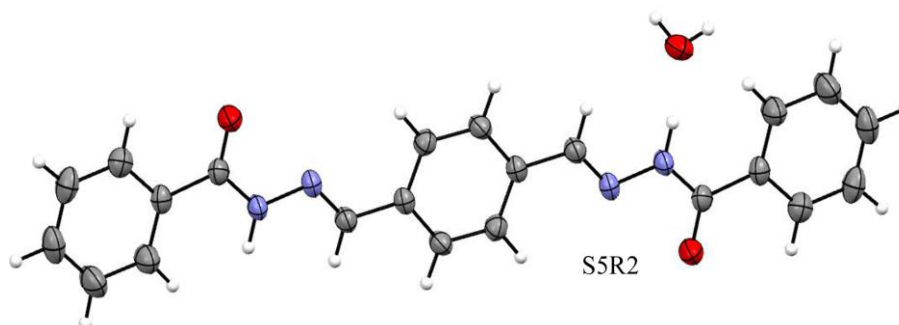


Fig. 6.1 The ORTEP diagram of receptor **S5R2** with 50% probability

The receptor **S5R2** crystallised in monoclinic lattice. Detailed crystallographic data of receptor **S3R2** is given in the Table 6.1

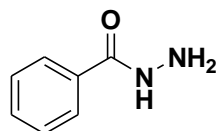
Table 6.1 Crystallographic data of receptor **S5R2**

Receptor	S5R2
Chemical formula	C ₂₂ H ₁₈ N ₄ O ₃
Formula weight	370.40
Crystal System	Monoclinic
Space group	C2/c
a (Å)	12.5507 (6)

b (Å)	4.6846 (2)
c (Å)	34.5126 (17)
α (°)	90.00
β (°)	96.507 (6)
γ (°)	90.00
V (Å)³	2016.1 (16)
Z	4
Crystal size	0.47 × 0.31 × 0.26
F (000)	776
R-factor (%)	4.58

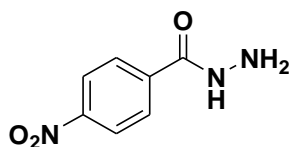
All intermediates and receptors were characterized by spectral analysis. The characterization data have been compiled and given below.

Benzohydrazide (S 6.3)



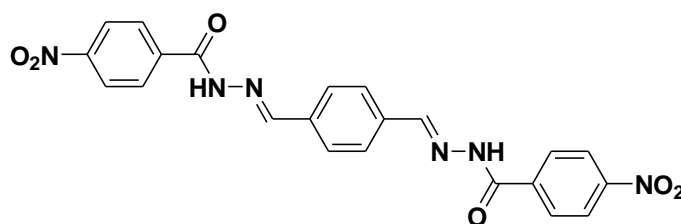
Yield: 92%. m.p.: 114.6°C. Elemental analysis: Calculated for C₇H₈N₂O (%): C 71.75, H 5.92, N 20.58. Experimental: C 71.65, H 5.98, N 20.38. FT-IR in cm⁻¹: 3292.9 (m), 3190.4 (s), 3010.4 (s), 1607.9 (s), 1559.5 (s), 1335.5 (s), 671.9 (s).

4-nitrobenzohydrazide (S 6.6)



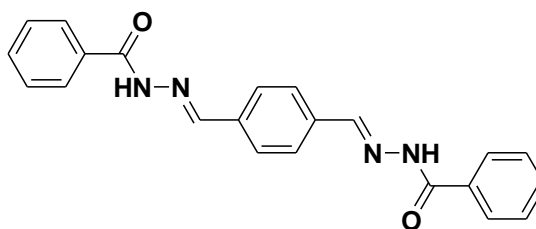
Yield: 89%; m.p.: 216.4°C. Elemental analysis: Calculated for C₇H₇N₃O₃: C 46.41, H 3.89, N 23.20. Experimental: C 46.25, H 3.62, N 23.38. FT-IR in cm⁻¹: 3316.8 (m), 3037.6 (w), 1608.6 (m), 1511.6 (s), 1313.8 (m), 926.2 (m), 857.1 (m), 589.7 (m).

N', N''-[benzene-1,4-diyl di(E)methylylidene]bis(4-nitrobenzohydrazide) (S5R1)



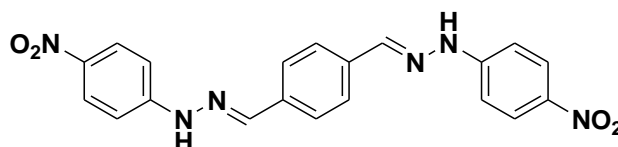
Yield: 84%; m.p.: > 350 °C. Elemental analysis: Calculated for C₂₂H₁₆N₆O₆ (%): C 57.39, H 3.50, N 18.25. Experimental: C 57.36, H 3.49, N 18.28. ¹H NMR (500 MHz, DMSO-*d*₆): δ 12.25 (s, 2H, -NH); δ 8.51 (s, 2H, =CH); δ 8.40 (d, 4H, Ar-H, *J*= 8.5 Hz), δ 7.18 (d, 4H, Ar-H, *J*= 8.5 Hz), δ 7.87 (s, 4H, Ar-H). FT-IR in cm⁻¹: 3511.8 (m), 3088.6 (w), 1654.7 (m), 1594.9 (s), 1562.4 (s), 1521.5 (s), 1334.7 (s), 1275.1 (s).

***N', N''*-[benzene-1,4-diyl-di(*E*)methylidene]dibenzohydrazide, (S5R2)**



Yield: 80%; m.p.: 330.6 – 331.2 °C. Elemental analysis: Calculated for C₂₂H₁₈N₄O₂ (%): C 71.34, H 4.90, N 15.13. Experimental: C 71.32, H 4.91, N 15.12. ¹H NMR (500 MHz, DMSO-*d*₆): δ 11.96 (s, 2H, -NH); δ 8.49 (s, 2H, =CH); δ 7.94 (d, 4H, Ar-H, *J*=9.5 Hz), δ 7.83 (s, 4H, Ar-H), δ 7.62 (t, 2H, Ar-H, *J*=7.25 Hz), δ 7.54 (t, 4H, Ar-H, *J*=7.5 Hz). FT-IR in cm⁻¹: 3251.4 (m), 1647.3 (s), 1538.1 (s), 1275.5 (s).

(1*E*, 1'*E*)-1, 1'-[benzene-1,4-diyl-di(*E*)methylidene]bis[2-(4-nitrophenyl)hydrazine] (S5R3)



Yield: 78%; m.p.: 274.5 – 275.3 °C. Elemental analysis: Calculated for C₂₀H₁₆N₆O₄ (%): C 59.40, H 3.99, N 20.78. Experimental: C 59.42, H 3.96, N 20.75. ¹H NMR (500 MHz, DMSO-*d*₆): δ 8.78 (s, 2H, =CH); δ 8.33 (d, 4H, Ar-H, *J*= 8.5 Hz), δ 8.16 (s, 4H, Ar-H), δ 7.52 (d, 4H, Ar-H, *J*= 9 Hz), δ 7.54 (t, 4H, Ar-H, *J*=7.5 Hz). FT-IR in cm⁻¹: 3271.4 (m), 1570.5 (s), 1503.8 (s), 1329.9 (s).

The representative spectra of receptors have been given below.

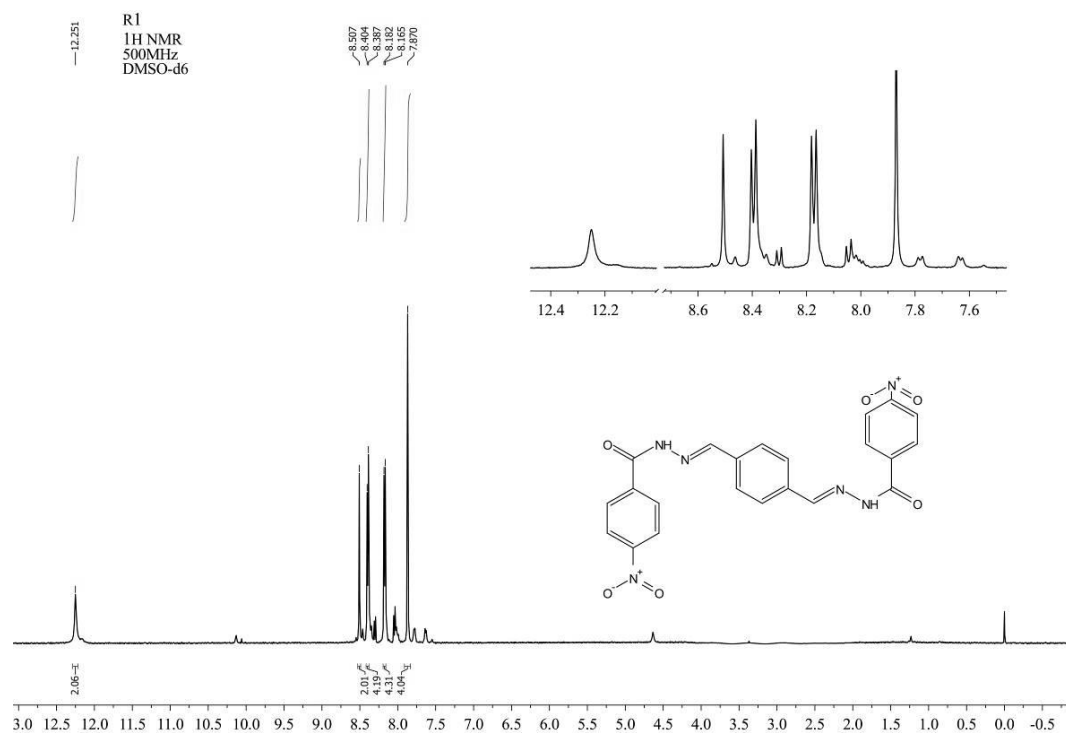


Fig. 6.2 ^1H NMR spectra of S5R1

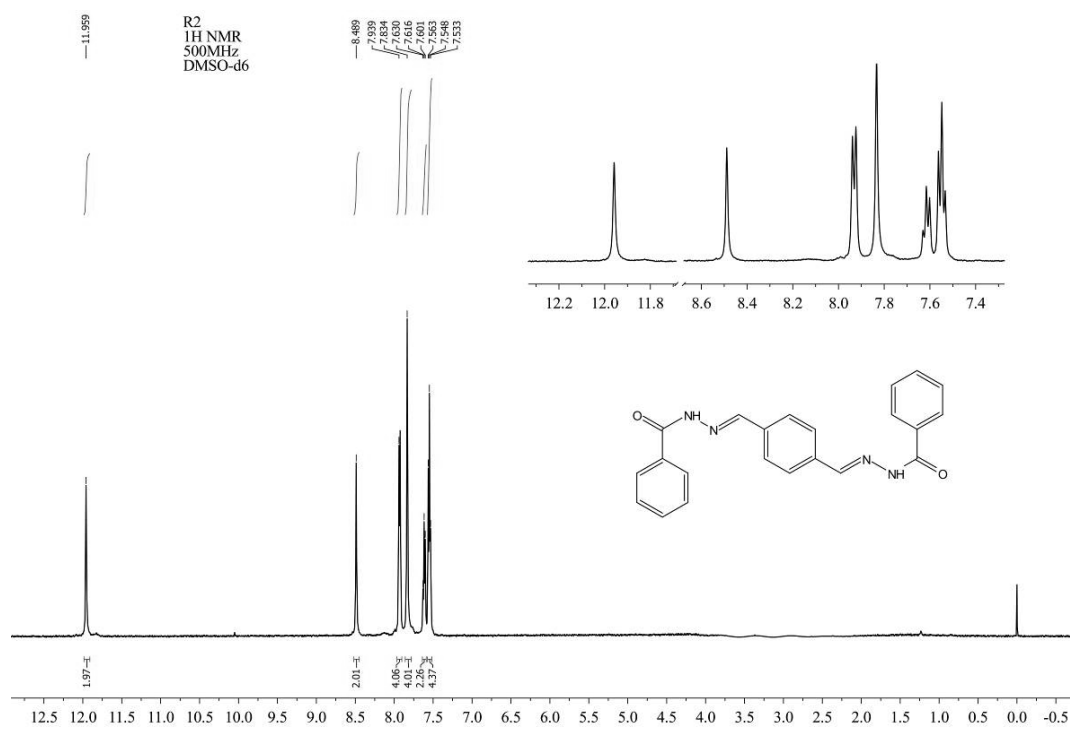


Fig. 6.3 ^1H NMR spectra of S5R2

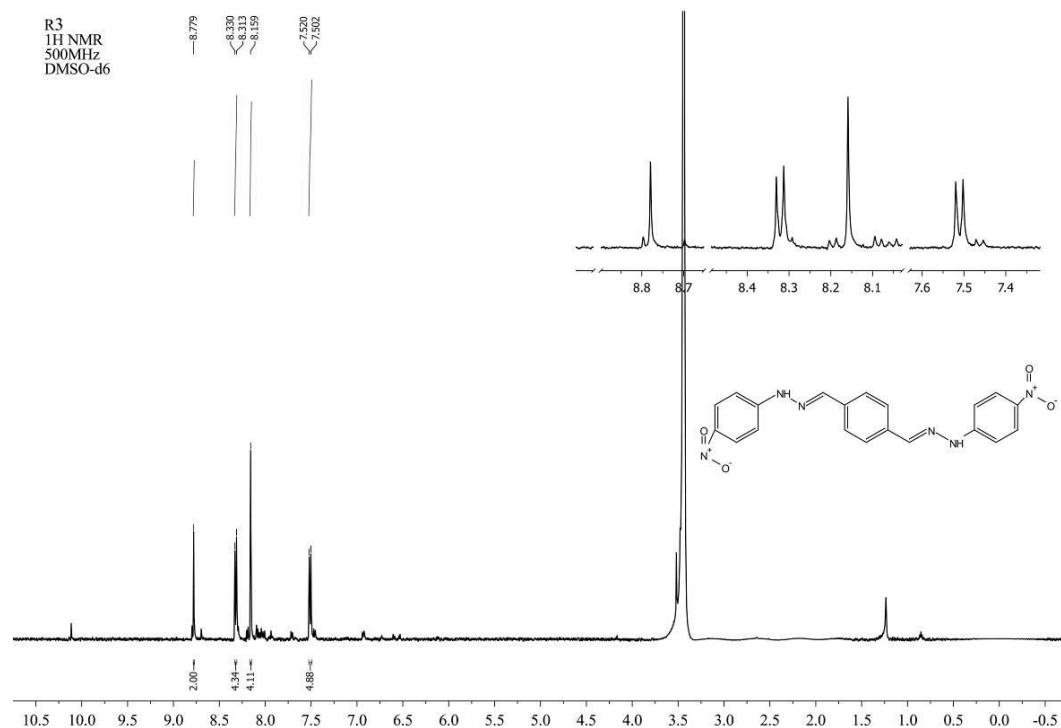


Fig. 6.4 ¹H NMR spectra of **S5R3**

6.2.5 General procedure for the synthesis of tetrabutylammonium salts

To a stirred solution of a dicarboxylic acid (2.5 mmol) in dry methanol (5 mL), a 1.0 M solution of tetrabutylammonium hydroxide in methanol (2.0 equiv.) was added. The reaction mixture was stirred at room temperature for 2 h. The solvent was evaporated under reduced pressure and dried over P₂O₅ to obtain tetrabutylammonium salt of corresponding dicarboxylic acid and the salt was used immediately for further applications.

6.3 RESULTS AND DISCUSSION

6.3.1 Discrimination of isomeric dicarboxylates

The isomeric selectivity of the receptors **S5R1**, **S5R2** and **S5R3** with maleate and fumarate anions in dry DMSO was investigated by UV-vis spectroscopy. Upon the addition of maleate ions (10 equiv.) in the form of tetrabutylammonium (TBA) salt to the receptor **S5R1**, a prominent change in the UV-vis spectrum was observed. However, no change was observed with the addition of fumarate ions (Fig. 6.5).

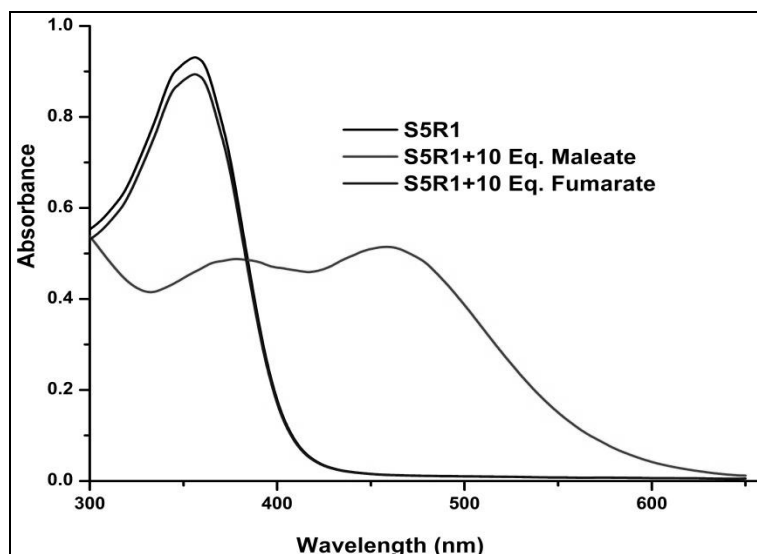


Fig. 6.5 UV-vis spectral change on addition of 10 equiv. maleate and fumarate ions to the receptor **S5R1** solution (5×10^{-5} M)

The UV-vis investigation was further extended to other receptor solutions (**S5R2** and **S5R3**) in dry DMSO. Upon addition of maleate ions to receptor **S5R2**, a slight change in the UV-vis spectra was observed (Fig. 6.6, i). However, the receptor **S5R3** did not show any significant change after adding 20 equiv. of anions (Fig. 6.6, ii).

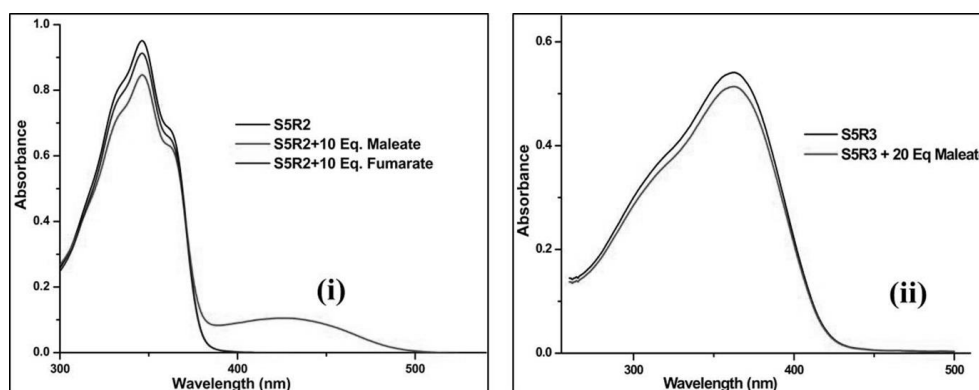


Fig. 6.6 (i) UV-vis spectral change on addition of 10 equiv. maleate ions and fumarate in the form of TBA salts to the receptor **S5R2** solution (5×10^{-5} M). (ii) UV-vis spectral changes of **S5R3** (5×10^{-5} M) in DMSO after addition of 20 equiv. of maleate

The dry DMSO solution of receptor **S5R1** (5×10^{-5} M) was tested for the colorimetric discrimination of maleate and fumarate ions by adding 1 equiv. of anion

solutions as TBA salts. The addition of maleate ions to the receptor **S5R1** showed a significant colour change instantaneously from colourless to orange red whereas fumarate ions did not show any visual changes (Fig. 6.7).

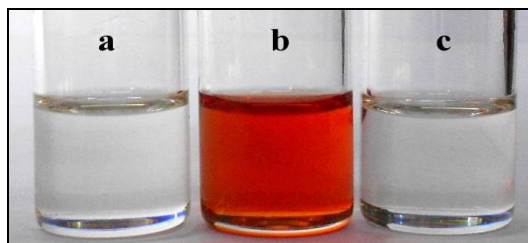


Fig. 6.7 Change in colour on addition 1 equiv. of anions in the form of TBA salt; (a) Free receptor **S5R1** (5×10^{-5} M), (b) **S5R1**+ 1 equiv. maleate ions and (c) **S5R1**+ 1 equiv. fumarate ions

The colorimetric discrimination study was extended to receptor **S5R2** (Fig. 6.8). The receptor **S5R2** showed significant colour change from colourless to yellow upon adding 1 equiv. of maleate ion in dry DMSO solution (5×10^{-5} M).

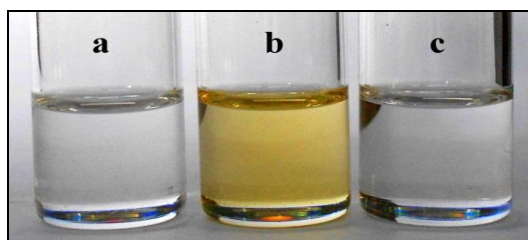


Fig. 6.8 Change in colour upon addition 1 equiv. of anions in the form of TBA salt; (a) Free receptor **S5R2** (5×10^{-5} M), (b) **S5R2**+ 1 equiv. maleate ions and (c) **S5R2**+ 1 equiv. fumarate ions

Further, the binding mechanism of maleate ions to the receptor **S5R1** was studied by ^1H NMR titration and UV-vis titration experiment. The ^1H NMR titration of receptor was performed with maleate ions in dry $\text{DMSO-}d_6$ solution (Fig. 6.9). With the incremental addition of maleate ion (0 to 2 equiv.) to receptor **S5R1**, the proton corresponding to benzohydrazide $-\text{NH}$ (Ha) involves in hydrogen bond formation with carboxylate group of maleate ion. As a result the electron density over proton Ha decreased and therefore, a downfield shift in signal at δ 12.25 corresponds to this proton was observed. As the concentration of maleate ion increased, an

intermolecular hydrogen bond complex was established between receptor **S5R1** and maleate ion. Consequently, the electron density over imine protons decreases and as a result a slight downfield shift in the signal at δ 8.51 corresponding to proton Hb was observed. Simultaneously, the splitting pattern of signal corresponding to *p*-nitrophenyl protons (Hc at δ 8.40 and δ 7.18) were disappeared. This observation was perhaps due to the fast proton exchange within the intermolecular hydrogen bond complex.

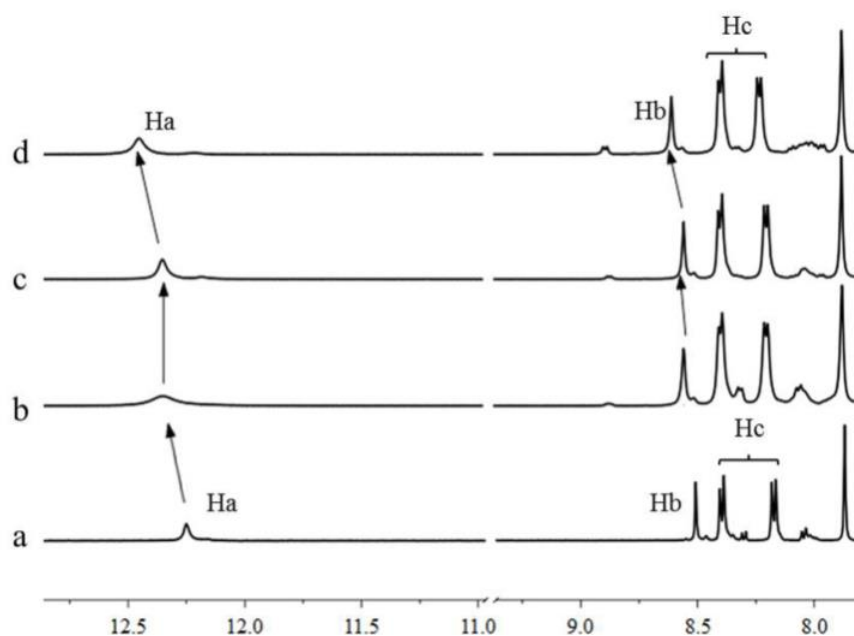


Fig. 6.9 Partial ^1H NMR spectra of receptor **S5R1** in presence of (a) 0 equiv., (b) 0.5 equiv., (c) 1 equiv. and (d) 2 equiv. of maleate ions in $\text{DMSO-}d_6$ solution

Fig. 6.10 shows UV-vis titration spectra of the receptor **S5R1** with maleate ions carried out in dry DMSO solvent. With the incremental addition of maleate ions to the standard receptor solution (5×10^{-5} M) a constant decrease in the absorption band at 356 nm followed by the appearance of new absorption band at 460 nm was observed. This bathochromic shift of 104 nm with a clear isosbestic point at 385 nm was ascribed to the establishment of intermolecular hydrogen bond complex between the receptor and maleate ion. The formation of clear isosbestic point at 385 nm specifies that the complex formation was due to hydrogen bonded electrostatic interactions (Yen and Ho 2006).

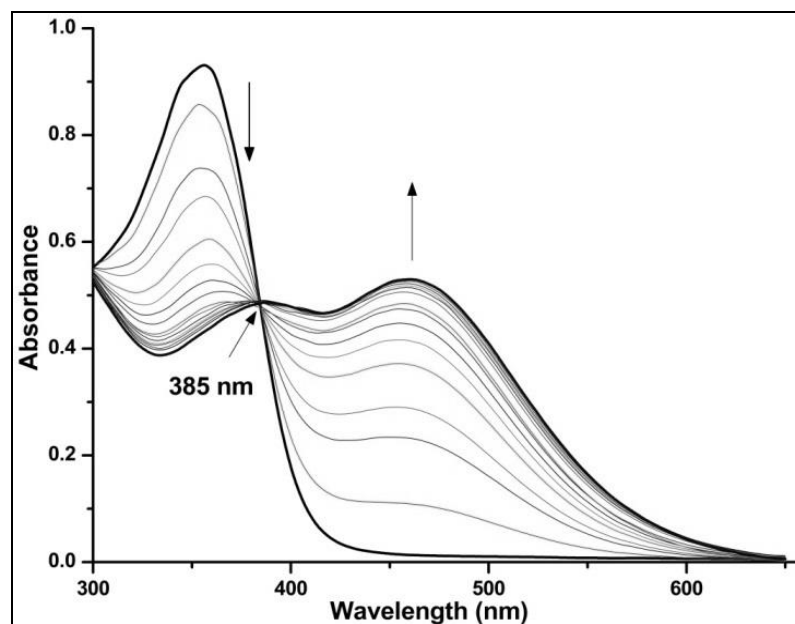


Fig. 6.10 UV-vis titration of receptor **S5R1** (5×10^{-5} M) in dr DMSO with standard solution of maleate ions (0–15 equiv.)

Binding stoichiometric ratio of the complex between receptor **S5R1** and maleate ion was determined using Job's method (Fig. 6.11). A maximum absorbance change was observed at 460 nm, when the mole fraction of **S5R1** versus maleate ion was 0.5.

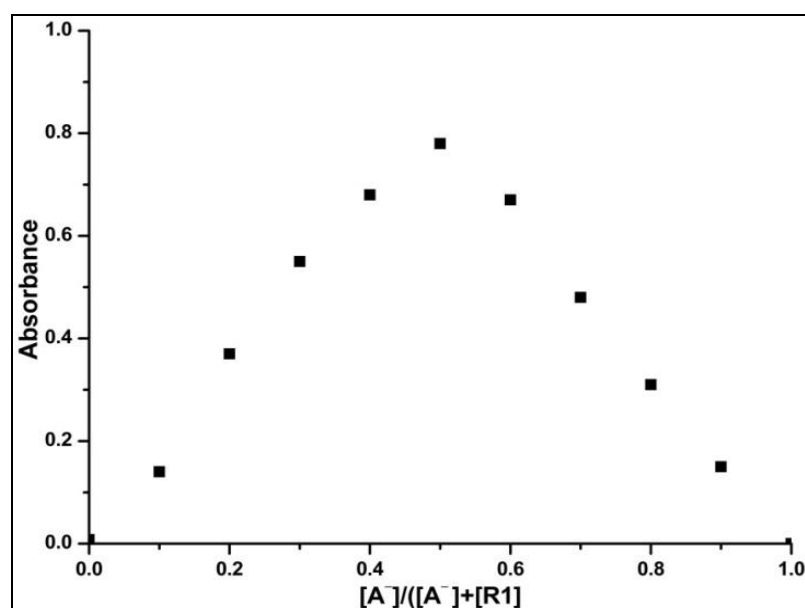


Fig. 6.11 Job's plot at 460 nm which indicates 1:1 complexation ratio between **S5R1** and maleate ion

This clearly confirmed the formation of 1:1 stoichiometry between **S5R1** and maleate ion. The binding constant was calculated using Benesi – Hildebrand equation (Benesi and Hildebrand, 1949) and found to be $3.29 \pm 0.78 \times 10^4 \text{ M}^{-1}$.

Further, the receptor **S5R2** was subjected to quantitative analysis using UV-vis titration experiment (Fig. 6.12).

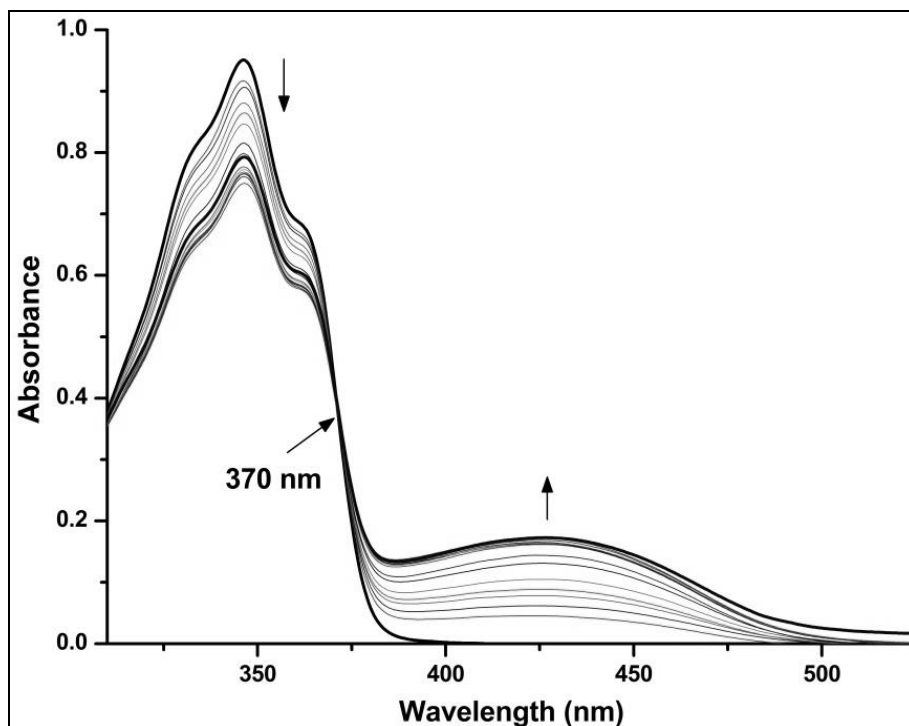


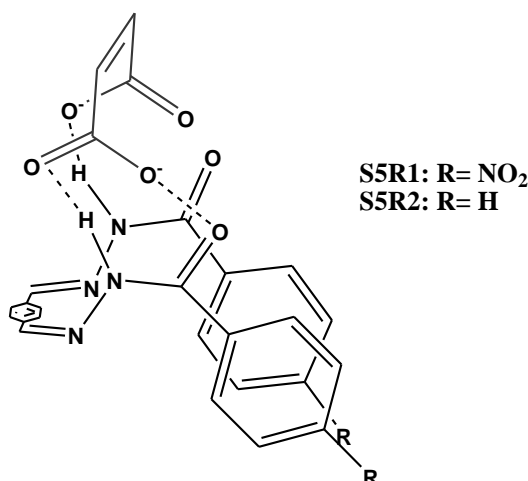
Fig. 6.12 UV-vis titration of receptor **S5R2** ($5 \times 10^{-5} \text{ M}$) in dry DMSO with standard solution of maleate ions (0 – 15 equiv.)

Upon increasing addition of the standard maleate ion solution to the receptor **S5R2** solution ($5 \times 10^{-5} \text{ M}$) in dry DMSO, a constant decrease in the intensity of absorption band at 346 nm was observed. Simultaneously, a new absorption band centred at 427 nm with a bathochromic shift of 81 nm was observed. The absorbance intensity of this new absorption band was constantly increased with increase in the concentration of maleate ions. This bathochromic shift with a clear isosbestic point at 370 nm was resulted due to the formation of intermolecular hydrogen bond complex between receptor **S5R2** and the maleate ions.

The stoichiometric ratio of the receptor-anion complex was decided by Job's method which was obtained from UV-vis titration data at 427 nm for DMSO solution

of receptor **S5R2**. The plot showed maximum absorbance when the mole fraction was 0.5, which corresponds to 1:1 stoichiometric ratio between receptor **S5R2** and maleate ion. The binding constant was calculated using Benesi – Hildebrand equation and found to be $2.88 \pm 0.08 \times 10^4 \text{ M}^{-1}$.

The isomeric discrimination ability of receptors **S5R1** and **S5R2** could be related with the receptor orientation. The orientation of receptors changes with the conformation of incoming guest (maleate ion) stereochemistry. The *cis* conformation of maleate ions can easily fit with benzohydrazide functionality of the receptors and can form hydrogen bonded complex structure as shown in Scheme 6.5. However, the fumarate ion cannot exactly fit with benzohydrazide group of the receptor because of its *trans* conformation.



Scheme 6.5 Proposed binding model for the receptors with maleate ion

Simultaneously, basicity of the maleate ion also play important role in the discrimination process. Maleate ion being more basic ($\text{pK}_{\text{a}1}$: 5.0, $\text{pK}_{\text{a}2}$: 18.8 in DMSO; Choi et al. 2002) can easily bind to acidic proton of the receptor whereas fumarate ion is not enough basic ($\text{pK}_{\text{a}1}$: 9.0, $\text{pK}_{\text{a}2}$: 11.0 in DMSO; Choi et al. 2002) to produce any electrostatic interaction with the receptor.

Due to the presence of carbonyl ($-\text{C}=\text{O}$) groups in receptors **S5R1** and **S5R2**, the adjacent $-\text{NH}$ protons are highly acidic in nature and these protons in receptors **S5R1** and **S5R2** readily binds to the basic anions. In case of receptor **S5R1** the electron withdrawing $-\text{NO}_2$ group at *p*- position further increases the acidity of $-\text{NH}$

protons, because of which the maleate ion binds more strongly to receptor **S5R1** than receptor **S5R2**. As result, receptor **S5R1** showed more intense colour change (colourless to orange red) with maximum bathochromic shift than receptor **S5R2** (colourless to yellow) upon binding with maleate ion. However, the receptor **S5R3**, being a hydrazine derivative do not have carbonyl group and hence, the $-NH$ proton is not acidic enough to bind with maleate ion. In addition to this, lack of carbonyl group gives restricted flexibility and steric hindrance to the receptor **S5R3**. As a result, the receptor **S5R3** do not show any colorimetric change either with the addition of maleate ions or with fumarate ions.

6.3.2 Detection of F^- ions

Further, the receptors **S5R1** and **S5R2** were examined for colorimetric detection of other important anions such as fluoride, chloride, bromide, iodide, nitrate, hydrogensulphate, dihydrogenphosphate and acetate in the form of tetrabutylammonium (TBA) salts. The absolute dry DMSO solutions of receptors were treated with 1 equiv. of different anions, in which the receptors were able to colorimetrically recognize F^- ions and AcO^- ions. Upon adding F^- ions and AcO^- ions to receptor **S5R1** displayed a colour change from colourless to orange and the colour of receptor **S5R2** changed from colour less to yellow for F^- ion and pale yellow for AcO^- ions (Fig. 6.13, A and B). However, the colour intensity was more on adding F^- ions because of strong binding.

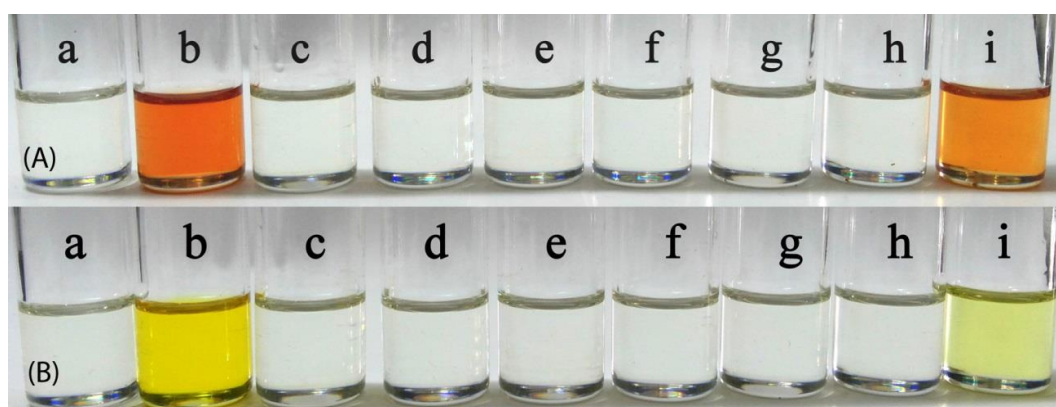


Fig. 6.13 Colour change of (A) **S5R1** and (B) **S5R2** (5×10^{-5} M) in dry DMSO upon adding 1 equiv. of TBA anions; (a) Free Receptor, (b) F^- , (c) Cl^- , (d) Br^- (e) I^- , (f) NO_3^- , (g) HSO_4^- , (h) $H_2PO_4^-$ and (i) AcO^-

The colorimetric study was further confirmed by UV-vis spectral studies. The UV-vis spectra of receptor **S5R1** and receptor **S5R2** were measured by adding 1 equiv. of different anions (Fig. 6.14, A and B) in DMSO.

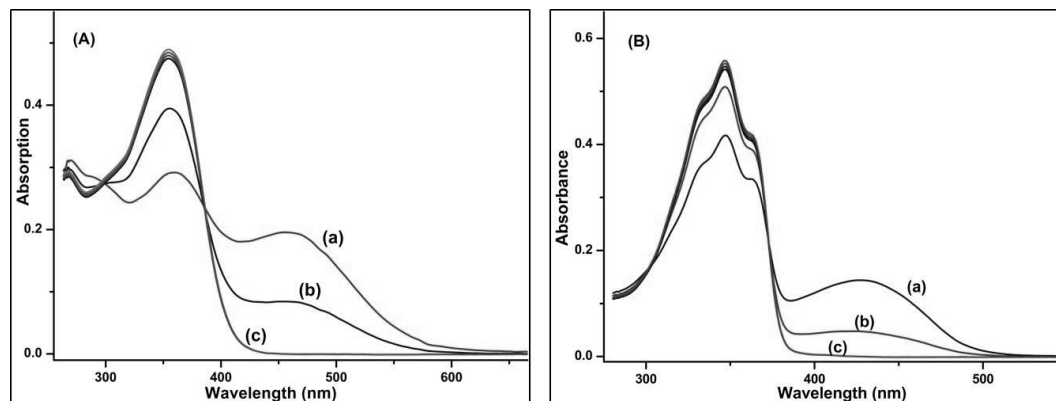


Fig. 6.14 UV-vis spectra of (A) **S5R1** and (B) **S5R2** in dry DMSO (5×10^{-5} M) upon adding 1 equiv. of (a) F^- ions, (b) AcO^- ions and (c) Cl^- , Br^- , I^- , NO_3^- , HSO_4^- , $H_2PO_4^-$ ions in the form of TBA salts

The UV-vis spectrum of receptor **S5R1** exhibited a strong absorption peak at 354 nm and the receptor **S5R2** displayed a strong absorption peak at 346 nm. Upon adding F^- ions to receptors **S5R1** and **S5R2**, a new absorption band at 458 nm and 423 nm were observed respectively. In presence of AcO^- ions the receptors **S5R1** and **S5R2**, showed a new broad absorption band with less intensity, while other anions produced no significant changes in UV-vis spectra. Thus, the receptor to anion interaction is strong with F^- ions and it is much weaker with AcO^- ions. On the other hand, all other anions either not interacted with receptors or the interaction was not enough to perturb any changes in UV-vis spectra. Therefore the receptors were highly selective to F^- ions and this selectivity could be ascribed to small size and the high charge density of F^- anion, which enables F^- ion to form a strong hydrogen bond with $-NH$ of the receptors.

To understand the binding phenomenon of receptors quantitatively, UV-vis titration experiments were performed (Fig. 6.15). Upon incremental addition of F^- ions (0 to 1 equiv.) to the receptor **S5R1** solution in DMSO, the UV-vis absorption band at 354 nm corresponding to imine ($-CH=N$) linkage decreased and a new absorption band at 458 nm with an isosbestic point at 384 nm was appeared. This

bathochromic shift was attributed to the formation of hydrogen-bond F^- ion complex with the receptor **S5R1**. The 458 nm peak corresponds to CT transition in the **S5R1**- F^- ion complex. Above 1 equiv., the band at 354 nm diminished completely and the peak at 458 nm gradually shifted bathochromically.

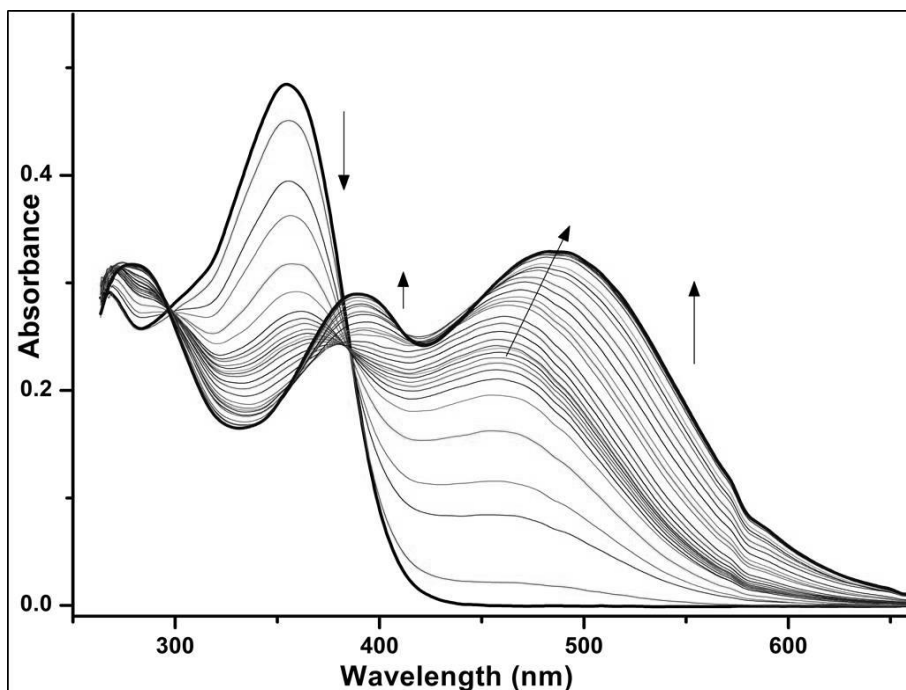


Fig. 6.15 UV-vis titration of receptor **S5R1** (5×10^{-5} M) in DMSO with standard solution of F^- ions (0 – 15 equiv.)

As the amount of F^- ions increased, the absorption band at 458 nm completely shifted to 488 nm. Meanwhile a new absorption band at 390 nm gradually appeared. This bathochromic shift of 30 nm and generation of new absorption band ascribed to the second step of the binding process where the higher concentration of F^- ions lead to the deprotonation of the receptor **S5R1** to form conjugate base (**S5R1** $^-$). Simultaneously a new absorption band at 390 nm generated which clearly confirms the formation and stabilization of deprotonated species receptor **S5R1** in the system. The binding process reached saturation after adding 10 equiv. of F^- ions where the conjugate base stabilizes. Therefore, the binding process involves two steps. At first, receptor **S5R1** forms adduct to give **S5R1** $\cdots F^-$ complex and in second stage receptor deprotonates to form **S5R1** $^-$ species.

The receptor **S5R2** showed similar trend upon titrating with F^- ions. As shown in the Fig. 6.16, with incremental addition of F^- ions, absorption band at 346 nm constantly decreased and a new band at 423 nm generated with an isosbestic point at 373 nm.

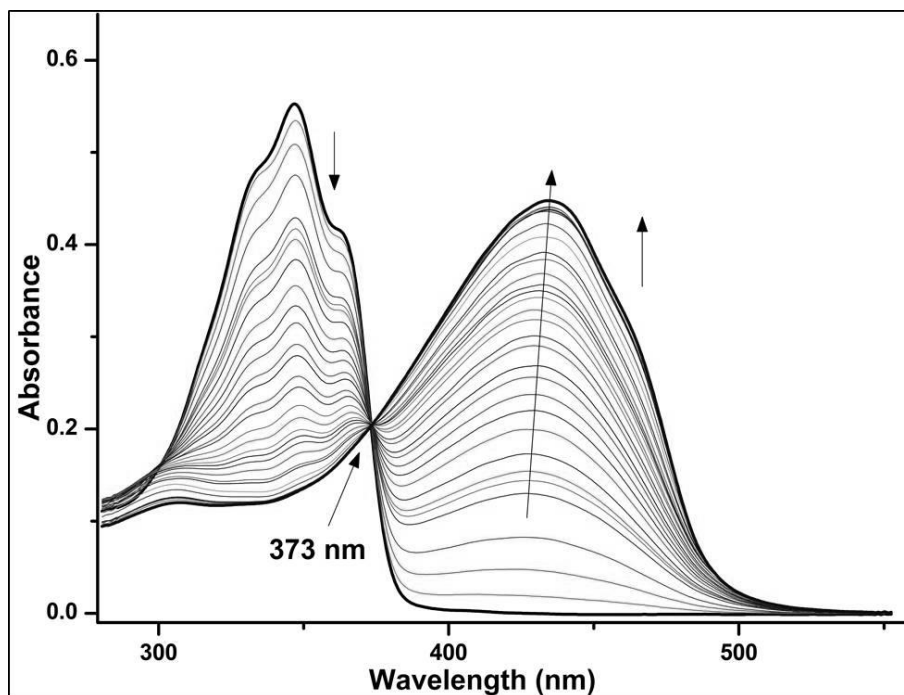


Fig. 6.16 UV-vis titration of receptor **S5R2** (5×10^{-5} M) in DMSO with standard solution of F^- ions (0–15 equiv.)

This new absorption band with a bathochromic shift of 77 nm was attributed to the formation of hydrogen-bonded F^- ion complex with receptor **S5R2**. When the F^- ion concentration increased above 1 equiv. the absorption peak at 423 nm shifted bathochromically to new absorption band 434 nm. At the same time absorption band at 346 nm disappeared completely. This second bathochromic shift of 11 nm at higher concentration of F^- ions was ascribed to the formation of new deprotonated species **S5R2⁻**. However, unlike in receptor **S5R1**, the receptor **S5R2** displayed less bathochromic shift. This was perhaps due to the substitution of strong electron withdrawing group ($-NO_2$) in receptor **S5R1**, owing to which the receptor exhibits extended conjugation.

In addition, the receptor-anion binding mechanism was confirmed by ^1H NMR titration experiment of **S5R1** with F^- ion (as TBA salt) which was carried out in $\text{DMSO-}d_6$ (Fig. 6.17).

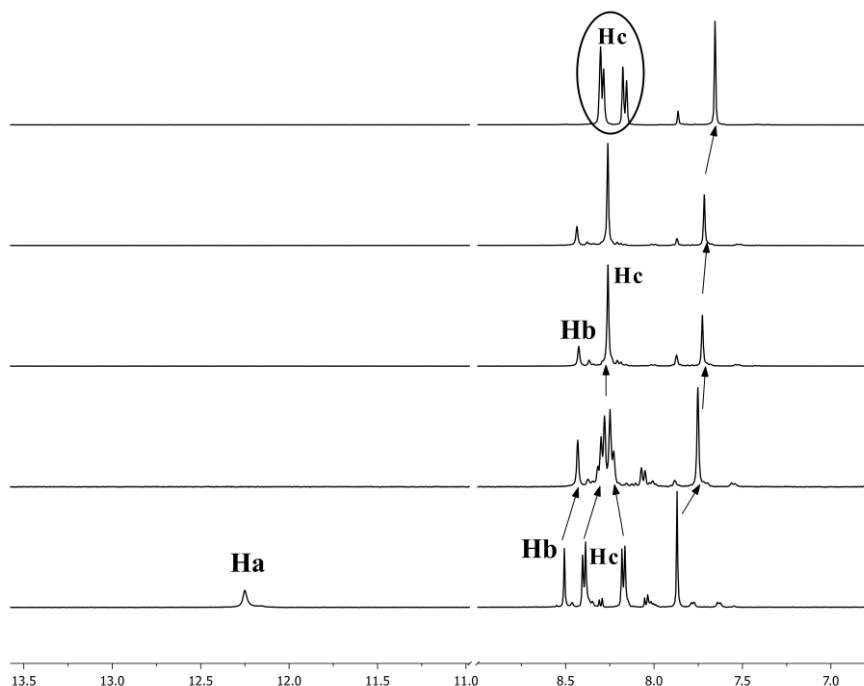
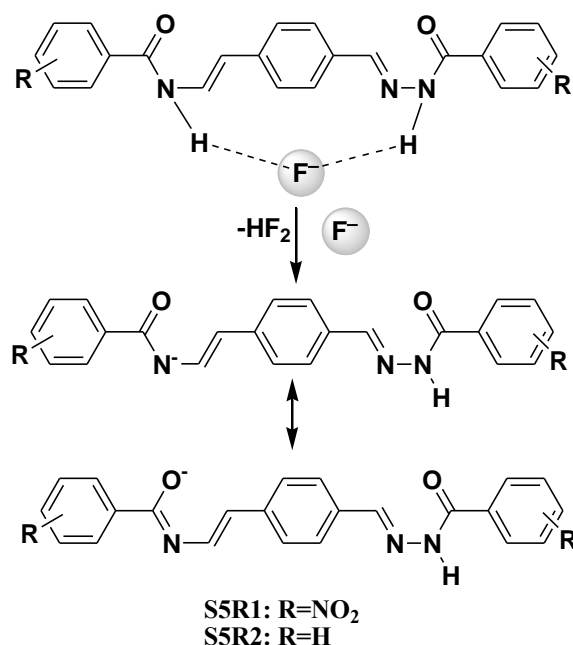


Fig. 6.17 Partial ^1H NMR spectra of receptor **S5R1** in $\text{DMSO-}d_6$ after the addition of (a) 0 equiv., (b) 1 equiv., (c) 2 equiv. and (d) 5 equiv. of F^- ions

The proton Ha at δ 12.25 corresponding to $-\text{NH}$ of receptor **S5R1** was disappeared completely upon adding TBAF which confirms the deprotonation process. The signals at δ 8.40 and δ 8.18 (Hc) corresponding to nitro phenyl group were merged together till 2 equiv. of F^- ions due to the fast proton exchange through the receptor R1 and at 5 equiv. of F^- ions the splitting of the signals corresponding to nitro phenyl group reappeared perhaps due to stabilization of conjugated quinonoid form of nitro phenyl group in receptor **S5R1**. As the concentration of F^- ion increased from 1 equiv. to 5 equiv., signal at δ 8.51 corresponding to imine proton (Hb) and signal at δ 7.87 corresponding to other aromatic protons respectively was experienced an upfield shift owing to the increase in electron density over receptor **S5R1**.

Based on the UV-vis titration and ^1H NMR titration experiment studies the binding mechanism of the F^- ions to the receptors can be proposed as showed in

Scheme 6.6 Initially, at lower concentration the F^- ion binds the receptors with hydrogen bond and at higher concentration of F^- ions the receptors experience the deprotonation. As a result, two step binding mechanism was observed.



Scheme 6.6 Proposed binding mechanism of F^- ions with receptors

Further, the results of UV-vis titration were correlated with the colour changes of receptors with different concentration of F^- ions. The receptor **S5R1** showed a colour change of colourless to orange upon adding 1 equiv. F^- ions. However, at higher concentration (above 4 equiv.) of F^- ions the colour transformed from orange to blood red (Fig 6.18-A). Similarly, as shown in Fig. 6.18-B receptor **S5R2** displayed a colour change from colourless to pale yellow at low concentration (1 equiv.) and pale yellow to dark yellow at higher concentration of F^- ions (above 4 equiv.). This variation with colour on incremental addition of F^- ions clearly justifies the two step binding mechanism of F^- ions to the receptors where the initial colour change is due to the formation of hydrogen-bonded F^- ion complex with the receptors and the second colour change owing to the deprotonation of the receptors.

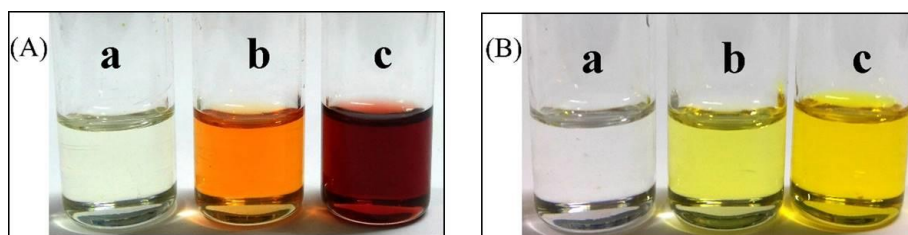


Fig. 6.18 Colour change of the receptors on addition of F^- ions to (A) **S5R1** and (B) **S5R2**; (a) Receptor, (b) Receptor + 1 equiv. F^- and (c) Receptor + 4 equiv. F^-

Further, the receptor **S5R1** was examined for UV-vis titration and two step colorimetric detection experiments with tetrabutylammonium hydroxide (TBAOH) in dry DMSO. The UV-vis titration displayed similar changes as that of TBAF, with incremental addition of TBAOH (Fig. 6.19). This clearly confirms the formation of hydrogen bond at lower concentration of anions followed by deprotonation at higher concentration is responsible for the two step binding process. Similarly, the two step binding process is resulted in two step colour change as shown in Fig. 6.19, Inset.

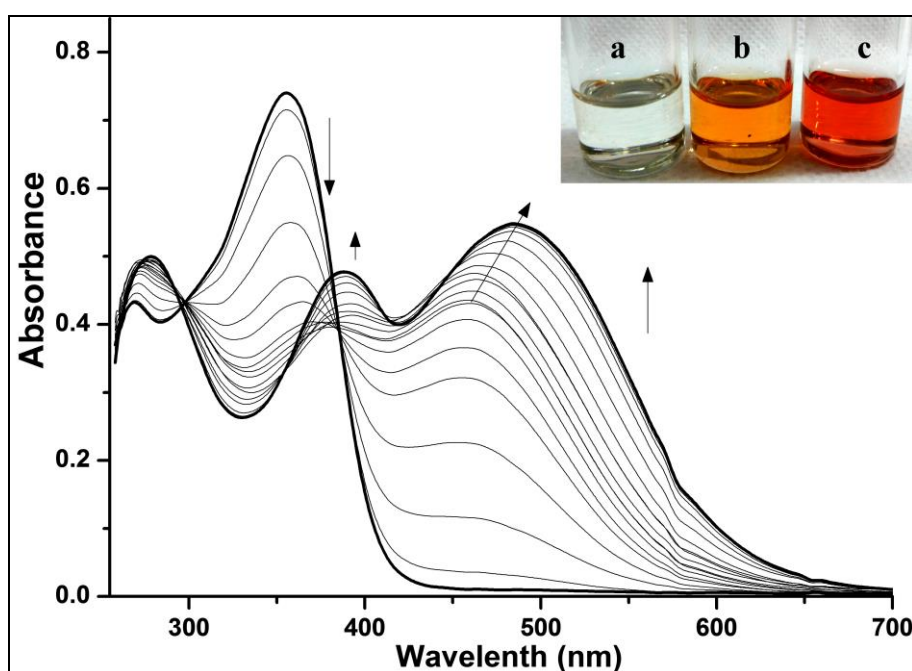


Fig. 6.19 UV-vis titration of **S5R1** (5×10^{-5} M) in dry DMSO with TBAOH (0 – 15 equiv.); Inset: Colour change of the receptor **S5R1** on addition of OH^- ions; (a) Receptor, (b) Receptor + 1 equiv. OH^- ions and (c) Receptor + 4 equiv. OH^- ions

The receptors **S5R1** was able to detect the presence of F^- ions at a concentration as low as 1 ppm. However, the same receptor detected maleate ion with a concentration of 10 ppm. This discrepancy is owing to the small size and strong electronegativity of F^- ion which binds more strongly to the receptor.

6.4 CONCLUSIONS

To conclude, new receptors **S5R1** and **S5R2** were designed and synthesised the colorimetric discrimination of maleate ions over fumarate ions. The receptors **S5R1** and **S5R2** with benzohydrazide functional group as a binding site showed significant colour change from colourless to orange red and colourless to yellow respectively, only with the addition of maleate ions, whereas fumarate ions failed to show any colour change with both the receptors. The colour change was due to the formation of intermolecular hydrogen bond complex between maleate ion and receptors, which was confirmed by 1H NMR titrations. On the other hand, receptor R3 which lacks carbonyl groups did not bind with maleate ion. Similarly, lack of carbonyl groups in **S5R3** resulted in restricted flexibility and steric hindrance. Therefore, the receptor **S5R3** did not show any response either with maleate ions or with fumarate ions. In addition, the receptors **S5R1** and **S5R2** were subjected to colorimetric detection of other biologically important anions such as F^- ions. These receptors colorimetrically detected the F^- ions and along with the concentration of F^- ions the colour of receptors changed. Receptors **S5R1** and **S5R2** showed a colour change of colourless to orange and colourless to pale yellow respectively upon adding 1 equiv. F^- ions. Further, at higher concentration of F^- ions the orange colour of receptor **S5R1** and yellow colour of receptor **S5R2** transformed to blood red and dark yellow respectively. This observation was attributed to initial hydrogen-bonded complex formation at lower concentration of F^- ions and at higher concentration the deprotonation of receptor. Thus, the receptors could be used not only as isomeric discriminative tools but also for the colorimetric detection of F^- ions with a minimum detection limit of 1 ppm.

CHAPTER 7

***DESIGN AND SYNTHESIS OF RECEPTORS WITH
ACTIVE METHYLENE GROUP AS BINDING SITE FOR
EXTRACTION OF FLUORIDE IONS FROM SEA WATER***

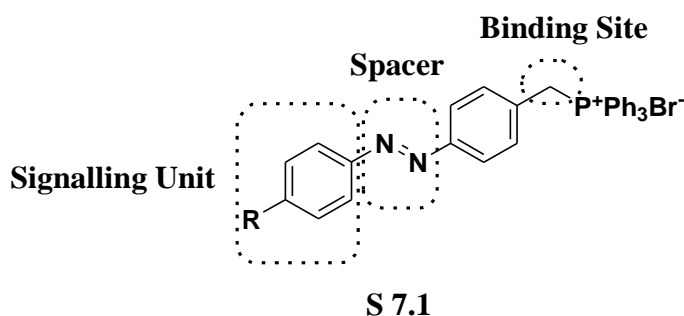
The chapter contains synthesis of triphenylphosphonium salt based receptors with active methylene group which acts as binding site. The selectivity of the receptors towards fluoride ions has been discussed. The practical applicability of these receptors has been showed by extracting inorganic fluoride ions from aqueous solutions and sea water.

7.1 INTRODUCTION

Many receptors with well-known functionalities such as urea/thiourea, amide, pyrrole and imidazolium as binding sites for the F^- ion have been reported where the conventional hydrogen bond formation has been used for the detection (Cametti and Rissanen 2009; Lu et al. 2011; Zhang et al. 2013; Tang, et al. 2013; Im et al. 2013; Li et al. 2013; Ajayakumar et al. 2013; Asthana, 2013. Sarkara and Thilagar 2013; Swamy et al 2013; Trembleau et al. 2013; Liu et al. 2013; Kumar et al. 2013; Cametti and Rissanen 2013; Huang e al. 2013; Sivaramana and Chellappa 2013; Yong et al. 2013; Li et al. 2013; Amendola et al 2013). Unfortunately, majority of them are capable of working only in absolute non-aqueous conditions for the detection of organic fluoride source such as tetrabutylammonium fluoride (TBAF). On the other hand, only few organic receptors have been reported for the detection of F^- ion in aqueous media (Shu et al 2012; Zheng et al. 2013; Yang et al. 2013; Rosen et al. 2013; Nishimura et al. 2013; Maiti et al. 2013). However, only one report (Das et al. 2011) has been published on the selective extraction of F^- ion form aqueous solution with the measurable visual detection till today.

The anion binding receptors with alkyl triphenylphosphonium salts with active/acidic methylene group as a binding site were not studied to the extent of receptors with $-NH$ or $-OH$ binding sites. Hamdi et al. (2004) synthesised a alkyl triphenylphosphonium salts attached to calix[4]arene and reported the formation of ion-pair type complexes with a range of anions like halides, AcO^- , HPO_4^{2-} and ClO_4^- . Das et al. (2011) synthesised alkyl triphenylphosphonium salts attached to anthraquinone skeleton which displayed high selectivity towards F^- ions. In addition, this receptor displayed a unique anion extraction from aqueous solution to organic solvent.

The receptors in this chapter are based on triphenylphosphonium salts which contain active methylene ($-\text{CH}_2-$) group as a binding site for anion detection. The receptors were designed on binding site-spacer-signalling unit approach where binding site and signalling unit were separated by a ‘spacer’ diazo group (**S 7.1**). The receptor **S6R1** contains ethoxyphenyl unit as ‘signalling unit’ and the receptor **S6R2** contains coumarine as ‘signalling unit’.



The receptors are used for the detection of F^- ions in organic media and to extract inorganic F^- ion from aqueous media to organic media. The extraction process has been visualised by instantaneous optical change in organic media. The receptor **S6R3** and **S6R4** were synthesised to evaluate the role of acidic methylene group in the detection process.

7.2 EXPERIMENTAL

7.2.1 Materials and methods

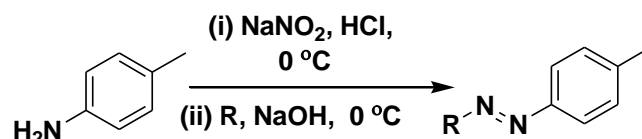
All chemicals were purchased from Sigma-Aldrich, Alfa Aesar or from Spectrochem and used without further purification. All solvents were procured from SD Fine, India with HPLC grade and used without further distillation.

The ^1H NMR spectra were recorded on a Bruker, Avance II (500 MHz) instrument using TMS as internal reference and $\text{DMSO}-d_6$ as solvent. The raw FID data was processed with MestReNova 7.0.0-8331 software. Resonance multiplicities are described as s (singlet), br s (broad singlet), d (doublet), t (triplet), q (quartet) and m (multiplet). The chemical shifts (δ) are reported in ppm and coupling constant (J) values are given in Hz. Melting points were determined with Stuart- SMP3 melting-point apparatus in open capillaries and are uncorrected. IR spectra were recorded on a Thermo Nicolet Avatar-330 FT-IR spectrometer; signal designations: s (strong), m (medium), w (weak), br.m (broad medium) and br.w (broad weak). Mass spectra were

recorded on Waters Micromass Q-Tof micro spectrometer with ESI source. UV-vis spectroscopy was carried out with Analytikjena Specord S600 Spectrometer in standard 3.5 mL quartz cells (2 optical windows) with 10 mm path length. Elemental analyses were done using Flash EA1112 CHNS analyser (Thermo Electron Corporation). All reactions were monitored by TLC on pre-coated silica gel 60 F₂₅₄ plates which were procured from Merck.

7.2.2 Synthesis of S 7.2 and S 7.3

Diazonium salt of p-toluidine was prepared by adding sodium nitrate (3.5 mmol) to a stirred solution of p-toluidine (2.33 mmol) in conc. HCl (2 mL) at 0 °C. A mixture of R (phenol, 2.33 mmol or 2-hydroxybenzaldehyde, 2.33 mmol) and NaOH (4.66 mmol) was slowly added to diazonium salt at 0 °C and allowed to stir for 10 min. The reaction mixture was then stirred at room temperature for 30 min and the pH was adjusted to 6 to obtain solid. The solid was filtered washed with water and dried to obtain desired products **S 7.2** (0.446 g) or **S 7.3** (0.5 g); Scheme 7.1.

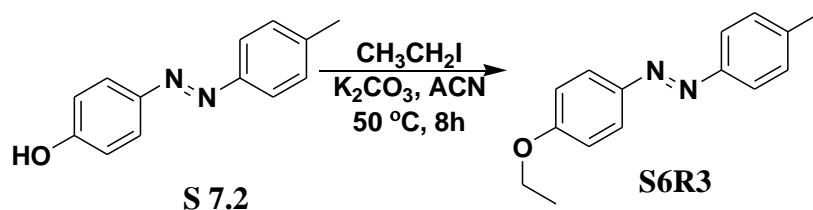


S 7.2: R = Phenol
S 7.3: R = 2-hydroxybenzaldehyde

Scheme 7.1 Synthesis of intermediates **S 7.2** and **S 7.3**

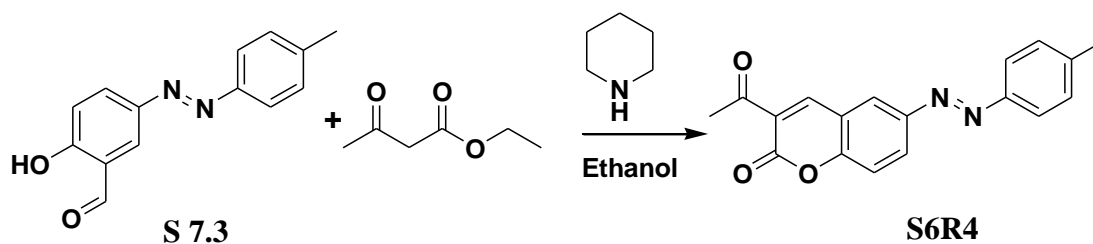
7.2.3 Synthesis of S6R3

To a solution of **S 7.2** (1.18 mmol) in dry acetonitrile, anhydrous K₂CO₃ (3.53 mmol) and ethyl iodide (1.48 mmol) were added. The reaction mixture was stirred at 50 °C for 8 h. The completion of reaction was checked by thin layer chromatography. Excess of K₂CO₃ was removed by filtration and the filtrate was evaporated under reduced pressure to yield pure brown coloured product **S6R3** (0.226 g; Scheme 7.2).

Scheme 7.2 Synthesis of receptor **S6R3**

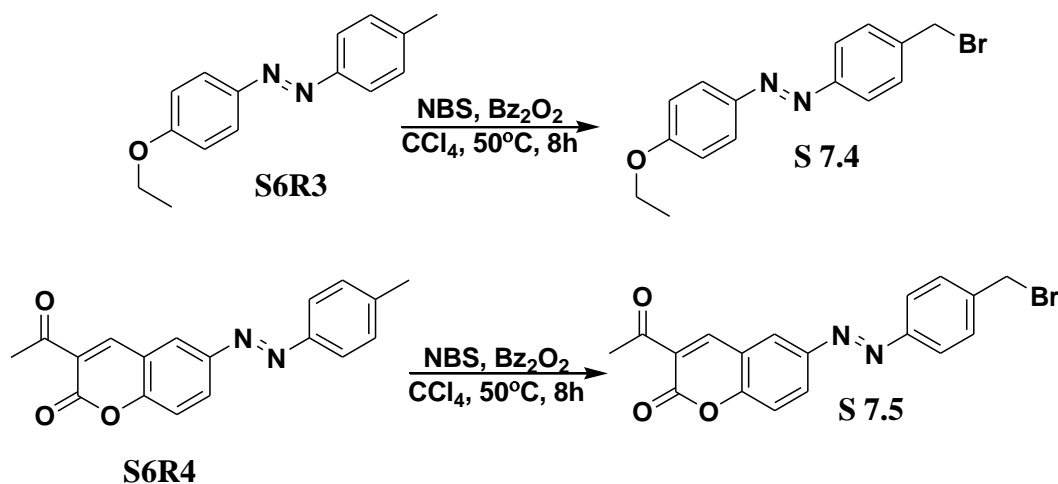
7.2.4 Synthesis of **S6R4**

To a mixture of **S 7.3** (1.04 mmol) and piperidine (0.21 mmol) in ethanol, ethylacetoacetate (1.04 mmol) was added and stirred for 5 h. at room temperature. The completion of reaction was confirmed by TLC. The solid obtained was filtered, washed with ethanol and dried to obtain yellow coloured pure product **S6R4** (0.316 g; Scheme 7.3).

Scheme 7.3 Synthesis of receptor **S6R4**

7.2.5 Synthesis of **S 7.4** and **S 7.5**

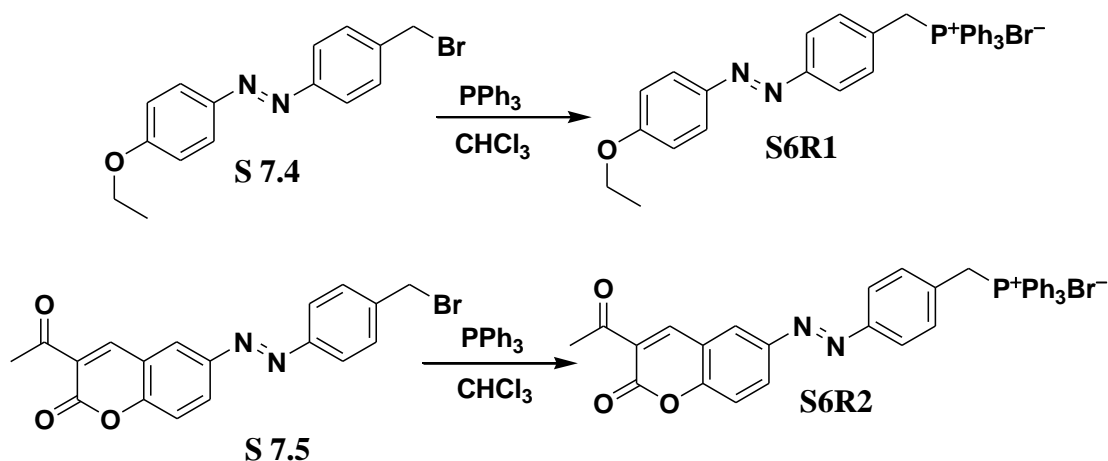
To a solution of **S6R3** or **S6R4** (0.83 mmol or 0.94 mmol) in 20 mL of CCl_4 , N-bromosuccinimide (NBS) (0.91 mmol for **S6R3** and 1.03 mmol for **S6R4**) and a catalytic amount of dibenzoylperoxide (Bz_2O_2) were added. The resulting mixture was refluxed for 8 h. The decomposed product of NBS was then separated by filtration and the filtrate was evaporated to dryness to afford a yellow coloured solid. The solid was triturated with diethylether to yield pure product **S 7.4** (0.24 g) or **S 7.5** (0.343 g; Scheme 7.4).



Scheme 7.4 Synthesis of intermediates S 7.4 and S 7.5

7.2.6 Synthesis of S6R1 and S6R2

A solution of S 7.4 or S 7.5 (0.63 mmol or 0.78 mmol) and triphenyl phosphine (0.693 mmol for S 7.4 and 0.858 mmol for S 7.5) in 20ml dry chloroform was refluxed for 4 h and then stirred at room temperature for 8 h. The reaction mixture was evaporated under reduced pressure to afford a hygroscopic residue which was stirred with diethyl ether till it forms solid residue. The solid was filtered and dried to get the pure product S6R1 (0.34 g) or S6R2 (0.47 g); Scheme 7.5.



Scheme 7.5 Synthesis of receptors S6R1 and S6R2

The single crystal of the receptors S6R3 suitable for X-ray diffraction analysis was grown by slow evaporation of ethanol-dichloromethane (1:1) solution at room temperature. The ORTEP diagrams (50% probability) of the receptor S6R3 is given in

Fig. 7.1. The receptor **S6R3** was crystallised in monoclinic lattice. Detailed crystallographic data of receptor **S6R3** is given in the Table 7.1.

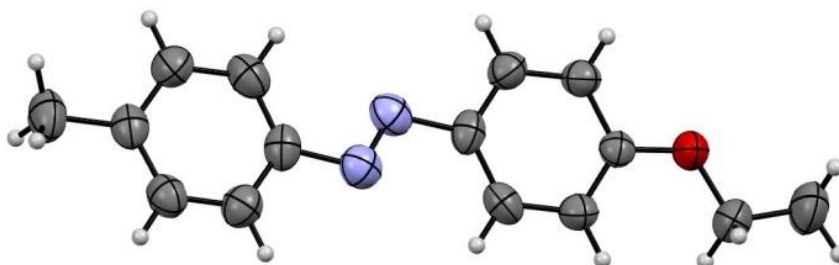
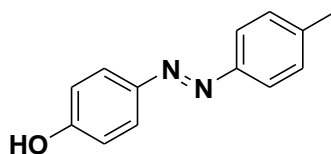


Fig. 7.1 ORTEP diagram (50% probability) of receptor **S6R3**

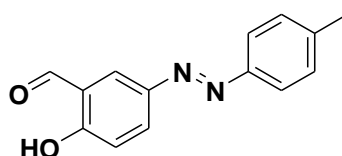
Table 7.1 Crystallographic data of receptor **S6R3**

Parameters	S6R3
CCDC	985440
Chemical formula	$C_{15}H_{16}N_2O$
Formula weight	240.30
Crystal System	Monoclinic
Space group	$P2_1/n$
a (Å)	8.1773(4)
b (Å)	7.5454(4)
c (Å)	21.9486(10)
α (°)	90.00
β (°)	98.890(3)
γ (°)	90.00
V (Å)³	1337.98
Z	4
Crystal size	$0.48 \times 0.35 \times 0.29$
R-factor (%)	7.26

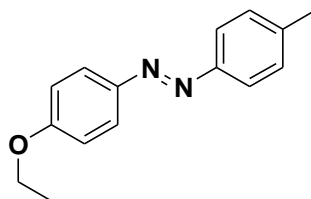
All intermediates and the receptors were characterized by spectral analysis. The characterization data have been compiled and given below.

(E)-4-(p-tolyldiazenyl) phenol (S 7.2)

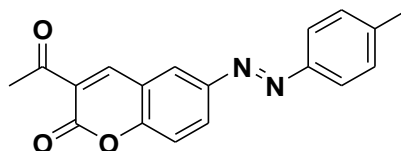
Yield: 90 %; m.p.: 135 – 136 °C. Elemental analysis Calculated for $C_{13}H_{12}N_2O$ (%): C 73.56; H 5.70; N 13.20. Experimental: C 73.59; H 5.66; N 13.19. FT-IR in cm^{-1} : 3356.9 (br. m), 3.40.3 (m), 2936.4 (m), 1601.2 (s).

(E)-2-hydroxy-5-[(p-tolylimino)methyl] benzaldehyde (S 7.3)

Yield: 89 %; m.p.: 119 – 121 °C. Elemental analysis Calculated for $C_{14}H_{12}N_2O_2$ (%): C 69.99; H 5.03; N 11.66. Experimental: C 70.02; H 5.06; N 11.69. FT-IR in cm^{-1} : 3364.9 (br. m), 3072.3 (w), 2835.7 (w) 1698.9 (s), 1602.3 (s).

(E)-1-(4-ethoxyphenyl)-2-p-tolyldiazene (S6R3)

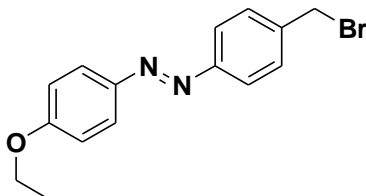
Yield: 80%; m.p.: 126 – 127 °C. Elemental analysis Calculated for $C_{15}H_{16}N_2O$ (%): C 74.97; H 6.71; N 11.66. Experimental: C 74.95, H 6.69, N 11.69. 1H NMR (DMSO- d_6) δ 7.88 (d, 2H, -Ar-H, $J=7$ Hz); δ 7.77 (d, 2H, Ar-H, $J=8$ Hz), δ 7.39 (d, 2H, Ar-H, $J=8$ Hz), δ 7.13 (d, 2H, Ar-H, $J=7$ Hz), δ 4.15 (q, 2H, -CH₂-, $J=7$ Hz) δ 1.38 (t, 3H, -CH₃, $J=7$ Hz). FT-IR in cm^{-1} : 3041.4 (m), 2940.3 (m), 1602.4 (s).

(E)-3-acetyl-6-(p-tolyldiazenyl)-2H-chromen-2-one (S6R4)

Yield: 95%; m.p.: 177 – 178 °C. Elemental analysis Calculated for $C_{18}H_{14}N_2O_3$ (%): C 70.58; H 4.61; N 9.15. Experimental: C 70.54; H 4.58, N 9.18. 1H NMR (DMSO- d_6) δ 8.82 (s, 1H, Ar-H); δ 8.50 (s, 1H, Ar-H); δ 8.22 (d, 1H, Ar-H,

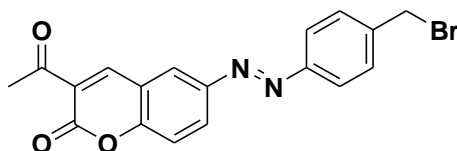
$J=9$ Hz), δ 7.85 (d, 2H, Ar-H, $J=8.5$ Hz), δ 7.66 (d, 1H, Ar-H, $J=8.5$ Hz), δ 7.44 (d, 2H, Ar-H, $J=8$ Hz), δ 2.61 (s, 3H, $-\text{COCH}_3$), δ 2.43 (s, 3H, $-\text{CH}_3$). FT-IR in cm^{-1} : 3042.4 (m), 2885.9 (m), 1699.4 (s), 1684.4 (s), 1601.5 (m).

(E)-1-(4-(bromomethyl) phenyl)-2-(4-ethoxy phenyl)diazene (S 7.4)



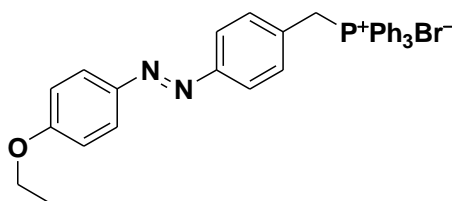
Yield: 90 %; m.p.: 156 – 158 °C. Elemental analysis Calculated for $\text{C}_{15}\text{H}_{15}\text{BrN}_2\text{O}$ (%): C 56.44; H 4.74; N 8.78. Experimental C 56.49, H 4.76, N 8.80. FT-IR in cm^{-1} : 3056.9 (m), 2986.4 (m) 1601.4 (s), 1247.3 (m).

(E)-3-acetyl-6-((4-(bromomethyl)phenyl)diazenyl)-2H-chromen-2-one, (S 7.5)



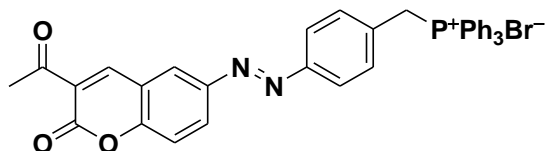
Yield: 91%; m.p.: 188 – 190 °C. Elemental analysis Calculated for $\text{C}_{18}\text{H}_{13}\text{BrN}_2\text{O}_3$ (%): C 56.12; H 3.40; N 7.27. Experimental: C 56.17, H 3.46, N 7.29. FT-IR in cm^{-1} : 3040.2 (w), 2889.3 (m), 1700.3 (s), 1687.4 (s), 1602.5 (m).

(E)-1-(4-ethoxyphenyl)-2-{4-[(triphenylphosphino)methyl]phenyl}diazene bromide (S6R1)



Yield: 92%; m.p.: 146 – 147 °C. Elemental analysis Calculated for $\text{C}_{33}\text{H}_{30}\text{BrN}_2\text{OP}$ (%): C, 68.16; H, 5.20; N, 4.82. Experimental: C 67.53; H 5.58, N 4.86. ^1H NMR ($\text{DMSO}-d_6$) δ 7.62-7.94 (m, 23H, Ar-H); δ 5.30 (d, 2H, P-CH $J=16$ Hz) δ 4.16 (q, 2H, $-\text{CH}_2-$, $J=7$ Hz) δ 1.38 (t, 3H, $-\text{CH}_3$, $J=7$ Hz). FT-IR in cm^{-1} : 3462.3 (m), 3045.6 (m), 2985.7 (m) 1604.3 (s). MS (ESI) m/z Calculated: 581.5 Experimental: 581.1

(E)-3-acetyl-6-[[4-((triphenylphosphino)methyl)phenyl]diazenyl]-2H-chromen-2-one bromide (S6R2)



Yield 92%; m.p.: 159 – 161 °C. Elemental analysis Calculated for $C_{36}H_{28}BrN_2O_3P$ (%): C, 66.78; H, 4.36; N, 4.33. Experimental: C 66.23; H 4.58, N 4.73. 1H NMR (DMSO- d_6) δ 7.24-7.64 (m, 23H, Ar-H); δ 5.36 (d, 2H, P-CH $J=16$ Hz) δ 2.42 (s, 3H, -CH $_3$). FT-IR in cm^{-1} : 3462.3 (m), 3045.6 (m), 2985.7 (m), 1604.3 (s). MS (ESI) m/z Calculated: 647.5; Experimental: 648.5

The representative spectra of receptors have been given below.

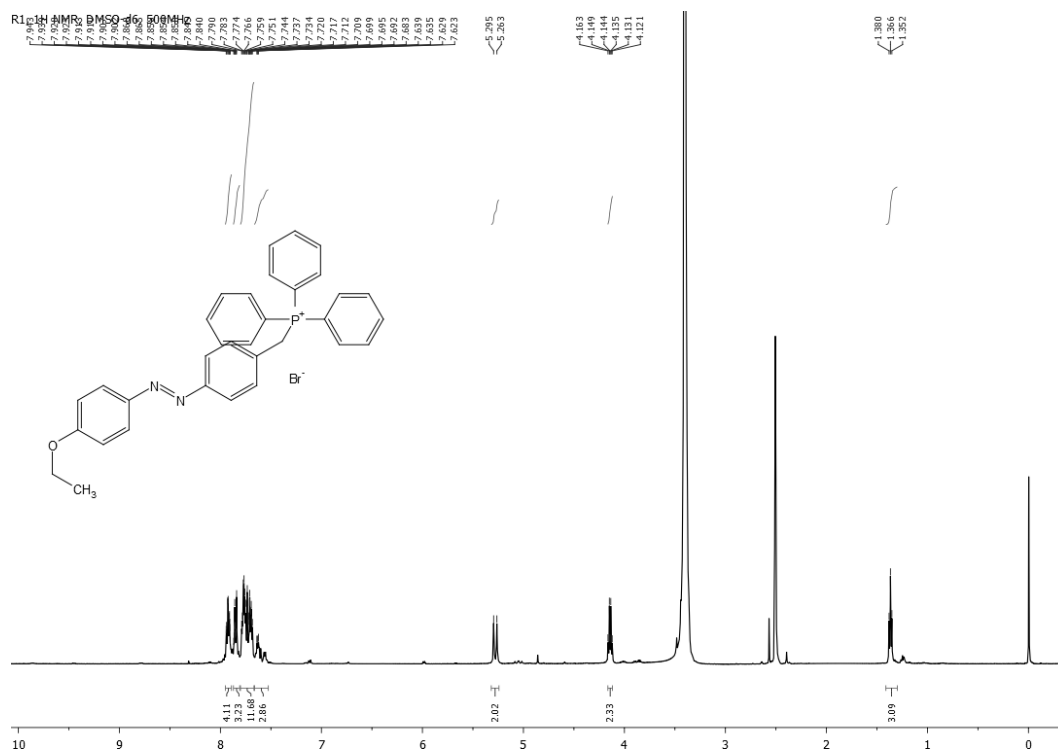


Fig. 7.2 1H NMR spectra of S6R1

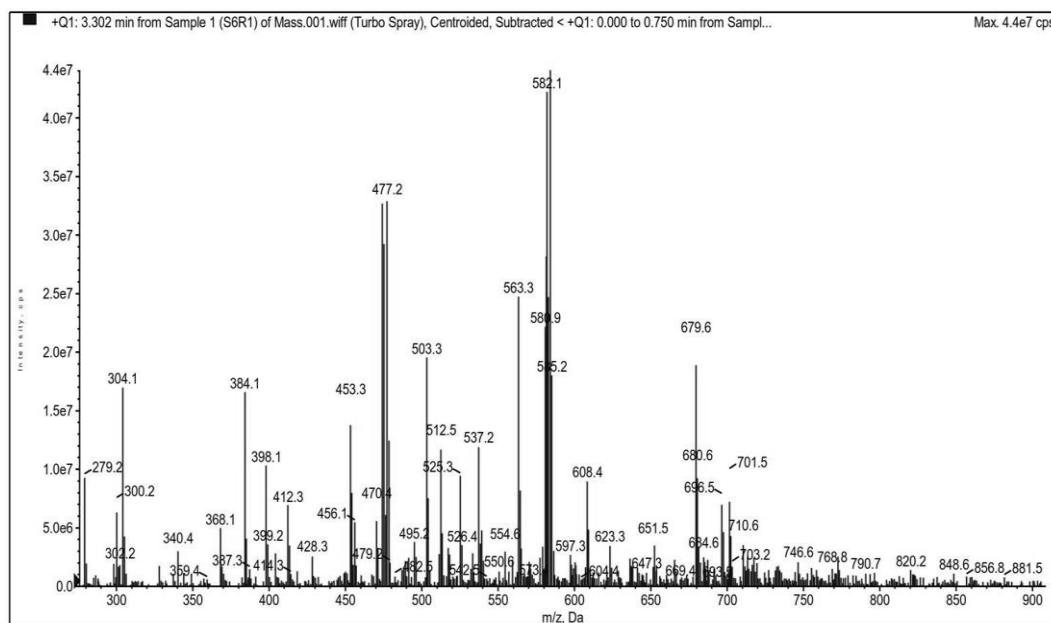
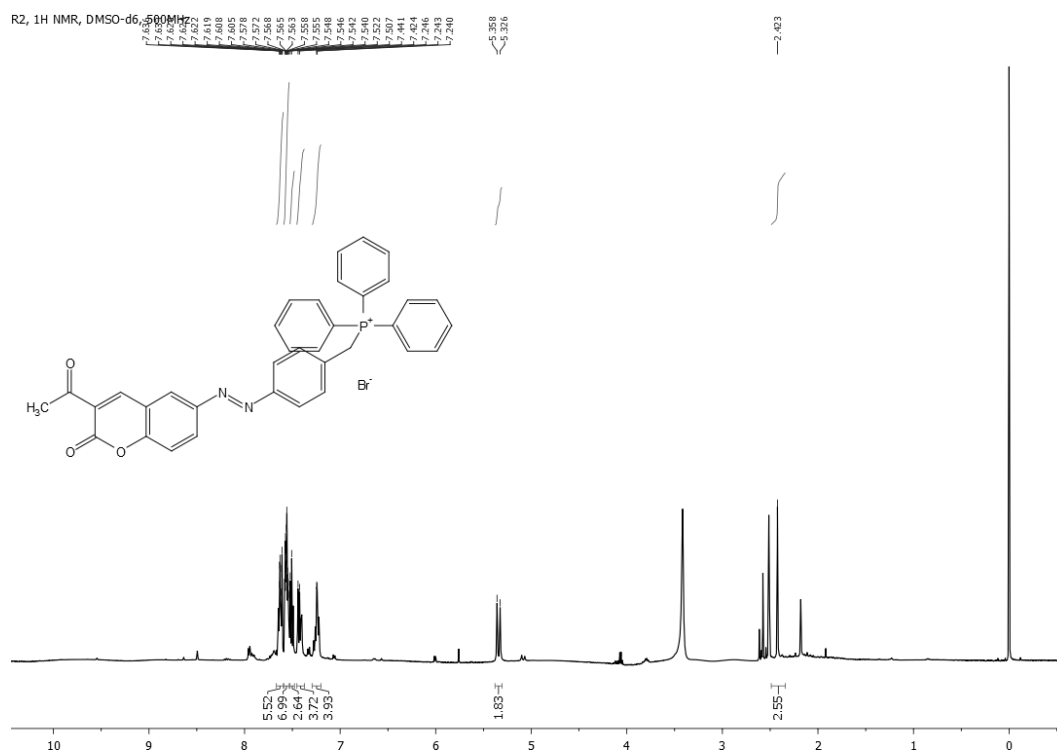


Fig. 7.3 Mass spectra of S6R1

Fig. 7.4 ^1H NMR spectra of S6R2

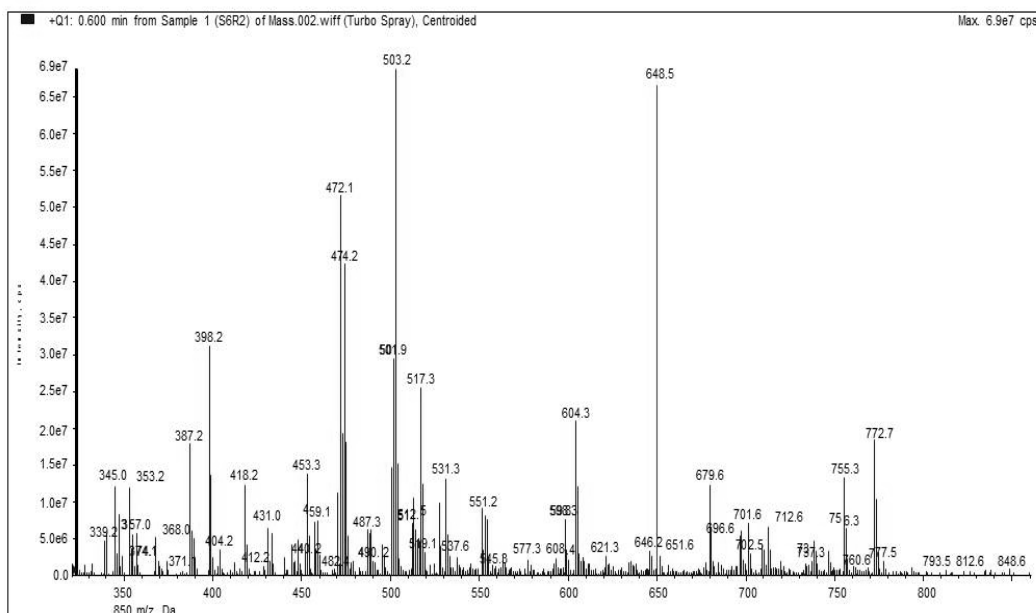


Fig. 7.5 Mass spectra of **S6R2**

7.2.7 Extraction efficiency measurement of receptor **S6R2**

A solution of 1×10^{-4} M TBAF (1 mL) was treated with 19 mL of receptor **S6R2** solution (1×10^{-5} M) in absolute dry DCM (20 mL of total volume). The absorbance was recorded in UV-vis spectrometer. A 1×10^{-4} M of aqueous NaF solution was prepared which was extracted three times with receptor **S6R2** solution in DCM. The extracted non-aqueous solutions were combined together and diluted to 20 mL and absorbance was recorded. Absorbance of the both solutions at 573 nm were compared to obtain extraction efficiency and the receptor was found to be 99% efficient.

7.3 RESULTS AND DISCUSSION

7.3.1 Fluoride ion detection

The selective anion detection study for receptors **S6R1-S6R4** was carried out with the help of UV-vis spectroscopy. The 1×10^{-5} M solutions of receptors **S6R1** and **S6R2** in dry DCM solutions were treated with 2 equiv. of different anions such as fluoride, chloride, bromide, iodide, nitrate, hydrogensulphate, dihydrogenphosphate and acetate in the form of tetrabutylammonium (TBA) salts. In case of receptor **S6R1** a significant shift in the absorbance was observed with the addition of F^- ions and

AcO⁻ ions (Fig. 7.6, A). The intensity of absorption band in UV-vis spectra for AcO⁻ ions was much less than that for F⁻ ions. This signifies the interaction between receptor **S6R1** and F⁻ ion is stronger and interaction between receptor **S6R1** and AcO⁻ ion is much weaker. All other anions did not show any change in UV-vis spectra which indicates that these anions either did not interact with receptor **S6R1** or the interaction is not enough to perturb any changes in the spectra. The receptor **S6R2** showed similar changes with the addition of different anions (Fig. 7.6, B).

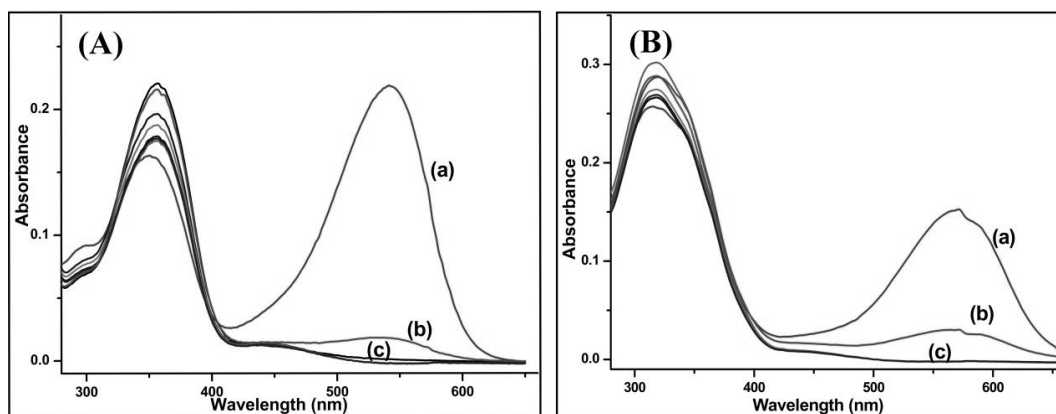


Fig. 7.6 UV-vis spectral change on addition of 2 equiv. anions to receptors (A) **S6R1** and (B) **S6R2** (1×10^{-5} M) in dry DCM (a) F⁻ ions, (b) AcO⁻ ions and (c) Receptor and other anions

In addition, the receptor **S6R1** was further evaluated for colorimetric detection of anions. The receptor **S6R1** solution (1×10^{-5} M) in dry DCM showed significant colour change from pale yellow to pink instantaneously with the addition of F⁻ ion. However, no colour change was noticed upon addition of other anions (Fig. 7.7). The addition of AcO⁻ ions showed slight change in the absorbance of UV-vis spectra, however, it failed to induce any significant colour change to the receptor **S6R1**.

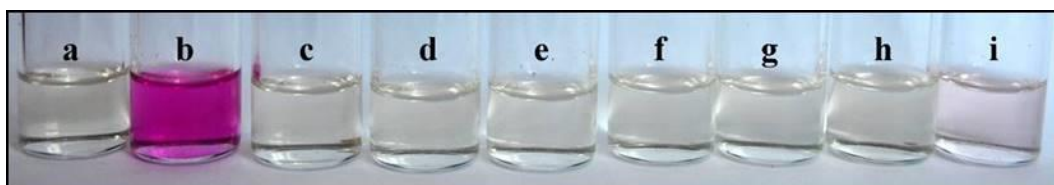


Fig. 7.7 Change in colour after addition of 2 equiv. of different anions as TBA salt to the receptor solution in dry DCM (1×10^{-5} M); (a) Receptor **S6R1**, (b) F⁻, (c) Cl⁻, (d) Br⁻ (e) I⁻, (f) NO₃⁻, (g) HSO₄⁻, (h) H₂PO₄⁻ and (i) AcO⁻

In order to understand the nature of the receptor–anion interactions, the UV-vis titration experiment was carried out between receptor **S6R1** and TBAF (Fig. 7.8). With the incremental addition of TBAF to receptor **S6R1** (1×10^{-5} M), the absorbance at 356 nm corresponding to the phenyldiazene group in the receptor **S6R1**, decreased constantly and a new absorption band at 544 nm was appeared and gradually increased. This is owing to the formation of CT transition involving electron rich methylene functionality as donor group and the phenylenediazene group as the acceptor unit. The intensity of absorption band attained saturation after adding 2 equiv. of F^- ions. The bathochromic shift of 188 nm with the formation of an isosbestic point at 401 nm attributed to the formation of CT complex between the receptor and F^- ion. The binding stoichiometry between the receptor **S6R1** and F^- ions was determined by Bensei-Hildebrand method using UV spectrometric titration data at 544 nm. The linearity in graph confirms the formation of a stable 1:2 receptor: F^- ion stoichiometric complex (Fig. 7.8, Inset).

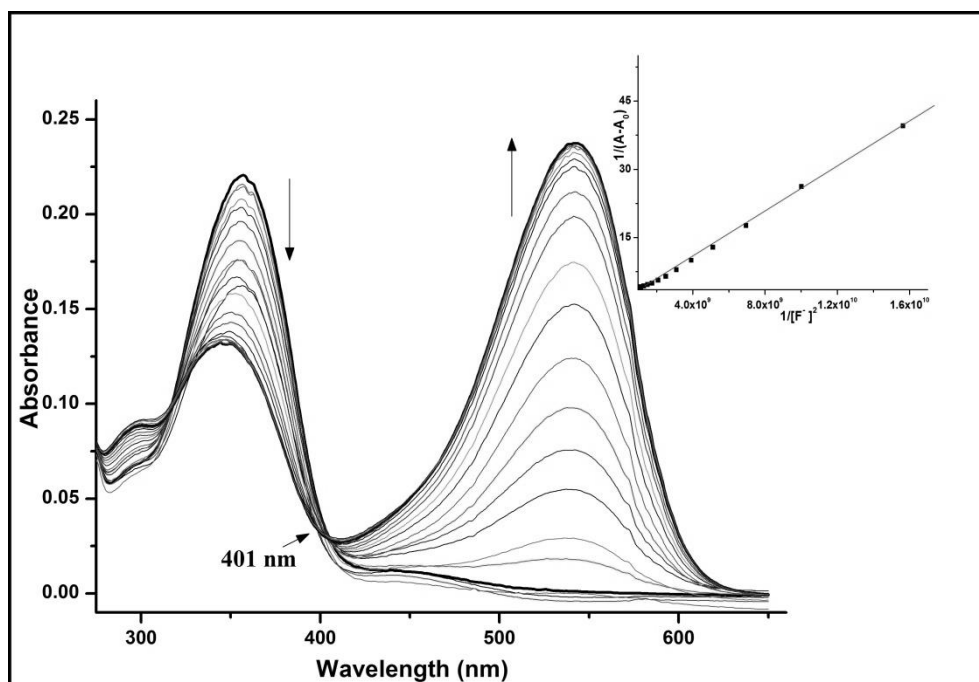


Fig. 7.8 UV-vis titration spectra of **S6R1** (1×10^{-5} M) with the increasing concentration of TBAF (0–3 equiv.) in dry DCM; Inset: Bensei-Hildebrand plot for **S6R1** at 544 nm

Further, the colorimetric investigation was extended to receptor **S6R2**. The receptor **S6R2** (1×10^{-5} M) was treated with 2 equiv. of different anions in dry DCM (Fig. 7.9). The addition of F^- ions showed a significant colour change from pale yellow to dark blue whereas AcO^- ions showed slight variation in colour from pale yellow to light blue. This difference in the colour intensity indicated a stronger binding interaction between receptor **S6R2** and F^- ion and a significantly weaker interaction between receptor **S6R2** and AcO^- ions. On the other hand, other anions either did not interact or feebly interacted with the receptor **S6R2** to show any visual colour change.

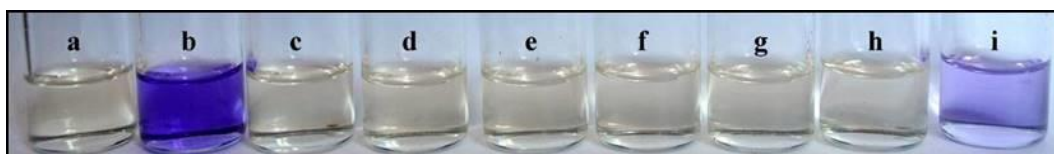


Fig. 7.9 Change in colour after adding 2 equiv. of different anions as TBA salt to the receptor solution in DCM (1×10^{-5} M); (a) Receptor **S6R2**, (b) F^- , (c) Cl^- , (d) Br^- (e) I^- , (f) NO_3^- , (g) HSO_4^- , (h) $H_2PO_4^-$ and (i) AcO^-

The receptor **S6R2** was further quantitatively analysed using UV-vis spectroscopic titration by adding TBAF to dry DCM solution (Fig. 7.10). The addition of TBAF resulted in the generation of new absorption band at 573 nm. With the incremental addition of F^- ion to the receptor **S6R2** solution, the absorbance band at 317 nm corresponding to phenyldiazene chromenone unit decreased gradually and simultaneously, the absorption band at 573 nm progressively increased owing to the development of CT transitions between electron rich methylene functionality as it acts as electron donor and phenylenediazene chromenone group which acts as the electron acceptor unit. The intensity of this new absorption band attained saturation after the addition of 2 equiv. of TBAF. The stoichiometric complexation ratio was determined using Bensei-Hildebrand method. The Bensei-Hildebrand plot was obtained using UV spectrometric titration data at 573 nm. The plot showed linearity only at square of the concentration of F^- ions. This clearly indicates the formation of 1:2 stoichiometric complex between the receptor **S6R2** and F^- ions (Fig. 7.10, Inset).

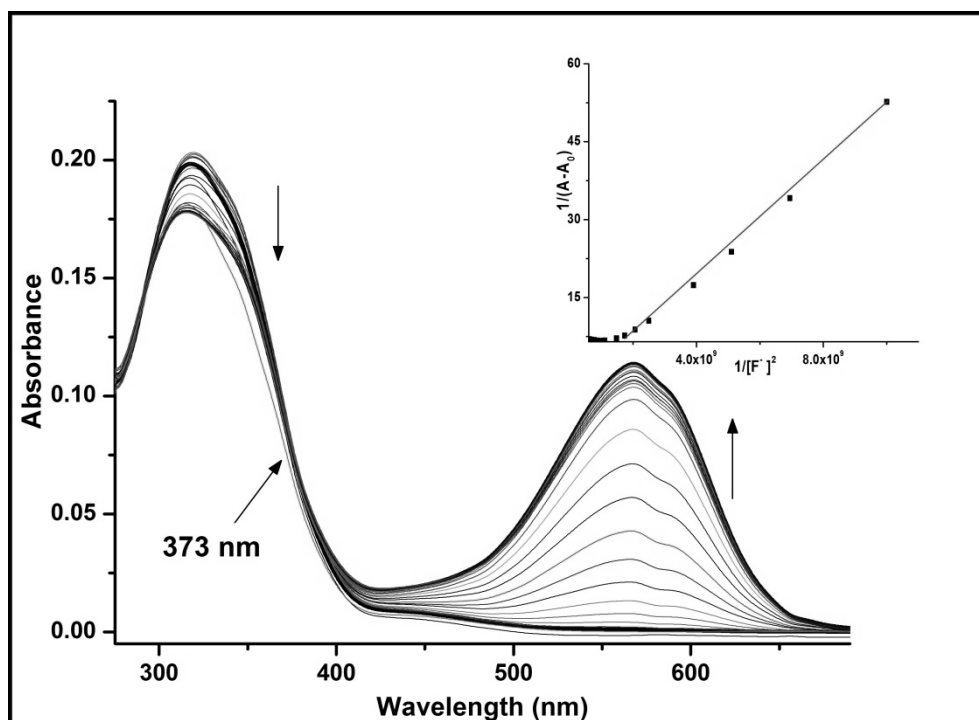
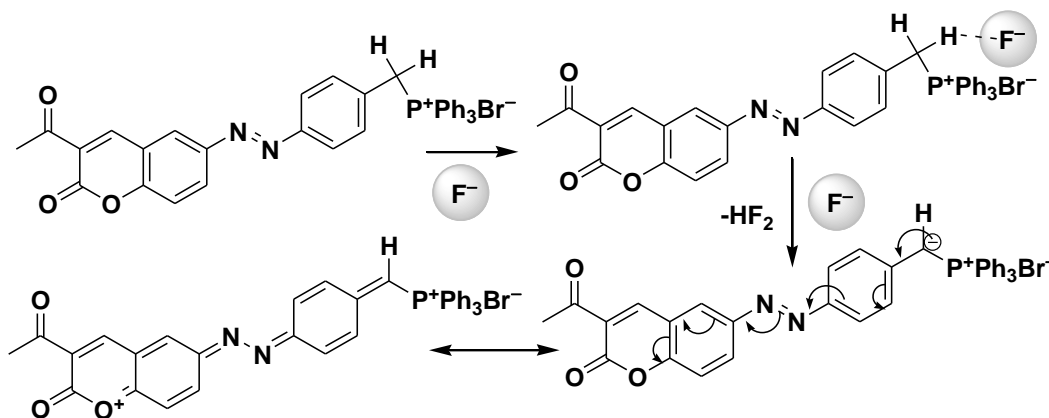


Fig. 7.10 UV-vis titration spectra of **S6R2** (1×10^{-5} M) with the increasing concentration of TBAF (0–3 equiv.) in dry DCM; Inset: Benesi-Hildebrand plot for receptor **S6R2** at 573 nm

The binding constant for both the receptors (**S6R1** and **S6R2**) was calculated using Benesi-Hildebrand equation and found to be $4.58 \pm 0.02 \times 10^7 \text{ M}^{-2}$ for receptor **S6R1** and $7.5 \pm 0.03 \times 10^7 \text{ M}^{-2}$ for Receptor **S6R2**. This shows that the F^- ion binds more strongly to receptor **S6R2** than receptor **S6R1**. This sensitivity is perhaps due to the presence of coumarine unit in receptor **S6R2** which is a strong signalling unit when compared to ethoxyphenyl group in receptor **S6R1**.

Further, the binding mechanism of receptor **S6R2** to F^- ions was proposed by evaluating the results obtained from UV-vis titration and Benesi-Hildebrand method. On compiling the results of UV-vis experiments, it is evident that the colorimetric detection of F^- ion using receptor **S6R2** is a two-step process. Initially, F^- ion binds to the active methylene ($-\text{CH}_2-$) group of the receptor **S6R2** through hydrogen bonding which results in 1:1 adduct to form **S6R1**•• F^- complex. As shown in Scheme 7.6, the second F^- ion leads to deprotonation of active methylene group to form **S6R2** $^-$ (Ghosh, et al. 2011). As a result, the electron density of the receptor

S6R2 increases which leads to the intramolecular charge transfer (ICT) interaction between electron rich phenyldiazeno-chromenone functionality and electron deficient $[\text{PPh}_3]^+$ group. Thus, receptor **S6R2** instantaneously shows intense colour change upon addition of F^- ions.



Scheme 7.6 Proposed binding mechanism of F^- ions with receptor **S6R2**

The binding mechanism was further confirmed by ^1H NMR titration (Fig. 7.11) of receptor **S6R2** carried out in $\text{DMSO-}d_6$ solution. The ^1H NMR signal at δ 5.32 corresponding to two protons of methylene ($-\text{CH}_2-$) group of receptor **S6R2**. The splitting pattern of this signal appeared as a doublet because of coupling with the adjacent phosphorous (Das et al. 2012). Upon adding 0.5 equiv. of F^- ions, slight downfield shift from δ 5.32 to δ 5.33 and δ 5.35 to δ 5.36 was observed. This downfield shift was owing to the formation of hydrogen bond between methylene proton and F^- ion. Upon increasing the concentration of F^- ions to 1 equiv., the signal corresponding to this methylene group disappeared completely which indicated the fast proton exchange between methylene proton and the F^- ion. Further, the addition of F^- ions (2 equiv.) resulted in the deprotonation of receptor to form **S6R2** $^-$ and simultaneously the electron density over the receptor molecule increased. Therefore, the signal corresponding to the protons of $-\text{CH}_2-$ group shifted downfield from δ 5.32 to δ 5.76. Concurrently, the splitting pattern was disappeared because of the fast proton exchange within the receptor. The multiplet signals for aromatic protons experienced downfield shift (from δ 7.24 – 7.63 to δ 7.54 – 7.64) and merged together

to form major two signals with multiple splitting. This further confirms the increase in electron density over the receptor **S6R2**.

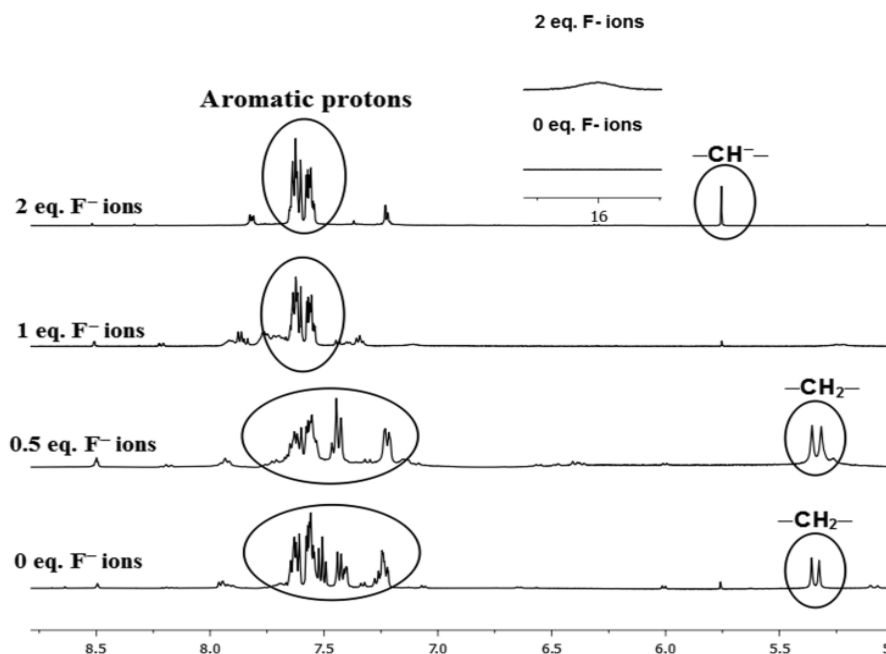


Fig. 7.11 Partial ^1H NMR titration spectrum of receptor **S6R2** in $\text{DMSO-}d_6$ after the addition of F^- ions; Inset: appearance of ^1H NMR signal at δ 16.1 corresponding to HF_2^- upon adding 2 equiv. of F^- ions

In addition, upon adding 2 equiv. of F^- ions to the receptor **S6R2** solution, the active methylene group undergoes deprotonation. This deprotonation process was confirmed from the appearance of ^1H NMR signal at δ 16.1 (Fig. 7.11, Inset) which corresponds to HF_2^- (Peng et al. 2005; Ashokumar et al. 2010).

As an evidence for the deprotonation mechanism, the UV-vis spectroscopic titration was carried out by adding tetrabutylammonium hydroxide (TBAOH) to dry DCM solution of receptors **S6R1** and **S6R2** (Fig. 7.12, A for receptor **S6R1** and Fig. 7.12, B for receptor **S6R2**, Supporting Information). The UV-vis spectra of TBAOH for both the receptors showed similar changes as that TBAF which clearly indicates the detection process follows deprotonation mechanism.

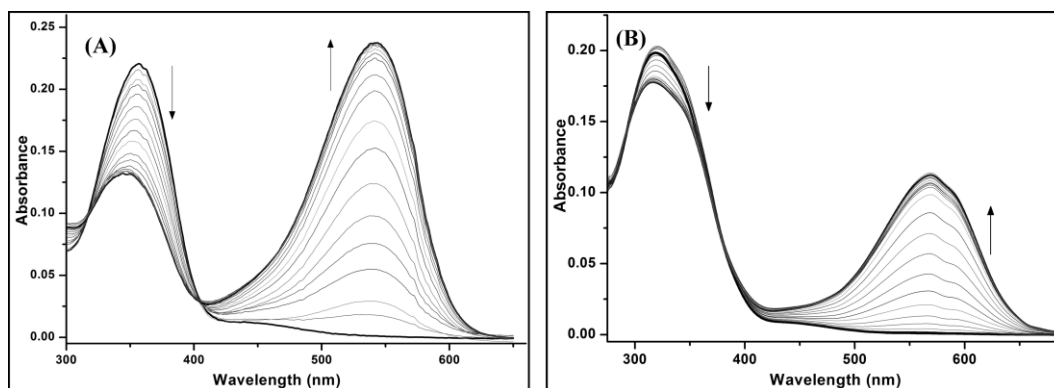


Fig. 7.12 UV-vis titration spectra of (A) **S6R1** and (B) **S6R2** (1×10^{-5} M) with the increasing concentration of TBAOH (0–3 equiv.) in dry DCM

The receptors **S6R3** and **S6R4** which do not contain active methylene group, studied for the anion detection ability in DCM.

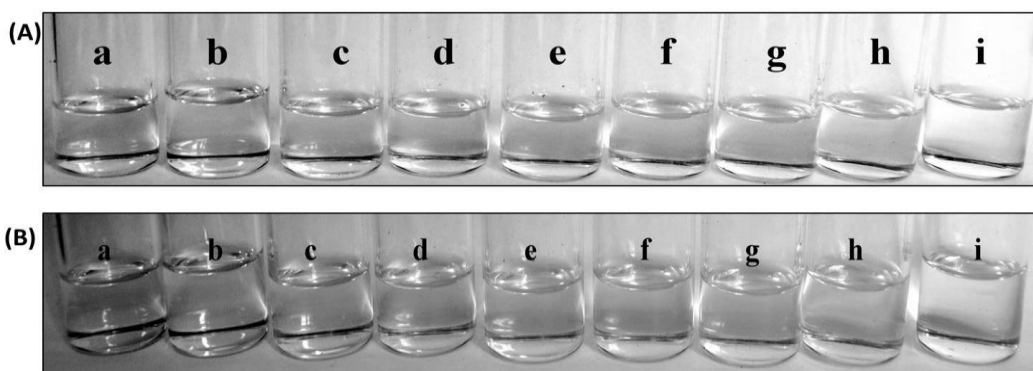


Fig. 7.13 Change in colour after adding 20 equiv. of different anions as TBA salt to the receptor solution in DCM (1×10^{-5} M); (A) **S6R3** and (B) **S6R4**; (a) Receptor (b) F^- , (c) Cl^- , (d) Br^- (e) I^- , (f) NO_3^- , (g) HSO_4^- , (h) $H_2PO_4^-$ and (i) AcO^-

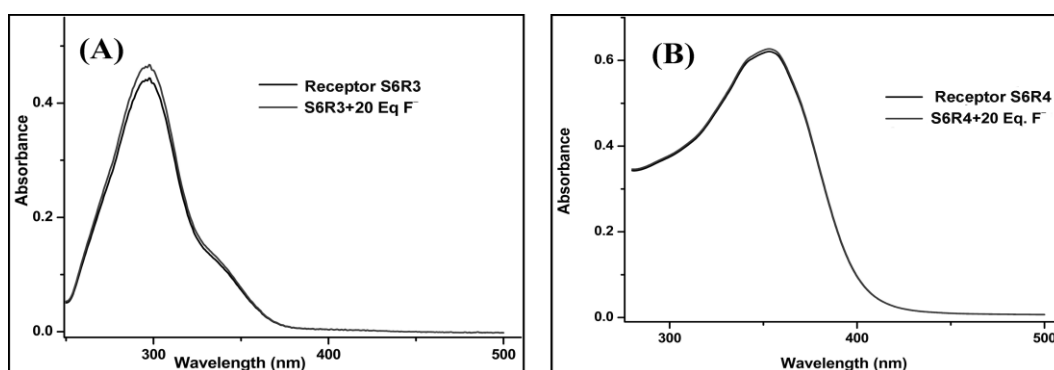


Fig. 7.14 UV-vis spectral change on addition of 20 equiv. anions to receptor solution (1×10^{-5} M) in DCM (A) **S6R3** and (B) **S6R4**

As expected, these receptors neither showed any colour changes (Fig. 7.13, A and Fig. 7.13, B) nor displayed any UV-vis spectral changes (Fig. 7.14, A and Fig. 7.14, B) even with the addition of 20 equiv. of anions. This clearly suggested that the active methylene is responsible for the F^- ion detection.

7.3.2 Extraction of inorganic fluoride ion from aqueous media

The inorganic fluoride such as NaF is an essential nutrient for living organisms, however, at higher concentration it is health hazardous. Therefore, World Health Organization restricted F^- ion concentration level to 1 ppm in drinking water (Fawell et al. 2001; WHO report 1994). Keeping this view in mind, the real-life applicability such as extraction of F^- ions from aqueous media to organic media has been evaluated using receptors **S6R1** and **S6R2**. Standard solutions of NaF in different concentrations were prepared and used as inorganic F^- ion source for the extraction study. These standard solutions were treated with receptors **S6R1** and **S6R2** solution in DCM. Upon vigorous shaking of these organo-aqueous mixtures, the receptor solutions were able to extract F^- ions from aqueous media. As a result, the colour of solutions of receptors **S6R1** and **S6R2** changed from yellow to pink and yellow to deep blue respectively. Further, these receptors were tested for the extraction of F^- ions from sea water collected from Arabian Sea (latitude $13^{\circ}0'33.99''$, longitude $74^{\circ}47'17.23''$) to examine the practical applicability. The extraction process of F^- ions from sea water using these receptors might have interfered by the other anions present in sea water. However, receptor **S6R2** was able to extract F^- ions from sea water successfully. This extraction was represented with the colour change of receptor solution from yellow to blue (Fig. 7.15).

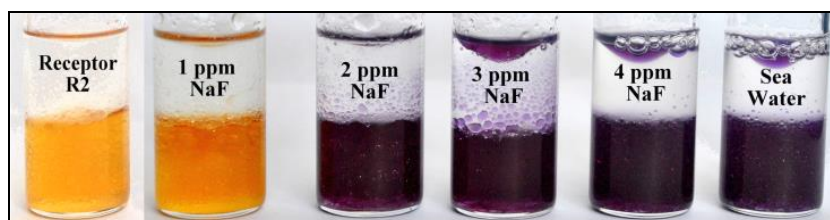


Fig. 7.15 Extraction process of F^- ions from aqueous solutions and sea water using receptor **S6R2** solution in DCM

The extraction experiment was carried out by treating standard solutions of NaF (1 - 4 ppm) and sea water (1.5 mL each) with DCM solutions of receptor **S6R2**, in glass vial. The organo-aqueous solutions were shaken well to extract the F^- ions. The vials containing above 1 ppm NaF solution showed significant colour change from yellow to blue which clearly indicates that the receptor is capable of extracting F^- ions from water. The experimental studies revealed that the receptor **S6R2** was able to extract 99% F^- ions from aqueous NaF solution as well as from sea water.

The extraction study was further quantified using UV-vis spectroscopy. The aqueous solution of F^- ion of different concentration was subjected to extraction (three times for each F^- ion solution) using receptor **S6R2** in DCM. The organic phase was separated, diluted four times and UV- vis spectra was measured. Same procedure was repeated for sea water. The calibration curve was obtained by plotting absorbance vs concentration (in ppm) of F^- ions (Fig. 7.16) where the concentration of F^- ions in sea water was found to be 1.4 ppm. This was comparable with the previously reported literature value (WHO report 1994).

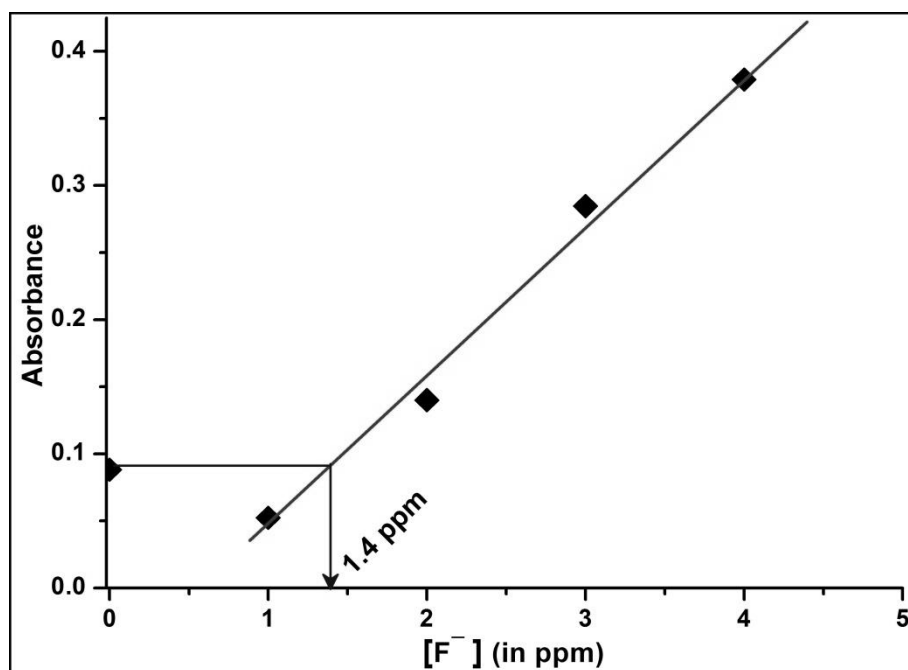


Fig. 7.16 Calibration curve for quantitative determination of F^- ions in sea water/sample

The similar extraction experiments were carried out for receptor **S6R1** which showed a significant colour change in the organic media only with the organo-aqueous solutions which contains minimum 1.5 ppm of NaF. Therefore, the receptor **S6R1** was unable to extract the F^- ions from sea water (Fig. 7.17). This is perhaps due to less extended conjugation as the ethoxyphenyl group is not participating in the detection process.



Fig. 7.17 Extraction process of F^- ions from aqueous solutions and sea water using receptor **S6R1** solution in DCM

7.4 CONCLUSIONS

To summarise, two new receptors with active methylene group as binding site have been designed and synthesised for the selective detection of F^- ions. On adding F^- ions, the receptors **S6R1** and **S6R2** displayed a colour change from pale yellow to pink and pale yellow to dark blue along with a significant bathochromic shift of 188 nm and 256 nm respectively. This colour change and bathochromic shift was owing to the charge transfer transitions in the receptors on adding F^- ions. These receptors were able to detect F^- ions even in the concentration as low as 0.2 ppm in organic media which is much less than the WHO permissible level. In addition, these receptors were able to extract the F^- ions from aqueous media to organic solutions with a substantial colour change. The real-life applicability of the receptors was evaluated by extracting F^- ions from sea water. The receptor **S6R2** was able to extract F^- ions from sea water with 99% efficiency. In addition, the amount of F^- ions present in sea water was determined using receptor **S6R2** and was found to be 1.4 ppm which is in well agreement with the literature reports.

CHAPTER 8

SUMMARY AND CONCLUSIONS

This Chapter describes the brief summary and conclusion of the present research work.

8.1 SUMMARY

Among the wide range of anions, the detection of fluoride ion has gained greater attention because of its privileged usage in clinical applications which made it beneficial to human health. However, the excess of fluoride consumption is health concern as it can be a cause of many lethal diseases including bone cancer. Owing to this dual functionality, it is significant to detect the fluoride ions. More precisely, it will be more advantageous if one can detect the presence of fluoride ion colorimetrically, using organic receptors. Looking at the literatures it has been aimed to design and synthesis new receptors which can colorimetrically detect fluoride ions over other anions, not only in organic media but also in aqueous media.

Apart from this fluoride ion detection, the detection of dicarboxylates is also a field of prominence as they play vital role in the numerous metabolic processes such as glyoxalate cycle, generation of high energy phosphate bonds and in dicarboxylate cycle for autotrophic carbon dioxide (CO₂) fixation. Among the widespread organic anions, the discrimination of geometrical isomers such as *cis/trans* dicarboxylates (maleate and fumarate ions) attains significance because of their different biological behaviours and owing to similar chemical and physical properties, it is gainful to discriminate these isomeric dicarboxylates with colorimetric approach.

Considering the significance of the field, it has been decided to develop new receptors for the colorimetric detection of fluoride ion and dicarboxylate ions. The overall research work is summarized below.

- ❖ Six different series of receptors based on various backbones such as 1-naphthohydrazide, benzohydrazide, aminophenol and triphenylphosphonium salts have been designed and synthesised for colorimetric detection of anions. These receptors have been utilized for versatile applications of environmental concern. All the receptors and intermediates were well characterised using different techniques such as ¹H NMR, FT-IR, elemental analysis and ESI-MS. The selected receptors have been considered for three-dimensional structural elucidation using Single Crystal X-Ray diffraction (SCXRD) studies.

-
- ❖ The quantitative studies of these receptors have been carried out using UV-vis titrations experiments. The stoichiometric ratios of anion to receptor have been determined with the help of either Job's Plot method or Benesi-Hildebrand method. Applying the stoichiometric ratios and quantitative studies, the binding mechanisms of anion to receptor have been derived. These binding mechanisms were justified by ^1H NMR titration of receptors with anions.
 - ❖ All the receptors were tested for different practical applications such as detection of inorganic F^- ions in aqueous media, solvatochromic behaviour of receptor upon adding F^- ions, applications of solvatochromism to determine the percentage composition of binary solvent mixture, discrimination of dicarboxylate ions and extraction of F^- ions from sea water.
 - ❖ The practical applicability of receptor has been tested by detecting and quantifying the amount of F^- ion present in commercial mouthwash and sea water.
 - ❖ A logic gate has been developed for the molecular switching applications using dual sensing property of the receptor.
 - ❖ The receptor containing triphenylphosphonium salt with active methylene group as binding site has been evaluated for the extraction of F^- ions from aqueous media and sea water.

8.2 CONCLUSIONS

Based on the experimental results, following important conclusions have been drawn.

- ❖ The colorimetric detection of F^- ions using receptors **S1R1** and **S1R2** based on 1-naphthohydrazide involve initial 1:1 receptor- F^- ion adduct formation followed by deprotonation at higher concentration of F^- ions. The receptor **S1R1** displayed prominent colour change in organic media, however, it failed to show the same result for the detection of inorganic fluoride ions in aqueous media as the binding site easily gets solvated with trace amount of water. The receptor **S1R2** was able to successfully detect inorganic fluoride in aqueous media which was owing to the presence of base labile $-\text{OH}$ functionality

which deprotonates with the addition of basic F^- ions in aqueous media. The receptor **S1R2** was able to colorimetrically detect the F^- ions with a minimum concentration of 1×10^{-6} M in organic media and 1×10^{-4} M in organo–aqueous mixture.

- ❖ Receptors **S2R1**, **S2R2** based on benzohydrazide derivatives were able to detect inorganic fluoride (NaF) in aqueous media with instantaneous colour changes. The receptors **S2R1** and **S2R2** possess high sensitivity for inorganic F^- ion with a detection level of 0.5 ppm in aqueous media which is much less than WHO permissible level (1 ppm) in drinking water. The mechanism of detection followed formation of stable imidic acid tautomer which was evidenced by 1H NMR titrations. The results were quantified to obtain the amount of F^- ion present in commercial mouthwash and sea water.
- ❖ The receptor **S3R1** based on aminophenol was able to instantaneously detect the F^- ions with a significant colour change. In addition, the receptor showed unique solvatochromic property by displaying different colorations in different solvents only in presence of F^- ions. This solvatochromic property was successfully applied to determine the percentage composition of binary solvent mixture. Along with the instantaneous F^- ion detection the receptor **S3R1** colorimetrically detected Cu^{2+} ions. It acts as a molecular switch which is said to be ‘switch ON’ in presence of F^- ions and ‘switch OFF’ when Cu^{2+} ions were added. An output signal corresponding to the INH circuit has been obtained with input signals in the logic gate operations of receptor **S3R1** which could be implemented to molecular computing operations and molecular devices.
- ❖ The receptors **S4R1** and **S4R3** were able to discriminate maleate ion over fumarate ion with a prominent and instantaneous colour change from pale yellow to reddish pink. The binding of maleate ion to the receptor was through hydrogen bond formation which was confirmed by 1H NMR titrations. The isomeric selectivity has been correlated with the change in receptor orientation upon binding with maleate ion. In addition, these receptors were able to

colorimetrically detect F^- ions by a instantaneous colour change from pale yellow to blood red.

- ❖ New receptors **S5R1** and **S5R2** were able to discriminate isomeric dicarboxylate anion namely maleate ions over fumarate ions by colorimetric approach. The colour change was owing to the formation of intermolecular hydrogen bond complex between maleate ion and the receptors, which was confirmed by 1H NMR titrations. In addition, the receptors **S5R1** and **S5R2** were able to detect other biologically important anions such as F^- ions colorimetrically with a minimum detection limit of 1 ppm. Upon adding 1 equiv. F^- ions to receptors **S5R1** and **S5R2**, a colour change from colourless to orange and colourless to pale yellow have been observed respectively. At higher concentration of F^- ions the orange colour of receptor **S5R1** and yellow colour of receptor **S5R2** have been transformed to blood red and dark yellow respectively. This observation has been attributed to the formation of hydrogen-bonded complex at lower concentration and the deprotonation of receptors at higher concentration of F^- ions. Thus, the receptors could be used not only as isomeric discriminative tools but also for the colorimetric and ratiometric detection of F^- ions.
- ❖ The instantaneous colorimetric detection of F^- ions using receptors **S6R1** and **S6R2** with active methylene group encompass the deprotonation of acidic methylene group. The detection limit of these receptors in organic media was found to be 0.2 ppm which is much less than the WHO permissible level. The receptors were able to extract the F^- ions from aqueous media to organic solutions which resulted in a colour change. The practical applicability of the receptors was evaluated by extracting F^- ions from sea water wherein, receptor **S6R2** extracted F^- ions from sea water with 99% efficiency. The amount of F^- ions present in sea water has been quantified and found to be 1.4 ppm which is comparable with the reported literature value.

REFERENCES

&

PUBLICATIONS

-
- Alberts, B., Bray, D., Lewis, J., Raff, M., Roberts K. and Watson, J.D. (1994). “*Molecular Biology of the Cell*, 3rd. edn, Garland Science, New York.
- Amendola, V., Bergamaschi, G., Boiocchi, M., Fabbrizzi, L. and Mosca, L. (2013). “The interaction of fluoride with fluorogenic ureas: An ON¹–OFF–ON² response.” *J. Am. Chem. Soc.*, 135 (16), 6345–6355.
- Amendola, V., Esteban-Goñi Mez, D., Fabbrizzi, L. and Licchelli, M. (2006). “What anions do to N–H-containing receptors.” *Acc. Chem. Res.*, 39, 343–353.
- Anderson, M.P., Gregory, R.J., Thompson, S., Souza, D.W., Paul, S., Mulligan, R.C., Smith, A.E. and Welsh, M.J. (1991). “Demonstration that CFTR is a chloride channel by alteration of its anion selectivity.” *Science*, 253, 202-205.
- Asakawa, M., Ashton, P.R., Balzani, V., Credi, A., Mattersteig, G., Matthews, O.A., Montalti, M., Spencer, N., Stoddart, J.F. and Venturi, M. (1997). “Electrochemically induced molecular motions in pseudorotaxanes: a case of dual-mode.” *Chem.–Eur. J.*, 3, 1992-1996.
- Aydogan, A., Coady, D.J., Lynch, V.M., Akar, A., Marquez, M., Bielawski, C.W. and Sessler, J.L. (2008). “Poly(methyl methacrylate)s with pendant calixpyrroles: polymeric extractants for halide anion salts.” *Chem. Commun.*, 1455–1457.
- Banthia, S. and Samanta, A. (2005). “Multiple logical access with a single fluorophore–spacer–receptor system: realization of inhibit (INH) logic function.” *Eur. J. Org. Chem.*, 4967-4970.
- Bao, Y., Liu, B., Wang, H., Tian, J. and Bai, R. (2011). “A “naked eye” and ratiometric fluorescent chemosensor for rapid detection of F[–] based on combination of desilylation reaction and excited-state proton transfer.” *Chem. Commun.*, 47, 3957-3959.
- Bassin, E.B., Wypij, D., Davis, R.B. and Mittleman, M.A. (2006). “Age-specific fluoride exposure in drinking water and osteosarcoma (United States).” *Cancer Causes Control*, 17, 421-428.

-
- Basu, A. and Das, G. (2012). "Neutral acyclic anion receptor with thiadiazole spacer: halide binding study and halide-directed self-assembly in the solid state." *Inorg. Chem.*, 51, 882–889.
- Bates, G.W., Gale, P.A., Light, M.E., Ogden, M.E. and Warriner, C.N. (2008). "Structural diversity in the first metal complexes of 2,5-dicarboxamidopyrroles and 2,5-dicarbothioamidopyrroles." *Dalton Trans.*, 4106-4112.
- Baytekin, H.T. and Akkaya, E.U. (2000). "A molecular NAND gate based on Watson-Crick base pairing." *Org. Lett.*, 2, 1725-1727.
- Beer, P.,D. and Gale, P.A. (2001). "Anion Recognition and Sensing: The State of the Art and Future Perspectives." *Angew. Chem. Int. Ed.* 40, 486-516.
- Benesi, H. and Hildebrand, H, (1949). "A spectrophotometric investigation of the interaction of iodine with aromatic hydrocarbons." *J. Am. Chem. Soc.* 71 (8), 2703-2707.
- Berg, J.M., Tymoczko, J.L., Stryer, L. and Gatto, Jr, G.J. (2012). "Biochemistry" W. H. Freeman and Company, New York.
- Beyramabadi, S.A., Bozorgmehr, M.R. and Morsali, A. (2011). "DFT study of solvent effects on tautomerization of 4-(2-thiazolylazo)-resorcinol." *Int. J. Phys. Sci.*, 6 (24), 5726-5730.
- Bhardwaj, V.K. Hundal, M.S. and Hundal, G. (2009). "A tripodal receptor bearing catechol groups for the chromogenic sensing of F^- ions via frozen proton transfer." *Tetrahedron*, 65, 8556–8562.
- Bhosale, S.V., Bhosale, S.V., Kalyankar, M.B. and Langford S.J., (2009). "A Core-Substituted Naphthalene Diimide Fluoride Sensor." *Org. Lett.*, 11, 5418-5421.
- Boiocchi, M., Boca, L.D., Gomez, D.E., Fabbrizzi, L., Licchelli, M. and Monzani, E. (2004). "Nature of urea–fluoride interaction: incipient and definitive proton transfer." *J. Am. Chem. Soc.*, 126, 16507-16514.

-
- Bose, P. and Ghosh, P. (2010). "Visible and near-infrared sensing of fluoride by indole conjugated urea/thiourea ligands." *Chem. Commun.*, 46, 2962–2964.
- Bowman-James, K., and Garcia-Espana, E. (1997) *Supramolecular Chemistry of Anions*, Wiley-VCH: New York.
- Browne, D., Whelton H. and O'Mullane, D. (2005). "Fluoride metabolism and fluorosis." *J. Dent.*, 33, 177–186.
- Buckland, D., Bhosale, S. V. and Langford, S. J. (2011). "A chemodosimer based on a core-substituted naphthalene diimide for fluoride ion detection." *Tetrahedron Lett.*, 2, 1990–1992.
- Caltagirone, C. and Gale, P.A. (2009). "Anion receptor chemistry: highlights from 2007." *Chem.Soc.Rev.*, 38, 520-563.
- Caltagirone, C., Hiscock, J.R., Hursthouse. M.B., Light, M.E. and Gale, P.A. (2008). "1,3-Diindolylureas and 1,3-Diindolylthioureas: Anion Complexation Studies in Solution and the Solid State." *Chem. Euro. J.*, 14, 10236–10243.
- Cametti, M. and Rissanen, K. (2009). "Recognition and sensing of fluoride anion." *Chem. Commun.*, 2809–2829.
- Cametti, M. and Rissanen, K. (2013). "Highlights on contemporary recognition and sensing of fluoride anion in solution and in the solid state." *Chem. Soc. Rev.*, 42, 2016-2038.
- Carton, R.J. (2006). "United States national research council report: fluoride in drinking water." *Fluoride*, 39, 163-172.
- Chen, S., Hou, P., Wang, J. and Song, X. (2012). "A highly sulfite-selective ratiometric fluorescent probe based on ESIPT." *RSC Adv.*, 2, 10869–10873.
- Chiu, C.-W. and Gabbai, F.P. (2006). "Fluoride ion capture from water with a cationic borane". *J. Am. Chem. Soc.*, 128, 14248–14249.

-
- Cho, E.J., Ryu, B.J., Lee, Y.J. and Nam, K.C. (2005). "Visible Colorimetric fluoride ion sensors." *Org. Lett.*, 7, 2607-2609.
- Choi, P.J., Petterson, K.A. and Roberts, J.D. (2002). "Ionization equilibria of dicarboxylic acids in dimethyl sulfoxide as studied by NMR." *J. Phys. Org. Chem.*, 15, 278–286.
- Clayden, J., Greeves, N., Warren, S., Wothers, P. (2001). *Organic Chemistry*; Oxford University Press: New York, Chapter 8, 197.
- Connet, P. (2007). "Professionals mobilize to end water fluoridation worldwide." *Fluoride.*, 40, 155-158
- Cooper, C.R., Spencer, N. and James, T.D. (1998). "Selective fluorescence detection of fluoride using boronic acids." *Chem. Commun.*, 1365–1366.
- Costero, A.M., Colera, M., Gavina P. and Gil, S. (2006). "Fluorescent sensing of maleate versus fumarate by a neutral cyclohexane based thiourea receptor." *Chem. Commun.*, 761–763.
- Credi, A., Balzani, V., Langford, S. J. and Stoddart, J.F. (1997). "Logic operations at the molecular level. An XOR gate based on a molecular machine." *J. Am. Chem. Soc.*, 119, 2679-2681.
- D'Souza, F. (1996). "Molecular recognition via hydroquinone–quinone pairing: Electrochemical and singlet emission behavior of [5,10,15-Triphenyl-20-(2,5-dihydroxy-phenyl)porphyrinato]zinc(II)–quinone complexes." *J. Am. Chem. Soc.*, 118, 923-924.
- Danil de Namor, A.F., Shehab, M., Khalife, R. and Abbas, I. (2007). "Modified Calix[4]pyrrole receptor: Solution thermodynamics of anion complexation and a preliminary account on the phosphate extraction ability of its oligomer." *J. Phys. Chem. B*, 111, 12177–12184.

-
- Das, P., Kesharwani, M.K., Mandal, A.K., Suresh, E., Ganguly, B. and Das, A. (2012). "An alternative approach: A highly selective dual responding fluoride sensor having active methylene group as binding site." *Org. Biomol. Chem.*, 10, 2263-2271.
- Das, P., Mandal, A.K., Kesharwani, M.K., Suresh, E., Ganguly, B. and Das, A. (2011). "Receptor design and extraction of inorganic fluoride ion from aqueous solution." *Chem. Commun.*, 47, 7398-7400.
- Davis, A.P. and Joos, J-B. (2003). "Steroids as organising elements in anion receptors." *Coord. Chem. Rev.*, 240, 143- 156.
- de Silva, A.P. and McClenaghan, N.D. (2004). "Molecular-Scale logic gates." *Chem.–Eur. J.*, 10, 574-586.
- de Silva, A.P., Dixon, I.M., Gunaratne, H.Q.N., Gunnlaugsson, T., Maxwell, P.R.S. and Rice, T.E. (1999). "Integration of logic functions and sequential operation of gates at the molecular-scale." *J. Am. Chem. Soc.*, 121, 1393-1394.
- de Silva, A.P., Guneratne, H.Q.N. and Maguire, G.E.M. (1994). "Off-on' fluorescent sensors for physiological levels of magnesium ions based on photoinduced electron transfer (PET), which also behave as photoionic OR logic gates." *J. Chem. Soc., Chem. Commun.*, 1213-1214.
- Devuyst, O., Christie, P.T., Courtoy, P.J., Beauwens, R. and Thakker, R.V. (1999). "Intra-Renal and subcellular distribution of the human chloride channel, CLC-5, reveals a pathophysiological basis for dent's disease" *Hum. Mol. Genet.*, 8, 247-257.
- Dreisbuch, R.H. (1980) *Handbook of Poisoning*, Lange Medical Publishers: Los Altos, CA.
- Duke, R.M. and Gunnlaugsson, T. (2011). "3-Urea-1,8-naphthalimides are good chemosensors: a highly selective dual colorimetric and fluorescent ICT based anion sensor for fluoride." *Tetrahedron Lett.*, 52(13), 1503-1505.
- Duke, R.M., Veale, E.B., Pfeffer, F.M., Kruger, P.E. and Gunnlaugsson, T. (2010). "Colorimetric and fluorescent anion sensors: an overview of recent developments in

the use of 1,8-naphthalimide-based chemosensors.” *Chem.Soc.Rev.*, 39(10), 3936-3953.

Dusemund, C., Sandanayake, K.R.A.S. and Shinkai, S. (1995). “Selective fluoride recognition with ferroceneboronic acid.” *J. Chem. Soc., Chem. Commun.*, 333–334.

Dydio, P. Lichosyt, D. and Jurczak, J. (2011). “Amide- and urea-functionalized pyrroles and benzopyrroles as synthetic, neutral anion receptors.” *Chem. Soc. Rev.*, 40(5), 2971-2985.

EiamOng, S., Spohn, M., Kurtzman, N.A. and Sabatini, S. (1995). “Insights into the biochemical mechanism of maleic acid-induced Fanconi syndrome.” *Kidney Int.*, 48, 1542–1548.

El-Sherif, A.A. (2010). “Synthesis, solution equilibria and antibacterial activity of Co(II) with 2-(Aminomethyl)-benzimidazole and dicarboxylic acids.” *J. Solution Chem.*, 39, 1562-1581.

Elstner, M., Weisshart, K., Mullen, K. and Schiller, A. (2012). “Molecular logic with a saccharide probe on the few-molecules level.” *J. Am. Chem. Soc.*, 134 (19), 8098-8100.

Fawell, J., Bailey, K., Chilton, J., Dahi, E., Fewtrell, L. and Magara, Y. (2001) *Fluoride in Drinking-water*, IWA Publishing, London, 32.

Featherstone, J.D. (1999). “Prevention and reversal of dental caries: Role of low level fluoride.” *Community Dent. Oral. Epidemiol.*, 27, 31–40.

Frant, M.S. and Ross, J.W. (1966). “Electrode for sensing fluoride ion activity in solution.” *Science*, 154, 1553–1555.

Galbraith, E., Fyles, T.M., Marken, F., Davidson, M.G. and James, T.D. (2008). “Fluorescent boron bis(phenolate) with association response to chloride and dissociation response to fluoride.” *Inorg. Chem.*, 47, 6236–6244.

-
- Gale, P.A. (2000). "Anion coordination and anion-directed assembly: highlights from 1997 and 1998." *Coord. Chem. Rev.*, 199, 181-233.
- Gale, P.A. (2001). "Anion receptor chemistry: highlights from 1999." *Coord. Chem. Rev.*, 213, 79-128.
- Gale, P.A. (2010). "Anion receptor chemistry: highlights from 2008 and 2009." *Chem. Soc. Rev.*, 39(10), 3746-3771.
- Gale, P.A. (2011). "Anion receptor chemistry." *Chem. Commun.* 47 (1), 82-86.
- Gale, P.A. and Gunnlaugsson, T. (eds.) (2010). "Supramolecular Chemistry of Anionic Species" *Chem. Soc. Rev.*, 39, 3581-4008.
- Gale, P.A., Busschaert, N., Haynes, C.J.E., Karagiannidis, L.E. and Kirby, I.L. (2014). "Anion receptor chemistry: highlights from 2011 and 2012." *Chem. Soc. Rev.*, 43, 205-241.
- Gale, P.A., Garcia-Garrido, S.E. and Garric, J. (2008). "Anion receptors based on organic frameworks: highlights from 2005 and 2006." *Chem. Soc. Rev.*, 37, 151-190.
- Garcia-Garrido, S.E., Caltagirone, C., Light, M.E. and Gale, P.A. (2007). "Acridinone-based anion receptors and sensor." *Chem. Commun.*, 43 (14), 1450-1452.
- Garg, B., Bisht, T. and Chauhan, S.M.S. (2010). "Synthesis and anion binding properties of novel 3,12- and 3,7-bis(40-nitrophenyl)-azo-calix[4]pyrrole receptors." *New J. Chem.*, 34, 1251-1254.
- Ghosh, A., Verma, S., Ganguly, B., Ghosh, H.N. and Das, A. (2009). "Influence of urea N-H acidity on receptor-anionic and neutral analyte binding in a Ruthenium(II)-polypyridyl-based colorimetric sensor." *Eur. J. Inorg. Chem.*, 2496-2507.
- Ghosh, K., Saha, I., Masanta, G., Wang, E.B. and Parish, C.A. (2010). "Triphenylamine-based receptor for selective recognition of dicarboxylates." *Tetrahedron Lett.*, 51, 343-347.

-
- Gong, W.-t., Hiratani, K. and Lee, S.S. (2008). "Macrocyclic bis(amidonaphthol)s for anion sensing: tunable selectivity by ring size in proton transfer process." *Tetrahedron*, 64, 11007-11011.
- Gougoux, A., Lemieux, G. and Lavoie, N. (1976). "Maleate-induced bicarbonaturia in the dog: a carbonic anhydrase-independent effect." *Am. J. Physiol.*, 231, 1010–1017.
- Graf, E., Lehn, J.M. (1975). "Cryptates. XVII. Synthesis and cryptate complexes of a spheroidal macrotricyclic ligand with octahedrotetrahedral coordination." *J. Am. Chem. Soc.*, 97, 5022–5024.
- Graf, E., Lehn, J.M. (1976). "Anion cryptates: highly stable and selective macrotricyclic anion inclusion complexes" *J. Am. Chem. Soc.*, 98, 6403–6405.
- Guliyev, R., Ozturk, S., Sahin, E. and Akkaya, E.U. (2012). "Expanded bodipy dyes: anion sensing using a bodipy analog with an additional difluoroboron bridge." *Org. Lett.*, 14, 1528-1531.
- Gunnlaugsson, T., Davis, A.P., O'Brien, J.E. and Glynn, M. (2002). "Fluorescent sensing of pyrophosphate and bis-carboxylates with charge neutral pet chemosensors." *Org. Lett.*, 4, 2449-2452.
- Gunnlaugsson, T., Glynn, M., Tocci, G.M., Kruger, P.E. and Pfeffer, F.M. (2006). "Anion recognition and sensing in organic and aqueous media using luminescent and colorimetric sensors." *Coordin. Chem. Rev.*, 250, 3094-3117.
- Gunnlaugsson, T., Mac Donail, D.A., Parker, D. (2001). "Lanthanide macrocyclic quinolyl conjugates as luminescent molecular-level devices." *J. Am. Chem. Soc.*, 123, 12866-12876.
- Gunnlaugsson, T., Kruger, P.E., Jensen, P., Tierney, J., Ali, H.D.P. and Hussey, G.M. (2005). "Colorimetric "naked eye" sensing of anions in aqueous solution." *J. Org. Chem.*, 70, 10875–10878.
- Guo, Z. Shin, I. and Yoon, J. (2012). "Recognition and sensing of various species using boronic acid derivatives." *Chem. Commun.*, 48, 5956-5967.

-
- Huang, C-Y., Wan, C-F., Chir, J-L. and Wu, A-T. (2013). "A Schiff-Based colorimetric fluorescent sensor with the potential for detection of fluoride ions, *J. Fluorescence*, 23, 1107-1111.
- Hudnall, T.W., Kim, Y.-M., Bebbington, M.W.P., Bourissou, D. and Gabbai, F.P. (2008). "Fluoride ion chelation by a bidentate phosphonium/borane lewis acid." *J. Am. Chem. Soc.*, 130, 10890–10891.
- Jadhav, V.D. and Schmidtchen, F.P. (2006). "Judging on host-guest binding mode uniqueness: association entropy as an indicator in enantioselection." *Org. Lett.*, 8, 2329-2332.
- Jose, D.A., Kumar, D.K., Ganguly, B. and Das, A. (2004). "Efficient and simple colorimetric fluoride ion sensor based on receptors having urea and thiourea binding sites." *Org. Lett.*, 6, 3445-3448.
- Jung, H.S., Kim, H.J., Vicens, J. and Kim, J.S. (2009). "A new fluorescent chemosensor for F₋ based on inhibition of excited-state intramolecular proton transfer." *Tetrahedron Lett.*, 50, 983–987.
- Kaminsky, L.S. Mahoney, M.C. Leach, J. Melius J. and Miller, M.J. (1990). "Fluoride: benefits and risks of exposure." *Crit. Rev. Oral Biol. Med.*, 1, 261–281.
- Kang, S.O., Llinares, J.M., Powell, D., VanderVelde, D. and Bowman-James, K. (2003). "New polyamide cryptand for anion binding." *J. Am. Chem. Soc.*, 125, 10152–10153
- Karl, V., Andrievsky, A. and Sessler, J.L. (1995). "A covalently linked sapphyrin dimer. a new receptor for dicarboxylate anions." *J. Am. Chem. Soc.*, 117, 2953-2954.
- Kata, J.E., Dumlao, S.D., Wasserman, J.I., Lansdown, M.G., Jung, M.E., Faull, K.F. and Clarke, S. (2004). "3-Isopropylmalate is the major endogenous substrate of the *saccharomyces cerevisiae* trans-aconitate methyltransferase." *Biochemistry*, 43, 5976–5986.

Kaur, N., Kumar, S. (2012). "Aminoanthraquinone-based chemosensors: colorimetric molecular logic mimicking molecular trafficking and a set–reset memorized device." *Dalton Trans.*, 41, 5217-5224.

Kim, F.M., Hayes, C., Williams, P.L., Whitford, G.M., Joshipura, K.J., Hoover, R.N., Douglass C.W. and the National Osteosarcoma Etiology Group. (2011). "An assessment of bone fluoride and osteosarcoma" *J. Dent. Res.* 90(10): 1171–1176.

Kim, H.N., Guo, Z., Zhu, W., Yoon, J. and Tian, H. (2011) "Recent progress on polymer-based fluorescent and colorimetric chemosensors." *Chem. Soc. Rev.*, 40, 79-93.

Kim, S-H., Hwang, I-J., Gwon, S-Y., Burkinshaw, S.M. and Son, Y-A. (2011). "An anion sensor based on the displacement of 2,6-dichlorophenol-indo-o-cresol sodium salt from a water-soluble tetrasulfonated calix[4]arene." *Dyes Pigments*, 88, 84-87.

Kim, Y. and Gabbai, F.P. (2009). "Cationic boranes for the complexation of fluoride ions in water below the 4 ppm maximum contaminant level." *J. Am. Chem. Soc.*, 131, 3363–3369

Kim, Y., Gabbai, F.P. (2009). "Cationic boranes for the complexation of fluoride ions in water below the 4 ppm maximum contaminant level." *J. Am. Chem. Soc.*, 131, 3363-3369.

Kirk, K.L. (1991). *Biochemistry of the Halogens and Inorganic Halides*, Plenum Press: New York, 13-53.

Kleerekoper, M. (1998). "The role of fluoride in the prevention of osteoporosis." *Endocrinol. Metab. Clin. North Am.* 27, 441-452.

Kornak, U., Kasper, D., Bosl, M.R., Kaiser, E., Schweizer, M., Schulz, A., Friedrich, W., Delling, G. and Jentsch, T.J. (2001). "Loss of the ClC-7 chloride channel leads to osteopetrosis in mice and man." *Cell*, 104, 205-215.

Kubik, K. (2010). "Anion recognition in water." *Chem. Soc. Rev.*, 39, 3648-3663.

-
- Kubik, S. (2009). "Amino acid containing anion receptors." *Chem.Soc.Rev.*, 38, 585-605.
- Kumar, M., Kumar, R. and Bhalla, V. (2013). "Differential fluorogenic sensing of F^- versus CN^- based on thiacalix[4]arene derivatives." *Tetrahedron Lett.*, 54, 1524-1527.
- Kumar, S., Luxami V. and Kumar, A. (2008). "Chromofluorescent probes for selective detection of fluoride and acetate ions." *Org. Lett.*, 10, 5549-5552.
- Kumar, V., Kaushik, M.P., Srivastava, A.K., Pratap, A., Thiruvenkatam, V. and Row, G.T.N. (2010). "Thiourea based novel chromogenic sensor for selective detection of fluoride and cyanide anions in organic and aqueous media." *Anal. Chim. Acta.*, 663,77-84.
- Kumari, N., Jha, S. and Bhattacharya, S. (2011). "Colorimetric probes based on anthraimidazolediones for selective sensing of fluoride and cyanide ion via intramolecular charge transfer." *J. Org. Chem.*, 76(20), 8215-8222.
- Kundu , T., Chowdhury, A.D., De, D., Mobin, S.M., Puranik, V.G., Datta, A. and Lahiri, G.K. (2012). "Selective recognition of fluoride and acetate by a newly designed ruthenium framework: experimental and theoretical investigations." *Dalton Trans.*, 41, 4484-4496.
- Lau, Y.H., Rutledge, P.J., Watkinson, M. and Todd, M.H. (2011). "Chemical sensors that incorporate click-derived triazoles." *Chem. Soc. Rev.*, 40, 2848-2866.
- Laurella, S. Sierra, M.G., Furlong, J. and Allegretti, P. (2012). "Analysis of tautomerism in b-ketobuanamides by nuclear magnetic resonance: substituent, temperature and solvent effects." *J. Appl. Solution Chem. Modeling*, 1, 6- 12
- Lee, H.N., Singh, N.J., Kwon, J.Y., Kim, Y.Y., Kim K.S., Yoon, J. (2007). "New imidazolium systems bearing two pyrene groups as fluorescent chemosensors for anions and anion induced logic gates." *Tetrahedron Lett.*, 48, 169-172.

-
- Lee, M.H. Agou, T. Kobayashi, J. Kawashima, T. and Gabbai, F.P. (2007). "Fluoride ion complexation by a cationic borane in aqueous solution." *Chem. Commun.*, 1133–1135.
- Lehn, J.M., Sonveaux, E. and Willard, A.K. (1978) "Molecular recognition. Anion cryptates of a macrobicyclic receptor molecule for linear triatomic species." *J. Am. Chem. Soc.*, 100, 4914–4916.
- Li, A.-F., Wang, J.-H., Wang, F. and Jiang, Y.B. (2010) "Anion complexation and sensing using modified urea and thiourea-based receptors" *Chem. Soc. Rev.*, 39 (10), 3729-3745.
- Li, J., Lin, H., Cai, Z. and Lin, H. (2009). "A high selective anion colorimetric sensor based on salicylaldehyde for fluoride in aqueous media." *Spectrochim. Acta A*, 72, 1062–1065.
- Li, T., Yu, L., Jin, D., Chen, B., Li, L., Chen, L. and Li, Y. (2013). "A colorimetric and fluorescent probe for fluoride anions based on a phenanthroimidazole–cyanine platform." *Anal. Methods*, 5, 1612-1616.
- Li, T., Yu, L., Jin, D., Chen, B., Li, L., Chen, L. and Li, Y. (2013). "A colorimetric and fluorescent probe for fluoride anions based on a phenanthroimidazole–cyanine platform." *Anal. Methods*, 5, 1612-1616.
- Li, Z., Rosenbaum, M.A., Venkataraman, A., Tam, T.K., Katz, E., Angenent, L.T. (2011). "Bacteria-based AND logic gate: a decision-making and self-powered biosensor." *Chem. Commun.*, 47 (11), 3060-3062.
- Lin, Y.D., Pen, Y.S., Su, W., Liao, K.L., Wen, Y.S., Tu, C.H., Sun, C.H. and Chow, T.J. (2012). "Reaction-based colorimetric and ratiometric fluorescence sensor for detection of cyanide in aqueous media." *Chem-Asian J.*, 7, 2864-2871.
- Lin, Y-S., Tu, G-M., Lin, C-Y., Chang, Y-T. and Yen, Y-P. (2009). "Colorimetric anion chemosensors based on anthraquinone: naked-eye detection of isomeric dicarboxylate and tricarboxylate anions." *New J. Chem.*, 33, 860–867.

-
- Lin, Z., Chen, H.C., Sun, S-S., Hsu, C-P. and Chow, T.J. (2009). "Bifunctional maleimide dyes as selective anion sensors." *Tetrahedron*, 65, 5216–5221.
- Lin, Z-h., Ou, S-j., Duan, C-y., Zhang, B-g. and Bai, Z-p. (2006). "Naked-eye detection of fluoride ion in water: a remarkably selective easy-to-prepare test paper." *Chem. Commun.*, 624–626.
- Lin, Z-h., Xie, L-x., Zhao, Y-g., Duan, C-y. and Qu, J-p. (2007). "Thiourea-based molecular clips for fluorescent discrimination of isomeric dicarboxylates." *Org. Biomol. Chem.*, 5, 3535–3538.
- Lin, Z-h., Zhao, Y-g., Duan, C-y., Zhang, B-g. and Bai, Z-p. (2006). "A highly selective chromo- and fluorogenic dual responding fluoride sensor: naked-eye detection of F⁻ ion in natural water via a test paper." *Dalton Trans.*, 3678–3684.
- Liu, B. and Tian, H. (2005). "A ratiometric fluorescent chemosensor for fluoride ions based on a proton transfer signaling mechanism." *J. Mater. Chem.*, 15, 2681–2686.
- Liu, C., Qian, X., Sun, G., Zhao, L. and Li, Z. (2008). "Chromogenic and fluorescent chemodosimeter for fluoride ion based on novel anion-catalyzed intramolecular hydrogen transfer." *New J. Chem.*, 32, 472-476.
- Liu, S-Y., Fang, L., He, Y-B., Chan, W-H., Yeung, K-T., Cheng, Y-K. and Yang, R-H. (2005). "Cholic-acid-based fluorescent sensor for dicarboxylates and acidic amino acids in aqueous solutions." *Org. Lett.*, 7, 5825-5828.
- Liu, X-M., Zhao, Q., Song, W-C. and Bu, X-H. (2012). "New highly selective colorimetric and ratiometric anion receptor for detecting fluoride ions." *Chem-Eur. J.*, 18, 2806-2811.
- Liu, Y., Li, M., Zhao, Q., Wu, H., Huang, K. and Li, F. (2011). "Phosphorescent Iridium(III) complex with an N[^]O Ligand as a Hg²⁺-selective chemodosimeter and logic gate." *Inorg. Chem.*, 50 (13), 5969-5977.
- Llinares, J.M., Powell, D. and Bowman-James, K. (2003). "Ammonium based anion receptors." *Coord. Chem. Rev.*, 240, 57-75.

-
- Lu, H., Wang, Q., Li, Z., Lai, G., Jiang, J. and Shen, Z. (2011). "A specific chemodosimeter for fluoride ion based on a pyrene derivative with trimethylsilylethynyl groups." *Org. Biomol. Chem.*, 9, 4558–4562.
- Lu, Q-S., Dong, L., Zhang, J., Li, J., Jiang, L., Huang, Y., Qin, S., Hu, C-W. and Yu, X-Q. (2009). "Imidazolium-Functionalized BINOL as a Multifunctional Receptor for Chromogenic and Chiral Anion Recognition." *Org. Lett.*, 11, 669-672.
- Luxami, V. and Kumar, S. (2008). "Molecular half-subtractor based on 3,3'-bis(1H-benzimidazolyl-2-yl)[1,1']binaphthalenyl-2,2'-diol." *New J. Chem.*, 32 (12), 2074-2079.
- Luxami, V. and Kumar, S. (2012). "A differential ICT based molecular probe for multi-ions and multifunction logic circuits." *Dalton Trans.*, 41, 4588-4593.
- Luxami, V. and Kumar, S. (2012). "ESIPT based dual fluorescent sensor and concentration dependent reconfigurable boolean operators." *RSC Adv.*, 2 (23), 8734-8740.
- Luxami, V., Kumar, A., Hundal, M.S. and Kumar, S. (2010). "Internal electric field driven chromofluorescent chemodosimeter for fluoride ions." *sensor actuat. B-chem.*, 145, 1-6.
- Magri, D.C. (2009). "A fluorescent AND logic gate driven by electrons and protons." *New J. Chem.*, 33, 457-461.
- Mahapatra, A.K., Hazra, G. and Sahoo, P. (2010). "Synthesis of indolo[3,2-b]carbazole-based new colorimetric receptor for anions: A unique colour change for fluoride ions." *Beilstein J. Org. Chem.*, 6, 1-8.
- Mahato, P., Saha, S. and Das, A. (2012). "Rare example of TICT based optical responses for the specific recognition of Cr³⁺ by a 2,2':6',2''-Terpyridine derivative and demonstration of multiple logic operations." *J. Phys. Chem. C*, 116 (33), 17448-17457.

-
- Maiti, D.K., Roy, S., Datta, A. and Banerjee, A. (2013). "Aqueous fluoride ion sensing by a new perylenediimide derivative: Interaction between the hydrated fluoride and the aromatic molecule." *Chem. Phys. Lett.*, 588, 76-81.
- Mandal, A.K., Das, P., Mahato, P., Acharya, S., Das, A. (2012). "A Taco Complex Derived from a Bis-Crown Ether Capable of Executing Molecular Logic Operation through Reversible Complexation." *J. Org. Chem.*, 77 (16), 6789-6800.
- Martinez-Manez, M. and Sancenó, F. (2003). "Fluorogenic and Chromogenic Chemosensors and Reagents for Anions." *Chem. Rev.*, 103, 4419-4476.
- Metz, B., Rosalky, J.M. and Weiss, R. (1976). "[3] Cryptates: X-ray crystal structures of the chloride and ammonium ion complexes of a spheroidal macrotricyclic ligand." *J. Chem. Soc., Chem. Commun.*, 533-534.
- Moragues, M.E., Máñez, R.M. and Sancenón, F. (2011). "Chromogenic and fluorogenic chemosensors and reagents for anions. A comprehensive review of the year 2009." *Chem. Soc. Rev.*, 40, 2593-2643.
- Moss, B. (1996). "A land awash with nutrients-The problem of eutrophication." *Chem. Ind.*, 11, 407-411.
- Ngo, H.T., Liu, X. and Jolliffe, K.A. (2012). "Anion recognition and sensing with Zn(II)-dipicolylamine complexes." *Chem. Soc. Rev.*, 41, 4928-4965.
- Nie, L., Li, Z., Han, J., Zhang, X., Yang, R., Liu, W.-X., Wu, F.-Y., Xie, J.-W., Zhao, Y.-F. and Jiang, Y.-B. (2004). "Development of N-benzamidothioureas as a new generation of thiourea-based receptors for anion recognition and sensing." *J. Org. Chem.*, 69, 6449-6454.
- Nigam, S. and Rutan, S. (2001). "Principles and applications of solvatochromism." *Appl. Spectrosc.*, 55 (11), 362A-370A.
- Nisbet, D.J., Callaway, T.R., Edrington, T.S., Anderson R.C. and Krueger, N. (2009). "Effects of the Dicarboxylic Acids Malate and Fumarate on E. coli O157:H7 and

Salmonella enterica Typhimurium Populations in Pure Culture and in Mixed Ruminant Microorganism Fermentations.” *Curr. Microbiol.*, 58, 488–492.

Nishimura, T., Xu, S-Y., Jiang, Y-B., Fossey, J.S., Sakurai, K., Bull, S.D. and James, T.J. (2013). “A simple visual sensor with the potential for determining the concentration of fluoride in water at environmentally significant levels.” *Chem. Commun.*, 49, 478-480.

Niu, H-T., Su, D., Jiang, X., Yang, W., Yin, Z., He, J. and Cheng, J-P. (2008). “A simple yet highly selective colorimetric sensor for cyanide anion in an aqueous environment.” *Org. Biomol. Chem.*, 6, 3038-3040.

Odago, M.O., Colabello, D.M. and Lees, A.J. (2010). “A simple thiourea based colorimetric sensor for cyanide anion.” *Tetrahedron*, 66, 7465-7471.

Ojida, A., Takashima, I., Kohira, T., Nonaka, H., Hamachi, I. (2008). “Turn-on fluorescence sensing of nucleoside polyphosphates using a xanthene-based Zn(II) complex chemosensor.” *J. Am. Chem. Soc.*, 130, 12095-12101.

Ozsvath, L. (2009) “Fluoride and environmental health: A review.” *Rev. Environ. Sci. Biotechnol.*, 8(1), 59-79.

Panzella, L., Pezzella, A., Arzillo, M., Manini, P., Napolitano, A. and d’Ischia, M. (2009). “A novel fluoride-sensing scaffold by a peculiar acid-promoted trimerization of 5,6-dihydroxyindole.” *Tetrahedron*, 65, 2032–2036.

Park, C.H. and Simmons, H.E. (1968). “Macrobicyclic amines. III. Encapsulation of halide ions by in,in-1,(k + 2)-diazabicyclo[k.l.m.]alkane ammonium ions” *J. Am. Chem. Soc.*, 90, 2431-2432.

Park, I.S., Heo, E-J. and Kim, J-M. (2011) “A photochromic phenoxyquinone based cyanide ion sensor.” *Tetrahedron Lett.*, 52, 2454-2457.

Park, J.J., Kim Y.-H. and Kim, C. (2011). “Naked eye detection of fluoride and pyrophosphate with an anion receptor utilizing anthracene and nitrophenyl group as signaling group.” *Tetrahedron Lett.*, 52, 2759-2763.

-
- Park, J.J., Kim, Y.-H., Kim, C. (2011). "Fine tuning of receptor polarity for the development of selective naked eye anion receptor." *Tetrahedron Lett.*, 52, 3361–3366.
- Pascal, R.A., Spergel, J. and Engen, D.V. (1986). "Synthesis and X-ray crystallographic characterization of a (1,3,5)cyclophane with three amide N-H groups surrounding a central cavity. A neutral host for anion complexation." *Tetrahedron Lett.*, 27, 4099-4102.
- Pfeffer, F.M., Lim, K.F. and Sedgwick, K.J. (2007). "Indole as a scaffold for anion recognition." *Org. Biomol. Chem.*, 5, 1795-1799.
- Piatek, P. and Jurczak, J. (2002). "A selective colorimetric anion sensor based on an amide group containing macrocycle." *Chem. Commun.*, 2450–2451.
- Qu, Y., Hua, J. and Tian, H. (2010). "Colorimetric and ratiometric red fluorescent chemosensor for fluoride ion based on diketopyrrolopyrrole." *Org. Lett.*, 12, 3320-3323.
- Raker, J. and Glass, T.E. (2002). "Selectivity via cooperative interactions: detection of dicarboxylates in water by a pinwheel chemosensor." *J. Org. Chem.* 67, 6113-6116.
- Rakow, N.A., Sen, A., Janzen, M.C., Ponder, J.B. and Suslick, K.S. (2005). "Molecular Recognition and Discrimination of Amines with a Colorimetric Array." *Angew. Chem. Int. Ed.* 2005, 44, 4528-4532.
- Rao, M.R., Mobin, S.M. and Ravikanth, M. (2010). "Boron–dipyrromethene based specific chemodosimeter for fluoride ion." *Tetrahedron*, 66, 1728–1734.
- Ren, J., Wu, Z., Zhou, Y., Li, Y., Xu, Z. (2011). "Colorimetric fluoride sensor based on 1,8-naphthalimide derivatives." *Dyes Pigm.* 91(3), 442-445.
- Riggs, B.L. (1984). *Bone and Mineral Research*, Annual 2; Elsevier: Amsterdam, 366-393.

Rosen, C.B., Hansen, D.J. and Gothelf, K.V. (2013). "Efficient colorimetric and fluorescent detection of fluoride in DMSO–water mixtures with arylaloximes." *Org. Biomol. Chem.*, 11 (45), 7916-7922.

Ros-Lis, J-V., Martinez-Manez, R. Sancenon, F., Soto, J. Rurack, K. and Weißhoff, H. (2007). "Signalling mechanisms in anion-responsive push-pull chromophores: the hydrogen-bonding, deprotonation and anion-exchange chemistry of functionalized azo dyes." *Eur. J. Org. Chem.*, 2449-2458.

Sancenon, F., Martinez-Manez, R., Miranda, M.A., Segui, M-J. and Soto, J. (2003). "Towards the development of colorimetric probes to discriminate between isomeric dicarboxylates." *Angew. Chem. Int. Ed.*, 42, (6), 647-650.

Santos-Figueroa, L.E. Moragues, M.E. Climent, E. Agostini, A. Martinez-Manez, R. and Sancenon, F. (2013). "Chromogenic and fluorogenic chemosensors and reagents for anions. A comprehensive review of the years 2010–2011." *Chem. Soc. Rev.*, 42, 3489-3613.

Santos-Figueroa, L.E., Moragues, M.E., Raposo, M.M., Batista, R.M., Costa, S.P., Ferreira, R.C., Sancenón, F., Martínez-Mañez, R., Ros-Lis, J.V. and Soto, J. (2012). "Synthesis and evaluation of thiosemicarbazones functionalized with furyl moieties as new chemosensors for anion recognition." *Org. Biomol. Chem.*, 10, 7418-7428.

Sarkara, S.K. and Thilagar, P. (2013). "A borane–bithiophene–BODIPY triad: intriguing tricolor emission and selective fluorescence response towards fluoride ions." *Chem. Commun.*, 49, 8558-8560.

Schmidtchen, F.P. (1980). "Synthese makrotricyclischer Amine." *Chem. Ber.*, 113, 864-874.

Schmidtchen, F.P. (1981). "Macrocyclic Quaternary Ammonium Salts, II¹⁾ Formation of Inclusion Complexes with Anions in Solution." *Chem. Ber.*, 114, 597-607.

-
- Schmidtchen, F.P. and Müller, G. (1984). "Anion inclusion without auxiliary hydrogen bonds: X-ray structure of the iodide cryptate of a macrotricyclic tetra-quaternary ammonium receptor." *J. Chem. Soc., Chem. Commun.*, 1115-1116.
- Schwarzenbach, R.P., Escher, B.I., Fenner, K., Hofstetter, T.B., Johnson, C.A., Gunten U.V. and Wehrli, B. (2006). "The challenge of micropollutants in aquatic systems." *Science*, 313, 1072-1077.
- Scott, D.A., Wang, R., Kreman, T.M., Sheffield V.C. and Karniski, L.P. (1999). "The Pendred syndrome gene encodes a chloride-iodide transport protein." *Nat. Genet.*, 21, 440- 443.
- Sessler, J.L., Gale, P.A., and Cho, W.S. (2006). *Anion receptor chemistry*; Royal Society of Chemistry.
- Shang, X.-F., Xu, X.-F., Lin, H., Shao, J. and Lin, H.-K. (2007). "Efficient fluoride-selective receptor: experiment and theory." *J. Inclusion Phenom. Macrocycl. Chem.*, 58, 275–281.
- Sharma, D., Mistry, A.R., Bera, R.K. and Sahoo, S.K. (2013a). "Spectroscopic and computational studies on the development of simple colorimetric and fluorescent sensors for bioactive anions." *Supramolecular Chemistry*, 25, 212-220.
- Sharma, D., Sahoo, S.K., Bera, R.K. and Kamal, R. (2013b). "Spectroscopic and computational study of a naphthalene derivative as colorimetric and fluorescent sensor for bioactive anions." *J. Fluorescence*, 23, 387-392.
- Sharma, D., Sahoo, S.K., Chaudhary, S., Bera, R.K. and Callan, J.F. (2013c). "Fluorescence 'turn-on' sensor for F⁻ derived from vitamin B₆ cofactor." *Analyst*, 138, 3646-3650.
- Shin, Y-J., Jang, S-A., Song, H-Y., Song, H-J. and Song, K.B. (2011). "Effects of combined fumaric Acid-UV-C treatment and rapeseed protein-gelatin film packaging on the postharvest quality of 'Seolhyang' strawberries." *Food Sci. Biotechnol.*, 20, 1161-1165.

-
- Shiraishi, Y., Adachi, K., Itoh, M. and Hirai, T. (2009). "Spiropyran as a selective, sensitive, and reproducible cyanide anion receptor." *Org. Lett.*, 11, 3482-3485.
- Shiraishi, Y., Maehara, H., Sugii, T., Wang, D. and Hirai, T. (2009). A BODIPY–indole conjugate as a colorimetric and fluorometric probe for selective fluoride anion detection." *Tetrahedron Lett.*, 50, 4293–4296.
- Shivarajashankara, Y.M. Shivashankara, A.R. Rao S.H. and Bhat, P.G. (2001). "Oxidative stress in children with endemic skeletal fluorosis." *Fluoride*, 34, 103-107.
- Shu, Q., Birlenbach, L. and Schmittel, M. (2012). "A Bis(ferrocenyl)phenanthroline Iridium(III) complex as a lab-on-a-molecule for cyanide and fluoride in aqueous solution, *Inorg. Chem.*, 51 (24), 13123–13127.
- Simon, D.B., Bindra, R.S., Mansfield, T.A., Nelson-Williams, C., Mendonca, E., Stone, R., Schurman, S., Nayir, A., Alpay, H., Bakkaloglu, A., Rodriguez-Soriano, J., Morales, J.M., Sanjad, S.A., Taylor, C.M., Pilz, D., Brem, A., Trachtman, H., Griswold, W., Richard, G.A., John, E. and Lifton, R.P. (1997). "Mutations in the chloride channel gene, *CLCNKB*, cause Bartter's syndrome type III." *Nat. Genet.* 17, 171 – 178.
- Singh, P. and Kumar, S. (2006). "Photonic logic gates based on metal ion and proton induced multiple outputs in 5-chloro-8-hydroxyquinoline based tetrapod." *New J. Chem.*, 30 (11), 1553-1556.
- Sivaramana G. and Chellappa, D. (2013). "Rhodamine based sensor for naked-eye detection and live cell imaging of fluoride ions." *J. Mater. Chem. B*, 1, 5768-5772.
- Sokkalingam, P. and Lee, C.–H. (2011). "Highly sensitive fluorescence "Turn-On" indicator for fluoride anion with remarkable selectivity in organic and aqueous media." *J. Org. Chem.*, 76, 3820–3828.
- Steed, J.W. (2009). "Coordination and organometallic compounds as anion receptors and sensors." *Chem.Soc.Rev.*, 38, 506-519.

-
- Steed, J.W., Atwood, J.L. (2009). *Supramolecular Chemistry, 2nd edition*, John Wiley & Sons, Ltd., United Kingdom.
- Su, H., Lin, H., Cai, Z-S. and Lin, H. (2010). "Anion receptor based on thiourea: via hydrogen bonding interaction and efficient deprotonation." *J. Incl. Phenom. Macrocycl. Chem.* 67, 183-189.
- Suksai, C. and Tuntulani, T. (2003). "Chromogenic anion sensors." *Chem. Soc. Rev.*, 32, 192–202.
- Suresh, M., Ghosh, A. and Das. A. (2007). "Half-subtractor operation in pH responsive N-heterocyclic amines." *Tetrahedron Lett.* 48, 8205-8208.
- Suresh, M., Ghosh, A. and Das. A. (2008). "A simple chemosensor for Hg²⁺ and Cu²⁺ that works as a molecular keypad lock." *Chem. Commun.*, 44, 3906-3908.
- Suresh, M., Jose, D.A. and Das. A. (2007). "[2,2'-Bipyridyl]-3,3'-diol as a molecular half-subtractor." *Org. Lett.*, 9, 441-444.
- Swamy, C.A., Mukherjee, P.S. and Thilagar, P. (2013). "Dual emissive borane–BODIPY dyads: molecular conformation control over electronic properties and fluorescence response towards fluoride ions." *Chem. Commun.*, 49, 993-995.
- Tang, Z., Yang, J., Yu, J. and Cui, B. (2010). "A Colorimetric Sensor for Qualitative Discrimination and Quantitative Detection of Volatile Amines." *Sensors*, 10, 6463-6476.
- Tetilla, M.A., Aragoni, M.C., Arca, M., Caltagirone, C., Bazzicalupi, C., Bencini, A., Garau, A., Isaia, F., Laguna, A., Lippolis, V. and Meli, V. (2011). "Colorimetric response to anions by a "robust" copper(II) complex of a [9]aneN₃ pendant arm derivative: CN⁻ and I⁻ selective sensing." *Chem. Commun.*, 47, 3805-3807.
- Trembleau, L., Smith, T.A.D. and Abdelrahman, M.H. (2013). "Receptor conformational change induces fluoride binding despite competitive water binding." *Chem. Commun.*, 49, 5850-5852.

-
- Trivedi, D.R. Fujiki, Y. Fujita, N. Shinkai, S. and Sada, K. (2009). "Crystal engineering approach to design colorimetric indicator array to discriminate positional isomers of aromatic organic molecules" *Chem. Asian J.*, 4, 254-261.
- Trivedi, D.R., Fujiki, Y., Goto, Y., Fujita, N., Shinkai, S. and Sada, K. (2008). "A naked-eye colorimetric indicator to discriminate aromatic compounds by solid-state charge-transfer complexation." *Chem. Lett.*, 37, 550-551.
- Tseng, Y-P., Tu, G-M., Lin, C-H., Chang, C-T., Lin, C-Y. and Yen, Y-P. (2007). "Synthesis of colorimetric sensors for isomeric dicarboxylate anions: selective discrimination between maleate and fumarate." *Org. Biomol. Chem.*, 5, 3592–3598.
- Upadhyay, K.K., Kumar, A., Mishra, R.K., Fyles, T.M., Upadhyay S. and Thapliyal, K. (2010). "Reversible colorimetric switching of thiophene hydrazone based on complementary IMP/INH logic functions." *New J. Chem.*, 34, 1862-1866.
- Valiyaveetil, S., Engbersen, J.F.J., Verboom, W. and Reinhoudt, D.N. (1993). "Synthesis and Complexation Studies of Neutral Anion Receptors." *Angew. Chem. Int. Ed.*, 32, 900-901.
- Villamil-Ramos, R. and Yatsimirsky, A.K. (2011). "Selective fluorometric detection of pyrophosphate by interaction with alizarin red S–dimethyltin(IV) complex." *Chem. Commun.*, 47, 2694-2696.
- Voet, D. and Voet, J.G. (1995). *Biochemistry*, 2nd ed.; wiley; Newyork, NY.
- Weatherall, J.A. (1969). "Pharmacology of fluorides." In *Handbook of Experimental Pharmacology XX/1*, Part 1; Springer-Verlag: Berlin, 141-172.
- WHO Technical Report Series- 846, Fluoride and Oral Health, Geneva, 1994.
- Wiseman, A. (1970). *Handbook of Experimental Pharmacology XX/2, Part 2*, Springer-Verlag, Berlin, 48.
- Xu, G. and Tarr, M.A. (2004). "A novel fluoride sensor based on fluorescence enhancement." *Chem. Commun.*, 1050–1051.

-
- Xu, G., Liu, L. and Chen, J. (2012). "Reconstruction of cytosolic fumaric acid biosynthetic pathways in *Saccharomyces cerevisiae*." *Microb. Cell Fact.*, 11, 1-10, doi:10.1186/1475-2859-11-24.
- Xu, L., Li, Y., Yu, Y., Liu, T., Cheng, S., Liu, H. and Li, Y. (2012). "A receptor incorporating OH, NH and CH binding motifs for a fluoride selective chemosensor." *Org. Biomol. Chem.*, 10, 4375-4380.
- Xu, Z. Kim, S.K. and Yoon, J. (2010). "Revisit to imidazolium receptors for the recognition of anions: highlighted research during 2006–2009." *Chem. Soc. Rev.*, 39, 1457-1466.
- Xu, Z., Chen, X., Kim, H.N. and Yoon, J. (2010). "Sensors for the optical detection of cyanide ion." *Chem. Soc. Rev.*, 39, 127-137.
- Yang, R., Liu, W.-X., Shen, H., Huang, H.-H. and Jiang, Y.-B. (2008). "Anion Binding in Aqueous Solutions by N-(Isonicotinamido)-N'-phenylthiourea-Based Simple Synthetic Neutral Receptors. Role of the Hydrophobic Microenvironment of the Receptor Molecule." *J. Phys. Chem. B*, 112, 5105–5110.
- Yang, S., Liua, Y. and Feng, G. (2013). "Rapid and selective detection of fluoride in aqueous solution by a new hemicyanine-based colorimetric and fluorescent chemodosimeter." *RSC Adv.*, 3, 20171-20178.
- Yen, Y-P. and Ho, K-W. (2006). "Development of colorimetric receptors for selective discrimination between isomeric dicarboxylate anions." *Tetrahedron Lett.*, 47, 7357–7361.
- Yen, Y-P. and Ho, K-W. (2006). "Synthesis of colorimetric receptors for dicarboxylate anions: a unique color change for malonate." *Tetrahedron Lett.*, 47, 1193–1196.
- Yin, C., Huo, F., Zhang, J., Máñez,R.M-., Yang, Y., Lv, H. and Li, S. (2013). "Thiol-addition reactions and their applications in thiol recognition." *Chem.Soc.Rev.*, 42, 6032-6059.

Yong, X., Su, M., Wan, W., You, W., Lu, X., Qu, J. and Liu, R. (2013). “2-Thiohydantoin containing OH and NH recognition subunits: a fluoride ion selective colorimetric sensor.” *New J. Chem.*, 37, 1591-1594.

Yong, X., Su, M., Wang, W., Yan, Y., Qu, J. and Liu, R. (2013). “A naked-eye chemosensor for fluoride ions: a selective easy-to-prepare test paper.” *Org. Biomol. Chem.*, 11, 2254–2257.

Yoshida, A., Taniguchi, S., Hisatome, I., Royaux, I.E., Green, E.D., Kohn, L.D. and Suzuki, K. (2002). “Pendrin is an iodide-specific apical porter responsible for iodide efflux from thyroid cells.” *J. Clin. Endo. Metab.*, 87, 3356-3361.

Yu, Y., Yang, W., Dong, Z., Wan, C., Zhang, J., Liu, J., Xiao, K., Huang Y. and Lu, B. (2008). “Neurotransmitter and receptor changes in the brains of fetuses from areas of endemic fluorosis.” *Fluoride.*, 41, 134-138.

Zhang, B.-G., Cai, P., Duan, C.-Y., Miao, R., Zhu, L.-G., Niitsu, T. and Inoue, H. (2004). “Imidazolidinium-based robust crypt with unique selectivity for fluoride anion.” *Chem. Commun.*, 2206–2207.

Zhang, G., Lin, W., Yang, W., Lin, Z., Guo, L., Qiu, B. and Chen, G. (2012). “Logic gates for multiplexed analysis of Hg^{2+} and Ag^+ .” *Analyst*, 137 (11), 2687-2691.

Zhang, Y.-M., Lin, Q., Wei, T.-B., Wang, D.-D., Yao, H. and Wang, Y.-L. (2009). “Simple colorimetric sensors with high selectivity for acetate and chloride in aqueous solution.” *Sens. Actuators, B*, 137, 447–455.

Zhao, Y., Li, Y., Qin, Z., Jiang, R., Liu, H., and Li, Y. (2012). “Selective and colorimetric fluoride anion chemosensor based on s-tetrazines.” *Dalton Trans.*, 41, 13338-13342.

Zheng, F., Zeng, F., Yu, C., Hou, X. and Wu, S. (2013). A PEGylated Fluorescent Turn-On Sensor for Detecting Fluoride Ions in Totally Aqueous Media and Its Imaging in Live Cells, *Chem. Eur. J.* 19, 936–942.

Zielinski, T. and Jurczak, J. (2005). "Thioamides versus amides in anion binding." *Tetrahedron*, 61, 4081–4089.

LIST OF PUBLICATIONS

Papers published/ communicated in international journals

1. **Madhuprasad**, Shetty, A. N. and Trivedi, D. R. (2012). “Colorimetric receptors for naked eye detection of inorganic fluoride ion in aqueous media using ICT mechanism.” *RSC Adv.* 2, 10499–10504.
2. **Madhuprasad**, Swathi, N., Manjunatha, J. R., Das, U.K., Shetty, A. N. and Trivedi, D. R. (2014). “Dual Colorimetric Receptor with Logic Gate Operations: Anion Induced Solvatochromism.” *New J. Chem.*, 38, 1484-1492.
3. **Madhuprasad** and Trivedi, D. R. (2014). ““Naked-eye” Detection of Inorganic Fluoride Ion in Aqueous Media Using Base Labile Proton: A Different Approach.” *J. Fluo. Chem.*, 160, 1–7.
4. **Madhuprasad** and Trivedi, D. R. “Colorimetric Receptors to Discriminate Maleate Ions over Fumarate Ions and Its Application in Fluoride Ion Detection.” Communicated.
5. **Madhuprasad** and Trivedi, D. R. (2014). “A New Colorimetric Receptor for Selective Detection of Maleate vs. Fumarate and Ratiometric Detection of F⁻ Ions.” *Ana. Methods*, 6, 3817–3825.
6. **Madhuprasad** and Trivedi, D. R. (2014). “A New Receptor with Active Methylene Group as Binding Site for Extraction of Inorganic Fluoride Ions from Sea Water.” *ChemPlusChem*, 79, 1001 – 1008.

Papers presented in international conferences

1. Madhuprasad, Trivedi, D. R. (2011). “Simple Amides as a Colorimetric Sensor for Rapid Detection of Fluoride Ion.” Paper presented in “International conference on Futuristic Science and Technology in Frontier Areas & 2nd Annual Conference of Indian JSPS Alumni Association” August 05-06, Tiruvananthapuram.
2. Madhuprasad, Trivedi, D. R. (2012). “Colorimetric Receptor for The Detection of F⁻ Ions And Its Solvatochromic Effect.” Paper presented in “New Age Science and Technology for Sustainable Development & 3rd Annual Conference of Indian JSPS Alumni Association” August 06-07, NEERI, Nagpur.

CURRICULAM VITAE

MADHUPRASAD

mchemkigga@gmail.com

+919900300625

EDUCATION

July 2010 to Present

PhD

Department of Chemistry,
National Institute of Technology Karnataka,
New Synthetic Receptors for Molecular
Recognition of Anions and Their Practical
Applications.

Title of the thesis

Supervisor

Dr. Darshak R. Trivedi

June 2004 to May 2006

Master of Science (71.8 %)

Department of Chemistry
Jnana Sahyadri, Kuvempu University
Organic Chemistry, Analytical Chemistry,
Physical Chemistry, Inorganic Chemistry

Major Subjects

June 2001 to May 2004

Bachelor of Science (60.3 %)

Sri J. C. B. M College, Sringeri,
Kuvempu University

Major Subjects

Chemistry, Physics and Mathematics

RESEARCH EXPERIENCE

July 2010 to Present

Research Scholar

Department of Chemistry
National Institute of Technology Karnataka,
Organic Chemistry, Material Chemistry,
Molecular recognition and Colorimetric
receptors.

Area of research

August 2006 to July 2010

Scientist

Syngene International Ltd – A Biocon
Company, Bangalore, India.
(<http://www.syngeneintl.com>)

Area of Research

R & D, Synthetic Organic and Medicinal
Chemistry, Purification and Interpretation of
organic molecule by various techniques.

SKILLS AND ABILITIES

EXPERTISE

Synthesis

- ❖ One dimensional library synthesis: 2000 compounds per year
- ❖ Three dimensional library synthesis: 3000 compounds per year
- ❖ Multistep scaffold synthesis using various hazardous/flammable reagents such as cyanide, DIBAL-H, BBr₃, BuLi, sodium triacetoxy borohydride etc. and/or hydrogenation reaction using Pd/C.
- ❖ Expertized in various reactions such as Suzuki, Grignard, Vilsmeier-Haack, etc.

Analytical

- ❖ Analytical interpretation of organic molecules by ¹H, ¹³C NMR, IR, HPLC and LCMS.
- ❖ Structural DATA collection using **Bruker APEX II Single Crystal XRD** and Structure solution (DATA reduction).
- ❖ **Instruments handled:** Many instruments including basic Semi/Fully automated purifiers to **advanced** instruments such as **Bruker APEX II Single Crystal XRD**.
- ❖ Route scouting and quotation for target compounds.
- ❖ Project report and campaign report on completion of project.

MANAGEMENT

- ❖ Handled a group of 8 chemists.
- ❖ Guided projects for 11 postgraduate/undergraduate students

PUBLICATIONS

1. **Madhuprasad**, A. Nityananda Shetty and Darshak R. Trivedi, "Colorimetric receptors for naked eye detection of inorganic fluoride ion in aqueous media using ICT mechanism." *RSC Advances*, 2012, 2, 10499–10504; **RSC Publications**.
2. **Madhuprasad**, N. Swathi, J. R. Manjunatha, Uttam Kumar Das, A. Nityananda Shetty and Darshak R. Trivedi. "Dual Colorimetric Receptor with Logic Gate Operations: Anion Induced Solvatochromism." *New Journal of Chemistry*, 2014, 38, 1484-1492; **RSC Publications**.
3. **Madhuprasad** and Darshak R. Trivedi. "Naked-eye" Detection of Inorganic Fluoride Ion in Aqueous Media Using Base Labile Proton: A Different Approach. *Journal of Fluorine Chemistry*, 2014, 160, 1–7; **Elsevier Publications**.

-
4. **Madhuprasad** and Darshak R. Trivedi. "A New Colorimetric Receptor for Selective Detection of Maleate vs. Fumarate and Ratiometric Detection of F⁻ Ions." *Analytical Methods*, 2014, 6, 3817–3825; **RSC Publications**.
 5. **Madhuprasad** and Darshak R. Trivedi. "Colorimetric Receptors to Discriminate Maleate Ions over Fumarate Ions and Its Application in Fluoride Ion Detection." Communicated.
 6. **Madhuprasad** and Darshak R. Trivedi. "A New receptor with Active Methylene Group as Binding Site for Extraction of Fluoride Ions from Sea Water." *ChemPlusChem*, 2014, 79, 1001 – 1008; **Wiley-VCH Publications**.

PERSONAL DETAILS

Date of birth : 16th May 1983
Marital Status : Married
Languages known : English, Hindi, Kannada and Tulu
Permanent address : Banginabailu House
Post Kigga, Sringeri TQ
Chikkamagaluru DT- 577 139
Karnataka, INDIA
Phone: 08265-258779

REFERENCE

Dr. Darshak R. Trivedi Assistant Professor Department of Chemistry NITK, Post Srinivasanagara, Surathal, Mangalore, Karnataka-575 025, INDIA Email: darshak_rtrivedi@yahoo.co.in	Dr. Subhendu Kumar Mohanty Lead Investigator Syngene International Ltd. Biocon Park, Plot No. 2&3, Bommasandra, Bangalore, Karnataka-560 099, INDIA Email: subhendu.mohanty@gmail.com
--	---